Characterising the Role of Mitochondrial Dysfunction in Ageing Liver Regeneration and Inflammation

Michelle Louise James

Doctor of Philosophy

Newcastle University

Institute of Cellular Medicine

August 2019

| Abstract

Ageing is a major risk factor for chronic liver disease in which reduced regeneration and age-associated chronic inflammation or “inflammageing” is observed. In ageing, mitochondrial respiratory chain dysfunction is shown to be a key arbitrator of the process, accruing somatic mitochondrial DNA (mtDNA) mutations with increasing time. Mechanisms linking these themes remain elusive; however, respiratory dysfunction is thought to be important in excess ROS production and apoptosis. Knock-in mitochondrial replicase γ (*PolgA*) mice are known to recapitulate some progeroid and phenotypic features of human ageing as a result of clonally expanded somatic mtDNA mutations. Basally whilst $PolgA^{+/mut}$ and $PolgA^{mut/mut}$ ageing mice livers was shown to be histologically normal, immunohistological analysis of tissues revealed reduced hepatocellular turnover in the presence of increasing mitochondrial respiratory deficiency. This proliferative defect was attributed to mitochondrial dysfunction within the liver parenchyma and specifically hepatocytes, observing reduced complex I expression. Subsequent subjection to mechanical stress by means of two-thirds partial hepatectomy in $PolgA^{+/mut}$ and $PolgA^{+/mut}$ mice also showed a blunted proliferative response. Additionally, accelerating ageing, mitochondrial dysfunction and downstream ROS production is linked to oxidative stress and altered proinflammatory signalling. Indeed, this study of $PolgA^{+/mut}$ and $PolgA^{mut/mut}$ mice reveals skewing towards a proinflammatory environment. Analysis revealed increased honing of neutrophils within the liver that when stimulated, releases increased amounts of ROS. Such a proinflammatory phenotype appears secondary to the proliferative defect, in which the $PolgA^{mut/mut}$ liver following exposure to acute oxidative CCl_4 stress revealed delayed regeneration and cell cycle p16 induction, as well as a failure to clear proinflammatory immune cells. Observations coincided with increasing induction of mitochondrial dysfunction and additional compensatory mechanisms of mitochondrial and antioxidant gene expression. The findings of this thesis suggests that complex I mitochondrial respiratory dysfunction plays a role in ageing hepatocellular regeneration, with ETC deficiency having further roles in regulating proinflammatory cell signalling. Dissecting the role of respiratory dysfunction in liver homeostasis and regeneration would enable understanding for therapeutic intervention in the context of ageing liver disease.

| Dedication and Thanks

First and foremost, I would like to give my deepest thanks to my supervisors Professor Fiona Oakley and Dr Laura Greaves for their tutelage, insight and guidance during my project. A special thanks to my main supervisor Fiona who has been there for me throughout my PhD and beyond: no matter how big or small the problem always made time to check-in.

I would like to give my thanks to the Fibrosis Research group, the Wellcome Trust for Mitochondrial Research and those involved in the Centre for Ageing and Vitality for all of their knowledge, help and above all friendship, making my time as a PhD student an enjoyable and most memorable experience. In particular, a special thanks to my lab bestie, Dr Julie Worrell, who throughout my PhD has supported my mad 'sciencing' ideas and given me the best motivational and pastoral care a PhD student could wish.

I would also like to thank my family and 'kapamilya', who without the wonderful support network would have made the PhD almost impossible. Specifically, a special thanks to Kalvin who, no matter the distance and obstacles, always found the time and way to be there for one another.

Above all, the utmost appreciation and deepest gratitude to my parents, Sonia and Barry James, who through the trials and tribulations have always been there for me - always guided me and supported me. I thank you both and to you this thesis is dedicated.

'If at first you don't succeed: try, try and try again'

| Acknowledgements

I would like to thank my colleagues at both the Fibrosis Research Group and Wellcome Trust for Mitochondrial Research Newcastle for their collaborative knowledge, insight and help during my PhD. In particular, I would like to acknowledge the following for their contributions:

For assistance in the animal work, I would like to firstly thank Ms Carla Bradshaw with her help in maintaining the *PolgA* colonies: without her efficiency and proficiency, the mouse models and thus PhD could not be completed. In addition, a big thanks to Dr Jack Leslie who helped to perform partial hepatectomy surgeries in chapter 5.

For assistance with chapter 4 (phenotypic characterisation of $PolgA^{+/mut}$ and $PolgA^{mut/mut}$ ageing livers) I would like to firstly thank Dr Caroline Wilson and Mr Jonathan Scott of the Simpson Lab Newcastle, who both initially assisted me in experimental set up and optimisation of neutrophil functional assays and data acquisition *via* flow cytometry. My gratitude also extends to Dr Julie Worrell who contributed to the hepatocyte functional assays, in particular the harvesting of isolated hepatocyte cell protein, LDH assays and assistance in the acquisition of hepatocyte photomicrographs. Lastly, I would also like to thank Dr Alex Laude, who kindly contributed to creating a quantifiable threshold suitable for COX/SDH staining analysis.

The work completed during this PhD was supported by a joint MRC and Barbour Foundation funded PhD studentship.

| Table of Contents

| List of Abbreviations

4-HNE	4-hydroxynonenal
8-OHdG	8-hydroxy-2-deoxyguanosine
aa	Amino acid
ACK	Ammonium-chloride-potassium
ADP	Adenosine diphosphate
ALT	Alanine transaminase
ANOVA	Analysis of variance
APC	Adenoma polyposis coli
αSMA	Alpha smooth muscle actin
AST	Aspartate transaminase
ATM	Ataxia-telangiectasia-mutated
ATP	Adenosine triphosphate
ATPB	ATP synthase subunit beta
ATR	Ataxia telangiectasia and Rad3-related
BAK	Bcl-2 homologous antagonist killer
BAX	Bcl-2 associated X protein
BCL	B cell lymphoma encoded protein
BEC	Biliary epithelial cell
BID	BH3 interacting domain death agonist
BMP	Bone morphogenetic proteins
BrDU	Bromodeoxyuridine
CCl_3*	Trichloromethyl
CCl_3OO^-	Trichloromethyl peroxy
CCl_4	Carbon tetrachloride
CD	Cluster of Differentiation
CDK	Cyclin Dependent Kinase
cDNA	Copy DNA
c-FLIP	Cellular FLICE-inhibitory protein
Chk	Checkpoint kinase
CKI	Cyclin dependent kinase (CDK) inhibitor
c-MET	Hepatocyte growth factor receptor
CM	Cristae membrane
C mtDNA	Circular mitochondrial DNA

CO_2	Carbon dioxide
CoA	Coenzyme A
COL1A1	Collagen Type I Alpha 1 Chain
COX	Cytochrome c oxidase
COX-2	Cyclooxygenase II
COX/SDH	Cyctochrome c oxidase/succinate dehydrogenase
CPS-1	Carbomoyl-phosphate synthase-1
CS	Cockayne Syndrome
CTD	C-terminal domain
CTGF	Connective tissue growth fctor
CYP2E1	Cytochrome P450 family 2 subfamily E member 1
CXCL	Chemokine (C-X-C motif) ligand
DAB	3,3’ diaminobenzidine tetrahydrochloride
DAMP	Damage-associated molecular pattern
DHR	Dihydrorhodamine 123
D-loop	Displacement loop
DMEM	Dulbecco’s Modified Eagle Medium
DPBS	Dulbecco’s phosphate buffered sale
dNTPs	Deoxynucleotide triphosphates
ECL	Electrochemiluminescent
ECM	Extracellular matrix
EDTA	Ethylenediaminetetraacetic acid
EGF	Epithelial growth factor
EGFP	Enhanced green fluorescent protein
EGFR	Epithelial growth factor receptor
ELISA	Enzyme-linked immunosorbent assay
ER	Endoplasmic reticulum
ETC	Electron transport chain
EYFP	Enhanced yellow fluorescent protein
FADH	Flavin adenine dinucleotide
FASTK	Serine-threonine kinase
FCS	Fetal calf serum
FMLP	N-formylmethionine-leucyl-phenylalanine
FOXM1B	Forkhead box protein M1 B
FSC-H	Forward scatter height

G	Gap phase
g	Gravity
gp	Glycoprotein
GFP	Green fluorescent protein
GPX	Glutathione peroxidase
GS	Glucose synthetase
GSS	Glutathione Synthetase
GSSG	Glutathione disulphide
H_2O_2	Hydrogen Peroxide
H&E	Haematoxylin and eosin
HB-EGF	Heparin binding EGF-like growth factor
HBSS	Hank's Balanced Salt Solution
HBSS+	Hank's Balanced Salt Solution with Ca^{2+} and Mg^{2+}
HCC	Hepatocellular carcinoma
HEPES	Hydroxyethyl piperazineethanesulfonic acid
HGF	Hepatocyte growth factor
HGFR	Hepatocyte growth factor receptor
HIFα	Hypoxia-inducible factor α
HM	Hepatic myofibroblasts
HPF	High power field
HRP	Horseradish peroxidase
HSC	Hepatic stellate cell
HSP	Heavy strand promoter
ICAM1	Intracellular Adhesion Molecule 1
IFN	Interferon
IHC	Immunohistochemistry
IκB	Inhibitor of kappaB
IKK	Inhibitor of kappaB (IκB) kinase
IL	Interleukin
IMDM	Iscove's modified Dulbecco's medium
IMM	Inner mitochondrial membrane
JAK	Janus kinase
LSEC	Liver sinusoidal endothelial cells
LDH	Lactate dehydrogenase
LP-BER	Long patch base excision repair

LPS	Lipopolysaccharide
LSP	Light strand promoter
M	M (mitotic) phase
MAPK	Mitogen-activated protein kinases
MB	Mitotic bodies
MCP-1	Monocyte chemoattractant protein-1
MDA	Malondialdehyde
MDM2	Mouse double minute 2 homolog
MELAS	Mitochondrial myopathy, encephalopathy, lactic acidosis and stroke
MERRF	Myoclonic epilepsy with ragged red fibres
MMLV	Moloney Murine Leukemia Virus
MMP	Matrix metalloproteinases
Mt-CO1	Mitochondrially encoded cytochrome c oxidase I
mtDNA	Mitochondrial DNA
mRNA	Messenger RNA
mTERF	Mitochondrial transcription termination factor
mtIF	Mitochondrial initiation factor
mtRF	Mitochondrial termination factor
NBT	NitroBlue tetrazolium
NADH	Nicotinamide adenine dinucleotide
NADPH	Nicotinamide adenine dinucleotide phosphate
NAFLD	Non-alcoholic fatty liver disease
ND	NADH dehydrogenase
NDUFB	NADH dehydrogenase [ubiquinone] 1 beta subcomplex subunit
NEMO	NF-kappaB (NF-κB) essential modulator
NER	Nucleotide excision repair
NET	Neutrophil extracellular trap
NF-κB	Nuclear factor kappa light-chain enhancer of activated B cells
NH_2	Amino radical
NO	Nitrous oxide
NOX2	NADPH oxidase 2
NPC	Non-parenchymal cell
NLR	Nod-like receptor
NLRP3	NLR family pyrin domain containing 3
O_2	Oxygen

O_2^*	Superoxide anions
OM	Outer membrane
ORF	Open reading frames
OXPHOS	Oxidative phosphorylation
PAF	Platelet activating factor
PBS	Phosphate buffered saline
PCNA	Proliferating cell nuclear antigen
PCR	Polymerase chain reaction
PCNA	Proliferating Cell Nuclear Antigen
PDGF	Platelet derived growth factor
PGC1α	Peroxisome proliferator-activated receptor gamma coactivator 1 alpha
PHx	Partial hepatectomy
PMS	Phenazine methosulphate
PolgA	Mitochondrial DNA Polymerase gamma
POLRMT	Mitochondrial RNA polymerase
pRb	Product of the retinoblastoma susceptibility gene
PRC	Pombe Repressor Complex
qRT-PCR	Quantitative real-time polymerase chain reaction
RANTES	Regulated on activation, normal T cell expressed and secreted
RIG-1	Retinoic acid inducible gene 1
RIPA	Radioimmunoprecipitation assay buffer
RIPK3	Receptor-interacting serine/threonine-protein kinase 3
RITOLs	Ribonucleotide incorporation throughout the lagging strand
RNF43	Ring finger 43
ROS	Reactive oxygen species
RPMI	Roswell Park Memorial Institute medium
rRNA	Ribosomal RNA
RSPO	Respondin
RT	Room temperature
S100A9	S100 calcium binding protein A9
SASP	Senescent-associated secretory phenotype
SDS	Sodium dodecyl sulphate
SIRT	Sirtuin
SOD	Superoxide dismutase

SOCS3	suppressor of cytokine signalling 3
SDH	Succinate dehydrogenase
SDHB	Succinate dehydrogenase subunit B
SMAD	Small mothers against decapentaplegic
SP-BER	Single-patch base excision repair
SSC-A	Side scatter area
STAT	Signal transducer and activator of transcription 3
TBS	Tris buffered saline
TBST	Tris buffered saline - Tween
TCA	Tricarboxylic acid cycle
TEFM	Mitochondrial elongation factor
TF	Transcription factor
TFAM	Mitochondrial transcription factor A
TFB2	Mitochondrial transcription factor B2
TGF	Transforming growth factor
TIMP	Tissue inhibitor of metalloproteinases
TLR	Toll-like receptor
TNF	Tumour necrosis factor
TOMM20	Translocase of outer mitochondrial membrane 20
tRNA	Transfer RNA
TUNEL	Terminal deoxynucleotidyl transferase dUTP nick end labelling
UCP	Uncoupling protein
UQCRC	Ubiquinol-cytochrome c reductase complex
UV	Ultraviolet
uPA	Urokinase plasminogen activator
WME	William’s media E
WT	Wild type
YAP	Yes-associated protein
ZNRF	Zinc and ring finger

| List of Figures

| List of Tables

Chapter 1 | Introduction

1.1 Overview of Liver physiology

1.1.1 The Liver: Gross Anatomy and Physiology

The human liver is a major organ located in the upper right quadrant of the abdomen, known for its integral physiological role across a variety of biological functions: from nutrient catabolism and protein synthesis to detoxification and energy metabolism. The liver accounts for around 2% of an individual's total body weight, weighing ~1.5 kg. Within this, the liver exhibits lobularity comprising four lobes: the posteriorly located caudate and quadrate lobes, and the anteriorly located left and right lobe (Strasberg, 2005). Of the four lobes, the right lobe exhibits the largest size: defined alongside the left lobe by the umbilical fissure and attachment by the falciform ligament (Strasberg, 2005). This differs from the murine liver in that it spans the entire subdiaphragmatic space and accounts for ~6% of the mouse's total body weight at 2 grams in weight. Also shown to demonstrate quad-lobularity: the left lobe is the largest; however, distinct hemi-section of the right lobe by the transverse septum, dichotomises the lobe into two nearly equal halves (Treuting *et al.*, 2018). In previous studies this can be described instead as two separate cranial and caudal lobes. Finally, the medial lobe sits the most ventrally and comprises two pyriform wings. The medial lobe connects to the remaining liver *via* a narrow central isthmus which protrudes the gallbladder (Treuting *et al.*, 2018).

Amongst its diverse profile of physiological functions, the mammalian liver is known uniquely for its regenerative capacity whereby lost cellular mass and function can be recovered following a variety of injurious insults. This remarkable function makes the liver of particular interest: whereby low cellular turnover and hepatocyte quiescence during homeostatic conditions gives way to a proliferative state to produce new cells: either by (1) mitotic division of existing cells or (2) expansion of the stem/progenitor cell portion, depending on the aetiology of injury (Miyaoka and Miyajima, 2013). Indeed, this integral role becomes particularly apparent in chronic liver injury if dysregulated, in which pathophysiological changes, if left unchecked are likely to result in further injurious changes and clinical advancement of disease.

Hepatocytes account for 80% of liver mass, residing within the liver tissue architecture as part of functional units known as hepatic lobules (figure 1-1). Within these, hepatocytes line basolaterally alongside liver sinusoidal endothelial cells (LSECs), resident Kupffer macrophages and hepatic stellate cells (HSCs), a capillary channel known as a sinusoid, in which blood supply from the portal vein and hepatic artery percolate for vascular egress from the liver *via* the central vein (Stanger, 2015). In parallel, the apical membranes of adjacent hepatocytes form tight junctions to create a canaliculus for hepatocyte-secreted bile acids, which together with bilirubin and cholesterol combine to form bile. Bile is then transported along the canaliculae *via* the bile ducts for subsequent release into the duodenum during digestive fat emulsification (Stanger, 2015). The other primary functional cells, the parenchymal biliary epithelial cells (BECs), act as ductular conduits for passage between hepatocytes and the small intestine (Stanger, 2015). Taken together, this lobular structure incorporating proper placement of parenchymal and non-parenchymal cells (NPCs) alike allows the liver to move blood counter-currently in a portal-to-centrilobular direction to the centrilobular-to-portal flow of bile – thus allowing the liver to conduct simultaneously its diverse metabolic, secretory, synthetic and detoxifying roles.

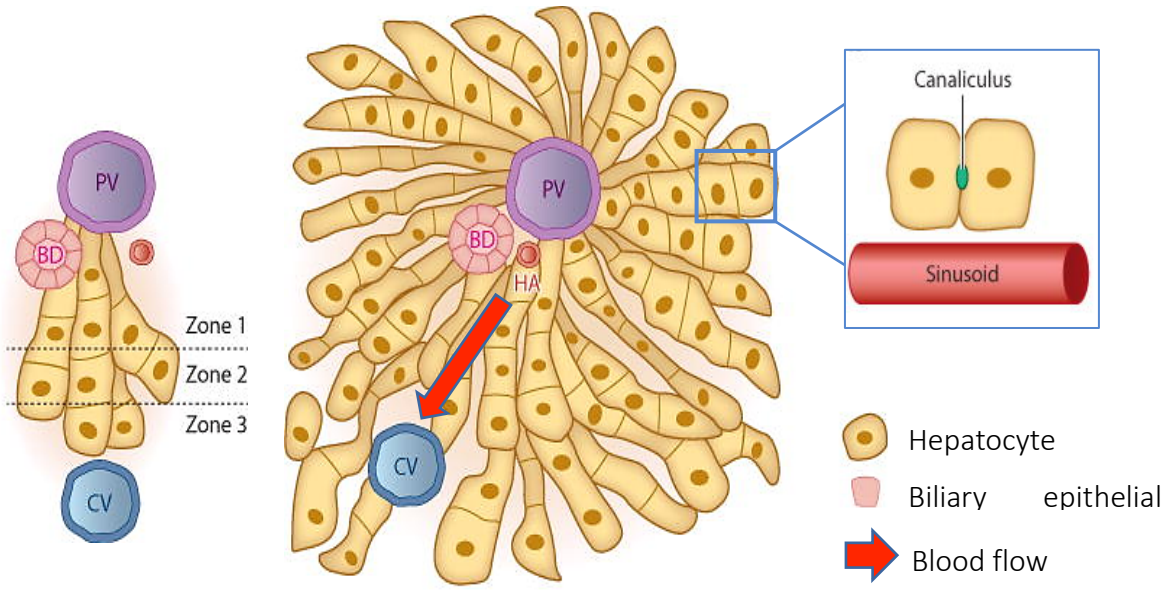

Figure 1-1: Schematic showing the liver lobule. *Hepatocytes and biliary epithelial cells are organised into liver functional units known as hepatic lobules. Hepatocytes line the sinusoids, forming tight junction canaliculus for the secretion of bile acids. A counter-current flow of blood and bile occurs in the liver in which blood flows in the direction from the portal vein (PV) towards the central vein (CV), whilst bile acids flow from a CV to PV direction. Along the sinusoid, there is a hepatocyte differentiation gradient comprised of three zones; each zone differentiated to meet specific liver functions. Adapted from Stanger et al., (2015). Bile duct (BD); hepatic artery (HA).*

1.1.1.1 Hepatocytes

As highlighted previously, hepatocytes form the majority population of cells within the liver. As a result, hepatocytes appear to execute the greatest body and range of work, from synthetic activities involving bile acid synthesis to cholesterol metabolism; equipped densely with mitochondria and endoplasmic reticulum to carry out such energetic processes. Other activities include serum protein and glutamine synthesis, as well as mediating energy metabolism for example through gluconeogenesis (Stanger et al., 2015). Finally, hepatocytes play an integral role in arbitrating the detoxification of digested products, in which absorbed molecules are fed into liver from the intestinal tract *via* portal circulation. This so-called 'first pass metabolism' allows the screening of potentially toxic compounds by the liver and removes them when encountered. Here, detoxification is mediated through the arsenal of hepatocyte P450 detoxifying enzymes allowing for elimination into the bile or urine (Park, 1982). Of which, urea formation is also part of the hepatocyte portfolio of functions.

1.1.1.2 Biliary Epithelial Cells/Cholangiocytes

BECs, also known as cholangiocytes, are cuboidal cells that form the other cell majority of the liver parenchyma and are known to line the hepatic biliary tracts. Understood to be less metabolically active than liver hepatocytes, findings show BECs to possess an element of plasticity: *in vitro* immature BECs demonstrate the potential to differentiate into hepatocytes, an ability which is lost following maturation of the hepatic bile ducts (Tanimizu *et al.*, 2013). As such, BECs have been proposed to be involved in the maintenance of liver homeostasis (see section 1.2.1). Collectively, BECs are long time established as conduits for hepatocyte-synthesised bile within the liver tissue, passing along from the intrahepatic bile ducts to the larger extrahepatic biliary tract for removal into the intestinal duodenum (Stanger, 2015). BECs that line these biliary tracts are specialised for collection, storage and concentration of bile, allowing intermittent delivery of bile, as required for fat emulsification. Consequently, given the concentrated toxic nature of bile acids, blockage of the bile ducts either by infection or disease, appears to manifest into liver pathogenesis: for example, autoimmune destruction of the intrahepatic bile ducts results in the retention of bile ducts and primes onset for primary biliary cholangitis.

1.1.1.3 Non-Parenchymal Cells and Hepatic Stellate Cells

NPCs encompass cell types not derived from hepatocytes and BECs and are predominantly involved in a variety of other liver functions; they may be endothelial cells or immune cells such as liver resident Kupffer macrophages, derived from non-endodermal origins (Stanger, 2015). Of particular note, NPCs of additional importance are fibroblasts, extracellular matrix (ECM) scar-forming cells involved in maintenance of normal hepatic tissue architecture through production of collagenous scaffolding proteins (Oakley and Mann, 2015). Here, hepatic fibroblasts can be divided in to two populations: HSCs and portal fibroblasts, of which the former is thought to be a major contributor to liver pathogenesis through chronic wound healing processes. Previous studies, including fate lineage-tracing, have shown that HSCs are a dominant contributor to fibrogenic pathogenesis, independent of the type of liver injury (Mederacke *et al.*, 2013). Central to this is stimulation of HSCs from a quiescent, vitamin A and retinoid storing phenotype to an activated alpha smooth muscle active (α-SMA) positive myofibroblast, that can result in the excess and chronic deposition of ECM scar forming tissue if the insult persists (Pinzani and Rombouts, 2004; Chakraborty *et al.*, 2012). This also coincides with the synthesis of fibrillar collagens, inhibitors of metalloproteinases and the induction of a proinflammatory response; the removal of α-SMA positive HSCs, demonstrates regression of the fibrogenic response and the induction of HSC apoptosis (Iredale *et al.*, 1998).

1.1.2 Liver Zonation and Ploidy

Despite morphological similarities, hepatocyte functions differentiate depending on the liver lobule location. Hepatocytes of the liver can be conceptually divided into three main areas: (1) zone 1 comprising periportal hepatocytes, (2) zone 2 comprising centrilobular hepatocytes, and (3) zone 3 hepatocytes located pericentrally, with hepatocytes for each zone adapted to specific liver functions (figure 1-1). Accordingly, zones are largely distinguished according to their metabolic function - under which liver patterning is seminally understood to be regulated by Wnt/β-catenin signalling (Sekine *et al.*, 2006; Gebhardt and Hovhannisyan, 2010). In the seminal paper by Benhamouche and colleagues (2006), differential expression of β-catenin is observed in pericentral hepatocytes whilst its negative regulator APC (adenoma polyposis coli) is expressed periportally, subsequently giving way to

metabolic zonation along the liver's portocentral axis (Benhamouche *et al.*, 2006). The subsequent ablation of β-catenin within this study induces a periportal phenotype within pericentral hepatocytes (Benhamouche *et al.*, 2006). Meanwhile, Wnt signalling ligands have been also been shown to act in concert to control metabolic zonation, proliferation and tissue homeostasis. In recent studies, Respondin 1 and 3 (RSPO1, RSPO3) ligands, for example, are shown not only to act in concert with cognate receptors LGR4/5 to regulate metabolic zonation but also control zone-specific parenchymal regeneration and the liver size in early stages of post-PHx when in combination with ZNRF3 (zinc and ring finger 3) / RNF43 (ring finger 43) (de Lau *et al.*, 2014; Planas-Paz *et al.*, 2016). These studies appear to highlight the complex interplay between metabolic zonation and liver growth control required to maintain liver homeostasis during hepatocellular turnover and active regeneration; abrogation of the various components of the Wnt signalling pathway resulting in the impaired hepatocyte differentiation and zonation, as well reduced hepatocyte proliferation (Planas-Paz *et al.*, 2016).

Other dynamic factors associated with zonal patterning may also include nutrients, growth factors (e.g. hepatocyte growth factor; HGF), and importantly blood oxygenation (Kietzmann, 2017). In zone 1 where periportal blood demonstrates higher oxygenation, mitochondrial numbers and hepatocyte intracellular pO_2 versus pericentral cells, the oxidative capacities of periportal hepatocytes predominantly facilitate oxidative liver functions such as gluconeogenesis and fatty acid β-oxidation, whereas zone 3 pericentral hepatocytes are largely involved in processes such glycolysis and cytochrome P450-based drug detoxification (Loud, 1968; Schmucker *et al.*, 1978; Jungermann and Kietzmann, 2000; Stanger, 2015). Evidence for zonal modulation by oxygen can be directed from earlier *in vivo* evidence showing anaemic transgenic mouse livers to induce erythropoietin (EPO) expression under sufficiently hypoxic conditions and appeared to be only detectable in pericentral hepatocytes (Koury *et al.*, 1991). Meanwhile, factors responsive to oxygen availability, like hypoxia-inducible factor α (HIFα), have been also shown to be transcriptionally upregulated in pericentral zones (Kietzmann *et al.*, 2001). Coincidentally, the literature collectively appears to suggest a complex link between oxygenation and Wnt/β-catenin-mediated control of metabolic zonation signalling, however not directly correlated. The liver-specific ablation of β-catenin, for example, results in reduced

HIFα signalling, likely ascribed to β-catenin in HIF1α transcriptional promoter binding to induce cell survival and adaptation to hypoxia (Kaidi *et al.*, 2007; Lehwald *et al.*, 2011). Under low conditions of oxygen, as in pericentral hepatocytes, APC is shown to be repressed leading to β-catenin-mediated induction of HIF signalling and cellular adaptation within zone 1, whilst periportal zones is reciprocally shown to repress β-catenin signalling *via* APC expression (Benhamouche *et al.*, 2006; Burke *et al.*, 2009). Clear phenotypes are yet to be seen however, when disruption of this zonal organisation is induced.

1.2 Overview of Liver Regeneration

The remarkable capability of the liver to recover lost cellular mass and function in response to injury makes the organ of particular interest. However, in contrast to other regenerative post-mitotic tissues such as the skin or colon, the liver demonstrates a quiescent (G_0) state of low hepatocellular turnover with only 1-2% hepatocytes entering cell cycle at any given time (Michalopoulos and DeFrances, 1997). Historically, the mechanisms of liver regeneration have been most classically understood through injurious models. The most notable and widely understood is partial hepatectomy (PHx), first described by Higgins (1931), in which regeneration follows removal of two-thirds (70%) of the liver, involving the median and left lateral lobes (see 1.2.1.1) (Higgins, 1931). Subsequent re-establishment of the liver's homeostatic environment and loss of cellular mass post-PHx, is thought to predominantly occur *via* pre-existing hepatocyte hypertrophy and cellular hyperplasia; however, regeneration can also occur through expansion and differentiation of hepatic stem and progenitor cell as outlined in the below sections (Miyaoka *et al.*, 2012; Miyaoka and Miyajima, 2013).

1.2.1 Theories of Liver Homeostasis

To date, many kinetic studies observing hepatophysiological homeostasis collectively propose normal hepatocyte turnover to occur in a so-called 'streaming liver' hypothesis-like manner. During which Zajicek and colleagues (1985) seminally describe the slow migration or "streaming" of hepatocytes along the portocentral axis, in the direction of the central vein through pulse-chase analysis of thymidine-injected rats. Furthermore, in populations of proliferating hepatocytes determined to be

clonally derived from the same cytochrome c oxidase-deficient source, units were shown to originate from close to the portal limiting plate and migrate in a direction towards the hepatic vein (Fellous *et al.*, 2009).

Additional evidence appears to support a periportal origin for hepatocytes: long-term cell DNA labelling retention studies have allowed investigation into hepatocyte 'stemness' and clonogenic potential, specifically showing that labelling retention appears to occur in greater density within niches located close to portal tract (Kuwahara *et al.*, 2008). Whilst in murine fate lineage tracing studies, X-gal staining of hepatocytes demonstrates their genetic lineage from SOX9-positive precursors that originate from the liver's biliary duct and migrate towards the hepatic central vein to replace the liver parenchyma every 8-12 months, following tamoxifen intoxication (Furuyama *et al.*, 2011). These observations would therefore appear to suggest that establishment of liver homeostasis through hepatocellular turnover is critically derived and maintained from the biliary tree compartment. However, these suggestions appear controversial due to the variation in data associated with biliary duct studies. For example, SOX9-postive ductal cells have been shown to have limited contribution towards the hepatocyte cell compartment following murine hepatic progenitor (oval) cell injury, whilst lineage tracing of Sox9-positive ductal progeny demonstrates generation of the intrahepatic biliary cells including a few periportal hepatocytes in the absence of extensive parenchymal replacement (Carpentier *et al.*, 2011; Tarlow *et al.*, 2014). Moreover, in models of PHx and carbon tetrachloride (CCl_4) intoxication, limited expression of hepatocyte specific fluorescent proteins (enhanced yellow fluorescent protein; EYFP) appears to conclusively reject the contribution of ductal liver progenitor cells in normal liver homeostasis (Malato *et al.*, 2011).

Taken together, the literature appears to refute the notion that liver homeostasis is maintained by hepatocyte streaming, instead proposing that liver homeostasis and cellular turnover occurs by division of pre-existing hepatocytes with minor input from progenitor cells within the bile ducts. Recent findings appear to propose that hepatocytes could derive from a progeny stem cell niche of hepatic vein endothelial cells, in which lineage tracing of Axin2-heptocytes alternatively shows migration of hepatocytes in a direction towards the portal vein from the central vein (Wang *et al.*,

2015). Axin2 is shown to promote phosphorylation and proteosomal degradation of β-catenin through negative regulation of Wnt, and in mice, forms a pericentral monolayer of Axin2-positive diploid hepatocytes (Jho *et al.*, 2002; Wang *et al.*, 2015). The subsequent observations made during lineage tracing appears to show hepatocytes to differentiate from progenitor cells with migration: becoming negative for progenitor marker Tbx3, as well as markers of pericentral and centrilobular/pericentral hepatocytes Wnt-mediated glucose synthetase (GS) and carbamoyl-phosphate synthase 1 (CPS-1) as they move towards the portal vein with time (Wang *et al.*, 2015). This suggestion of centro-portal migration, however, failed to be recapitulated elsewhere in which Planas-Paz and colleagues (2016) failed to observe Lgr5-positive pericentral hepatocytes able to basally repopulate the liver, including after PHx, through observation of the RSPO-LGR4/5-ZNRF3/RNF43 module involved in Wnt-potentiated metabolic liver zonation and regeneration. As such, the mechanism and population by which liver homeostasis is maintained, remains unclear.

1.2.2 Liver Regeneration Models

Animal models, and the ability to genetically manipulate them, exploit a variety of investigative tools that aid the understanding of the complex mechanisms that underpin liver regeneration. Much of our current understanding derives from commonly used acute and chronic liver damage models such as PHx and toxic drug injury; however, such models are only partially representative of the large range of pathophysiology observed within the human liver. For specific example, PHx is rarely undertaken in humans without the presence of cancers. Outlined below are classic examples of regenerative models commonly used in mice.

1.2.2.1 Partial Hepatectomy (PHx)

As previously highlighted, the most classical mode of hepatic injury to study regeneration, PHx, involves the two-thirds surgical removal of the liver in which the remnant caudate and right lateral lobes undergo tissue proliferation to recover lost cellular mass (Higgins, 1931). Recovery of the original liver mass transpires within 5-7 days with peak proliferation occurring between 24 and 48 hours in rat and mice respectively, during which levels of compensatory hepatocyte hypertrophy and

hyperplasia are highest and precedes a wave of cellular proliferation from non-parenchymal cells (Michalopoulos, 2007; Miyaoka *et al.*, 2012; Miyaoka and Miyajima, 2013; Mao *et al.*, 2014).

1.2.2.2 Carbon Tetrachloride Toxic Injury Model

As well as PHx, the liver is able to regenerate in response to chemical-induced injury, the nature of which appears to hold more clinical relevance to certain liver diseases due to the induction of necrotic injury (Abu Rmilah *et al.*, 2019). Specifically, carbon tetrachloride (CCl_4) is a classical hepatoxic model, iteratively used to induce pathways of inflammatory and profibrotic injury. When acutely administered, CCl_4 results in the transient induction of an acute inflammatory phase with some extracellular matrix (ECM), followed by DNA synthesis and tissue recovery during parenchymal regeneration, which peaks at 24-48 hours post-toxic injury (Hatta, 1985; Doolittle *et al.*, 1987). Conversely, repeated exposure from CCl_4 induces chronic activation of the proinflammatory and profibrotic signalling pathways, resulting in the persistent activation of HSCs and their ECM scar forming phenotype. Chronic exposure subsequently results in the progressive development of liver scarring and cirrhosis, with loss of normal hepatocellular regeneration and function ascribed to significant losses of the liver parenchyma to collagenous ECM deposition unable to be degraded.

Mechanistically, CCl_4 exerts its hepatotoxic effect following its metabolism *via* the liver's detoxification enzymes. Cytochrome P450 (CYP)2E1 metabolises CCl_4 into highly reactive and toxic radicals trichloromethyl (CCl_3^*), and in the presence of oxygen, trichloromethyl peroxy (CCl_3OO^-) (Manibusan *et al.*, 2007). Subsequently, these metabolite products are able to induce free radical propagation reactions with surrounding cellular structures, forming adducts with hepatocyte DNA, protein and carbohydrate macromolecules, as well as promoting lipid peroxidation to form propagating cytotoxic reactive aldehydes, 4-hydroxynonenal (4-HNE) and malondialdehyde (MDA), ultimately inducing hepatocellular damage (Hartley *et al.*, 1999; Abu Rmilah *et al.*, 2019). Following intoxication, CCl_4-induced toxic injury appears to induce pathogenic changes within 12-48 hours, peaking at 36 hours as marked by the significant serological release of liver enzyme and hepatocellular damage marker alanine transaminase (ALT) (Hartley *et al.*, 1999). Key features

include the induction of hepatocyte ballooning and cell death, centrilobular fat deposition or ‘steatosis’ and tissue necrosis within 12-48 hours post-intoxication. Moreover, intoxication leads to the activation of Kupffer macrophages that negatively impacts the damaged tissue environment through additional release of damaging reactive oxygen species (ROS) and cytokines (Sipes *et al.*, 1991; Edwards *et al.*, 1993; Seki *et al.*, 2000). This damage appears to be concentrated pericentrally (zone 3), in which centrilobular necrosis occurs in areas where CYP2E1 is highly expressed. Conversely, this type of injury is reversible if the CCl_4 toxic insult is acute: liver regeneration ensues following cessation of injury and insult, in which an acute inflammatory response comprising recruited macrophages and polymorphonuclear leukocytes, such as neutrophils, mediate the removal of necrotic hepatocyte debris.

1.2.3 Cellular Response to Liver Injury

The process of liver regeneration is complex, involving a plethora of growth factors and cytokines that act in concert to regulate liver growth and size in the recovery period following injury. Involvement of regulating factors first came to light in studies by Moolten and Bucher (1967), in which cross carotid-to jugular circulatory parabiosis from hepatectomised to normal rats revealed the induction of hepatocyte mitosis in the absence of injury in the later, whereas this was absent in normal-to-normal parabiosis. Taken together, the study reveals the importance of serologically-present factors in driving liver regeneration in response to injury. To date, there are three distinct and critical steps of hepatic regeneration: (1) the priming phase, (2) proliferation phase and (3) termination phase (figure 1-2; sections 1.2.3.1 – 1.2.3.3).

1.2.3.1 Cell Cycle

In the human adult liver, approximately 0.05% of hepatocytes are in cell cycle at any given time (Furchtgott *et al.*, 2009). Cell cycle is fundamental to growth; defined as a ubiquitous cellular process involving a chronological series of events that include DNA replication (S-phase) and the division of an individual’s genome (M-phase), in which the cell partitions into two daughter cells (figure 1-3) (Salazar-Roa and Malumbres, 2017). The process of cell cycle is complex and is regulated at many differing levels. Most notably, cyclin dependent kinases (CDKs; table 1-1) are understood to be critical drivers of cell cycle progression, first identified in mutagenic

yeast by Hartwell and colleagues (1970). CDKs, in turn, are regulated by CDK inhibitors (CKIs), whilst CDK activating proteins, cyclins, are able to be mediated through ubiquitin ligase-dependent degradation to arrest cell cycle (Salazar-Roa and Malumbres, 2017). Regulation in this manner gives rise to breaks in the cell cycle, also known as 'gap phases', each occurring before and after key DNA synthesising and mitotic stages in the cell cycle as key control system checkpoints, namely G1 and G2 (before and after S phase-before cellular mitosis respectively) and the resting G0 phase (Vermeulen *et al.*, 2003). Regulation at each of these phase checkpoints is key, preventing progression of defective cells through cell cycle and the possibility of their expansion.

Checkpoint prevention of defective cell replication appears to be dependent on cell size and most notably the presence of DNA damage within these cells. DNA damage, for example, prevents S-phase DNA synthesis during G1 by means of Chk1 and Chk2 phosphorylation by protein kinase ATR (ataxia telangiectasia and Rad3-related) to maintain inactivity of Cdc25A and kinase CDK2 (Barnum and O'Connell, 2014). Meanwhile at stages prior to M phase, cell cycle can be stalled at G2 by means also involving the Chk1/Chk2 and ATR/ATM kinases; however, involving the sequestration of cdc25 phosphatases that activate CDK1 within the CDK1/cyclin B complex (Lukas and Bartek, 2004; Lukas *et al.*, 2004).

As previously highlighted, CDKs are understood to be critical drivers of the cell cycle; however, require the additional partnering with cyclin proteins that regulate CDK substrate specificity and kinase activity to encourage progression. Cyclins are therefore likened to gears that regulate the driving activity of CDKs, assisting cyclin kinases in the transition between each cell cycle phase (Lim and Kaldis, 2013). The formation of CDK/cyclin complexes is therefore key; early yeast studies show the role for these complexes, whereby yeast CDK1 demonstrates the promotion of cycle phase transition *via* interactions with a number of cyclins (Nurse *et al.*, 1976; Nurse and Thuriaux, 1980; Beach *et al.*, 1982; Reed *et al.*, 1982; Evans *et al.*, 1983). When conditions are unfavourable, however, including during the presence of DNA damage, these complexes halted in turn – namely *via* negative regulation by CKIs. CKIs are of two types: belonging to the INK4 or Cip/Kip family of inhibitory proteins - their negative action employed within the cell cycle to regulate formed CDK/cyclin

complexes (Lim and Kaldis, 2013). Of the former, INK4 proteins ($p16^{INK4a}$, $p15^{INK4b}$, $p18^{INK4c}$and $p19^{INK4d}$) all comprise ankyrin repeat domains, showing preferential binding to CDK4 and CDK6 through monomeric interactions (Jeffrey *et al.*, 2000). These interactions are understood to distort the CDK/cyclin interface at the CDK adenosine triphosphate (ATP)-binding pocket, preventing cell cycle progression by prohibiting interaction between CDK4 and CDK6 with their corresponding D-type cyclins (Jeffrey *et al.*, 2000). By contrast, Cip/Kip family members ($p21^{Cip1}$, $p27^{Kip1}$ and $p57^{Kip2}$) comprise N-terminal CDK inhibitory domains and demonstrate inhibitory activity preferential to CDK2/cyclin E and CDK2/cyclin A complexes. Cip/Kip activity is mediated through heterodimeric binding to both CDK and cyclin subunits in a simultaneous manner – adding an additional level of regulation to CDK/cyclin complex formation (Russo *et al.*, 1996; Pavletich, 1999). Binding of INK4 and Cip/Kip proteins, however, is not solely exclusive: Cip/Kip proteins have been previously demonstrated to bind CDK/cyclin D complexes, whilst p16-CDK4/6 interactions induces redistribution of p21 and p27 to induce CDK2 inactivation within the CDK2/cyclin E complex (McConnell *et al.*, 1999; Mitra *et al.*, 1999; Vermeulen *et al.*, 2003) Nonetheless, the subsequent elevation of CKIs, by various inducible means, is widely observed to promote cell cycle arrest (Stein *et al.*, 1999; Alani *et al.*, 2001)

Unsurprisingly CKIs are also regulated, the most basic mechanism by which is at a transcriptional level. CKI $p21^{Cip1}$ for example, is widely understood to be under the transcriptional control of p53, following the transcription factor's binding to p21 promoter response elements (Thornborrow and Manfredi, 1999). Less well known, however, is the transcriptional regulation of INK4 proteins, although regulation for the most prominent family member $p16^{INK4A}$ is thought involve a complex plethora of molecular regulators. The best studied is mediation through transcription factors ETS1 and ETS2, downstream of ERK MAPK pathway stimulation; however, $p16^{INK4}$ is also shown to receive involve tight regulation from variety other factors including Pombe Repressor Complex (PRC) 1, PRC2, Bmi1 and transcriptional repressor ID1 (Ohtani *et al.*, 2001; Rayess *et al.*, 2012). Elsewhere, it has been shown that mutations of activating molecules within the transcriptional pathway leads to an increase in INK4A expression, leading to the repression of the cell cycle (Bruce *et al.*, 2000).

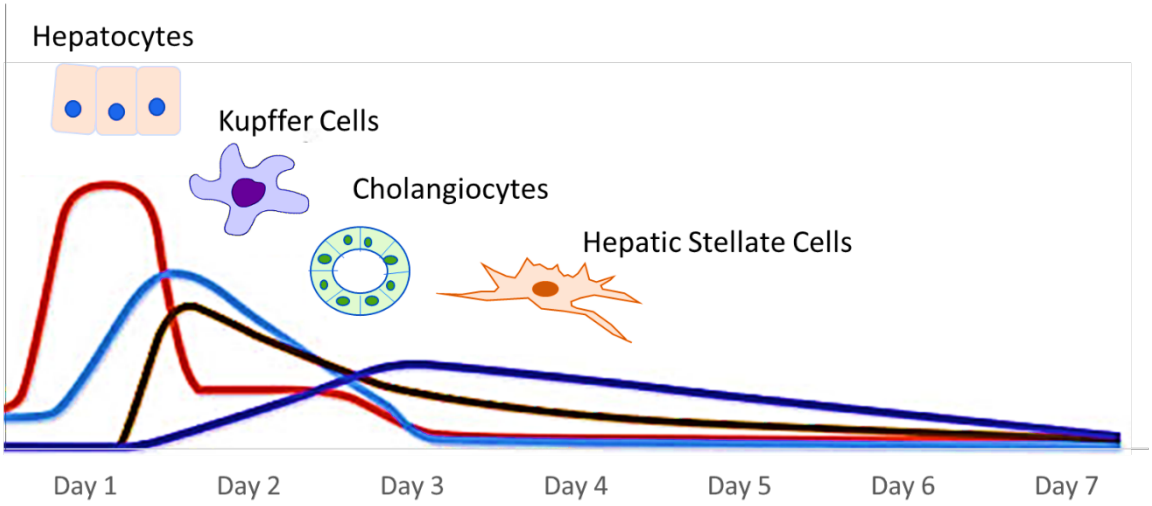

Priming	Proliferation	Termination
TNFα	HGF	TGFβ
IL-6	EGF	
	HB-EGF	

***Figure 1-2 (above): Timeline of liver regeneration**. Schematic showing timing kinetics of different liver cell types across the liver's priming, proliferation and termination phases of liver regeneration. Hepatocyte DNA synthesis (red) peaks 24 hours, followed by DNA synthesis of cholangiocytes (black) and Kupffer cells (blue), as well as hepatic stellate cells (dark blue). Each phase characterised by gene expression profiles of cytokines and growth factors associated with liver parenchymal regeneration (table): tumour necrosis factor α (TNFα), interleukin-6 (IL-6), hepatocyte growth factor (HGF), epithelial growth factor (EGF); heparin-binding epithelial like growth factor (HB-EGF); tumour*

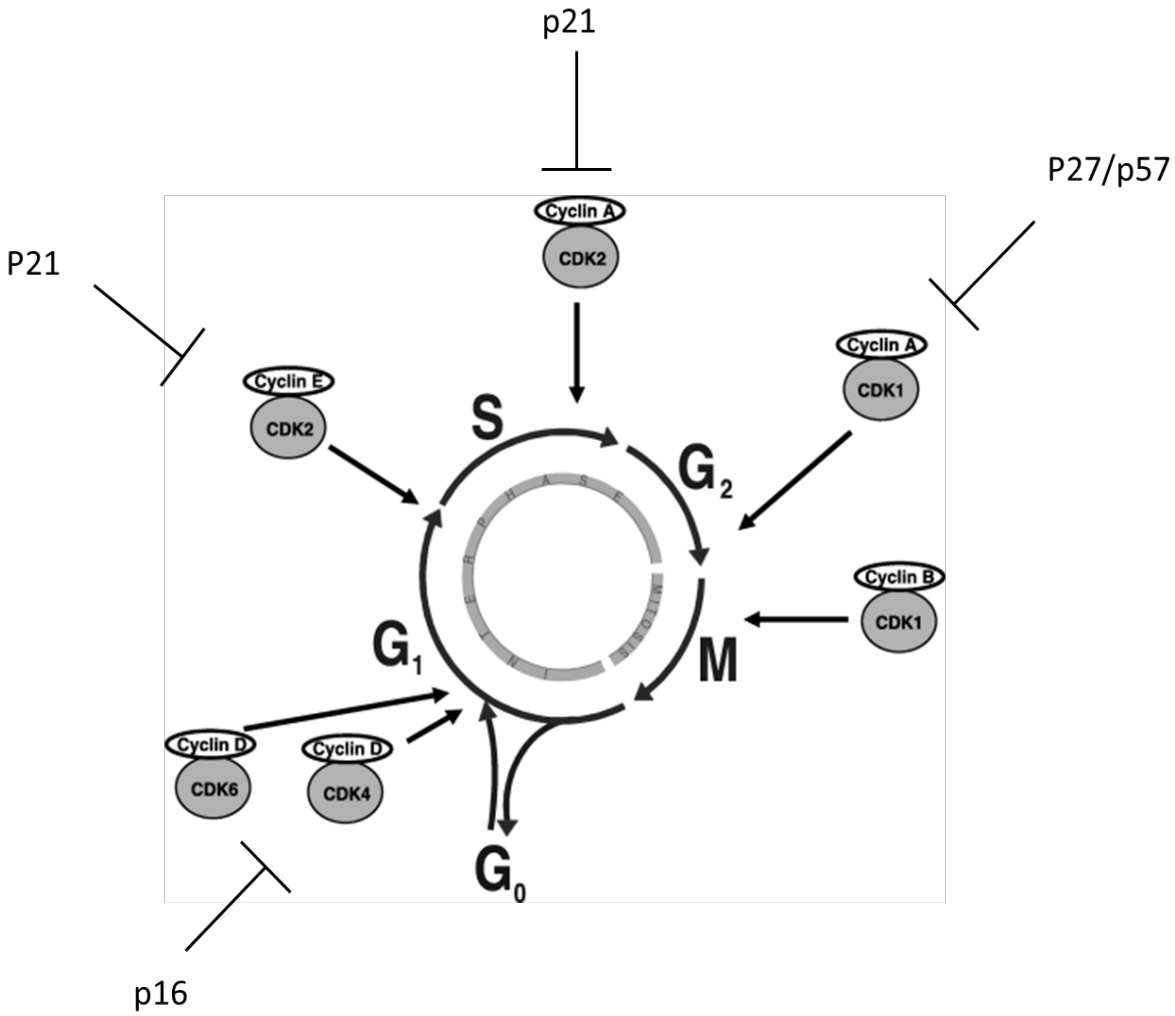

Figure 1-3: Stages of cell cycle as regulated by CDK/Cyclin complexes. *CDKs are regulated in turn by cyclin kinase inhibitors (CKIs) which in the presence of aberrant cellular changes such as DNA damage, induces cell cycle inhibition by repressing kinase activity. (Adapted from Vermulen et al., 2003).*

CKI Family	Family Member		Cell Cycle	Inhibits
INK4 Family	p15	INK4b	G1	CDK4/6
	p16	INK4a		CDK4/6
	p18	INK4c		CDK4/6
	p19	INK4d		CDK4/6
Cip/Kip Family	p21	Waf1, Cip1	G1/S	CDK2
	p27	Cip2	G2	CDK1
	p57	Kip2	G2/M	CDK1

Table 1-1: Cell cycle inhibitors belonging to cyclin kinase inhibitor (CKI) families INK4 and Cip/Kip. *CKI target specific cyclin dependent kinases (CDKs) and arrests cell cycle at different stages.*

1.2.3.2 Priming Phase

The priming phase of liver regeneration following injury begins with the activation of inflammatory cells, in which quiescent (G_0) hepatocytes are stimulated to rapidly re-enter the cell cycle for parenchymal restoration. The process is centrally coordinated by cytokines, including tumour necrosis factor-α (TNFα) and interleukin-6 (IL-6) secreted by tissue resident Kupffer macrophages activated in a MyD88-NF-κB dependent manner in response to resultant tissue debris (Iwai *et al.*, 2001; Schwabe *et al.*, 2006). Specifically, increased TNFα secretion is observed following PHx, demonstrating a critical role for the initiation of hepatocyte proliferation, as well as subsequent IL-6 expression following transient secretion in the murine liver 24-48 hours post-surgery (Satoh *et al.*, 1991; Yamada *et al.*, 1997). Studies by Yamada and colleagues (1997) further demonstrate effects to mediated *via* TNF-corresponding receptor type I (TNFR-1), with regenerative impairment observed during ablation of TNFR-I but not ablation of type II receptor (TNFR-II) (Yamada *et al.*, 1997; Yamada *et al.*, 1998).

Subsequent secretion of IL-6 assists and primes the proliferative response through binding to its cognate receptor IL-6R – glycoprotein (gp) 130 complex, eliciting an immediate-early gene expression response through several downstream effector pathways, including Janus kinase (JAK)/STAT (Signal Transducer and Activator of Transcription 3) and P13k/Akt signalling. Amongst mitogenic factors expressed is transcription factor AP-1 *c-fos* and *c-jun,* known to functionally regulate cell cycle *via* its potentiation of cyclins including cyclin D1, as well as negative regulator SOCS3 (suppressor of cytokine signalling) to prevent further hepatocyte cell cycle entry (Bakiri *et al.*, 2000; Su *et al.*, 2002). Whilst gp130 is readily present in most cells, IL-6R is limited in its expression to hepatocytes. As such, the pleotropic cytoprotective and mitogenic effects of IL-6 appears to be limited to these cells (Schmidt-Arras and Rose-John, 2016). In line with this, data previously shows that singly administered IL-6 appears to rescue hepatocyte proliferation in hepatectomised IL-6 knockout mice; however, when solely administered to laparotomy controls, parenchymal regeneration does not ensue (Blindenbacher *et al.*, 2003). Taken together, the literature suggests that IL-6 alone does not exert a mitogenic effect. Accordingly, gp130 is able to induce hepatoregenerative signalling independent of IL-6R through YAP and Notch mediatory proteins: YAP-mediated expression of Jag-1 can activate

Notch in mouse hepatocytes and HCC, yet the mechanisms are yet to be fully characterised within the context of classic liver regeneration and repair.

Taken together, TNFα and IL-6 appears to control hepatocyte progression from G_0 into G_1 phase, mediated through stimulation of an immediate-early transcriptional programme of gene expression. The subsequent loss or inhibition of TNFα and IL-6 is therefore unsurprisingly shown to delay post-PHx regeneration, ascribed to cell cycle arrest *via* reduced receptor signal transduction.

1.2.3.3 Proliferation Phase

The proliferation phase of hepatic regeneration denotes the transition of G_1 hepatocytes into mitotic cell division. In rodents, the majority of mitotic division and ensuing parenchymal hyperplasia post-PHx already occurs by ~3 days and completes recovery of liver mass within 5-7 days. Driving this, progression of hepatocellular proliferation through G_1 to mitosis is mediated by mitogenic factors, most importantly by growth factors. One of the first circulatory factors identified is HGF, shown previously to induce proliferative gene expression during delayed cell cycle in serum-free primary cultured hepatocytes, as well as cause liver hyperplasia *in vivo* (José Gómez-Lechón *et al.*, 1995). HGF is therefore critical to liver regeneration, with conditional genetic ablation shown to compromise PHx liver regeneration (Nejak-Bowen *et al.*, 2013). Accordingly, within 2 hours of injury plasma, HGF has been shown to significantly rise (between 13- and 17-fold) post-CCl_4 and PHx injury respectively, mediated through its active conversion to pro-HGF by urokinase plasminogen activator (uPA) that binds and initiates activation of its cognate tyrosine kinase receptor HGFR or Met (Lindroos *et al.*, 1991; Mars *et al.*, 1993). HGF stores are located within the ECM, in which uPA is a critical mediator and which prompts transformation of plasminogen and pro-matrix metalloproteinases (pro-MMPs) into plasmin and active MMPs within 24-48 hours - enzymes actively involved in ECM remodelling during liver regeneration (Kim *et al.*, 1997). When depleted HGF stores are actively synthesised elsewhere, predominantly thought to involve contribution from activated non-parenchymal endothelial and HSCs in response to hepatocyte stimulation (Kinoshita *et al.*, 1991; Skrtic *et al.*, 1999).
The subsequent delay of cellular mitosis as a result of diminished HGF signalling highlights the growth factor's role in liver regeneration. Specifically, knockout or RNA

silencing (shRNA) of the Met gene, *c-met,* delays mature hepatocellular recovery through cell cycle arrest, as well as increases hepatocyte sensitivity to Fas-mediated apoptosis and persistent activation of proinflammatory reactions (Borowiak *et al.*, 2004; Huh *et al.*, 2004; Paranjpe *et al.*, 2007). Experimental analysis understands HGF to mediate these effects by cascade mitogen-activated protein kinase (MAPK)/Erk and phosphatidylinositol 3-kinase (PI3K)/Akt signalling downstream of cognate HGF receptor binding (Xiao *et al.*, 2001; Borowiak *et al.*, 2004; Suzuki *et al.*, 2009). Of the former, persistent Erk1/2 activation by HGF/Met binding is molecularly described within G_2/M phase transition in activating downstream expression of checkpoint/cell cycle arrest genes including kinases CDK1, Plk1 and Aurora A and B - genes known to act in concert to aid execution of M phase gene transcription *via* transcription factor FoxM1 activation (Fu *et al.*, 2008; Laoukili *et al.*, 2008; Factor *et al.*, 2010; Suryadinata *et al.*, 2010). Other transcription factors, such as STAT3 and C/EBPβ, are also noted as functionally involved in the mitogenic signalling activity of HGF-mediated hepatocellular proliferation (Schaper *et al.*, 1997; Wang *et al.*, 2005).

Corresponding ligands of the epithelial growth factor receptor (EGFR) comprise other mitogens besides HGF, including epithelial growth factor (EGF), heparin binding EGF-like growth factor (HB-EGF), amphiregulin and transforming growth factor-α (TGFα). Mobilised initially from sequestered ECM stores within the portal triad, EGF is thought critical in the stimulation of hepatocyte DNA synthesis ‘S phase’ transition at 24 hours, shown to significantly rise prior to this within 1-8 hours post-surgery (Noguchi *et al.*, 1991). In line with this EGFR activation demonstrates mitogenic hepatoproliferative activity and liver hyperplasia following EGF stimulation, with subsequent depletion by submandibular gland removal shown to slow ensuing DNA synthesis (Bucher *et al.*, 1977; McGowan *et al.*, 1981; Noguchi *et al.*, 1991). When treated post-PHx with exogenous EGF, this regenerative phenotype is able to be rescued (Noguchi *et al.*, 1991).

By comparison, HB-EGF, amphiregulin and TGFα are synthesised as precursor mitogens and are converted to their mature secretory forms following processing by extracellular proteases. Like EGF, HB-EGF, amphiregulin and TGFα are promptly synthesised following liver injury (within 1-6 hours) and exert their effects *via* EGFR signalling (Ito *et al.*, 1994; Tomiya *et al.*, 1998; Kiso *et al.*, 2003). Utilisation of

experimental murine models outline the importance of each of these mitogens: specifically, ablation of amphiregulin and HB-EGF are demonstrated to impact negatively on liver regeneration, whilst TGFα$^{-/-}$ ablation in mice appear to have no observable effect (Oe *et al.*, 2004). The overexpression of HB-EGF in transgenic mice accordingly shows accelerated parenchymal recovery as well as mediation of ECM fibrotic activity, whilst amphiregulin is predominantly implicated in tissue remodelling *via* regulation of ECM-producing cells, such as HSCs, inducing not only release of HGF but expression of hepatic growth-related transcription factors such as *c-fos* (Kiso *et al.*, 2003; Perugorria *et al.*, 2008; Guo *et al.*, 2017). Taken together with HGF, examination of the proliferative phase reveals a complex interplay of signalling factors which in its absence, delays liver regeneration.

1.2.3.4 Termination Phase

Termination of liver regeneration ensues once 2.5% times the normal liver to body weight ratio is restored. The proliferative and mitogenic effects of growth factors understood to be predominantly counteracted by the tumour-suppressive cytokine transforming growth factor β (TGFβ), in which TGFβ peak increases in mRNA expression at ~72 hours post-PHx is consistent with late stages of liver regeneration (Hayashi and Carr, 1985; Nakamura *et al.*, 1985; Braun *et al.*, 1988; Fausto, 2000). Synthesised in both the spleen and non-parenchymal liver cells, TGFβ, in specific TGFβ1, is reported to elicit its anti-proliferative effects in a paracrine signalling manner on binding to its cognate TGFβ receptors I and II (TGFβR1/TGFβR2) located on surface of hepatocytes (Fausto *et al.*, 2006). These effects follows the induction of downstream cytostatic and apoptotic gene expression: SMAD (Small Mothers Against Decapentaplegic) effector signalling, for example, is show to induce both cell cycle kinase inhibitor p21 and pro-apoptotic gene expression, such as Bim and CARD11 downstream of TGFR hepatocyte receptor binding, in turn halting cell cycle progression (Oberhammer *et al.*, 1992; Schwall *et al.*, 1993; Yasuda *et al.*, 1993; Moustakas and Kardassis, 1998; Ramesh *et al.*, 2008). It is therefore unsurprising that reduced activation of TGFβ is likely able to enhances hepatocyte susceptibility to persistent mitogenic activity; however, in the absence of TGFβ-signalling, hepatocyte proliferation is still able to be terminated once liver mass is restored - consequently suggesting a lesser role for TGFβ in regenerative termination (Oe *et al.*, 2004).

Other TGFβ family members are also shown to have a role during the termination phase of liver regeneration, including the involvement of activins and bone morphogenetic proteins (BMPs). Whilst such proteins are not solely committed to the termination of liver regeneration, of those prominently studied such as Activin A, their expression is consistent with the latter stages of liver regeneration and exerts anti-proliferative cytostatic effects *via* a variety of signalling effectors, including SMAD-dependent arrest via cyclin D1 and cyclin E suppression (Takamura *et al.*, 2005; Chen *et al.*, 2014). Supporting this is the subsequent antagonization of activin A by follistatin, in which hepatocyte proliferation is prolonged *via* enhanced hepatocyte DNA synthesis (Kogure *et al.*, 1995). On the other hand, however, BMP7 and BMP4 are shown to repress proliferation in vitro, alluded to the delineation of these BMPs in a paracrine inhibitory role (Kan *et al.*, 2009). These studies therefore suggest the incomplete understanding of the extent to which activins and BMPs are involved in liver regeneration, more specifically whether in a proliferative or antiproliferative context.

1.3 NF-κB Signalling in Liver Regeneration

The transcription factor NF-κB regulates multiple aspects of liver homeostasis, serving as a pivotal mediator in a variety of downstream effector pathways: these include the careful coordination of hepatocyte survival and cell death, differentiation and immune cell signalling that ensues during liver regeneration (Iimuro and Fujimoto, 2010). The NF-κB family comprises five key member subunits: p50 (NF-κB1), p52 (NF-κB2), p65 (RelA), RelB and c-Rel, which bind following their release from their inhibitory κB proteins (IκB) to NF-κB DNA response elements either as hetero- or homodimers to induce gene transcription during classical canonical signalling (figure 1-4) (Hayden and Ghosh, 2012). During liver regeneration, NF-κB DNA binding activity is shown to promptly increase after PHx, transcriptionally targeting a diverse profile of proliferative and inflammatory genes, including cytokines TNFα and IL-6 *via* activated Kupffer, PMNs and endothelial cells; *c-fos* and *c-jun* (Libermann and Baltimore, 1990; Tewari *et al.*, 1992; Cressman *et al.*, 1994; Liu *et al.*, 2000). These genes form part of the immediate-early gene transcription profile quickly induced following tissue injury, as previously mentioned during the priming phase (section 1.2.3.1).

Unsurprisingly NF-κB is shown to blunt liver regeneration when inhibited, the repression of signalling on adenoviral IκB suppression and inactivation through inhibitor of κB kinase β (IKK2) subsequently shown to negatively impact post-PHx recovery (Iimuro *et al.*, 1998; Maeda *et al.*, 2005). In these studies, inhibition induces hepatocyte apoptosis, implicating NF-κB is not only a critical mediator of liver regeneration through transcription of immediate-early genes involved in hepatocellular proliferation, but through eliciting antiapoptotic effects. Conversely, further studies report that hepatocyte-specific adenoviral IκBα repression does not induce hepatocyte apoptosis post-PHx, but only in the presence of TNFα stimulation (Chaisson *et al.*, 2002). By bypassing NF-κB signalling in this manner, it is proposed that NF-κB within hepatocytes is less critical, instead mediating liver regeneration through activation of the innate immune signalling arm. Accordingly, early NF-κB activation is shown to primarily occur in transgenic *cis*-NF-κB-EGFP mice Kupffer macrophages during post-PHx liver regeneration, whilst conditional NF-κB inactivation in haemopoetic-derived cells, including Kupffer macrophages reduces parenchymal recovery (Maeda *et al.*, 2005; Yang *et al.*, 2005). The activation of Kupffer cells is therefore thought to be critical in liver regeneration, specifically in the priming of hepatocyte G_0-G_1 phase transition, *via* NF-κB-depending transcription of cytokines TNFα and IL-6.

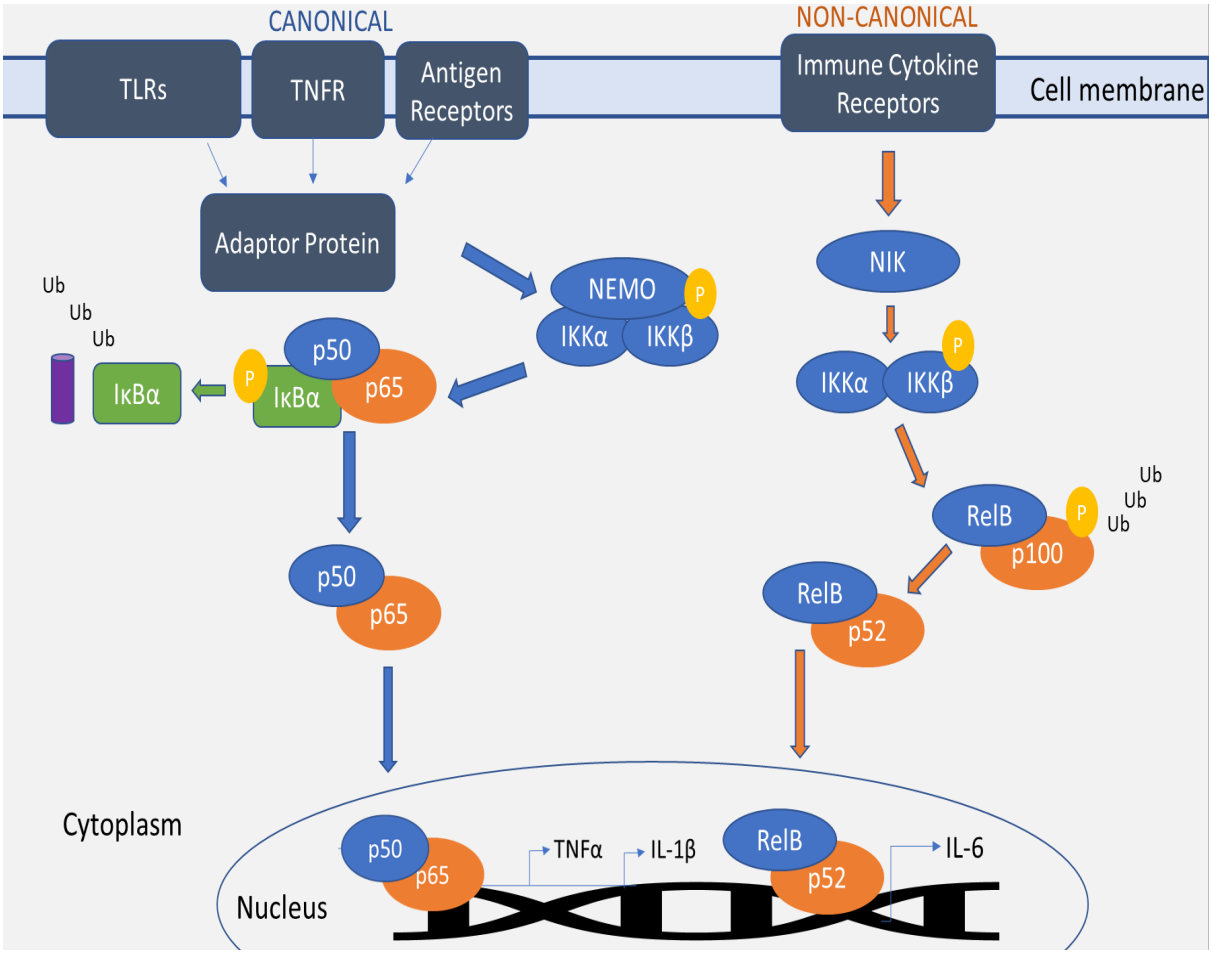

Figure 1-4: The canonical (left) and non-canonical (right) pathways of NF-κB signalling. *Canonical NF-κB signalling involves the binding of ligands to cognate surface receptor to induce adaptor protein stimulation such as MyD88 and tumour necrosis factor receptor (TNFR)-associated proteins that in turn mediates activation of the Inhibitor of κB kinase (IKK). IKK activation targets inhibitor of κB (IκB) for ubiquitination and proteasomal degradation which in turn allows for free NF-κB subunits to translocate to the nucleus to induce or repress gene transcription. Non-canonical NF-κB signalling involves the activation of IKKα by NF-κB inducing kinase (NIK). p100 is phosphorylated for further proteasomal processing by IKKα to p52 before nuclear translocation as a dimer to induce gene transcription.*

1.4 Liver Regeneration and Ageing

1.4.1 Ageing, Hepatic Regeneration and Liver Disease

Whilst advancement in medical care and research has ensured a steady increase in human lifespan with 13% of the population comprising the elderly aged >65 years and older, prolonged living does not necessarily correlate to a longer health span (United Nations, 2017). Increasing age or “ageing” presents a number of challenges, most notably the greater vulnerability of the elderly to morbidity and premature mortality as a result of the progressive homeostatic decline experienced during the ageing process (Lopez-Otin *et al.*, 2013). This deterioration contributes a primary risk factor for many chronic human diseases such as cancers, neurodegenerative and cardiovascular disease, diabetes, as well as for the context of this thesis, pathologies of the liver.

In relation to ageing, gradual alterations to liver physiology and function occur under both normal and pathological conditions. Current research outlining structural or functional phenotypes in the ageing liver is less well documented, with initial reports on the aged livers suggesting any age-associated hepatic decline to be largely protected against due to hepatic regenerative capacity and compensatory mechanisms (O'Mahony and Schmucker, 1994; Schmucker, 2005; Frith *et al.*, 2009) Frith *et al.,*2009; Schmucker and Sanchez, 2011). Nonetheless, studies also report increases in the incidence of hepatic pathologies and liver-associated mortality, associated with chronic liver disease within the elderly (Schmucker, 2005; Schmucker and Sanchez, 2011). Of the available comprehensive studies on ageing liver biology, a number of hepatic specific changes are observed with age: including the reduction in liver volume and hepatocyte cell numbers, hepatocyte hypertrophy, increased polyploidy and decreased mitochondrial density (Tauchi and Sato, 1968; Premoli *et al.*, 2009; Gan *et al.*, 2011). With these changes, reduced liver functionality is also reported as denoted by loss of hepatic phase I pharmacokinetics; however, it is important to note that clinical function tests often fail to capitulate liver function deficits associated with increasing age (Marchesini *et al.*, 1988; Wynne *et al.*, 1989; Schmucker, 2005).

Whilst no liver disease is specific to older ages, increasing lifespan appears to correlate to the greater frequency of chronic liver diseases managed in older patients. Studies have shown, for example, increased clinical determinants observed in the older population, such as liver inflammation or ‘steatohepatitis' due to hepatic fat accumulation (steatosis), advanced fibrosis and severe histological markers like ballooning degeneration and megamitochondria, typically associated with diseases such as non-alcoholic fatty liver disease (NAFLD). NAFLD is a common spectral liver disease that affects 20-30% of the general UK population, of which frequency in the elderly is increased (Frith *et al.*, 2009; Noureddin *et al.*, 2013). Prevalence and severity of NAFLD, as with other studies, are positively associated with changes in the participant’s metabolic and anthropometric traits such as obesity, dyslipidaemia and diabetes; however, at a molecular basis, manifestation is thought to arise from cellular alterations primarily centred around mitochondrial dysfunction (Mansouri *et al.*, 2018). Increased mitochondrial respiratory dysfunction, leading to ATP depletion and ROS generation, as well as impaired lipid metabolism and apoptosis are resultant key features of chronic disease and is also increasingly observed with age (section 1.6) (Chavin *et al.*, 1999; Cortez-Pinto *et al.*, 1999; Sanyal *et al.*, 2001; Koliaki *et al.*, 2015; Mansouri *et al.*, 2018).

Perhaps more clinically significant to this report is the marked decline in liver regeneration with age as seen in increasing mortality rates following tissue injury. Fatality following human liver resection is specifically shown to increase by 15% between 55 and 75 years of age, whilst in well-established murine models, survival post-PHx is reduced to between 40-60% in aged groups (Fortner and Lincer, 1990; Enkhbold *et al.*, 2015). This reduction in mortality is likely ascribed to a variety factors, including the reduction in hepatocellular proliferation as observed in aged rat livers when compared to young controls (Stocker and Heine, 1971). Accordingly, HGF and its cognate HGFR are also shown to deplete with age, delaying the regenerative ability of aged murine subjects, as well as increasing post-PHx mortality following *c-met* genetic ablation (Huh *et al.*, 2004; Enkhbold *et al.*, 2015). Meanwhile, TGFβ expression is shown to be increased in aged mice, suggesting any delays in liver regeneration are ascribed to the constitutive stimulation of hepatocyte apoptosis (Zhou *et al.*, 1993). Other examples of signalling pathways and genes associated with age-related hepatic decline also include CCAAT/enhancer-binding protein

(C/EBP family members) and Forkhead Box gene (FOXM1B), GSK3β and sirtuin (SIRT) 1 (Wang *et al.*, 2001; Jin *et al.*, 2009; Jin *et al.*, 2011). Interestingly, in transgenic mice ablated for the hepatoproliferative-associated gene FOXM1B, subsequent adenovirus FOXM1B transfection is shown to restore regenerative capacity in aged animals beyond that of younger controls, whilst targeting of GSK3β and SIRT1 pathways are proposed to improve the prognosis of various age-associated conditions (Lucas *et al.*, 2001; Wang *et al.*, 2001; Guarente, 2011).

1.5 The *PolgA* mtDNA mutator mouse

The development of the homozygous knock-in *PolgA* mouse ($Polg^{D257A/D275A}$) by two separate research groups, demonstrating error-prone/exonucleases-deficient mitochondrial replicase DNA polymerase-γ, has been a critical driving force in elucidating the molecular mechanisms of the ageing process: proposing the role of mitochondrial dysfunction *via* mitochondrial DNA (mtDNA) mutagenesis (Trifunovic *et al.,* 2004; Kujoth *et al.,* 2005).

Used as the model of interest for the present study, *PolgA* mice partially phenocopy some progeroid features of normal human ageing ranging from alopecia, kyphosis and frailty, reduced fertility, thymic atrophy, splenomegaly and bone marrow dysplasia, cardiomyopathy, and haemopoetic stem cell decline which coincides with increased frequency of mtDNA mutations in some tissues - including the liver (Trifunovic *et al.*, 2004; Kujoth *et al.*, 2005). Progressive deterioration of the mitochondria's electron transport chain (ETC) is observed, resulting in reduced respiratory capacity and subsequently decreased ATP production from approximately 12 weeks (Trifunovic *et al.,* 2004; Kujoth *et al.,* 2005). *PolgA* mice also demonstrate no markers of oxidative stress, nor show upregulation of antioxidants in earlier studies. Recent studies, however, using more sensitive *in vivo* detection methods show significant increases in oxidative stress marker H_2O_2 (Trifunovic *et al.*, 2004; Kujoth *et al.*, 2005; Logan *et al.*, 2014). Instead, stochastic accumulation of mtDNA mutations is proposed as a mechanism of ageing for this model through increased activation of apoptotic cell death, as observed *via* increased TUNEL staining and cleaved caspase-3 assays.

Whilst these mice suggest a correlative role of mtDNA mutation to ageing, critical review of the model reveals mtDNA mutation frequency to be moderately higher in heterozygotes and vastly increased in homozygous mice compared to WTs - even exceeding those observed in aged humans (Vermulst *et al.*, 2007). Despite this, *PolgA* heterozygotes appear phenotypically normal. Further scrutiny also establishes mutational burden of *PolgA* homozygous mice to be 500-fold higher than WTs before any obvious signs of progeroid ageing (Vermulst *et al.*, 2007). Whereas on one hand it can be suggested that mitochondrial mutations does not appear to limit lifespan of normal ageing mice and thus fails to recapitulate the ageing process in humans, one key consideration is the continual turnover or 'half-life' of mtDNA over the vastly different lifespans between mice (~2-3 years) and humans (Khrapko and Vijg, 2007; Payne and Chinnery, 2015). MtDNA turnover is very similar between mice and humans; however, it is clear that aged mice turnover less cycles of mtDNA replication than their human counterpart over a lifespan (Payne and Chinnery, 2015). As such, the link between mtDNA mutations and ageing is not redundant: this is substantiated by recent data in which mtDNA mutations may be intrinsically linked to cycles of mtDNA replication by means of clonal expansion (see section 1.6.2.3 for an overview of mitochondrial theories of ageing).

1.6 Mechanisms of Ageing

Defined as a gradual loss of physiological integrity, resulting in an increased vulnerability to external stress, damage and even death, human ageing has been subject to increasing scientific scrutiny as a primary risk factor in most chronic pathologies (Lopez-Otin *et al.*, 2013). Despite an incomplete understanding of its mechanisms, it is generally agreed that liver ageing and indeed the ageing process arises from damage to cellular, tissue and ultimately organ systems upon which over time accumulate (Payne and Chinnery, 2015). How this damage initiates presents a number of theories borrowed from the ageing field, including mtDNA dysfunction that arises from various postulated mechanisms such as clonal expansion of mutant mtDNA to the popular free radical theory. The latter of which proposes the mitochondrial organelle as the primary source of ROS, whose release has deleterious and mutagenic effects upon various cell compartments as well as mtDNA (Harman, 1956).

1.6.1 Evolutionary Theories of Ageing

Variations in organismal longevity and lifespan posits evolutionary theories of ageing to be part genetically regulated, resulting in the inexorable, stochastic deterioration of an organism's cell, tissue and organ homeostasis with increasing age (Finch and Tanzi, 1997; DiLoreto and Murphy, 2015). Genetic control of ageing was first postulated by August Weismann (1889): an 'ageing gene' as a means to naturally limit and minimise population growth (Weismann, 1891, 1889; reviewed Gavrilov and Gavrilova 2002). Subsequent updated arguments have since taken shape – including Medawar's Mutation Accumulation Theory (1952), suggesting that ageing is an adverse sum of deleterious genomic mutations; William's Antagonistic Pleiotropy Theory of Ageing (1957; reviewed Gavrilova and Gavrilova, 2002), proposing positive selection of genes for reproductive advantage that may prove detrimental in later life; and lastly Kirkwood's Disposable Soma Theory. The latter of which makes a key influential hypothesis that ageing arises due to metabolic trade-offs between an organism's cell repair mechanisms, and growth and reproduction due to the body's finite resources (Kirkwood, 1977; Kirkwood *et al.*, 1979; Kirkwood, 1997). Accordingly, the phenomenon of ageing and deterioration lies in the budgeting of energy towards cell repair and maintenance mechanisms, during which ageing cellular repair is continuous; however, somatic cell damage still accumulates due ineffective allocation of energy and thereby further drives the ageing process (Kirkwood, 1977). Energy is proposed to be pooled towards reproductive pathways to ensure propagation of a species rather than towards cell repair and maintenance. Whilst this is seemingly incompatible with William's antagonistic pleiotropy, disposable soma appears to trace the onset of ageing to a place where repair mechanisms take place at an early stage (Choi, 2016). However, Kirkwood argues that the idea of negative selection against survival genes in favour of those favourable to organismal decline seems unlikely – thereby leading to the inconclusive argument on how an organism ages (Kirkwood, 1997).

1.6.2 Molecular Theories of Ageing

1.6.2.1 The (mitochondrial) Free Radical Theory of Ageing

The free radical theory proposes that age-related disruptions to cellular, tissue and organ homeostasis arises from the accumulative oxidative damage to cellular compartments caused by endogenous ROS (Harman, 1956). The production of damaging ROS, chiefly superoxide ($O_2^{\cdot}$) and hydroxyl radicals, is believed to be predominantly derived from mitochondrial oxidative phosphorylation (OXPHOS), in which premature leakage of electrons from the mitochondria's ETC (see section 1.7 and 1.7.4 for mitochondrial biology overview), chiefly complex I and III, is able to reduce the high levels of oxygen consumed during cellular respiration to produce freely diffusing $O_2^{\cdot}$ and sequentially, hydroxyl radicals (Trifunovic and Larsson, 2008). Indeed, it has been suggested that of the total cellular ROS produced, around 90% can be traced back to the mitochondria; however, in early oxygen consumption studies with palmitoyl carnitine as substrate, only 0.15% is converted into detectable ROS (St-Pierre *et al.*, 2002).

With mitochondria identified as the dominant site of ROS production, key observations around the close proximity of mtDNA to the ETC proposes mtDNA as increasingly vulnerable to ROS-induced oxidative damage (Payne and Chinnery, 2015). Alongside the mtDNA's lack of protective histones, Harman's free radical theory goes on to suggest a 'vicious cycle' hypothesis in which acquired mutations within the mtDNA disrupts functionality of respiratory complexes and causes partial uncoupling of the ETC by UCPs (uncoupling proteins). The latter in turn has been shown to augment ROS production and oxidative damage, reduce ATP production and lastly increase mtDNA mutagenesis (Harman, 1956).

Interestingly, where organisms and individuals observe a longer or extended lifespan, correlative links are seen with reduced ROS production (Sohal *et al.*, 1989; Sanz, 2016). Longevity studies comparing pigeons with rats showed greater lifespan in the former, ascribed to a ~30% lower electron leakage and thus a consistently lower antioxidant activity in pigeon tissues (Ku and Sohal, 1993; Barja *et al.*, 1994; Herrero and Barja, 1997). Meanwhile studies involving genetic manipulation or inhibition of pro-oxidant signalling appear to vary in support for the free radical theory. For example, specific ablation of antioxidant superoxide dismutase (SOD) is shown to

have no effect in *C. elegans*; however, in *Drosophila* reduces ROS leakage without significant lifespan alterations (Sanz *et al.*, 2010; Van Raamsdonk and Hekimi, 2012). Furthermore, direct inhibition of complex I by the ubiquinone binding inhibitor rotenone, appears to increase *C. elegans* lifespan despite an increased generation of ROS (Yang and Hekimi, 2010). This contrasts with transgenic mice models in which ablation of antioxidants such as SOD2 has a deleterious effect on cellular DNA and proteins, as well as curtails lifespan due to increased oxidative DNA damage (Lebovitz *et al.*, 1996; Williams *et al.*, 1998; Huang *et al.*, 2001; Melov *et al.*, 2001).

Mitochondrial ROS and the onset of ageing therefore appears to product conflicting results; however, mitochondrial function is still largely recognised to decline with age. In a number of studies, mammalian ageing appears to occur concomitantly with a number of structural and morphological changes to the mitochondria, including a tissue decrease in mitochondrial density, swelling, cristae abnormalities, reduced mtDNA copy numbers and protein levels (Sastre *et al.*, 1996; Le Couteur *et al.*, 2001). Outlined changes are further exemplified in rat liver comparisons between old (24 months) and juvenile animals (3-4 months), whereby respiratory capacity is reduced ~40% and ATP levels decline (Stocco *et al.*, 1977). Reduced mitochondrial respiration is also observed for example in human and rodent liver, heart and skeletal muscle tissues, with additional deteriorations observed for ETC complexes I and IV; however, activities remain unchanged in complexes II, III and V (Lenaz *et al.*, 1997; Manczak *et al.*, 2005; Navarro and Boveris, 2007). Reasons for such disproportionate declines remain elusive, though one review suggests that methodical differences as well as changes in cell type composition in tissue homogenates such as fibrosis or vascularisation may compound interpretation of mitochondrial function results (Bratic and Larsson, 2013). Nonetheless, the mitochondria play an integral role in cellular homeostasis through its OXPHOS functionality. As such, any disruptive change to the organelle is likely to be contributory factor towards disrupted homeostasis during the ageing process.

1.6.2.2 Mitochondria and ageing: Clonal Expansion Theory

Recent findings appear to challenge the mitochondrial free radical theory, with ageing proposed to be linked to tissue mitotic activity, whereby mtDNA mutations are harboured within ageing tissues due to clonally expanded mtDNA point mutations

from a single origin (Nekhaeva *et al.*, 2002; Baines *et al.*, 2014). Using a variety of techniques to capture mutation loads, experimental data shows mtDNA mutagenic frequency (as an indirect measure of mutation rate) to change very little over age, yet clonally expanded mtDNA mutations dramatically increase (Greaves and Turnbull, 2009; Payne *et al.*, 2013; Greaves *et al.*, 2014). This expansion may be observed as mosaic events, visualised in practice by histochemical assay of COX/SDH activity. Multiple human tissues, for example, show mosaic COX deficiencies with age including the liver, brain, and muscle tissues (Cao *et al.*, 2001; Bua *et al.*, 2006; McDonald *et al.*, 2008; Fellous *et al.*, 2009). A causal role for mtDNA mutations in ageing is further elucidated in one study *via* the analysis of mitotic colorectal mucosal biopsies, in which next generation sequencing also shows 'mosaic like' COX deficiency in aged patients' colonic crypts, originating from expansion of single point mutations (Taylor *et al.*, 2003; Greaves *et al.*, 2014). These findings therefore appear to propose a mechanistic link between the clonal expansion of mtDNA point mutations and the deterioration of tissues observed with age: expanded mtDNA point mutations are thought to either be positively selected during cellular replication or via random genetic drift, with recent studies in mitotic gut tissue appearing to strongly support an argument in favour of the latter (figure 1-5) (Elson *et al.*, 2001; Baines *et al.*, 2014; Stamp *et al.*, 2018).

Meanwhile, cellular mitotic activity appears important in the clonal expansion of mutations in ageing tissue, as highlighted in variations in the mutation frequency detected between mitotic and post-mitotic tissues (Nekhaeva *et al.*, 2002). Differences in mitotic buccal epithelia and post-mitotic cardiomyocytes, revealing two different mechanisms for the origin and clonal expansion in ageing mitotic versus post-mitotic tissues. As such, the lower incidence of mtDNA mutations in post-mitotic tissues is most likely ascribed to reduced cellular turnover and capacity to progress through cell cycle, characteristic of post-mitotic cells.

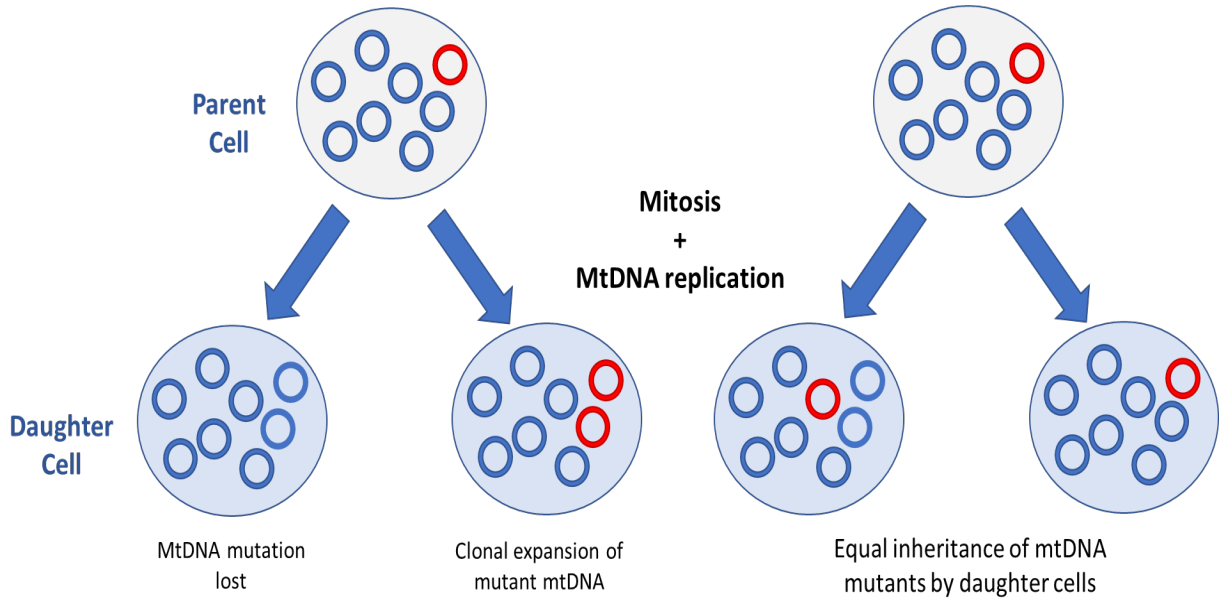

Figure 1-5: Clonal expansion of mutant mtDNA molecules by random intracellular drift in mitotic tissues following cellular and mitotic replication. *During cellular mitosis, mtDNA may be randomly lost or replicated in resultant daughter cells, in which inheritance of mutant mtDNA (red circles) may be further expanded and mutations propagated during relaxed mitochondrial replication and subsequent cycles of cell cycle progression (left diagram). Equally, parent cell division results in equal distribution of mutant mtDNA between daughter cells in the absence of clonal expansion (right diagram). Blue circles represent WT mtDNA molecules. Figure adapted from Baines (2014).*

A revised theory correlating mitochondrial dysfunction and ageing is therefore proposed, indicating oxidative damage and mtDNA replication errors result from early life events that give rise to mtDNA mutations that clonally expand throughout adulthood (Elson *et al.*, 2001; Coller *et al.*, 2005; Greaves *et al.*, 2014). Accordingly, murine studies involving the progeroid *PolgA* mouse have demonstrated that there is progressive age-associated accumulation of mtDNA mutations within tissues, which are thought to clonally expand and cause OXPHOS defects in individual cells (Trifunovic *et al.*, 2004; Kujoth *et al.*, 2005; Baines *et al.*, 2014). Early life events may be a critical factor in the development and expansion of mtDNA point mutations over time: maternal germline transmission studies showing wild type (WT) offspring from heterozygous *PolgA*$^{+/mut}$ mothers have a mild ageing phenotype, despite normal proof-reading capability (Ross *et al.*, 2013). In the broader context, it is likely that ageing and its related deficits are a consequence of clonal expansion of early life mutagenesis as opposed to *de novo* mutagenesis that disrupts mitochondrial-associated pathways including energy metabolism, apoptosis and senescence pathways, subsequently explored in section 1.7.

1.6.2.3 MtDNA mutations in ageing

MtDNA mutations are ~10-17 times more likely to occur than that of mutations within the nuclear genome, with mutation errors likely to occur during mtDNA replication (Neckelmann *et al.*, 1987; Wallace *et al.*, 1987; Taylor and Turnbull, 2005; Zheng *et al.*, 2006). Of the first mtDNA mutations identified, the 'common' 4977 bp deletion, spanning the mitochondrial ATP*ase8* and ND5 gene, and flanked by a 13 bp homologous repeat, is often reported in numerous ageing tissue studies (Cortopassi and Arnheim, 1990; Cortopassi *et al.*, 1992; Bua *et al.*, 2006). In the majority of these studies, this mutation is detected in post-mitotic tissues, indicating mtDNA deletions are likely to occur in a tissue-dependent manner during ageing (Corral-Debrinski *et al.*, 1992; Cortopassi *et al.*, 1992). Accordingly, multiple mtDNA deletion mutations have also been observed elsewhere: for example, in isolated ageing skeletal muscle fibres stained negatively for COX/SDH activity, multiple age-accumulated deletions are associated with focal regions of respiratory function within the tissue (Kopsidas *et al.*, 1998). Deletions appear to vary between different skeletal fibres; however, when subsequently isolated, single fibres revealed the presence of clonally expanded mtDNA deletions harboured within heteroplasmic cells (Brierley *et al.*, 1998; Cao *et*

al., 2001). Since increasing prevalence of mtDNA deletions correlates with the ageing process, it is believed that these mtDNA deletions expand until a phenotypic threshold is exceeded whereby mitochondrial respiratory dysfunction and ageing tissue-related pathology ensues, for example ageing muscle fibre degeneration during sarcopenia (Herbst *et al.*, 2007; Herbst *et al.*, 2016).

Interestingly, in the study by Taylor and colleagues (2003), no mtDNA deletion mutations were observed in the epithelial crypts of the aged human colon, rather an age-associated accumulation of mtDNA point mutations was observed. These mtDNA point mutations resulted in COX deficiency, with up to 15% of crypts being COX deficient by the age of 75 (Taylor *et al.*, 2003). Subsequently, point mutations have been observed in other mitotic tissues, particularly in those that in some part rely on stem cell renewal: including the stomach and liver, for which a random intracellular drift is proposed to account for clonal expansion (Elson *et al.*, 2001; McDonald *et al.*, 2008; Fellous *et al.*, 2009). Conversely, the absence of mitosis in post-mitotic tissues, is likely to account for the rare incidence of point mutations observed in previous studies (Wang *et al.*, 1997; Durham *et al.*, 2006).
First reports outlining mtDNA point mutation involvement in ageing are outlined in two studies by Munscher and colleagues (1993) and Zhang and colleagues (1993), in which investigations into A3243G and A8344G mutations, typically associated with MELAS (Mitochondrial myopathy, Encephalopathy, Lactic acidosis and Stroke) and MERRF (Myoclonic Epilepsy with Ragged Red Fibres) respectively revealed low level presence, even in aged brain tissues (Munscher *et al.*, 1993; Zhang *et al.*, 1993). Low levels may be ascribed to less sensitive methods which subsequent measurements utilising PCR-based methods, revealed 10 times higher incidence of the m.3243A>G in adult mitotic and post-mitotic tissues when compared to younger subjects (Liu *et al.*, 1997). Increasing levels in adult tissues are likely ascribed to the induction of mtDNA mutations in early life that expand with age. When modelling the incidence of point mutations in murine models, they were shown to increase during ageing. Specifically, the ageing *PolgA*$^{mut/mut}$ mice (section 1.6.2.4) harbour a 10-fold increase in the frequency of mtDNA point mutations than their WT siblings due to replicative errors, and the majority of these mutations are transitions (Kujoth *et al.*, 2005; Vermulst *et al.*, 2008). As previously highlighted, these point mutations are understood to clonally expand from early life, with subsequent sequencing analysis

showing no increased frequency in transversion mutations with time (Vermulst *et al.*, 2008; Edgar and Trifunovic, 2009; Ameur *et al.*, 2011). As such, the literature appears to propose age-related decline to be correlated with the increase in mtDNA mutations and subsequent respiratory dysfunction, in which the onset of an observable phenotype is seen once the threshold for mtDNA mutations within affected cells is reached. Ageing decline may therefore be secondary to pathogenic changes within mutant cells, ascribed to the role of mitochondria in a number of physiological pathways (see section 1.7). However, such implications must remain cognisant, especially given that mtDNA mutation levels remain relatively low in WT mice when compared to progeroid ageing murine models (Vermulst *et al.*, 2008).

1.7 Overview of Mitochondrial Biology

Mitochondria are maternally inherited, dynamic and multifunctional organelles renowned for their principal function of energy metabolism through synthesis of high-energy ATP molecules during OXPHOS. Located in all nucleated mammalian cells regardless of function, mitochondria form comprehensive dynamic networks, intricately maintained by the balance of mitochondrial fusion, fission, biogenesis and mitophagy pathways. Believed to be derived from eukaryotic progenitors following endosymbiotic engulfment or “symbiogenesis” with a α-proteobacterium, mitochondria form a bacterial-like organelle comprising a distinct outer and inner membrane that surround the intermembrane space, and a matrices compartment (figure 1-6A) (Wallin, 1926; Yang *et al.*, 1985; Martin *et al.*, 2015).

It is hypothesised that the evolution of mitochondria arises by two proposed theories: (1) the serial endosymbiotic hypothesis and (2) the hydrogen hypothesis (Margulis, 1971; Martin and Muller, 1998). Of the former and more classical model, mitochondrial formation is hypothesised to arise from successive symbiogenesis events in aerobically respiring eukaryotic cells. This follows thermoplastic archaebacteria nucleus formation, merging with spirochete-like eubacteria and finally the incorporation of photosynthetic bacteria (Margulis, 1971; Witzany, 2006). Meanwhile, the hydrogen hypothesis proposes mitochondrial formation to follow the uptake of hydrogen-producing eubacterium by hydrogen-dependent archaebacterium - resulting in the presence of both aerobic and anaerobic respiratory enzymes and clear gene classes within an eukaryotic cell (Martin and Muller, 1998). Over time, numerous studies seem to support the hydrogen hypotheses; however, despite the differences, both proposed hypotheses demonstrate a symbiotic relationship between the endosymbiotic transfer of mitochondria and its genes from eubacteria to mammalian cell (van der Giezen, 2011; Poole and Gribaldo, 2014).

1.7.1 Mitochondrial Structure and Genome

Termed initially as “sacrosomes”, the word ‘mitochondria’ was initially coined by Benda (1898) following observations of the organelle during spermatogenesis (van der Giezen, 2011). Subsequent electron microscopy studies depict mitochondria as small tissue organelles 1-4 μm in length and 0.3-0.7 μm in diameter, taking form as

elongated, rod or oval shaped structures (Palade, 1953). The size of which is dependent on the metabolic activity and function of the cell in which the mitochondria reside. The highest mitochondrial density occurs at the greatest sites of high energy consumption and correspondingly, ATP synthesis demand: for example, mitochondrial density index analysis shows cardiac tissue to have a higher mitochondrial concentration over a number of other tissues (Forner *et al.*, 2006; Park *et al.*, 2014). This variation in tissue-dependent density patterning is also seen in an array of organisms, including humans and rodents.

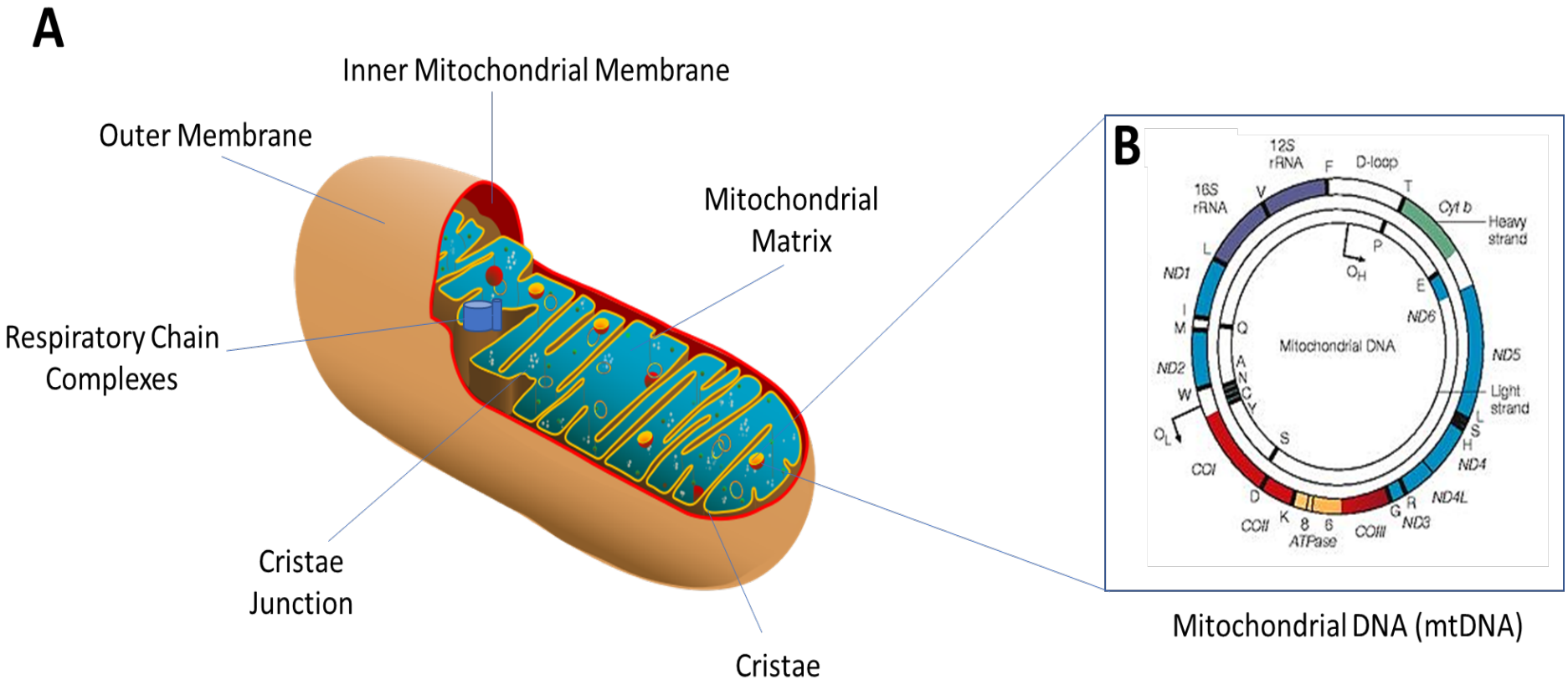

Figure 1-6: (A) Simplified representation of mitochondrial structure. (B) The human mitochondrial genome. Human mtDNA comprises a continuous circular 16,596 molecule comprised of a heavy and light strand. The mtDNA encodes 37 genes: 13 protein encoding mRNAs, 2 rRNAs and 22 tRNAs. Transcriptional and replication machinery is primarily housed within the non-coding displacement loop (D-loop), of which the origin of the heavy strand replication (O_H) is located. The outer heavy strand encodes 12 of the protein encoding genes, these include complex I subunits (ND1-5), complex III CytB and 3 subunits of complex IV (COX1-3), as well subunits of complex V (ATPase 6 and ATPase) On the inner light strand complex I subunit ND6 is encoded. In between protein encoding genes are sequences encoding for tRNAs. Adapted from Taylor and Turnbull (2005) and Potterton (2014).

1.7.1.1 Mitochondrial Structure

As abovementioned, mitochondria (figure 1-6A) are structurally double-membraned, housing an internal matrix comprising metabolic enzymes, transcription and translational machinery and numerous copies of mtDNA (Palade, 1953). Of the outermost layer, the outer membrane (OM) encompasses a lipid bilayer spanned by transmembrane protein channels, known as porin, which allows two-way passage of small molecules between the cytoplasm and the intermembrane space (Alberts *et al.*, 2002). Such small molecules are largely impermeable to the subsequent inner mitochondrial membrane (IMM) lipid bilayer, with exception to H_2O, hydrogen peroxide (H_2O_2), O_2, CO_2 and NH_2 for example. The inner mitochondrial membrane (IMM) comprises a continuous closed membrane that protrudes into the mitochondrial matrix. Known as cristae, the IMM comprises two of main workings: (1) the inner boundary membrane and (2) the cristae membrane (CM) (which houses the majority of OXPHOS protein complexes) that interconnect by tubular cristae junctions (Frey and Mannella, 2000; Vogel *et al.*, 2006). Inner foldings of the CM into the cristae allows increased surface area, which alongside the electrochemical insulating lipid components of the IMM, specialise the mitochondria (specifically the CM) for its respiratory function. By contrast, membrane-associated proteins of the IMM allow import of products such as intermediary metabolites and carrier molecules into the mitochondria for subsequent processing.

1.7.1.2 Mitochondrial Genome

MtDNA, is circular and double stranded in nature and is comprised of a guanine rich heavy strand and a cytosine rich light strand (figure 1-6B). It is estimated that with multiple mitochondria present in human somatic cells, the number of mtDNA copies lies somewhere between 10^3 and 10^4, although this may be higher in certain cell types, such as maternal germ cells in which mtDNA copies can increase to over a million during oocyte maturation (Lightowlers *et al.*, 1997; Coller *et al.*, 2001). The complete sequence of mtDNA was originally elucidated in 1981 by Anderson and colleagues (1981) and was subsequently reviewed in 1999 (Andrews *et al.*, 1999). MtDNA comprises 16,596 base pairs (bp) that encode 37 genes in total (13 protein encoding mRNAs, 2 ribosomal RNAs (rRNAs) and 22 transfer RNAs (tRNAs)), as well as housing within the non-coding displacement loop (D-loop) cis-acting elements recognised by nuclear genome encoded mtDNA transcriptional and replication

machinery (Anderson *et al.*, 1981; Gustafsson *et al.*, 2016). MtDNA also differs from nuclear DNA through the absence of introns and termination codons, the latter of which are alternatively created through post-transcriptional polyadenylation of mRNAs (Anderson *et al.*, 1981). Therefore, the mitochondrial genome relies on a synergistic relationship with nuclear DNA to encode much of its inventory, including the other ~77 respiratory chain subunits that are transported into the mitochondria for subsequent assembly into macromolecular protein complexes (Neupert and Herrmann, 2007; Schmidt *et al.*, 2010).

Originally believed to be of their own free-floating genetic entities, current understanding reveals mtDNA molecules to be compacted into inner mitochondrial membrane-associated nucleoprotein complexes known as nucleoids (mt-nucleoids) (Gustafsson *et al.*, 2016). Mt-nucleoids are thought to contain between 1-2 molecules of DNA, giving a 'string on a bead' like appearance; these can be visualised by various methods including immunocytochemical staining and GFP tagging as seen in human studies (Spelbrink *et al.*, 2001). Super-resolution fluorescent imaging also reveals nucleoids to be ~100 nm, compared with ~200-300 nm in previous conventional microscopy studies; however, there is much debate whether nucleoids contain a single copy or ~6-10 copies of mtDNA (Kukat *et al.*, 2011; Bogenhagen, 2012; Kukat and Larsson, 2013). Meanwhile, the abundant mitochondrial transcription factor A (TFAM) protein is integral to the structural formation of mt-nucleoids: wrapping mtDNA to their respective nucleoid in patches *via* cross-strand binding and loop formation with mtDNA as identified by electron microscopy (Kukat *et al.*, 2015). Furthermore, mtDNA is shown to be fully coated with TFAM, consequently giving rise to the elongated but irregularly shaped mt-nucleoids as observed as observed by electron cryotomography within bovine mitochondria (Kukat *et al.,* 2015). The levels of TFAM appear correlated to mtDNA copy number, as seen in murine studies (Larsson *et al.*, 1998).

Finally, it is important to note that differences in mtDNA exist between organisms. Mouse mtDNA, for example, is thought principally homologous in terms of encoding gene location; however, is smaller than human mtDNA at 16,259 bp due to a smaller 879 bp D-loop (Bibb *et al.*, 1981). Promoter and stop codon sequences required for transcriptional initiation and termination during murine mtDNA replication also differs

from those within the human D-loop (Bibb *et al.*, 1981). When packaged into mt-nucleoids, mouse somatic cells are shown to comprise of a single mtDNA copy per nucleoid (average ~1.1-1.5) that is packaged into a slightly more elongated nucleoid shape (Kukat *et al.*, 2011). Increases in mtDNA copy numbers show unaltered nucleoid size and shape; however, resulted in more nucleoids per cell.

1.7.2 MtDNA Transcription, Translation and Replication

1.7.2.1 MtDNA Transcription

Transcription of the mitochondrial genome occurs in a bidirectional manner and originates from three different promoter regions housed within the non-coding D loop: two heavy stand promoters (HSP1 and HSP2) and one light strand promoter (LSP) (Gustafsson *et al.*, 2016). Transcription from these promoters results in the production of a single polycistronic precursor RNA transcripts, the length of which predominantly depending on the promoter. Transcripts emanating from HSP2 results in near genome length products, whilst transcribes originating at HSP1 contain the 2 mitochondrial rRNAs and tRNAs, $tRNA^{Phe}$ and $tRNA^{Val}$, and terminate at a specific site in the $tRNA^{Leu}$ gene (Rebelo *et al.*, 2011). Meanwhile, the remaining 8 tRNAs and mitochondrial ND6 gene are transcribed under the LSP promoter on the light strand. Resultant RNA transcripts are then processed into their constituent tRNAs, mRNAs and 12S and 16S rRNAs for subsequent translation.

Mammalian mtDNA transcription requires machinery distinct from that used by the nuclear genome, requiring the help of TFAM, mitochondrial RNA polymerase (POLRMT) and mitochondrial transcription factor B2 (TFB2M) and TFB2M1 proteins to initiate gene expression (Gustafsson *et al.*, 2016). Utilising these, transcription starts 10-15 bp upstream of the starting origin, beginning with TFAM binding to unwind and relax the surrounding DNA region, as part of allosteric protein bubble coalescences with neighbouring TFAM monomers - in preparation for POLMRT-DNA binding at the transcriptional promoter (Traverso *et al.*, 2015). Subsequently, TFAM can act as a regulator of POLRMT/TFB2M and POLMRT/TFB21 complexes (Falkenberg *et al.*, 2002). TFB2M is primarily recruited to the transcription start site, allowing the fully assembled complex to induce structural changes at the promoter region and encourage initial phosphodiester bond formation during the transcription process (Sologub *et al.*, 2009; Lodeiro *et al.*, 2010; Yakubovskaya *et al.*, 2014).

POLMRT is then able to follow and elongates transcription, requiring additional aid from the mitochondrial elongation factor (TEFM) to which POLMRT interacts *via* its catalytic C-terminus. Interestingly, *in* vitro depletion of TEFM is shown to impair elongation of the copied DNA transcript (Minczuk *et al.*, 2011; Posse *et al.*, 2015).

1.7.2.2 MtDNA Transcription Termination

Termination of mtDNA transcription involves a specific set of events mediated by the transcription termination factor (mTERF), a 39 kDA protein of which there are four types (Gustafsson *et al.*, 2016). Amongst the best characterised is mTERF1, which through its three putative leucine-zipper motifs, terminates short HSP1-initated transcription at a 28 bp binding region located within the $tRNA^{Leu}$ gene (Bonawitz *et al.,* 2006). MTERF1 is believed to mediate mtDNA transcription termination through the physical modulation of the DNA duplex followed by stabilised binding of the termination factor by base flipping, such activity dependent, *in vivo,* on the trimeric conformation of mTERF and its post-translational phosphorylation (Asin-Cayuela *et al.*, 2004; Prieto-Martin *et al.*, 2004; Yakubovskaya *et al.*, 2010). By contrast, less is known about the termination events that follow HSP2- and LSP-initiated transcription and the other homologues of mTERF, as such further studies are required to clarify function (Gustafsson *et al.*, 2016). Once terminated, the resulting RNA transcripts are translated into corresponding proteins.

1.7.2.3 MtDNA Translation

Primary transcripts produced by mtDNA transcription are long and polycistronic in nature, requiring subsequent maturation processes prior to mtDNA translation. In general, maturation begins with excision of interspersed mitochondrial tRNA, in which tRNAs sequences are cut from mRNA and rRNA *via* endonucleolytic excision by RNase Z – in a model described as 'tRNA Punctuation' (Anderson *et al.*, 1981; Ojala *et al.*, 1981). Here, excision by RNase P is thought to cleave the primary transcript at the 5'-end of pre-tRNAs, whilst the endonuclease ELAC2 is described to execute the maturation of the mtDNA transcript *via* cleavage at the 3'-end of tRNA (Brzezniak *et al.*, 2011; Rossmanith, 2011). The absence of tRNA flanking of some mRNA regions, however, proposes use of alternate cleavage mechanisms, of which the role of serine/threonine kinase (FASTK) proteins has been recently proposed (Popow *et al.*, 2015; Boehm *et al.*, 2017). Following excision from the primary transcript, mRNAs

and tRNAs undergo maturation and stability involving various post-transcriptional modifications that facilitate subsequent mtRNA translation (D'Souza and Minczuk, 2018).

Decoding of mitochondria mRNA is understood to utilise the 22 mitochondrially encoded tRNAs only, in which tRNAs undergo extensive post-transcriptional chemical modifications to facilitate translation of the mitochondrial genome (Anderson *et al.*, 1981; Bibb *et al.*, 1981; D'Souza and Minczuk, 2018). Amongst alterations is the introduction of chemical modifications at the 'wobble' base (position 34) at the tRNA anticodon: in which the first position of the anticodon (corresponding to the third position of DNA) is altered to facilitate a larger repertoire of codon recognition during mitochondrial translation through non-Watson-Crick base pairing (Barrell *et al.,* 1980). Alterations include introduction of 5-formylcytosine of mitochondrial $tRNA^{Met}$ (f_5C34) by NSUN3 and ABH1, MTO1 and GTPBP3-mediated biogenesis of taurinomethyluridine and catalysis of 5-taurinomethylridine thiolation to allow for subsequent translation (Villarroya *et al.*, 2008; Sasarman *et al.*, 2011; Haag *et al.*, 2016; Nakano *et al.*, 2016; Wu *et al.*, 2016; Van Haute *et al.*, 2017).

The subsequent translation of mammalian mitochondrial mRNAs comprises four stages: (1) initiation, (2) elongation, (3) termination and (4) recycling. Translation is carried out on the mitoribosome that structurally comprises a large 39S subunit and a smaller 28S subunit, as well as two matrix rRNAs (12A and 16S) (Sharma *et al.*, 2003; Greber *et al.*, 2014; Kaushal *et al.*, 2014; Greber *et al.*, 2015). Due to the small number and content of rRNA components within the mitoribosome, 36 additional mitochondrial-specific proteins are recruited that together form a protein-protein network around a highly catalytic rRNA core (Amunts *et al.*, 2015). Accordingly, nuclear-encoded regulatory proteins are required to facilitate each stage of mRNA translation into polypeptides: mitochondrial initiation factors (mtIF) 2 and mtIF3, for example, are shown to position AUG or AUA start codons at the 28S subunit, whilst TEFMs direct tRNAs to form base pairs with mRNA at the codon-anticodon site to mediate elongation of translation (Bhargava and Spremulli, 2005; Haque and Spremulli, 2008; D'Souza and Minczuk, 2018). Finally, mitochondrial translation is terminated by the presence of A-site stop codons, predominantly UAA and UAG as

recognised by mtRF1a (mitochondrial termination factor 1a) (Barrell *et al.*, 1980; Anderson *et al.*, 1981).

Shown to catalyse the hydrolysis of the peptidyl tRNA, MtRF1a is understood to be the only release factor able to terminate translation across 13 mtDNA-encoded polypeptides at UAA and UAG codons; the exceptions being the termination at Mt-CO1 and ND6 open reading frames (Soleimanpour-Lichaei *et al.*, 2007; Huynen *et al.*, 2012; Lind *et al.*, 2013). In this context, AGA and AGG are understood to encode the stop codon; yet, as these codons occur only once at each end of the ORF, it is proposed that termination of mtDNA translation occurs in a non-adherent manner to the genetic code: a -1 frameshift of the mitoribosome ensuring termination at these rarer codons (Temperley *et al.*, 2010a; Temperley *et al.*, 2010b). ICT1 is previously proposed to mediate this function *via* the hydrolysis of peptidyl tRNAs at stop codons; however, this role remains widely debated (Akabane *et al.*, 2014). ICT1, for example, is unable to terminate translation in A-site extended RNA templates as in Mt-CO1 and ND6 and as such, is therefore likely to utilise alternative termination release factors, at least in this context (Chrzanowska-Lightowlers *et al.*, 2011; Chrzanowska-Lightowlers and Lightowlers, 2015). Nonetheless, following termination at the stop codon, recycling factors mtRRF and EGF2 mediates the release of ribosomal subunits, tRNAs and mRNAs from the resultant polypeptide, allowing for quaternary folding and arrangement of mtDNA-encoded proteins (D'Souza and Minczuk, 2018).

1.7.2.4 MtDNA Replication

MtDNA replication occurs in a continuous and autonomous manner, independent of cell cycle and nuclear DNA replication (Bogenhagen and Clayton, 1977). Replication is thought to occur by either of the two main models proposed as: (1) the synchronous model and (2) the asynchronous (strand displacement) model (Clayton, 1992; Holt *et al.*, 2000).

Asynchronous mtDNA replication occurs in a continuous manner, summarised by the interdependency of H strand synthesis on transcription initiation *via* the LSP promoter; the coordination of both heavy and light stands resulting in complementary DNA synthesis without the production of Okazaki fragments (Gustafsson *et al.*, 2016). During the asynchronous model, replication begins at the heavy strand origin

(O_H), with first phase mtDNA replication occurring in a clockwise manner to produce a single H strand without complementary replication of the L strand. Synthesis of the heavy leading strand advances two-thirds of the way, subsequently allowing the light strand origin (O_L) to be exposed for subsequent binding and complementary L strand synthesis to be initiated by an additional molecule of POLRMT in the opposite direction. In addition, random mtDNA transcription is also prevented here, by way of mitochondrial single stranded-binding protein (mtSSB) binding to the displaced parental H strand and preventing transcriptional assembly of POLRMT on ssDNA (Miralles Fusté *et al.*, 2014). Interestingly, synthesis of the L strand is highly dependent on the POLRMT transcription enzyme: subsequent looping of the exposed L strand obstructs mtSSB binding, allowing POLRMT to transcribe primer sequences from a poly-T stretch to which the mitochondrial DNA polymerase γ (Polγ) subsequently binds and executes L strand DNA replication (Miralles Fusté *et al.*, 2014; Gustafsson *et al.*, 2016). MtDNA daughter molecules are then ligated; forming closed circular molecules known as C mtDNA (Clayton, 1991). Supporting this notion of strand displacement are a number of studies, including notably the mapping of free ‘5 ends of O_H and O_L by atomic force microscopy; replication by this, however, is thought to take approximately 1 hour – a slow rate for DNA replication (Brown *et al.*, 2005).

By contrast, synchronous replication comprises synthesis of leading and lagging strands in a synchronous and symmetrical manner, allowing replication to occur bidirectionally (Gustaffson *et al.,* 2016). This is seminally described in 2D gel electrophoresis work by Holt and colleagues (2000), in which replication is observed *via* production of two classes of mtDNA intermediates, differentially sensitive to single-strand nuclease digestion (Holt *et al.*, 2000; Yasukawa *et al.*, 2005). During the synchronous model, replication appears to predominantly initiate at the O_H, however, work by Bowmaker and colleagues (2003) shows that replication also begins at multiple initiation zones spanning the broad zone (OriZ), namely at genes encoding ND5, ND6 and cytochrome b (Bowmaker *et al.*, 2003). Intriguingly, subsequent revisions of this work by atomic force microscopy and 2D gel electrophoresis appear unable to confirm synchrony as a model of mtDNA replication, instead providing evidence only for strand-displacement (Brown *et al.*,

2005).

Finally, two additional models for mtDNA replication have been recently suggested, based on mtDNA replication intermediates identified by 2D gel electrophoresis: (1) model of ribonucleotide incorporation throughout the lagging strand (RITOLS) and (2) the model of strand-coupled mtDNA replication (Holt *et al.*, 2000; Gustafsson *et al.*, 2016). Initially thought that replication may occur *via* two parallel mechanisms, slow incorporation of DNA precursor labelling into intermediates argue against mtDNA maintenance *via* strand-coupled approaches in favour of RITOLs (Holt *et al.*, 2000; Reyes *et al.*, 2013). Correspondingly, RITOLS demonstrates similarity to strand displacement replication, albeit the circumvented role of mtSSB, thus allowing asynchronous POLRMT-mediated transcription of the lagging L strand for later DNA conversion (Yasukawa *et al.*, 2006). Subsequently, RNA intermediates are successively threaded in a 'bootlace' manner onto a lagging-strand template as the replication fork advances until further DNA synthesis processing (Reyes *et al.*, 2013). Unfortunately, enzymes required for the process are yet to be identified, thus a firm conclusion of the mtRNA replication mechanism remains undefined.

1.7.2.5 MtDNA Mutagenesis

The introduction of mutations into mtDNA is understood to be higher in frequency than nuclear DNA, at an around a 10-17 fold increase (Neckelmann *et al.*, 1987; Wallace *et al.*, 1987). This observation is made on the long-time basis of the mitochondrial genome's close proximity to the electron transport chain (ETC) and its resultant oxidative by-products (section 1.5.4) (Yakes and Van Houten, 1997; Michikawa *et al.*, 1999; Zinovkina, 2018). Both deletions and point mutations, as well as insertions and large-scale rearrangements are found in mtDNA: specifically, point mutations are found to occur at a ~$6x10^{-8}$ frequency per bp per year, whilst deletions occur at ~$6\ x10^{-6}$ per mitochondrial genome replication (Shenkar *et al.*, 1996; Marcelino and Thilly, 1999). This deterioration in the mtDNA is originally thought to be due to poor DNA repair mechanisms or a lack thereof, as well as a lack of protective histones (Richter *et al.*, 1988; Zinovkina, 2018). It is now understood that the existence of DNA repair processes are beyond doubt, with many mechanisms shared with those for the nuclear DNA; however, these are much more diverse beyond typical base excision, mismatch repair and strand-break repair mechanisms

seen in the nuclear DNA (Liu and Demple, 2010; Zinovkina, 2018).

Mitochondrial replication is a key process by which mutations are thought to be introduced into the mitochondrial genome. Of the 17 DNA polymerases, DNA polymerase gamma (Polγ) is the only replicative polymerase known to exist in mammalian mitochondria and is proposed to principally introduce replication errors through spontaneous misincorporation and miscopying (DeBalsi *et al.*, 2017). This is despite a high fidelity that results in misinsertion only every 1 in 500,000 bp synthesised (Longley *et al.*, 2001). Accordingly, studies showing recapitulation of *in vivo* mtDNA mutations by Polγ *in vitro*, appears to support the notion that endogenous errors mediated by Polγ during mtDNA replication constitutes the primary source of mtDNA point mutations (Zheng *et al.*, 2006). Moreover, when mtDNA Polγ 3' exonuclease activity is inactivated, this is shown to increase levels of mtDNA mutations, as well as the loss of mitochondria and onset of ageing (Zhang *et al.*, 2000; Trifunovic *et al.*, 2004). Meanwhile. mtDNA deletions are proposed to occur either by repair mechanism errors that follow the induction of double-strand DNA damage or slippage replication (Shoffner *et al.*, 1989; Krishnan *et al.*, 2008).

1.7.2.6 MtDNA Repair Mechanisms

Despite some protection from mtDNA-associated proteins, the mitochondrial genome is still susceptible to insult from mutagenic agents. As such, the mitochondria comprises a number of systems to mediate mtDNA repair; however, the precise molecular mechanisms by which are still poorly understood (Zinovkina, 2018). Amongst those more widely established is the single-patch base excision repair (SP-BER) pathway, in which mutated regions are 'marked' by DNA glycosylases for cleavage from the DNA strand by apurinic/apyrimidinic (AP) endonuclease, followed by sealing of the mtDNA by Polγ lyase activity (Zinovkina, 2018). Onset of SP-BER is dependent on the lyase activity and the ability to remove the 5' terminal group of the abasic site by Polγ: if not in this this instance, repair occurs *via* long patch base excision repair (LP-BER) (DeBalsi *et al.*, 2017; Zinovkina, 2018). LP-BER typically proceeds when repair involves removal of several mtDNA-inserted nucleotides, resulting in the formation of a flap structure as mediated by DNA2 nuclease/helicase activity and EXOG1 (exo/endonuclease G) (Kroeger *et al.*, 2003; Liu *et al.*, 2008; Zheng *et al.*, 2008; Boesch *et al.*, 2011). Termination of BER (long and short patch)

involves the ligation of ends by DNA ligase 3 (Zinovkina, 2018). Meanwhile, repair of double-strand breaks and mismatches (mismatch repair; MMR) have been also described elsewhere in the removal of mis-incorporated and missense bases, of which the latter still remains in favour due to the presence of essential factors within the mitochondria, including MSH and YB-1 proteins (de Souza-Pinto *et al.*, 2009; Kazak *et al.*, 2012).

Finally, recent literature exploring Cockayne syndrome (CS), a defective ageing disorder involving mutations in ERCC6 (CSB) and ERCC8 (CSA), appears to have invigorated the argument for nucleotide excision repair (NER) during mtDNA repair mechanisms, previously thought be absent from mitochondria. Follow mutagenic H_2O_2 pro-oxidant inducing injury, NER enzymes CSA and CSB increase in expression and interaction with BER-associated mitochondrial glycosylases to implement mtDNA repair (Kamenisch *et al.*, 2010). Mutations in CSA and CSB proteins have indicated cellular sensitivity to the accumulation of damaged mitochondria and oxidative stress which promotes the ageing phenotype, of which rescue using serine protease inhibitors appears to reverse mitochondrial defects (Pascucci *et al.*, 2012; Cleaver *et al.*, 2014).

1.7.3 Heteroplasmy and the Threshold Effect

Heteroplasmy is described as a state in which a mixture of normal wild type (WT) mtDNA and mutated mtDNA can exist within an individual cell and is expressed as a percentage of total mtDNA genomes comprising mtDNA mutations (Larsson and Clayton, 1995). Cells may also exist as homoplasmic WT or homoplasmic mutant states, whereby all genomes are genetically or mutagenically identical (figure 1-7). Since mtDNA mutations are coupled to mtDNA copy numbers and are highly recessive, it is likely that individual cells can tolerate a level of mutation before a dysfunctional phenotype is observed (Sciacco *et al.*, 1994). Consequently, once a threshold is reached that induces respiratory deficiency, mutation-harbouring cells can be identified by assaying complex IV and complex II activity by cytochrome c oxidase/ succinate dehydrogenase (COX/SDH) histochemistry. The threshold for mitochondrial heteroplasmy to induce such a phenotype is unclear; however, it is estimated to be around ~60-85% dependent on the mutation type (Boulet *et al.*, 1992; Chomyn *et al.*, 1992; Sciacco *et al.*, 1994). How a threshold is exceeded is

less clear; however, it is thought that as mtDNA replicates independently of the cell cycle, and not all molecules are always replicated, mtDNA mutations can clonally expand within individual cells through the simple process of random genetic drift (figure 1-5) (Elson *et al.*, 2001).

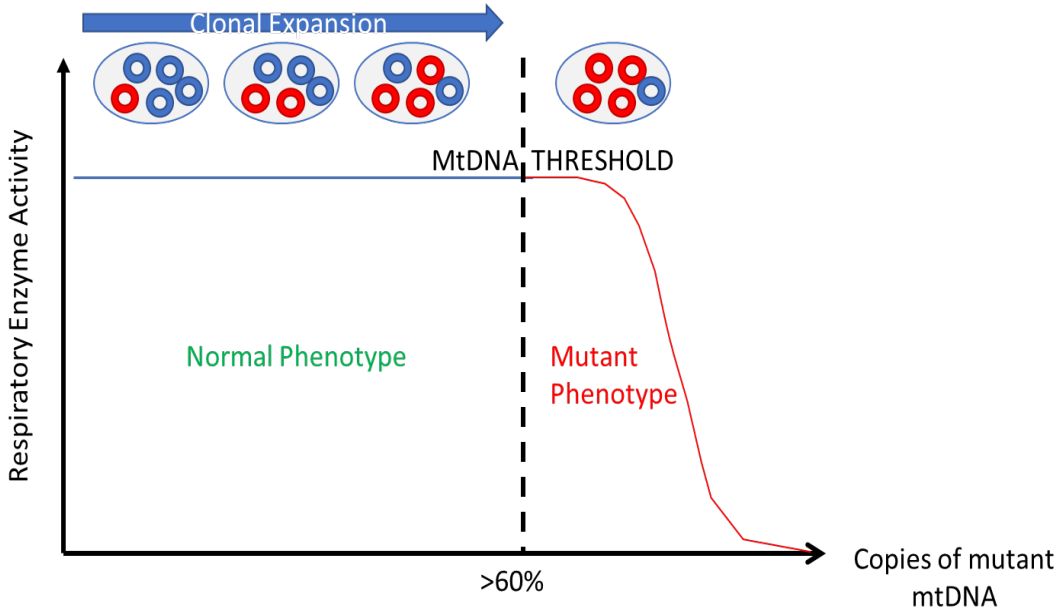

Figure 1-7: Heteroplasmic cells harbouring mutant mtDNA and the onset of a mutant phenotype when a threshold is exceeded. *Heteroplasmy is a state whereby a single cell harbours both normal and mutant mtDNA; cells may also exist as homoplasmic WTs (i.e. all normal mtDNA) or homoplasmic mutant states (all mutant mtDNA). Cells are able to tolerate the presence of mutant mtDNA until a certain threshold is reached (~60-85%), which in turn induces the onset of respiratory decline within the cell. Blue rings denote normal WT mtDNA; red rings denote mutant mtDNA. Adapted from Baines (2014).*

1.7.4 Mitochondrial Electron Transport Chain

Dubbed as 'cellular powerhouses of the cell', mitochondria are important arbitrators of energy metabolism through their part in the generation of high-energy adenosine triphosphate (ATP) molecules. The process by which is largely driven by the electron transport chain's (ETC) respiratory complexes (complexes I-IV) and ATP synthase (complex V) located on the IMM during the process of oxidative phosphorylation (OXPHOS) (figure 1-8). However, production begins prior within the cellular cytoplasm: glucose is catabolised in the presence of oxygen into pyruvate, the process of which leads to the generation of 2 ATP molecules and 2 electron carrier molecules nicotinamide adenine dinucleotide (NADH) that are subsequently transported into the mitochondrial matrix alongside pyruvate. Pyruvate is then converted to acetyl Coenzyme A (CoA) by decarboxylation, generating a further molecule of NADH and CO_2. Accordingly, CoA is a key substrate for the tricarboxylic acid cycle (TCA) cycle that occurs within the mitochondrial matrix, undergoing oxidation to CO_2, whilst coenzymes NAD+ and flavin adenine dinucleotide (FADH+) are reduced to functional carrier molecules NADH and $FADH_2$ during the cyclical breakdown of citrate. The process of TCA generates 10 NADH and 2 $FADH_2$ molecules that are fed into the ETC for the process of OXPHOS.

As previously highlighted, the OXPHOS system comprises five transmembrane protein complexes (complexes I-V) that form the ETC. Electrons from NADH and $FADH_2$ generated from glucose catabolism and the TCA cycle are transferred to oxygen at the ETC, initiating sequential reduction reactions at complexes I through to complex IV that result in proton (H^+ ion) translocation from the mitochondrial matrix to intermembrane space. This creates a ~150-180mV proton gradient membrane potential that encourages matrix proton flux *via* a hydrophilic passage across the IMM through complex V. Passage drives ATP synthesis, in which adenosine diphosphate (ADP) is phosphorylated to ATP, dependent on the bioavailability of ADP (Alberts *et al.*, 2002). Accordingly, when ADP:ATP ratios are high within the mitochondrial matrix, oxygen is consumed to execute ATP synthesis whilst simultaneously restoring the electrochemical gradient in a state III respiration state due to H^+ flux (Chance and Williams, 1955; Chance and Williams, 1956). Meanwhile low ADP:ATP is associated with low oxygen consumption and static H^+ flow across the IMM, known as state IV respiration (Chance, 1956). Synthesis is therefore

regulated by state III and IV respiration and the control of mitochondrial membrane potential. One ATP molecule is synthesised for every 3 protons that pass complex V (Alberts *et al.*, 2002).

- Glucose metabolism
- TCA Cycle

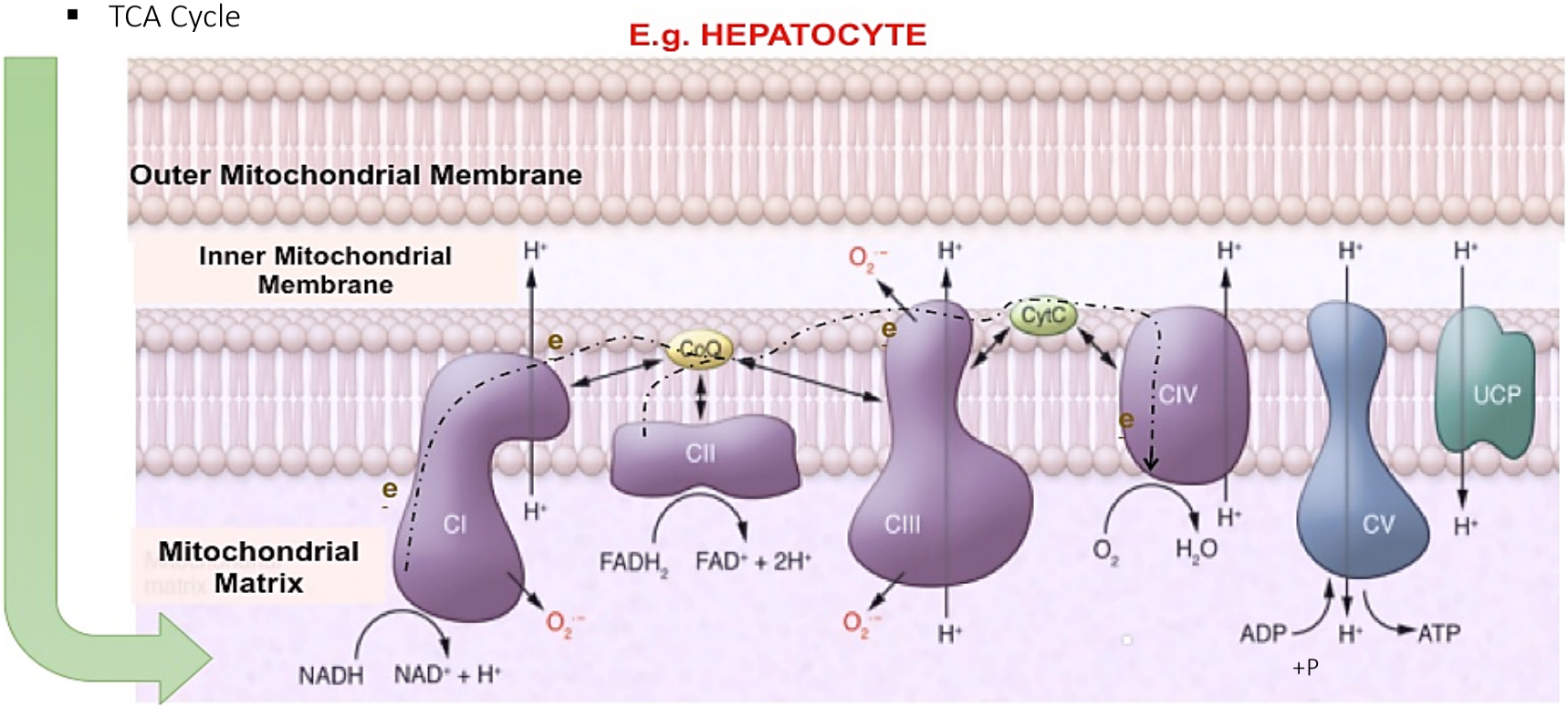

Figure 1-8: The Oxidative Phosphorylation System. *Mitochondrial DNA encodes 13 essential proteins which form enzymes complexes involves in mitochondrial respiration. Electrons (e) are donated to the electron transport train (ETC) by reduced carrier molecules nicotinamide adenine dinucleotide (NADH) and flavin adenine dinucleotide ($FADH_2$) formed during glucose and TCA cycle metabolism at the Complex I (via NADH) and Complex II (via $FADH_2$) site. Complex I catalyses reduction of NADH by transfer of electrons from ubiquinone (coQ) whilst complex II catalyses succinate oxidation to fumerate to catalyse the reduction of ubiquinone to ubiquinol using $FADH_2$. Subsequent oxidation of ubiquinol to ubiquinone occurs at complex III, during which protons are translocated across the inner mitochondrial membrane. Complex IV subsequently terminates the ETC by means of reducing oxygen to water by transfer of 4 electrons; proton translocation is also observed here. Translocation creates a difference in membrane potential, inducing proton flux through complex V. Comprising two components F_1 ATP synthase and F_0 proton translocator, the movement of protons down the electrochemical gradient converts ATP and inorganic phosphate (P_i) to high-energy ATP molecules. Adapted from Trifunovic and Larsson (2008).*

1.8 Mitochondria, Inflammation and Senescence in Ageing

Chronic low-grade systemic inflammation is a pervasive feature of human ageing, thought to result in the cumulative damage to macromolecules - referred to frequently as “inflammageing” (Chung *et al.*, 2009; Franceschi and Campisi, 2014). In the elderly, inflammageing is measured as a significant risk factor for morbidity and mortality, with several elevated markers of inflammation observed in age-associated pathologies (Saito and Papaconstantinou, 2001; Gomez *et al.*, 2010; Kim *et al.*, 2011). Inflammageing occurs in a sterile manner: specifically, the increasing prolonged release of “normal” endogenous molecules during cellular injury, recognised as damage associated molecular patterns (DAMPs) by pattern recognition receptors (PRRs) that are typically expressed on innate immune cells. This is consistent with the idea that low-grade inflammation with age arises from chronic stimulation of the inflammatory programme: indeed, circulating endogenous mtDNA, for example, is shown to increase in individuals aged 50 years and older, with highest plasma mtDNA in individuals coinciding with the greatest amount of IL-6, TNFα and RANTES (Regulated on Activation Normal T Cell Expressed and Secreted) proinflammatory cytokines (Pinti *et al.*, 2014). Similar exposure of these *in vivo* mtDNA concentrations to monocytes increases TNFα production, therefore suggesting unregulated mtDNA release with age may contribute to inflammageing (Pinti *et al.*, 2014).

1.8.1 Mitochondria and Inflammation

1.8.1.1 Mitochondria and proinflammatory signalling

Since mitochondria are known to be endosymbionts derived from bacteria, the release of mtDNA and other mitochondrial debris is unsurprisingly demonstrated to stimulate host inflammatory signalling. The cognate binding of mitochondrial-derived ligands to PRRs induces a wide variety of signalling pathways: for example, mtDNA is shown to bind to TLR9 and induce NF-κB signalling, of which proinflammatory cytokines form part of the downstream transcriptional programme (Bao *et al.*, 2016). The induction largely ascribed to CpG DNA motifs housed within the mitochondrial genome that make mtDNA bacterially homologous. Activation of other pathways are also noted, including the stimulation of the NOD-like receptor family pyrin domain-containing 3 (NLRP3) inflammasome that results in IL-1β and caspase-3 expression (Gurung *et al.*, 2015). Interestingly, NLRP3 activation is not solely limited to activation

via mito-DAMPs: extracellular ATP for example has been shown to activate the inflammasome and induce the proinflammatory response. ATP is subsequently implicated in previous studies of aberrant physiological inflammation as a key mechanism in initiating early innate immune responses (Bao *et al.*, 2016; Amores-Iniesta *et al.*, 2017).

Improper release of mtDNA and mito-DAMPs is thought to occur by increased cell death signalling (see section 1.7.2), with reported data showing induction of necroptotic cell death to activate the inflammasome and its downstream neutrophilic chemokine gradient following mitochondrial release of ATP (Iyer *et al.*, 2009; McDonald *et al.*, 2010). Similarly, the NLRP3 inflammasome is reported to be activated on apoptotic cell death by released oxidised mtDNA into the cytosol; in this respect, it is possible that increased mito-DAMP release may contribute to inflammageing (Shimada *et al.*, 2012). Accordingly, several studies provide correlative evidence of age-related changes in cell death signalling that provide such an opportunity: activity of apoptotic executioner caspases -2, -3, -6, -7 and -9, for example, is shown to increase in aging rat liver, lung and spleen (24-26 months) when compared to young (6 months) and middle aged (12-14 months) controls, whilst in post-mitotic hippocampal tissues increased caspase activity is observed in older murine groups (Lynch and Lynch, 2002; Zhang *et al.*, 2002). However, less is clear about necrotic cell death, although necroptosis activity of markers receptor-interacting serine/threonine-protein kinase 3 (RIPK3) and mixed lineage kinase domain-like protein (MLKL) are demonstrated to increase with age, at least in adipose tissue (Deepa *et al.*, 2018). It is therefore possible that in ageing, with increased cell death may come increased release of inflammatory inducing mito-DAMPs.

1.8.1.2 Mitochondria and redox signalling

Mitochondria are implicated in the production of ROS and are subsequently proposed to be a critical mediator in redox-sensitive proinflammatory pathways. As such, increasing evidence supports the notion, with studies previously demonstrating inflammatory pathway activation in response to a variety of ROS-mediated activities, whether directly or indirectly. Amongst them, intermediate ROS signalling is shown to activate the NF-κB-COX2 axis, as well as TLR9 and NLRP3 inflammasome signalling on release, inducing a downstream transcriptional programme of proinflammatory

cytokines chemotactic for immune cells (Ichimura *et al.*, 2003; Amma *et al.*, 2005; Zhou *et al.*, 2011; Jurk *et al.*, 2014). Consequently, mitochondrial dysfunction may be implicated in the stimulation of immune cell recruitment, including macrophages and neutrophils of the innate immunity arm (Chen *et al.*, 2018). Indeed, mtDNA induction of TLR9/NF-κB signalling, for example, is shown to induce apparent IL-6, IL-10 and TNFα cytokine release by activated macrophages, with an ensuing neutrophil infiltration thereafter within lung tissue during stimulation of a systemic inflammatory response (SIRS) (Zhang *et al.*, 2010). This proinflammatory-mediatory role may be further delineated during inhibition of respiratory function *via* TNFα or pharmacological inhibitors antimycin A or oligomycin, in which experimental disruption of mitochondrial respiratory enzymes exacerbates $O_2^{\cdot}$ production and incites an observable tissue phenotype that includes oxidative tissue damage, immune cell recruitment and cytokine expression in both human and murine models (Schulze-Osthoff *et al.*, 1993; Mariappan *et al.*, 2009; Vaamonde-Garcia *et al.*, 2012; Vaamonde-Garcia *et al.*, 2017). Subsequent inhibition of pro-oxidant signalling appears to alter the proinflammatory-phenotype, thereby supporting the role of oxidant signalling as a critical driver of inflammation (Ishihara *et al.*, 2015; Rehman *et al.*, 2016).

Of particular interest, mitochondrial dysfunction has also been shown to stimulate proinflammatory signalling as a consequence of augmented ROS generation and subsequent NF-κB induction. Earlier evidence appears to directly correlate ROS production to NF-κB activation, in which H_2O_2 is reported to activate IKK, as well as possibly promoting dimerisation of IKK with NEMO (Kamata *et al.*, 2002; Herscovitch *et al.*, 2008). Following inhibition of respiratory function by antimycin A, enhanced cell sensitivity to TNF-induced NF-κB cytotoxicity is also observed as a consequence of exacerbated ROS production (Schulze-Osthoff *et al.*, 1993). In this context, mitochondrial dysfunction and ROS would appear important together in the exacerbation of NF-κB mediated immune responses, with downregulation of ROS synthesising complex III subunit UQCRC2 shown to increase epithelial hypersensitivity and immune cell infiltration as a result of redox imbalance, whilst pharmacological inhibition of complex I is also shown to elicit similar effects of exacerbated ROS production and concurrent inflammatory signalling (Turrens and Boveris, 1980; Chen *et al.*, 2003; Aguilera-Aguirre *et al.*, 2009; Fato *et al.*, 2009). Conversely, such ROS NF-κB mediated inflammatory processes can be attenuated,

thereby supporting the role for mitochondrial dysfunction in redox proinflammatory signalling. For example, pharmacological inhibition of NF-κB with resveratrol and pyroolidinedithiocarbamate administration appears to reduce proinflammatory gene expression and monocyte adhesion in ageing rat blood vessels, in locations where both NF-κB and ROS levels were elevated significantly (Ungvari *et al.*, 2007). Meanwhile, murine ablation of the NF-κB p50 subunit appears to accelerate chronic inflammation and ageing due to absent p50-dimer repression of inflammatory genes and is proposed to cause inflammatory-mediated activation of the NF-κB-COX2 ROS-producing axis (Ungvari *et al.*, 2007; Jurk *et al.*, 2014).

Converse to the role of mitochondria serving as important mediators of proinflammatory signalling, a number of cytokines and oxidant signalling intermediates like nitrous oxide (NO) and peroxynitrite are able to disrupt normal mitochondrial function (Maneiro *et al.*, 2005). Amongst those discussed here are TNFα and IL-1β, which through binding to the complex I subunits is able to deplete ATP synthesis, as well as alter mitochondria membrane potential (Stadler *et al.*, 1992; Lopez-Armada *et al.*, 2006; Mariappan *et al.*, 2009). TNFα is also able to induce pronounced changes to mitochondrial morphology, including the loss of IMM cristae which arises from changes to mitochondrial dynamic mitofusion and mitofission proteins, at least in adipocytes (Chen *et al.*, 2010). Although the precise molecular mechanisms are not fully clear, these changes propose a role for inflammation to augment ROS levels observed experimentally. It is therefore possible that in ageing, chronic inflammatory stimulus induces mitochondrial decline, which in a vicious cycle is able to promote inflammageing. The origins of the inciting inflammation, however, are unclear, although are suggested either to be microbial in the case of infection, or sterile – in which one mechanism implicated is the development of dysregulated apoptosis or a role for the accumulation of senescent cells (see section 1.5.3).

1.8.2 Apoptosis

Programmed cell death or apoptosis is vital for organismal homeostasis and ensures the proper removal of damaged or dangerous cells from the body. Initially described by Kerr and colleagues (1972) in *C. elegans*, findings to date agree that apoptosis largely occurs in a caspase-mediated manner following their activation from their zymogen forms. As a result, apoptosis is characterised by a number of distinguishable morphological changes including chromatin condensation, cell shrinkage and ultimately the formation of apoptotic bodies for subsequent clearance (Elmore, 2007). The pro-apoptotic signalling process of which is understood to comprise two mechanistic parts: (1) extrinsic or death receptor-mediated apoptosis and (2) intrinsic apoptosis; carefully balanced by several pro- and anti-apoptotic factors to prevent improper induction or prevention of cell death.

Signalling pathways leading to apoptosis involve the ligand binding to corresponding surface membrane receptors that activate extrinsic pathway mechanisms. For example, FasL or CD95, binds to Fas, a death receptor often highly expressed in hepatic cell types (Leithauser *et al.*, 1993). Stimulation following ligand binding subsequently initiates a signalling cascade through activated membrane bound FADD and TRADD to induce recruitment of procaspase-8 and its downstream apoptotic effector caspase-3 (Hsu *et al.*, 1995; Kischkel *et al.*, 1995). In turn, extrinsic apoptosis appears to be regulated by cellular FLICE-inhibitory proteins (cFLIP), a caspase-8 homologous protein recruited to sequester the downstream signalling effects of caspase-8 (Scaffidi *et al.*, 1999; Wang and El-Deiry, 2003).

By contrast, mitochondria play an integral direct role in mediating the intrinsic pathway of apoptosis, through the release of several proapoptotic proteins from the intermembrane space. Amongst those is cytochrome *c,* with release occurring after permeabilisation of the mitochondrial outer membrane on inducible ligand binding or cellular stress (Kroemer *et al.*, 2007). Mediating mitochondrial permeabilisation and cytochrome *c* release is the BH3-domain only protein, Bid, which following truncation, translocates to the mitochondria and oligomerizes with the pro-apoptotic channel forming Bcl-2 proteins, Bak and Bax (Shimizu *et al.*, 1999). The resultant release of cytochrome *c* results in the activation and formation of the apoptosome comprising Apaf-1, cleaved apical procaspase-9 and cytochrome c proteins to induce cell death (Saelens *et al.*, 2004).

1.8.3 Mitochondrial Dysfunction and Senescence

Seminally discovered in primary human cells undergoing limited rounds of cell division by Hayflick and Moorehead (1961), senescence is a cellular state of permanent proliferative arrest, recently linked to ageing and inflammageing (Childs *et al.*, 2015). Senescent cells have multiple distinguishing characteristics from normal entities, including hypertrophy and telomere attrition, expression of cell cycle arrest proteins ($p16^{INK4a}$,p21 and p53), increased lysosomal hydrolase enzyme senescent-associated β-galactosidase activity (SA-β-Gal), and the upregulated expression of anti-apoptotic survival pathways (Dimri *et al.*, 1995; Alcorta *et al.*, 1996; Wong and Riabowol, 1996; Zindy *et al.*, 1997; Chen *et al.*, 2008). Moreover, senescent cells are associated with development of SASP, a senescent associated secretory phenotype comprising a transcriptional programme of growth factors, proteases and immune cell chemotactic factors, thought to have a limiting function *via* immune-cell mediated clearance of senescent cells within a variety of settings (Coppe *et al.*, 2010; Hoenicke and Zender, 2012; Demaria *et al.*, 2014). Predominantly activated by NF-κB signalling and maintained in an autocrine fashion by IL-1α, increased SASP is observed in a number of age-related pathologies including diabetes, atherosclerosis and hepatic steatosis (Childs *et al.*, 2016; Prattichizzo *et al.*, 2016; Ogrodnik *et al.*, 2017). Therefore in ageing models of senescence, inflammageing and ageing are causally linked: with formative work involving the periodic clearance of $p16^{INK4a}$-positive senescent cells to coincide with prolonged life and health span, attenuated proinflammatory signalling in the kidney and heart, as well as the reversal of pathogenesis, for example, in steatosis of the liver (Baker *et al.*, 2016; Ogrodnik *et al.*, 2017).

Cumulative evidence suggests that the induction of senescence and its secretory phenotype appears to be critically mediated by mitochondrial respiratory chain dysfunction. Indeed, senescent cells feature mitochondrial alterations that include decreased mitochondrial membrane potential, increased ROS production and increased mitochondrial mass: the selective removal of mitochondria was shown to ameliorate the senescent phenotype including mitochondrial ROS production (Moiseeva *et al.*, 2009; Correia-Melo *et al.*, 2016; Chapman *et al.*, 2019). In this context senescence is thought to be a downstream mechanistic effect of mitochondrial-induced oxidative stress and in which earlier steps to minimise ROS

species production delays cellular senescence (Packer and Fuehr, 1977; Chen *et al.*, 1995). Adding to this, ROS is shown to have a direct potentiating effect on senescent effector pathways including p16, p21 and p53 cell cycle mediators as a means to stabilise cell cycle arrest, with supporting evidence showing exacerbation of ROS following the stimulation of senescent cell cycle arrest (Macip *et al.*, 2002; Macip *et al.*, 2003; Takahashi *et al.*, 2006). The literature therefore appears to support the notion that mitochondrial dysfunction mediates the induction of senescence through exacerbated ROS production, in turn inducing a senescent associated phenotype and further stabilising permanent arrest through pro-oxidant signalling as part of SASP inventory.

Chapter 2 | Aims and Objectives

The principle aim of the project was to investigate the role of mitochondrial dysfunction and inflammation in ageing liver regeneration. Both mitochondrial dysfunction and chronic inflammation are key hallmarks in organismal decline: specifically, exacerbated inflammatory processes are implicated in hepatic pathophysiology, whilst the onset of mitochondrial dysfunction is noted to elicit a number of dysregulated physiological responses including stimulation of pro-oxidant, apoptotic and immune cell signalling. However, limited evidence has specifically linked these biological observations within the context of liver regeneration, also widely accepted to decline with age. The present study therefore aims to delineate the mechanistic link between mitochondrial dysfunction and hepatic regenerative decline.

Aim 1: *To further validate the core role of mitochondrial dysfunction in liver physiology with age, utilising a global progeroid PolgA$^{+/mut}$ and PolgA$^{mut/mut}$ mouse model, with the aim to identify the basal contribution and mechanisms behind mitochondrial dysfunction during age-associated tissue decline, specifically within the liver.*

Aim 2: *To determine the contribution of age-associated mitochondrial dysfunction in response to mechanical tissue injury and how this contributes to the liver's regenerative processes. PolgA$^{+/mut}$ mice will be aged before undergoing partial hepatectomy and markers of regeneration will be accessed to understand how PolgA accumulation of mtDNA mutations and subsequent mitochondrial respiratory dysfunction affects liver regeneration.*

Aim 3: *To investigate the relative contribution of oxidative stress during liver regeneration in the presence of mitochondrial dysfunction. Marks of cellular proliferation will be assessed in PolgA$^{+/+}$ (PolgA* WT) *and PolgA mice, following acute exposure to oxidative-stress induced CCl_4 toxic injury. By doing so, we hope to delineate the role of hypothesised mitochondrial reactive oxygen species in liver wound healing post-injury.*

Aim 4: *Investigate the relative contribution of mitochondrial dysfunction in inflammation and how this contributes to basal hepatocellular turnover and active liver regeneration. PolgA$^{+/+}$, PolgA$^{+/mut}$ and PolgA$^{mut/mut}$ mice will be assessed for inflammatory markers with age, as well as during regenerative models of injury.*

Chapter 3 | Materials and Methods

3.1 Mice and Models of Injury

3.1.1 Generation of *PolgA* mutator (*PolgA*$^{mut/mut}$) mice

Mitochondrial mutator mice (*PolgA*$^{mut/mut}$) were generated by knock-in insertion of the missense mutation (D257A) that changes aspartic acid to alanine within the second endonuclease proofreading domain into the *PolgA* catalytic subunit of the mtDNA polymerase gamma (Trifunovic *et al.*, 2004; Kujoth *et al.*, 2005). Mutator mice colonies were initially established from *PolgA*$^{+/mut}$ males (n=4) kindly donated by Tomas Prolla, Departments of Genetics and Medical Genetics, University of Wisconsin, Madison, USA and mated with C57Bl/6J female pure wild-type mice to generate *PolgA*$^{+/mut}$ female and *PolgA*$^{+/mut}$ male mice. Colonies were propagated and subsequently maintained in house to generate *PolgA*$^{+/mut}$ and *PolgA*$^{mut/mut}$ mice (figure 3-1). Mice were housed in accordance with the UK Animals Scientific Procedures Act, 1986 with 12-hour light/dark cycles at 25^{o}C. All injury models were performed under a UK Home Office licence on male C57BL/6J background (*PolgA*$^{+/+}$; WT), *PolgA*$^{+/mut}$ and *PolgA*$^{mut/mut}$ mice and following approval from the Newcastle Ethical Review Committee.

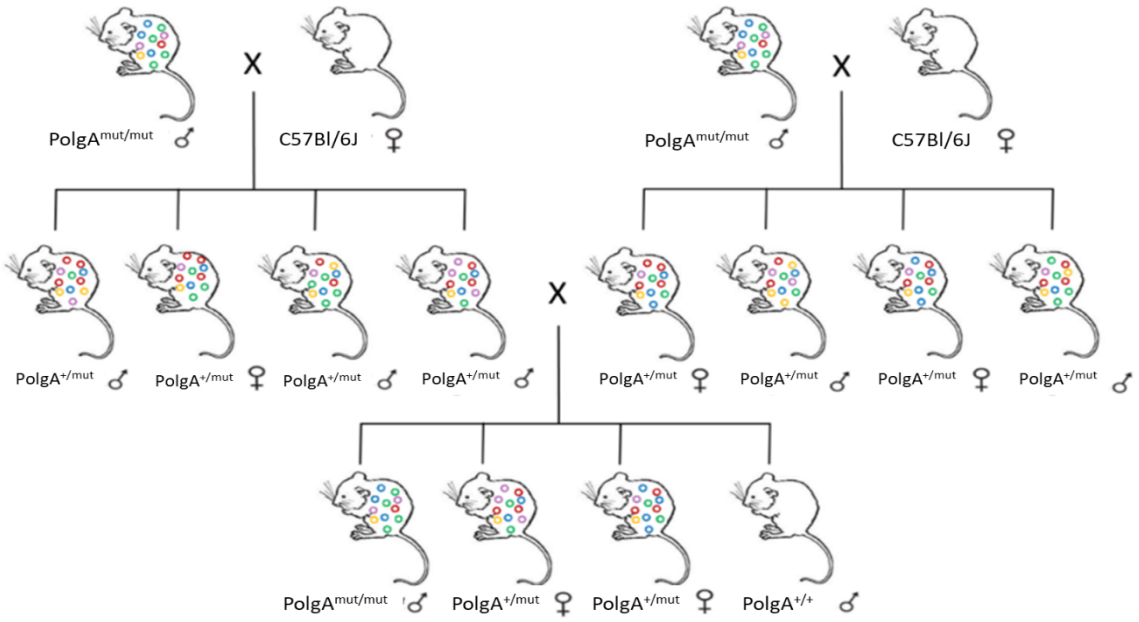

Figure 3-1: Breeding strategy for PolgA$^{+/+}$ (WT), PolgA$^{+/mut}$ and PolgA$^{mut/mut}$ mice *(Taken from Baines, 2014). Initial establishment of colony required mating of Polg$^{mut/mut}$ male mice with a C57Bl/6J WT female to generate PolgA$^{+/mut}$ progeny. Mating of PolgA$^{+/mut}$ males and PolgA$^{+/mut}$ females enabled propagation and sustenance of PolgA$^{+/+}$ (PolgA WT), PolgA$^{+/mut}$ and PolgA$^{mut/mut}$ mice.*

3.1.2 Isolation of genomic DNA for mouse genotyping

Genotyping of *PolgA* WT, *PolgA*$^{+/mut}$ and *PolgA*$^{mut/mut}$ mice was carried out from amplified genomic DNA extracted from mouse ear biopsies. Ear punches were digested at 55^{o}C overnight in digestion buffer comprising 50 mM KCl, 1 mM Tris-HCl (pH 9.0), 0.1% Triton X-100 and 0.4 mg/ml Proteinase K. Sample mixture was subsequently heated to denature the Proteinase K at 94^{o}C and centrifuged at full speed for 15 minutes. Supernatant was subsequently used for PCR amplification of genomic DNA.

3.1.3 PCR of genomic DNA

Genotypes of *PolgA* WT, *PolgA*$^{+/mut}$ and *PolgA*$^{mut/mut}$ was determined by amplification of *PolgA* genomic DNA under specific primer sequences (table 3-1) by polymerase chain reaction (PCR) using Veriti Thermal Cycler (ThermoFisher Scientific). PCR reaction mixture comprising 2.5 µl EDTA-Tris Buffer, 2.5 µl dNTPs, 1 µl of each 10 µM forward and reverse primer, 0.25 µl ExTaq (Takara) and nuclease free water to make a total volume of 23 µl. PCR amplification of genomic DNA was performed using the reaction template of 1 minute at 94^{o}C for DNA polymerase activation within ExTaq solution followed by 35 cycles of the following: 94^{o}C for 20 seconds, annealing at 64^{o}C for 30 seconds and elongation at 72^{o}C for 45 seconds. This was followed by a final elongation for 5 minutes at 72^{o}C. Mouse genotyping bands were determined by visualising amplified polymerase chain reaction (PCR) products onto a 2% agarose gel containing 0.01% ethidium bromide (appendix I).

Table 3-1: Genotyping primer sequences for mice

Primer	Primer Sequence
PolgA Forward	5'-GCCTCGTTTCTCCG-3'
PolgA Reverse	5'-GGATGTGGCCCAGGCTGTAACTCA-3'

3.1.4 Partial hepatectomy

Median laparotomy and resection of the left lateral and medial lobes (70%) were performed on WT, *PolgA*$^{+/mut}$ and *PolgA*$^{mut/mut}$ mice at 3 (n=≥3) and 6 (n=≥3) months of age following isofluorane anesthetisation. Excised lobes were weighed and subsequently processed for both RNA and protein extraction and immunohistochemical analysis by snap freezing and fixing tissue in 10% PBS buffered formalin (Sigma) respectively. Mice were monitored daily and kept in a heated cabinet at 27^{o}C until harvest at 48 hour and 72 hour post-surgery. 2 hours prior to harvest, mice were singly injected with 5-chloro-2'-deoxyuridine thymidine-labelling analogue at 100ug/g; mice were then humanely killed and blood samples collected. Liver tissues were harvested for subsequent RNA, Protein and immunohistochemical analysis. Naïve control groups received anaesthetisation and median laparotomy only.

3.1.5 Acute carbon tetrachloride injection

Mice were injected with a single dose of carbon tetrachloride (CCl_4) intraperitoneally at 2 µl/g body weight (CCl_4: olive oil at 1:1 [vol/vol] to induce acute liver injury. Mice were monitored daily and kept incubated at 27^{o}C until harvest either 48 hours or 5 days post-injection. Mice were subsequently humanely killed and liver tissues excised for fixing in 10% PBS buffered formalin for histology and snap freezing in liquid nitrogen for RNA and protein analysis. Control groups received olive oil as a vehicle control.

3.2 Cell Culture

3.2.1 Isolation of primary mouse hepatocytes

Primary mouse hepatocytes were isolated as previously described in Gieling and colleagues (2010). Female WT, *PolgA*$^{+/mut}$ and *PolgA*$^{mut/mut}$ were administered ketamine/xylaxine overdose and livers perfused with Krebs-ringer bicarbonate buffer (Sigma) supplemented with 0.1 mM EDTA. Livers were digested *in situ* with Krebs-ringer bicarbonate buffer (Sigma) supplemented with 50 mg/ml *Clostridium histolyticum* collagenase (Sigma) and 0.15 mM $CaCl_2$ and subsequently excised into EDTA-supplemented Krebs-ringer buffer. The bile duct was separated from liver and the liver capsule ruptured to allow hepatocytes to disperse. Cells were filtered, washed twice in Krebs-ringer bicarbonate buffer and resuspended into William's

medium E culture media (WME; Gibco) *via* centrifugation at 500rpm for 2.5 minutes. *WME:* William's media E (Gibco), 10% FCS, 100 U/ml penicillin (Lonza), 100 µg/ml streptomycin (Lonza), 2 mM glutamine, 2 mM pyruvate (Lonza). Hepatocytes were plated into 6 and 96-well tissue culture plates (Greiner) pre-coated with rat tail collagen (50 µg/ml 0.02 M acetic acid, 1 hour, RT; ThermoFisher Scientific) and incubated at 37^{o}C, 5% CO_2 for 4 hours to allow cells to adhere. Following incubation, cells were washed in 1 x DPBS (Lonza) and serum starved overnight: WME was replaced with low serum WME supplemented with 0.5% FCS and incubated for 16 hours at 37^{o}C, 5% CO_2 for subsequent analysis.

3.2.2 Isolation of primary mouse hepatic stellate cells

Primary mouse hepatic stellate cells (HSCs) were isolated from excised livers of female WT, *PolgA*$^{+/mut}$ and *PolgA*$^{mut/mut}$ mice, perfused *in vivo* with HBSS+ (with Ca^{2+} and Mg^{2+}). In sterile conditions, livers were homogenised in HBSS+ (Lonza) supplemented with 10 mg/ml pronase I (Roche), 3 mg/ml collagenase B (Roche) and washed with 10 mg/ml DNase (Roche) in HBSS+ *via* a 125 µm nybolt mesh. Flow through was suspended in HBSS+, centrifuged at 1800 rpm for 7 minutes and resultant cell pellet resuspended in DNase-HBSS+ media for further centrifugation. Final pellet was resuspended in 11.5% Optiprep-HBSS+ mixture and HSCs isolated by density gradient centrifugation at 1500 g for 23 minutes (acceleration 7, deceleration 2). A resultant cell layer containing HSCs was carefully collected, resuspended in DNase-HBSS+ media and centrifuged at 1800 rpm, 7 minutes. Pelleted cells were resuspended in Dulbecco's modified Eagle's medium (DMEM) supplemented with 16% fetal calf serum (Biosera), 100 U/ml penicillin (Lonza), 100g/ml streptomycin (Lonza), 2 mM glutamine and 1 mM pyruvate and seeded onto a T75 flask (Greiner Bio-One) for 20 minutes incubation at 37^{o}C, 5% CO_2 to allow separation of Kupffer cells. Flasks were washed to remove non-adherent HSCs and re-seeded onto fresh T75 flasks. HSCs were maintained at 37^{o}C, 5% CO_2 overnight and medias changed the following morning to remove cell debris; culture media was subsequently replaced every 2-3 days. Day 0 freshly isolated HSCs were considered quiescent and maintained until harvest approximately 7-10 days post-isolation - at which point they were considered activated.

3.2.3 Isolation of liver neutrophils

WT, *PolgA*$^{+/mut}$ and *PolgA*$^{mut/mut}$ mice were humanely killed and livers removed. Livers were then placed into a 10cm cell culture dish (Greiner) containing HBSS+ (with Ca^{2+} and Mg^{2+}) supplemented with 3 mg/ml Collagenase (Roche) and 10 mg/ml DNase (Roche) and mechanically disrupted. Cells were filtered through a 40 µM cell strainer and centrifuged at 800g for 5 minutes, 4^{o}C. Liver neutrophils were isolated by percoll gradient (33% vol/vol), centrifuged 800g for 30 minutes, RT and supernatant collected. Cells were washed and resuspended in 500 µl FACs buffer (1 x PBS supplemented with 5% serum) and purity established by Ly6G, CD11b and CD45B (BD Biosciences) flow cytometry (BD FACScantoII).

3.2.4 Isolation of bone marrow neutrophils

Bone marrow was extracted from femurs and tibias taken from WT, *PolgA*$^{+/mut}$ and *PolgA*$^{mut/mut}$ mice and flushed with 1x HBSS-Prep. Briefly, 8 x HBSS-Prep: 10 x PBS (without Ca^{2+} and Mg^{2+}), 2M HEPES (appendix II) buffer supplemented with 0.5% FCS, diluted from 8x to 1x using sterile distilled water. Extracted marrow was pelleted at 400g, 5 minute RT and red blood cells lysed in 0.2% and 1.6% saline gradients respectively. Cells were filtered through a 70 µM cell strainer and suspension centrifuged at 400g, for 5 minutes at RT. Supernatant was collected and neutrophils isolated by percoll gradient (62%). Isolated neutrophils were washed and resuspended in assay medium of choice for subsequent analysis.

3.3 Liver Culture Assays

3.3.1 Hepatocyte BrdU proliferation assay

Primary hepatocytes were seeded in 96 well plates (Greiner) at a density of 1 x 10^4 cells/well in WME supplemented with 10% FCS and incubated for 4 hours at 37^{o}C, 5% CO_2 to allow cells to adhere. Cells were washed in 1 x DPBS (Lonza) and serum starved for 16 hours as above. Concentrations of epithelial growth factor (EGF; Sigma) treatments at 5, 50 and 250 ng/ml were added to hepatocytes and cells allowed to incubate at 37^{o}C, 5% CO_2 for a further 1 hour. BrdU labelling solution 10 µM (BrdU colorimetric assay, Roche) was added to hepatocytes and incubated for 24 hours at 37^{o}C, 5% CO_2. Hepatocytes were subsequently fixed in 200 µl FixDenat solution for 30 minutes RT and anti-BrdU-POD working solution diluted 1:100 added. Cells were washed twice in 1 x PBS and colorimetrically detected at 450nm

spectrophotometrically following addition of 100 µl substrate solution and 1 M H_2SO_4 to hepatocytes.

3.3.2 Hepatocyte Alamar Blue assay

Cell viability and cytotoxicity was determined by the reduction of oxidised redox indicator resazurin (Sigma) to resorufin *via* Alamar Blue assays (White *et al.*, 1996; Vega-Avila and Pugsley, 2011; Rampersad, 2012). Primary hepatocytes were seeded in 96 well plates (Greiner) at a density of 1 x 10^4 cells/well, allowed to adhere for 4 hours, washed in 1 x DPBS (Lonza) and serum starved 16 hours overnight in 0.5% FCS supplemented WME as above. Cells were treated with EGF (Sigma) at 5, 50 and 250 ng/ml for a further 24 hours and media replaced with 100 µl/well warmed Resazurin solution diluted 1:100 in low serum culture media. Briefly, Resazurin salt (Sigma) stock was dissolved in PBS and sodium hydroxide at pH 7.4 and sterile filtered at a concentration of 880 mM. Hepatocytes were incubated for a further 3 hours, 37^{o}C, 5% CO_2 and kept out of direct light. Supernatants were harvested in duplicate and transferred to a black 96 well plate (Corning) for spectrophotometric measurement at 535/595 nm and analysed with SoftMax® Pro software.

3.3.3 LDH cytotoxicity assay

Aliquots of culture media were transferred (~50 µl) into 96 well plate (Greiner) during each media change; culture media was centrifuged at 400g for 3 minutes and supernatants harvested. Harvested aliquots were transferred to a flat bottomed 96-well plate (Corning) for enzymatic analysis. Lactate dehydrogenase (ThermoScientific) was performed on cell supernatants: assay reaction mixture was prepared by mixing LDH assay buffer (0.6ml) with substrate mix (11.4 ml) and kept out of direct light. Assay mixture was added in equal amount to supernatants (25 µl LDH mix to 25 µl sample) and incubated at 30 minutes RT in the dark. The assay was terminated by adding 25 µl stop solution and the absorbance at 490 nm was measured spectrophotometrically. Background absorbance was measured at 690 nm and subtracted from primary wavelength measurement.

3.4 RNA and Protein Lysis

3.4.1 Cell lysis

Primary cells were washed twice in 1 x DPBS (Lonza) and lysed for RNA extraction *in vitro* on addition of 350 µl RLT Buffer (Qiagen) supplemented with 1% 2-β-mercaptoethanol (Sigma). Culture plates were agitated by plate rocker and allowed to lyse for 5 minutes. An equal volume of 70% ethanol was added to plates and RNA isolated from lysed cells using the RNeasy Plus Mini Kit (Qiagen) as per manufacturer's instructions. Resulting RNA was eluted into Rnase-free water and quantified using a Nanodrop 2000c spectrophotometer. RNA samples were stored at -80^{o}C.

For protein, primary cells were washed twice in 1 x DPBS (Lonza) and 300 µl RIPA lysis buffer (appendix III) containing protease inhibitors (Roche) was added to culture plates. Cells were mechanically disrupted by cell scraper and lifted cells transferred to 1.5 ml Eppendorfs (Starlab). Homogenate was sonicated for 20 minutes and subsequently pelleted by cold centrifugation, 10 minutes 10,000rpm. Supernatant was harvested for further protein analysis.

3.4.2 RNA isolation from frozen liver tissue

In round bottomed Eppendorfs containing a single 7 mm stainless steel bead, frozen liver samples was added to 350 µl RLT Buffer (Qiagen) supplemented with 1% 2-β-mercaptoethanol (Sigma) and homogenised using a Qiagen TissueLyser II, 20.0 1/S frequency, 2 x 2 minutes. Tissue lysate was transferred through Qiashredder columns for homogenisation at ≥ 8000 x g for 15 seconds; RNA was subsequently isolated using the RNeasy Plus Mini Kit (Qiagen) as per manufacturer's instructions. Briefly, liver homogenate was transferred to RNeasy spin columns and centrifuged at ≥ 8000 x g for 15 seconds. Flow through was discarded and sample washed further with buffer RW1 at ≥ 8000 x g for 15 seconds and then buffer RPE twice at ≥ 8000 x g for 2 minutes, discarding flow through each time. Column was dried to remove remaining ethanol contaminates at full speed for 1 minute. RNA was eluted into fresh collection tube from column by adding directly to membrane 30-50 µl RNase-free water and spun ≥ 8000 x g for 1 minute. Extracted RNA was quantified using a Nanodrop 2000c spectrophotometer and samples stored at -80^{o}C.

3.4.3 RNA quantification by Nanodrop

Isolated RNA was quantified and purity assessed spectrophotometrically using a nanodrop 2000 spectrophotometer at 260 nm and 280 nm wavelength; nanodrop was blanked with a loaded 1 µl RNase free water sample prior to measurement. Acceptable purity of RNA samples was indicated as an A260/A280 ratio greater than 1.8.

3.4.4 Protein extraction from frozen liver tissue

In round bottomed Eppendorfs containing a single 7 mm stainless steel bead, frozen liver samples were lysed in 500 µl RIPA lysis buffer, homogenised *via* a Qiagen TissueLyser II, 20.0 1/S frequency, 2 x 2 minutes and followed by sonication for 20 minutes. Tissue homogenate was pelleted by cold centrifugation, 10 minutes at 10,000 rpm and supernatant collected for protein analysis.

3.4.5 Protein quantification for protein-based assay

Protein concentration was quantified using the BioRad Protein Assay Kit as per manufacturer's instructions and measured spectrophotometrically at 750 nm wavelength. Briefly, 2 µl of protein sample or control buffer sample was diluted 1:10 in distilled water and added to 100 µl of mixture comprising 98 µl buffer A and 2 µl buffer S. 800 µl of buffer B was added and samples incubated at room temperature for 20 minutes to allow for colour change. Protein concentration was determined at 750 nm by spectrophotometry and absorbance value divided by coefficient 0.0157 and then 2 to determine concentration in µg/µl.

3.5 Western Blotting

Protein samples for western blot were prepared as follows: 20 µg of protein lysate was diluted in 1 x Laemelli buffer (2% SDS, 0.06 M Tris-HCl 5% β-mercaptoethanol, 10% glycerol and bromophenol blue) denatured at 95^{o}C for 5 minutes. Protein was then fractionated by 12% SDS-PAGE and blotted onto nitrocellular membranes. Membranes were blocked for 1 hour with 5% milk powder in TBS-Tween and incubated with primary antibodies (table 3-2), 4^{o}C overnight. Membranes were subsequently washed in TBS-T, incubated for 1 hour with HRP-conjugated secondary antibodies (table 3-2) and washed again; specific antigens were detected on addition of enhanced-chemiluminescence (ECL; Amersham Biosciences).

3.6 cDNA synthesis and standard PCR gel electrophoresis

cDNA synthesis was carried out by Promega Reverse Transcription System: 1 µl of DNase was added to 500-1000 ng of RNA in a 1:1 ratio with DNase buffer, incubated at 37^{o}C, 30 minutes and DNase activity terminated on incubation with 1 µl stop solution and for 2 minutes, RT. Per every 1000 ng RNA extracted, 1 µl random hexamer primers (Promega) was added and incubated for 5 minutes, 70^{o}C and transferred immediately to ice. Intermediary products were subsequently added to a 6.5 µl real-time (RT) mix comprising 4 µl MMLV RT buffer, 1 µl Moloney Murine Leukaemia Virus Reverse Transcriptase (MMLV), 0.5 µl RNasin, 1 µl dNTPs (all reagents Promega) and incubated for 1 hour at 42^{o}C. Synthesised cDNA was stored at -80^{o}C.

Selective nucleotide sequence amplification was carried out by PCR using a 2720 Geneamp thermal cycler (Applied Biosystems). PCR amplification was facilitated by DreamTaq master mix comprising DNA polymerase, $MgCl_2$, dNTPs and optimised buffer. A total volume reaction for PCR of 25 µl was mixed: comprising 2 µl of 10 ng/µl cDNA, 12.5 µl X2 Dreamtaq master mix (ThermoFisher), 1 µl of corresponding 10 µM forward and reverse primer and nuclease water. PCR amplification of sequences was carried out at varying annealing temperatures 55-60^{o}C, with thermocycling reaction template comprising the following steps: 5 minute polymerase activation step at 95^{o}C, followed by 28 cycles of 30 second denaturation of cDNA at 95^{o}C, annealing for 45 seconds and extension at 72^{o}C for 60 seconds, followed by a final 10 minutes at 72^{o}C. Amplified PCR products were visualised by gel electrophoresis, in which samples were diluted 1:6 and mixed with 6 x Blue/Orange Loading Dye (Promega). Samples were loaded onto a 2% agarose gel and ran at 100 V for approximately 30 minutes. Nucleotide products were visualised by UV transilluminator alongside PCR molecular weight markers (Promega).

Table 3-2: Antibodies for western blot

Primary Antibodies					
Antigen	Antibody	Company	Source	Dilution	Code
GAPDH	Polyclonal	Abcam	Rabbit	1:2000	ab22555
β-actin	Polyclonal	Sigma	Mouse	1:1000	A2228
NDUFB8	Monoclonal	Abcam	Mouse	1:2000	ab110242
SDHB	Monoclonal	Abcam	Mouse	1:200	ab14714
ATPB	Monoclonal	Abcam	Mouse	1:2000	ab14730
UQCRC2	Monoclonal	Abcam	Mouse	1:1000	ab14745
Mt-CO1	Monoclonal	Abcam	Mouse	1:2000	ab14705
Cytochrome P450 2E1	Polyclonal	Abcam	Rabbit	1:5000	ab28146
αSMA	Monoclonal	Sigma	Mouse	1:1000	A2547
CDKN2A/p16	Polyclonal	BioRad	Rabbit	1:500	AHP1488
4HNE	Monoclonal	JaICA	Mouse	1:500	MHN-020P
Cyclin A2	Monoclonal	Cell Signalling	Mouse	1:1000	4656
Cyclin B1	Polyclonal	Cell Signalling	Rabbit	1:1000	4138
Cyclin D1	Monoclonal	Cell Signalling	Rabbit	1:1000	2978
Cyclin D2	Monoclonal	Cell Signalling	Rabbit	1:1000	3741
Cyclin D3	Monoclonal	Cell Signalling	Mouse	1:1000	2936
Cyclin E1	Monoclonal	4129	Mouse	1:1000	4129
Cyclin E2	Polyclonal	4132	Rabbit	1:1000	4132
Cyclin H	Polyclonal	2927	Rabbit	1:1000	2927
Secondary Antibodies					
Primary Mouse Ab	Anti-mouse HRP	Sigma	Goat	1:2000	A4416
Primary Rabbit Ab	Anti-rabbit HRP	Cell Signalling	Horse	1:2000	7074

3.7 qRT-PCR

Oligonucleotide primers were designed using Primer Blast analysis software for exon coding regions of nuclear-encoded genes (table 3-3). Qualitative PCR tested primer specificity at 10 µM concentration. For quantitative real time PCR (qRT-PCR), cDNA samples were diluted to 10 ng/µl and added to 0.5 µM forward and reverse primer, 6.5 µl SyBR Green Jumpstart (Sigma) and nuclease-free water. Quantitative analysis for each gene primer was carried out on an Applied Biosystems 7500 Fast Real-time PCR machine at various annealing temperatures 53-60^{o}C. The reaction template comprised a 10 second polymerase activation step at 95^{o}C followed by a 95^{o}C denaturation step, 5 seconds, annealing for 1 minute and extension at 72^{o}C. For mitochondrial-encoded genes (table 3-4), qRT-PCR was performed on an Applied Biosystems StepOne Real-time PCR machine and analysed by means of the TaqMan Gene Expression Assay (Applied Biosystems). 25 ng cDNA was added to a 20 µl reaction comprising, 10 µl 2 x TaqMan Gene Expression Mastermix No AmpErase UNG, RNase-free water and Taqman probes for mitochondrial genes (table 3-4). Reaction was run as 10 minutes 95^{o}C activation step, 40 cycles of 15 seconds cDNA denaturation and 20 second 60^{o}C step to allow for the annealing of TaqMan probes. Template temperatures of 95^{o}C 15 seconds, 60^{o}C 1 minute and 95^{o}C 15 seconds calculated a dissociation curve from which relative expressions were analysed by means of the $2^{-\Delta CT}$ method. CT values for the gene of interest were normalised to the reference housekeeping genes by calculating $\Delta CT^{(\text{gene of interest} - \text{housekeeping gene})}$. Mean changes in experimental groups were adjusted to the *PolgA* WT groups using POWER(2, [housekeeping gene-target gene]).

Table 3-3: Validated qRT-PCR mouse primer sequences

Gene	Forward Sequence	Reverse Sequence	Annealing Temperature (^{O}C)
GAPDH	CACAGTCAAGGCCGAGAAT	GCCTTCTCCATGGTGGTGAA	57
KC / CXCL1	CTGGGATTCACCTCAAGAACATC	CAGGGTCAAGGCAAGCCTC	60
MIP2a / CXCL2	CCAACCACCAGGCTACAGG	GCGTCACACTCAAGCTCTG	60
TNFα	GACCAGGCTGTCGCTACATCA	CGTAGGCGATTACAGTCACGG	57
IL-6	ACCAGAGGAAATTTTCAATAGGC	TGATGCACTTGCAGAAAACA	58
S100A9	CACCCTGAGCAAGAAGGAAT	TGTCATTTATGAGGGCTTCATTT	55
MCP1	AGGTCCCTGTCATGCTTCTG	TCTGGACCCATTCCTTCTTG	55
RANTES	TGCTGCTTTGCCTACCTCTCC	TGGCACACACTTGGCGGTTCC	55
αSMA	TCAGCGCCTCCAGTTCCT	AAAAAAAACCACGAGTAACAATCAA	60
COL1A1	TTCACCTACAGCACGCTTGTG	GATGACTGTCTTGCCCCAAGTT	57
TIMP1	GCAACTCGGACCTGGTCATAA	CGGCCCGTGATGAGAAACT	57
TGFβ	CTCCCGTGGCTTCTAGTGC	GCCTTAGTTTGGACAGGATCTG	57
SOD1	GAGACCTGGGCAATGTGACT	GTTTACTGCGCAATCCCAAT	60
SOD2	CCGAGGAGAAGTACCACGAG	CCGAGGAGAAGTACCACGAG	60
GSS	GCCTCCTACATCCTCATGGA	CCACATGCTTGTTCATCACC	60
GPX	ACTACACCGAGATGAACGA	GACGTACTTGAGGGAATTCAG	57

Table 3-4: qRT-PCR Taqman probes for mitochondrial genes

Gene	Company	Code	Annealing Temperature (^{O}C)
beta-2-globulin	ThermoFisher Scientific	Mm00437762_m1	60
ND1	ThermoFisher Scientific	Mm04225274_s1	60
ND4	ThermoFisher Scientific	Mm04225294_s1	60
COX1	ThermoFisher Scientific	Mm04225243_g1	60
COX3	ThermoFisher Scientific	Mm04225261_g1	60
ATP6	ThermoFisher Scientific	Mm03649417_g1	60
TOMM20	ThermoFisher Scientific	Mm01609022_g1	60
Cytochrome b	ThermoFisher Scientific	Mm00439560_m1	60

3.8 Serum aminotransferase assays

Blood samples were collected from sacrificed WT, *PolgA*$^{+/mut}$ and *PolgA*$^{mut/mut}$ mice and incubated at room temperature for 20 minutes to allow for blood clotting. Samples were centrifuged at 8000g for 15 minute, room temperature and supernatant serum collected; samples were stored at -80^{o}C. For analysis, alanine aminotransferase activity assays (AST Assay; Sigma) were kindly performed by Ms. Hannah Paish. Serum samples were diluted 1:8 and added to 25 µl of reaction mix per well of a 96 well plate comprising: 20 µl AST assay buffer, 0.5 µl AST enzyme mix, 2 µl AST developer and 2.5 µl AST substrate. Assay plate was mixed, incubated in dark at 37^{o}C for 3 minutes and initial absorbance determined at 450 nm ($(A_{450})_{Initial}$). Final absorbance ($(A_{450})_{Final}$) was measured following 15 minutes further incubation, in dark at 37^{o}C and difference from (A_{450}) initial calculated. Standards for assay were generated as follows from manufacturer's glutamate standard solutions as follows (table 3-5):

Table 3-5: Standards for serum AST assay

Standard	mM		Assay Buffer
1	1	5µl Std solution	495µl
2	0.8	400µl of 1mM	100µl
3	0.6	375µl of 0.8mM	125µl
4	0.4	333µl of 0.6mM	167µl
5	0.2	250µl of 0.4mM	250µl
6 (Blank)	0	0	500µl

Concentration of serum AST was determined from equation:
[AST = B x sample dilution factor/ reaction time x V], where B denotes amount of glutamate generated between initial and final A_{450}; reaction time is time of assay reaction and V denotes sample volume (mL).

3.9 Staining

3.9.1 Haematoxylin and Eosin (H&E) staining

Formalin fixed tissue was paraffin-embedded and cut *via* a microtome onto slides at 4 µm at least 2 hours prior to staining. Slides were deparaffinised; 2 x 5 minutes in clearene, 5 minutes in 100% ethanol, 5 minutes in 70% ethanol, and placed into tap water. Sections were incubated for 2-5 minutes in Mayer's haematoxylin (Sigma) followed by 30 seconds in Scotts water. Slides were counterstained 2-3 minutes in eosin and washed in tap water. Slides were briefly dehydrated in increasing alcohol grades and mounted in Pertex (Histolab).

3.9.2 Dual Cytochrome c Oxidase (COX) / Succinate Dehydrogenase (SDH) Histochemistry

Frozen liver (µm) tissue sections were cryosectioned onto glass slides and dried for at least 1 hour, RT prior to staining. Sections were incubated in 50 µl COX medium at 37^{o}C for 8 minutes; stock media comprising 500 µM cytochrome *c* 0.2 M phosphate buffer pH 7.0, diluted 1 in 5 with 3,3' diaminobenzidine tetrahydrochloride (DAB; 5 mM DAB in 0.2 M phosphate buffer pH 7.0) and supplemented with 20 µg/ml catalase (Sigma). Sections were washed 2 x 5 minutes in 3 x PBS and 50 µl SDH medium added to sections. SDH medium: 800 µl NitroBlue tetrazolium (NBT; 1.5 mM NBT in 0.2 phosphate buffer pH 7.0), 100 µl phenazine methosulphate (PMS; 2 mM PMS in 0.2 phosphate buffer pH 7.0), 100 µl sodium succinate (1.3 M sodium succinate in phosphate buffer pH 7.0) and 10 µl sodium azide (100 mM sodium azine in 0.2 phosphate buffer pH 7.0). SDH media was removed from section by washes 3 x 5 minutes in 1 x PBS and dehydrated *via* increasing alcohol gradient and two concentrations of Histoclear (National Diagnostics, Atlanta, USA). Slides were mounted in DPX.

3.9.3 Immunohistochemistry

Formalin fixed tissue was paraffin-embedded and cut onto slides at 4 µm by microtome at least 2 hours prior to staining. Slides were deparaffinised and rehydrated in clearene and graded alcohols as above before incubating in 3% hydrogen peroxidase (Sigma)/methanol, 15 minutes RT. Antigens specific to each antibody (table 3-6) were retrieved by various methods. Briefly, slides requiring a 0.01% pronase (BioScientific) were incubated for 20 minutes at 37^{o}C whilst sections

requiring antigen retrieval in Vector Unmasking solution (Vector Laboratories), 10 mM Sodium Citrate Buffer pH 6 or 1 mM EDTA pH 8 were heated in a microwave for 15-25 minutes at 600W (table 3-6). Slides were allowed to cool and blocked for 20 minutes, RT with avidin/biotin (Vector Laboratories), washing slides in 1 x PBS between each step. Sections were blocked with either 20% swine serum or 1 x casein for 45 minutes prior to 4^{o}C overnight incubation with primary antibody (table 3-6). Slides were washed in 1 x PBS and incubated 1-2 hours, RT with a biotinylated secondary antibody. Positively detected antigens were amplified for detection by ABC R.T.U Vectorstain kit (Vector Laboratories), incubated 1 hour RT and presence detected by 3,3-diaminobenzidine tetrahydrochloride (DAB; Vector Laboratories and Sigma). Tissue nuclei were counterstained 2-5 minutes using Mayer's haematoxylin and slides dehydrated in graded alcohols and clearene. Stained sections were mounted with Pertex (Histolab).

Table 3-6: Antibodies and retrieval methods for immunohistochemistry

Antigen	Antigen Retrieval	Primary Antibody	Secondary Antibody
PCNA	Citric saline (pH 6.0) Microwave 20 minutes	Rb pAb to PCNA (ab18197) 1:7000 dilution	Swine anti-rabbit biotin conjugated 1:200 dilution
CD3	1 mM EDTA (pH 9.0) Microwave 15 minutes	Rat pAb to CD3 (MCA1477) 1:100 dilution	Goat anti-rat biotin conjugated 1:200 dilution
CD68	Citric saline (pH 6.0) Microwave 20 minutes	Rb pAb to CD68 (OABB00472) 1:200 dilution	Swine anti-rabbit biotin conjugated 1:200 dilution
CD45R	Citric saline (pH 6.0) Microwave 20 minutes	Rat mAb to CD45R (ab64100) 1:200 dilution	Goat anti-rat biotin conjugated 1:200 dilution
NIMP	Pronase 0.01% Microwave 20 minutes	Rab mAb to NIMP (ab2557-50)	Goat anti-rat biotin conjugated 1:200 dilution
αSMA	Citric saline (pH 6.0) Microwave 20 minutes	Mouse mAb to αSMA FITC (F3777) 1:3000 dilution	Goat anti-fluorescein biotin conjugated 1:300 dilution
Caspase 3	10 mM Sodium Citrate (pH 6.0)	Rb mAb to cleaved caspase 3 (Asp175) 1:200 dilution	Swine anti-rabbit biotin conjugated

	Microwave 25 minutes		1:200 dilution
Secondary Antibodies			
Primary Antibody	Antigen	Source	Vendor/ Product Code
Primary Mouse Ab	Anti-mouse HRP	Goat	Sigma (A4416)
Primary Rabbit Ab	Anti-rabbit HRP	Swine	DAKO (E0353)
Primary Rat Ab	Anti-rat HRP	Goat	Serotec (STAR80B)
Primary FITC-Conjugated Ab	Anti-fluorescein biotin conjugated	Goat	Dako (V0403)

3.9.4 cIdU Immunofluorescence

Formalin fixed tissue was paraffin-embedded and cut by microtome to 4 µM thickness onto slides. Sections were deparaffinised and rehydrated in clearene and graded alcohols as above and rinsed in distilled water. Sections were subjected to antigen retrieval in 10 mM citrate buffer pH 6 in a pressurised cooker for ~20 minutes and blocked in 10% normal donkey serum, 1 hour RT. Washing slides in 1 x TBST between each step, sections were blocked with avidin/biotin (Vector Laboratories) for 20 minutes each, incubated overnight with primary rat anti-cldU antibody (Novus Biologicals) and cIdU detected for with secondary antibody donkey anti-rat IgG (H &L) Cy5 647 (Jackson ImmunoResearch) incubated at RT for 2 hours. Sections were washed in 1 X TBST and nuclei counterstained for with Hoescht (Life Technologies) diluted 1:1200 in TBST for 15 minutes. Stained sections were mounted with Prolong Gold (Life Technologies) and stored at 4^{o}C in dark until imaging.

3.9.5 Image analysis of staining

Representative photomicrographs of stained sections were taken using a Nikon Eclipse Ni-U upright microscope for bright field images or Zeiss AxioImager Z2 for cldU immunofluorescent images. Positively stained cells and areas were analysed in 20 high power fields (HPF) and analysed using NIS-Elements BR Analysis (Nikon).

3.10 MSD V-PLEX proinflammatory panel 1 mouse assay

3.10.1 Principle of Meso Scale Discovery cytokine assay

Meso Scale Discovery (MSD) V-Plex Cytokine assays allows rapid detection of soluble cytokine proteins by method of sandwich immunoassay. This involves the addition of samples to plates with a working electrode surface pre-coated with capture antibodies. Sample analytes are captured by immobilising capture antibodies and detected by the addition of solution containing cytokine detection antibodies conjugated with electrochemiluminescent (ECL) labels (MSD SULFO-TAG) to complete the sandwich. Buffer is added to maintain ECL signals and plate is loaded onto an MSD instrument for voltage application. Subsequent emission of light is detected and emission is measured quantitatively for intensity proportional to amount of cytokine present in sample.

3.10.2 Detection of cytokines in mouse sera

Inflammatory cytokines IFN-γ, IL-1β, IL-2, IL-4, IL-5, IL-6, KC/GRO, IL-10, IL-12p70 and TNFα were detected and measured by V-Plex Proinflammatory panel 1 mouse Assay (MSD) in female mouse sera taken from ageing *PolgA* WT, *PolgA*$^{+/mut}$ and *PolgA*$^{mut/mut}$ mice as per manufacturer's instructions. Briefly, calibrator stock standards were prepared by reconstitution in 1000 µl of diluent 41 and diluted serially 4-fold to generate a further 7 standard calibrators. The 8th calibrator comprised of diluent 41 only. Subsequently, serum samples were diluted 2-fold in diluent 41 for assay detection and 50 µl added to a pre-washed plate, washed with 150 µl of 1 X Wash Buffer. 50 µl of calibrator standards and controls were also added to corresponding wells. Plates were sealed, allowed to incubate at room temperature for 2 hours and washed again 3 times with Wash Buffer. To detect cytokines, 25 µl of detection antibody solution was added; prior to use X50 stock detection antibody solution comprising cytokine-specific antibodies conjugated with SULFO-TAG was prepared as a 1X working solution. Plate was then sealed and further incubated at

room temperature for 2 hours. To measure detected antibodies, plate was washed 3 times with Wash Buffer and 150 µl of 2X Read Buffer T added to each well. Plate was analysed on a MSD instrument and concentration of cytokine present measured proportional to intensity of light emitted from assay.

3.11 Neutrophil Assays

3.11.1 Neutrophil functional chemotaxis assay

Chemotaxic migration was assessed as previously established by Newcastle University's Simpson Lab. Briefly in each half of slide, three 2.5 mm circular chambers, separated by 2.5 mm were inserted into a gel comprising 2% agarose prepared in HBSS- (Sigma) and supplemented with 25% bovine serum albumin (BSA; Sigma), 2% gelatin solution (Sigma) and Iscove's Modified Dulbecco's Medium (IMDM), 5 x 10^5 neutrophils in 10 µl of 1% autologous serum supplemented IMDM was added to central chamber whilst autologous serum supplemented IMDM and 10 mM of chemoattractant N-Formyl-Met-Leu-Phe (fMLP; Sigma) was added to the other two wells; slides were incubated at 37^{o}C, 5% CO_2 for 2 hours and then fixed in 2.5% paraformaldehyde overnight. To measure migration of neutrophils, slides were stained with Giema solution diluted 1:10 in PBS-Tween and analysed using a Zeiss Axio Observer Inverted microscope.

3.11.2 Neutrophil functional phagocytosis assay

Bone marrow derived neutrophils were isolated from *PolgA* WT, *PolgA*$^{+/mut}$ and *PolgA*$^{mut/mut}$ mice as previously described above and seeded into a 24 well plate at 1 x 10^5 in 400 µl. Phagocytosis was assessed *via* addition of 40 µl Zymosan A: heat or chemically inactivated, fluorescin-labelled bacterial bioparticles derived from *Saccharomyces cerevisiae* (Invitrogen) and incubated for 2 hours at 37^{o}C, 5% CO_2. Plates containing neutrophils and zymosan particles were PBS washed, fixed in 4% formaldehyde for 10 minutes and subsequently analysed for phagocytosis by Zeiss Axio Observer Inverted microscope. Neutrophil phagocytosis was assessed by the presence of two or more phagocytosed zymosan particles within the cell and percentage cell phagocytosis calculated.

3.11.3 Isolation of blood neutrophils

Blood samples were collected from sacrificed 3-6 and 9-12 month old WT, *PolgA*$^{+/mut}$ and *PolgA*$^{mut/mut}$ mice and incubated at room temperature for 20 minutes to allow for blood clotting. Samples were subsequently diluted 1:2.5 in 200 µl calcium-free 1 x PBS prior to staining with fluorescent antibodies for flow cytometry analysis.

3.12 Flow Cytometry

3.12.1 Principle of flow cytometry

Flow cytometry permits the multi-parameter characterisation of single cells in an otherwise 'impure' heterogenous cell population by laser-based technologies. Parameters such as cell size, cell surface expression markers, intracellular molecules and intracellular signalling are characteristics frequently used. The technology involves the passing of a cell suspension containing cells of interest through small opening to allow single passage only *via* a laser light. Forward scattering of light (light in front of laser beam) and sideward scattering of light induced by the cell is collected by detectors and converted to electrical current with voltage proportional to amount of light.

Cell characteristics may also be observed by fluorescently labelling them *via* fluorochrome conjugated antibodies binding to cell specific markers. Light can be emitted and detected from antibody-bound cells when excited by an appropriate excitation wavelength; this can be separated from forward and side scatter parameters using combinations of mirrors and filters to allow separation of light into defined wavelengths. Such specific wavelength parameters are detected by a photomultiplier tube sensor. When using multi-parameter fluorescent detection it is imperative to minimise spectral overlap between different wavelengths: applying electronic compensation to avoid false positive detection of fluorescently labelled cells as well as the appropriate use of several controls including: stained and unstained cells, compensation controls and fluorescence minus one controls (FMO).

3.12.2 Fluorescent cell viability staining of neutrophils

Neutrophils were checked for cell viability before fluorescent labelling with conjugated antibodies. Neutrophils were added to a 96 well plate and centrifuged at 400 x g for 4 minutes, supernatant discarded and pelleted cells resuspended in 30 µl of Live/Dead

viability dye (ThermoFisher Scientific) at 1:120 in PBS for subsequent incubation at 4^{o}C for 15 minutes. Live/Dead cells were washed in FACs buffer (PBS supplemented with 1% FCS; Lonza and BioSera respectively) to quench unbound dye and resuspended in 30 µl of 1:30 FACs buffer diluted Fc block to prevent further non-specific binding. Cells were washed again in FACs buffer.

3.12.3 Staining, induction of ROS production and acquiring of fluorescently labelled neutrophils

Fluorescent labelling of neutrophils was undertaken to determine reactive oxygen species (ROS) release during respiratory burst in response to stimulatory factors. As above, neutrophils from blood and liver neutrophils were isolated into a final volume of 500 µl FACs buffer (1 x PBS supplemented with 5% FCS) and subsequently stained with fluorescent antibodies Ly6G, CD45R and CD11b (table 3-7) added at 1:50 dilution. Neutrophils were fluorogenically labelled with 1 µM Dihydrorhodamine 123 (DHR; ThermoFisher Scientific) ROS probe, prior prepared in FACs buffer and incubated for 10 minutes in the dark at 37^{o}C. Neutrophils were then either primed through the addition of 100 mM platelet activating factor (PAF; Sigma) or primed and stimulated through addition of PAF plus 1:1000 diluted fMLP (Sigma) to give the following flow cytometry assay controls: DHR only; DHR plus PAF; and DHR plus PAF and fMLP. Between the addition of each stimulatory factor, neutrophils were incubated at 37^{o}C in the dark for 10 minutes.

Prior to analysis, blood neutrophils were lysed with 1 X ACK (Ammonium-Chloride-Potassium) lysis buffer (ThermoFisher Scientific) and incubated for 10 minutes at 37^{o}C in the dark. All neutrophil isolates were spun at 500 x g for 5 minutes, supernatant removed and resuspended into 500 µl of FACs buffer. Neutrophils were then spun a further time at 500 x g for 5 minutes and remaining cell pellet resuspended in a total final volume of 100 µl for data acquisition by flow cytometry. All flow cytometry was performed on either a FACSCanto II or BD FACSDIVA v8, acquiring sufficient number of events for subsequent export and analysis.

3.12.4 Analysis of flow cytometry data

Raw flow cytometry data was analysed with software FlowJo v8 (BD Biosciences). Subsequent workflow of analysis followed plotting forward scatter height (FSC-H) versus side scatter area (SSC-A) for exclusion of contaminating red blood cells and cellular debris within cell isolate. FSC-H against FSC-A removed doublet cells and remaining cell population positively gated within the 405-450 nm channel to select for cells with area proportional to height and to remove permeable dead and necrotic cells with increased uptake of Live/Dead dye. Neutrophil populations were then characterized and analysed according to expression of their fluorescently labelled intracellular and extracellular markers.

Table 3-7: Flow cytometry antibodies

Antigen	Fluorophore	Vendor	Dilution
Live/Dead	BV241	Life Technologies	1:100
CD45R (for liver neutrophils only)	BV510	Biolegend	1:50
CD11b	PerCP-Cy5.5	Biolegend	1:50
LY6G	APC	Biolegend	1:50

3.13 NAD+/NADH Glo™ Assay

Levels of NAD+ and NADH were measured from frozen liver samples taken from aged *PolgA* WT, *PolgA*$^{+/mut}$ and *PolgA*$^{mut/mut}$ mice. Samples were cut and sliced to 20 mg and homogenised at room temperature in PBS-bicarbonate supplemented with 0.5% dodecyltrimethylammonium bromide. Samples were diluted 2-fold and 50 µl transferred into a 96 well plate. Standards of NAD+ and NADH were prepared from a 500 nM working solution of NAD+ and NADH diluted in PBS (table 3-8).
As per manufacturer's instructions for the NAD+/NADH Glo™ Assay (Promega) to corresponding wells, 25 µl of 0.4N HCl was added, plate covered and incubated for 15 minutes at 60-65^{o}C. Plate was cooled for 10 minutes at room temperature and 25 µl 0.5 M Trizma base added to neutralise HCl. In a 1:1 mixture add 50 µl of 0.4 N

HCl to 0.5 M Trizma base. To measure NADH and NAD+, 20 µl of samples were transferred into a 96 well white assay plate and spectrophotometrically measured at 647 nm.

Table 3-8: Standards for NAD+ and NADH measurement

NAD+ and NADH Standard Dilutons			
Standard	nM	Working Solution (µl)	Bicarb Assay Buffer (µl)
1	200	40	60
2	100	20	80
3	50	10	90
4	25	5	95
5	12.5	2.5	97.5
6	6.25	1.25	98.75
7 (Blank)	0	0	0

3.14 Statistical Analysis

Statistical analysis was performed using GraphPad Prism 7 for Windows (GraphPad) for ageing cohorts and *in vivo* damage models of *PolgA* WT, *PolgA*$^{+/mut}$ and *PolgA*$^{mut/mut}$ mice. Prior, data were checked prior for skewness and normality using Shapiro-Wilk and Kolmogorov-Smirnov tests. Data was reported and plotted graphically as means +/- standard error of mean (SEM); statistical analysis was performed using analysis of variance (ANOVA) test. Due to presence of multiple experimental groups and multiple time points, statistical analysis for ageing and *in vivo* models comprised two-way ANOVA with Bonferroni post-hoc test for multiple comparisons. Given values of P = ≤0.05 were accepted as *, P = ≤0.01 **, P = ≤0.001 ***, P = ≤0.0001 **** statistically different.

Chapter 4 | Phenotypic Characterisation of Polg$^{mut/mut}$ Ageing Livers Compared with Wild-Type Mice

4.1 Introduction

The accumulation of somatic mtDNA mutations and resulting respiratory dysfunction is implicated in the inexorable homeostatic decline of an organism and has been examined in the literature in a variety of mitotic and post-mitotic tissues (Zhang *et al.*, 1997; Cottrell *et al.*, 2001; McDonald *et al.*, 2008; Gutierrez-Gonzalez *et al.*, 2009). In the human liver, clonal expansion of COX-deficient hepatocytes has been observed with increasing occurrence during human ageing (Fellous *et al.*, 2009). The functional relevance of these clonally deficient populations remains unclear, in part, due to the difficulty in performing representative studies within static mitotic tissues samples, such as the liver. More significantly, there is an accompanied decline in hepatic regeneration with age, despite the organ's renowned unique capacity to fully recover lost cellular mass and function in response to injury. Most studies have focused on models of regeneration and utilised injurious interventions, such as two-thirds partial hepatectomy (PHx). Such studies have demonstrated that following PHx, survival is reduced by 40% in aged mice and in humans fatality increased by 15% in the elderly, perhaps owing to increased apoptosis, lower hepatocyte response to proliferative signals and halted progression of hepatocytes through the cell cycle with age (Huh *et al.*, 2004; Enkhbold *et al.*, 2015). Alterations are also accompanied by a number of mitochondrial changes including modification to the ultrastructure, a decrease in mitochondrial number and membrane potential, and an increase in peroxide reactive oxygen species (ROS) generation (Tauchi and Sato, 1968; Sastre *et al.*, 1996). Elsewhere, in mitotic aged human colonic crypts, clonally expanded respiratory chain deficiency is found to be associated with decreased cell proliferation and accompanied by increased apoptosis of deficient crypt cells (Taylor *et al.*, 2003; Nooteboom *et al.*, 2010; Baines *et al.*, 2014). Subsequently the biological contribution of age-accumulated mtDNA mutations and ensuing mitochondrial dysfunction in relation to liver ageing and regulation of hepatocellular proliferation was investigated in the present study.

The *PolgA*$^{mut/mut}$ mtDNA mutator mouse expresses a proof-reading deficient version of the mitochondrial DNA polymerase gamma (γ) which stochastically accumulates mtDNA mutations with time, providing experimental support that respiratory chain

dysfunction can promote an accelerated ageing phenotype (Trifunovic *et al.*, 2004; Kujoth *et al.*, 2005). Such studies on the *PolgA*$^{mut/mut}$ mouse have shown that premature ageing arises from mtDNA point mutations accumulating within tissues, including the liver, at a rate 3-5 fold faster per mtDNA molecule than wild type (WT) mice. Unlike age-associated mtDNA mutations in human tissues that occur sporadically and heterogeneously, *PolgA*$^{mut/mut}$ mutagenesis occurs during embryogenesis and expands clonally across all tissues (Khrapko *et al.*, 2006). Propagation of the ageing phenotype within these mice was originally proposed to occur in the absence of oxidative stress and attributed to the increasing loss of vital cells with respiratory chain dysfunction by apoptosis (Trifunovic *et al.*, 2004; Kujoth *et al.*, 2005; Hiona *et al.*, 2010). However, technological advances have more recently shown that mitochondrial ROS may contribute to *PolgA*$^{mut/mut}$ ageing by demonstrating the increasing *in vivo* detection of hydrogen peroxide with age and the extension of lifespan following antioxidant intervention (Dai *et al.*, 2010; Ahlqvist *et al.*, 2012; Logan *et al.*, 2014). Homeostatic decline observed in these mice has also been shown to be attributed to the early onset of stem cell dysfunction in which *PolgA*$^{mut/mut}$ progeny develop abnormal lineage differentiation and altered numbers and proliferative capacity of stem cells (Norddahl *et al.*, 2011; Ahlqvist *et al.*, 2012).

Since normal ageing WT mice accumulate low levels of mtDNA point mutations and demonstrate lower mtDNA mutation frequencies in the aged liver than the mutator mouse, *PolgA*$^{mut/mut}$ were used to investigate the role of mitochondrial respiratory dysfunction on the ageing regenerative liver (Vermulst *et al.*, 2007; Ameur *et al.*, 2011). In addition and more representative of the multi-factorial ageing process in humans, the present study included use of *PolgA*$^{+/mut}$ heterozygous mice; these mice also accumulate mtDNA mutations but at a lower rate of ~4 point mutations per mtDNA molecule and without the premature progeroid ageing phenotype (Kraytsberg *et al.*, 2009). Studies have also shown that within tissues such as the brain, heart and intestinal duodenum, respiratory deficiency occurs: quantified at ~20% in duodenal cells that correlates to the 100-fold increase in mtDNA mutations over WT mice at 15 months of age (Vermulst *et al.*, 2008).

4.2 Aims

The aim of this chapter was to phenotypically characterise the effects of mitochondrial respiratory chain function in the *PolgA*$^{+/mut}$ and *PolgA*$^{mut/mut}$ liver in relation to basal hepatocellular regeneration with age.

4.3 Histology and ageing phenotype of WT and *PolgA* liver tissues

Concomitant with increased age-related incidence of liver pathologies, morphological changes are increasingly recognised within the hepatic sinusoid with age. As well as evidence suggesting a link to the ageing process, evidence shows morphological changes to mitochondria ultrastructure as well as elevated mtDNA mutational load observed within the ageing liver. As such, liver tissues were analysed within *PolgA*$^{+/mut}$ and *PolgA*$^{mut/mut}$ mice to determine if mtDNA mutations induced histological perturbations that could underlie age-related changes to normal hepatic functions, including the possible reduction in liver regeneration. Tissues from WT, *PolgA*$^{+/mut}$ and *PolgA*$^{mut/mut}$ were characterised by H&E staining from 3, 6, 9 and 12 month old mice; however, no obvious changes to the hepatic ultrastructure was observed with age, despite an obvious ageing phenotype and increases in liver to body weight ratios in both *PolgA*$^{mut/mut}$ mice age groups ($p<0.05$, $n=5$) and across the 12 month old genotypes ($p<0.001$, $n=5$) (figure 4-1A, B).

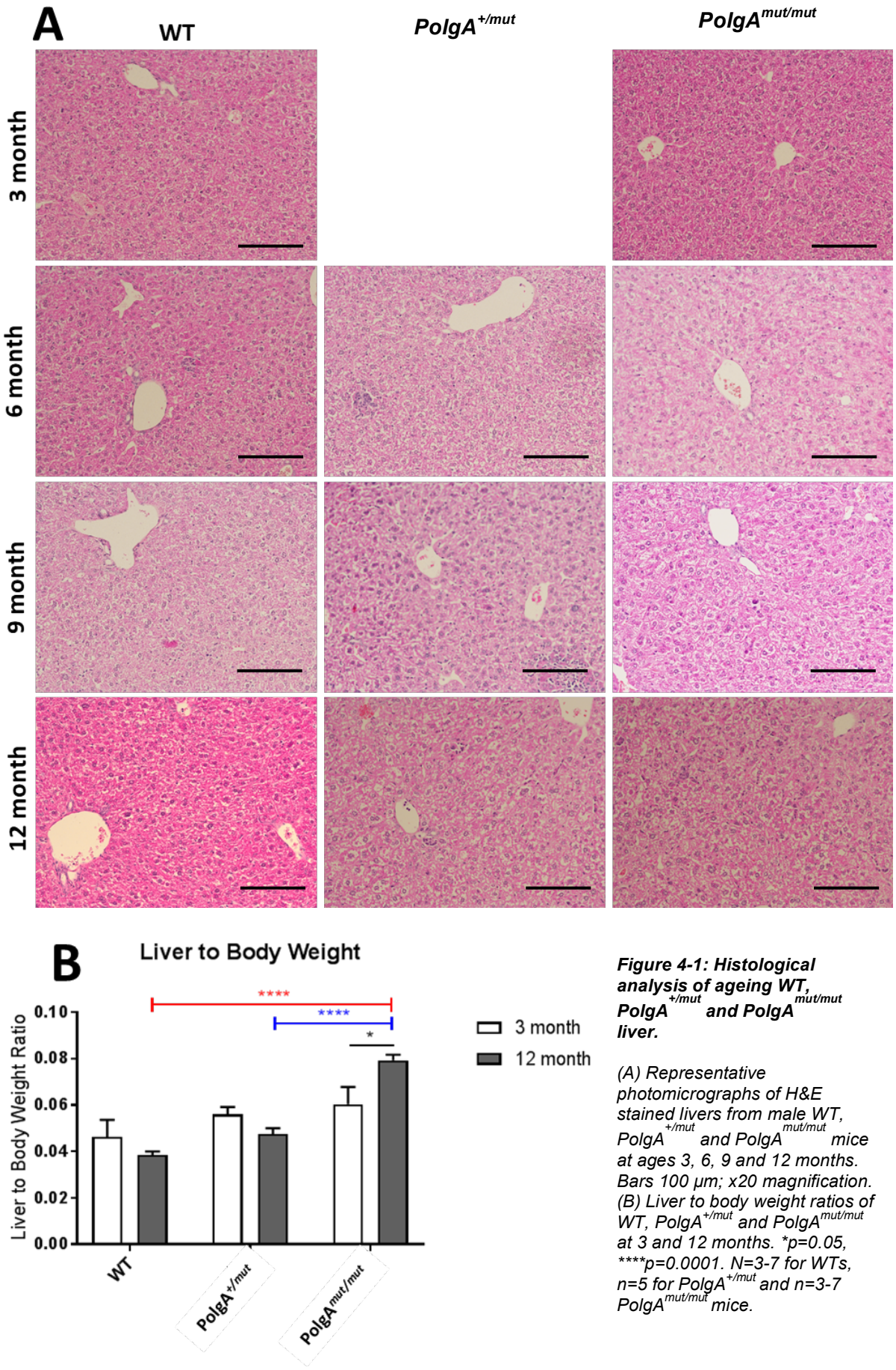

Figure 4-1: Histological analysis of ageing WT, PolgA$^{+/mut}$ and PolgA$^{mut/mut}$ liver.

*(A) Representative photomicrographs of H&E stained livers from male WT, PolgA$^{+/mut}$ and PolgA$^{mut/mut}$ mice at ages 3, 6, 9 and 12 months. Bars 100 µm; x20 magnification. (B) Liver to body weight ratios of WT, PolgA$^{+/mut}$ and PolgA$^{mut/mut}$ at 3 and 12 months. *p=0.05, ****p=0.0001. N=3-7 for WTs, n=5 for PolgA$^{+/mut}$ and n=3-7 PolgA$^{mut/mut}$ mice.*

4.4 Mitochondrial OXPHOS deficiency in *PolgA*$^{mut/mut}$ livers

4.4.1 COX/SDH staining analysis of livers

PolgA$^{mut/mut}$ mice are characterised by an accelerated ageing phenotype due to tissue accumulation of mtDNA mutations, exhibited by symptoms such as thymic involution, loss of bone mass, reduced subcutaneous fat and cardiomyocyte respiratory dysfunction (Trifunovic *et al.*, 2004; Kujoth *et al.*, 2005). In *PolgA*$^{+/mut}$ mice, no accelerated ageing is documented, however, mitochondrial respiratory deficiency is observed in mitotic colon crypts, which accumulate with age (Baines *et al.*, 2014). Interestingly for *PolgA*$^{mut/mut}$ mice, progressive deterioration of respiratory chain function is observed from 12 weeks and symptomatic onset within 6-8 months of age – a reflection of augmented mutational loads in *PolgA*$^{mut/mut}$ mice. To therefore determine if the liver also harnesses respiratory deficiency with age, frozen sections (15 µm) were subjected to dual COX/SDH staining from 3 month and 12-month WT (n=5, n=5) and *PolgA*$^{mut/mut}$ (n=3) mice. The subsequent colouration from the assay resulting from respiratory enzyme activity of nuclear encoded complex II succinate dehydrogenase (SDH) and mitochondrially encoded complex IV cytochrome c oxidase (COX). Accordingly, cells with normally functioning COX activity saturate with brown coloured reduced 3,3'-diaminobenzidine (DAB), whilst blue colouration occurs due to complex IV deficiency, as detected by the reduction of nitroblue tetrazolium (NBT) by SDH, in the absence of cellular saturation with reduced DAB product (Ross, 2011). Utilising this assay, mitochondrial deficiency was therefore calculated in WT and *PolgA*$^{mut/mut}$ livers as a percentage of the total tissue area *via* microscopy thresholding (figure 4-2A-B).

Even at 3 months of age, *PolgA*$^{mut/mut}$ mice displayed trends of elevated COX deficiency compared to WT controls (figure 4-2, C). Deficiency appeared visibly mosaic-like with possible respiratory dysfunction emanating from the hepatic periportal regions - given the greater COX deficient density observed closer to the portal vein (figure 4-2, C). In 12-month livers, deficiency was significantly elevated in these *PolgA*$^{mut/mut}$ mice ($p<0.01$) (figure 4-2, C); periportal staining appeared to extend towards the pericentral zones, coinciding with similar lineage tracing studies in the human liver (Fellous *et al.*, 2009). However, COX deficiency was not statistically different between 3 and 12-month *PolgA*$^{mut/mut}$ mice nor between all WT ages. Whereas some evidence of COX negativity was observed in 12-month WT

mice and similarly located in the periportal regions, this was less detectable by microscopic threshold analysis (figure 4-2, B, C). *PolgA*$^{mut/mut}$ mice livers unsurprisingly showed augmented levels of hepatic COX deficiency when compared to age-matched WTs and were considered similarly COX deficient between 3 and 12 months of age.

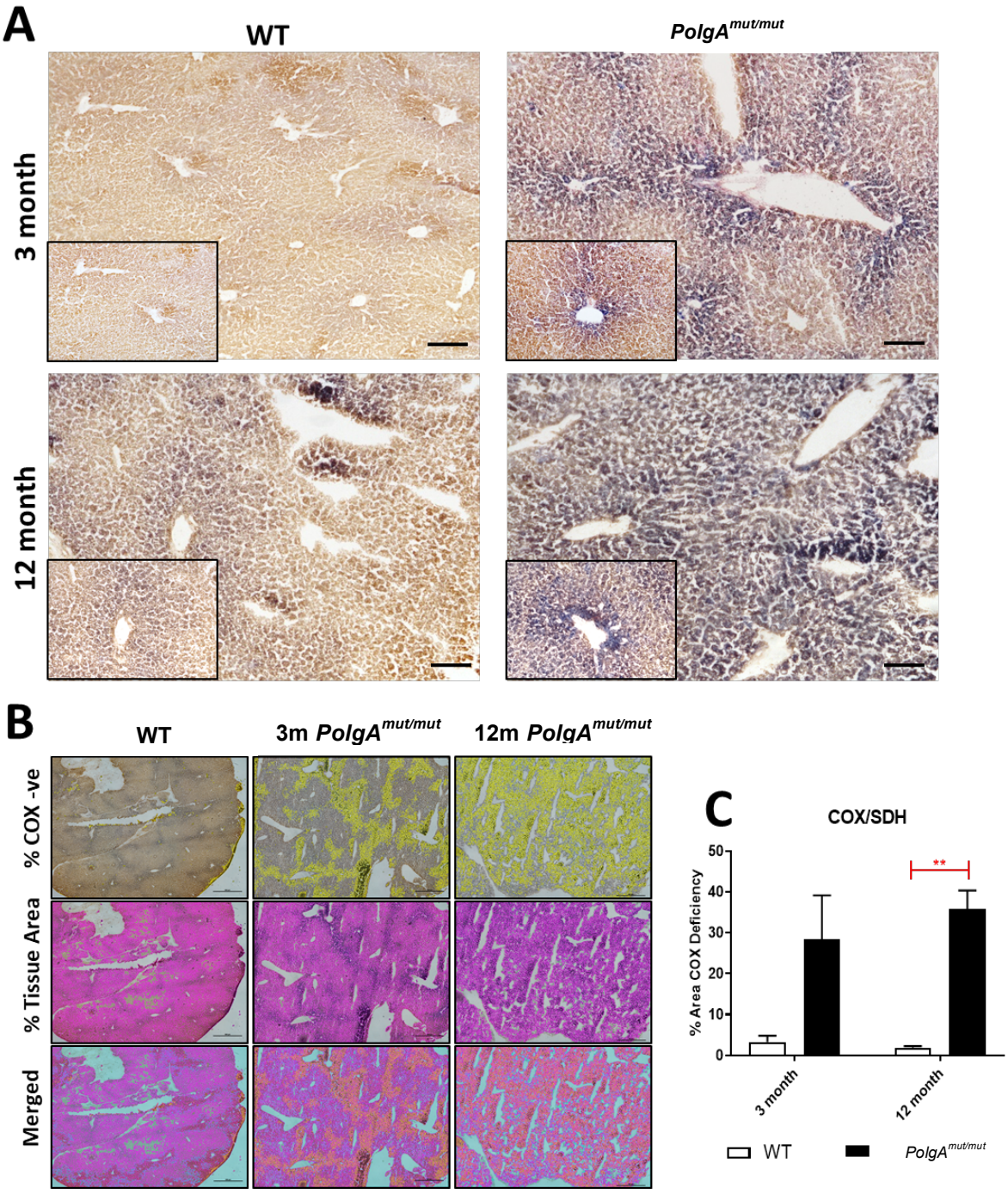

Figure 4-2: Histological analysis of basal mitochondrial function in young (3 month) and old (12 month) WT and PolgA$^{mut/mut}$ mice.

(A) Representative photomicrographs of COX/SDH staining in WT and PolgA$^{mut/mut}$ mice livers at 3 and 12 months. Outset images taken at x10 magnification, Bars 100 µm; inset images taken at x20 magnification (B) Representative photomicrographs of thresholds analysing COX/SDH staining in young and old WT and PolgA$^{mut/mut}$ livers. Area of liver tissue shown to be COX deficient is shown in yellow; total tissue area is highlighted in purple. Bars 500 µm. (C) Mitochondrial dysfunction shown by COX/SDH staining calculated as a percentage of total tissue area.

4.4.2 Respiratory chain deficiency in *PolgA*$^{mut/mut}$ livers

The utility of COX/SDH tissue staining in locating mitochondrial dysfunction is attributable to the reduction of electron acceptor nitroblue tetrazolium (NBT) in the absence of COX functionality. Yet, a caveat of COX/SDH staining is the limited detection of respiratory deficiencies for other specific ETC complexes. For example, complex I deficiency is readily detected in musculoskeletal tissues in the presence of COX negativity - identified only by specific immunofluorescent labelling for complex I (Rocha *et al.*, 2015). Ageing liver tissues from WT, *PolgA*$^{+/mut}$ and *PolgA*$^{mut/mut}$ mice were therefore tested for specific ETC complex deficiencies; however, due to the liver's auto-fluorescent nature, possible tissue deficiencies were alternatively detected by western blot (Croce *et al.*, 2010).

Protein expression of complexes I (NDUFB8), complex II (SDHB), complex III (UQCRC2), complex IV (Mt-CO1) and complex V (ATPB), determined *via* western blot, confirmed respiratory deficiency. Interestingly, no observable differences in Mt-CO1 expression could be detected in the liver from all aged genotypes, despite previous complex IV (COX) deficient staining (figure 4-3). Instead, reduced expression was observed in whole livers for NDUFB8 in *PolgA*$^{mut/mut}$ mice at 3, 6 and 12-month, deducing a complex I deficiency. In addition, NDUFB8 in *PolgA*$^{+/mut}$ whole livers was also found to observe reduced protein expression at 12 months of age but not at young ages (figure 4-3, C).

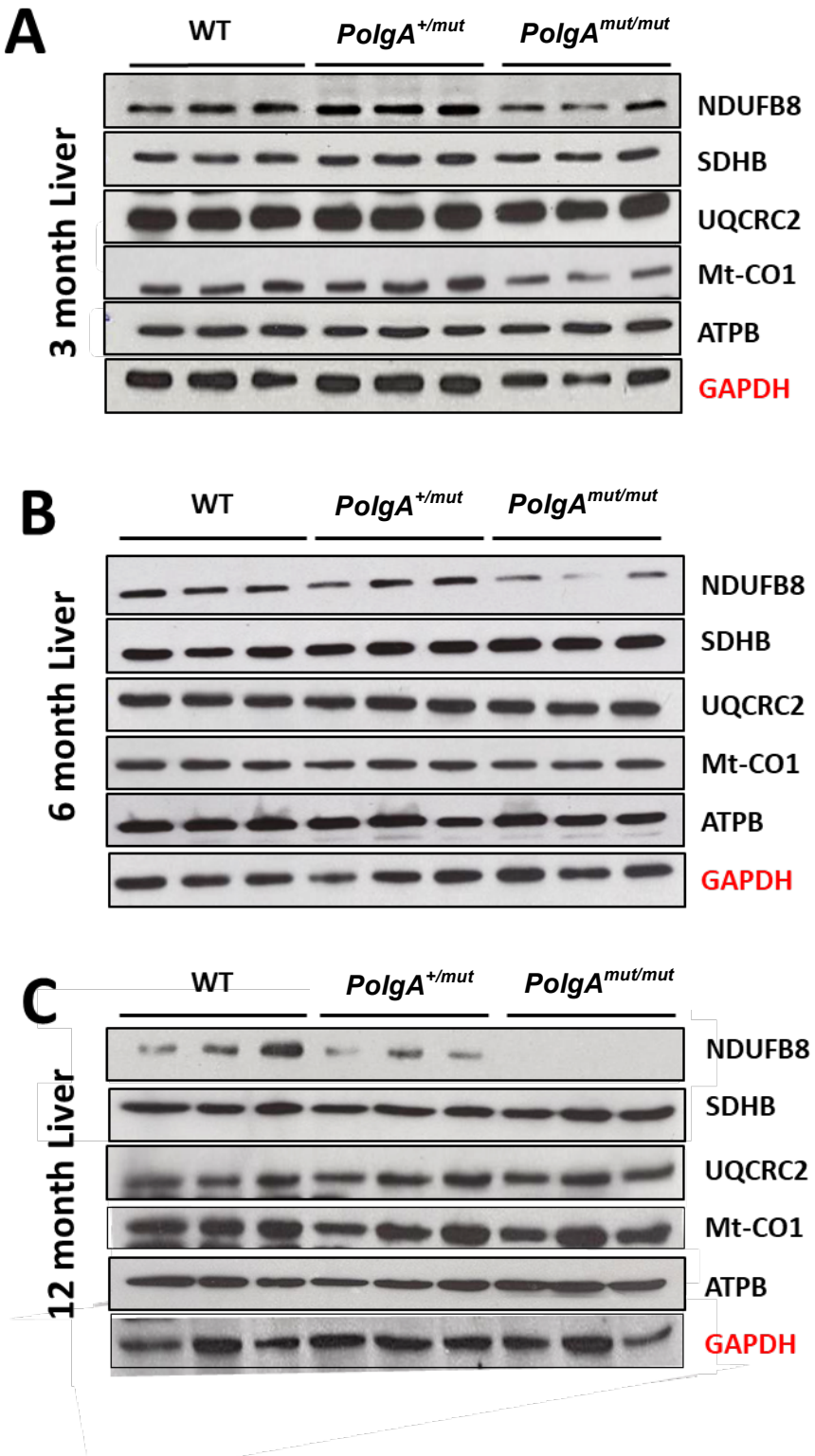

Figure 4-3: Western blot detection of mitochondrial respiratory complex enzyme proteins complex I (NDUFB8), complex II (SDHB), complex III (UQCRC2), complex IV (Mt-CO1) and complex V (ATPB)

Western blot detection of NDUFB8, SDHB, UQCRC2, Mt-CO1 and ATPB in (A) 3 month WT, PolgA$^{+/mut}$ and PolgA$^{mut/mut}$ mice livers, (B) in 6 month WT, PolgA$^{+/mut}$ and PolgA$^{mut/mut}$ mice livers and (C) in 12 month WT, PolgA$^{+/mut}$ and PolgA$^{mut/mut}$ mice livers. N=3 mice shown, representative of each genotype.

4.5 Basal proliferation and apoptosis in the ageing liver cohort

4.5.1 MtDNA mutations reduce basal hepatocyte proliferation in the ageing liver

Indications of reduced hepatocellular regeneration is previously outlined in the literature, describing diminished post-PHx survival in aged cohorts, as well as increased elderly incidence of liver pathologies (Enkhbold *et al.*, 2015; Kim *et al.*, 2015). With somatic mtDNA mutations highly implicated in the ageing process, it was hypothesised that the presence of mtDNA mutations would have an aberrant effect on hepatocyte proliferation. Liver sections dissected from aged WT, *PolgA*$^{+/mut}$ and *PolgA*$^{mut/mut}$ mice were therefore immunohistochemically labelled for proliferating cell nuclear antigen (PCNA), an auxiliary protein of DNA polymerase δ and a marker of cell proliferation (figure 4-4, A). The analysis of PCNA positive hepatocytes revealed hepatocellular proliferation in WT mice to remain relatively constant between the ages of 3 and 12 months, yet as *PolgA*$^{+/mut}$ and *PolgA*$^{mut/mut}$ mice aged to 9 and 12 months, this capacity compared with WTs was significantly reduced ($p<0.001$) (figure 4-4, B). Though trending, the effect at these ages did not appear to be significantly gene dose dependent when comparing *PolgA*$^{+/mut}$ and *PolgA*$^{mut/mut}$ mice, thus suggesting accumulation of mtDNA mutations has an effect in some part to reduce basal hepatocellular turnover.

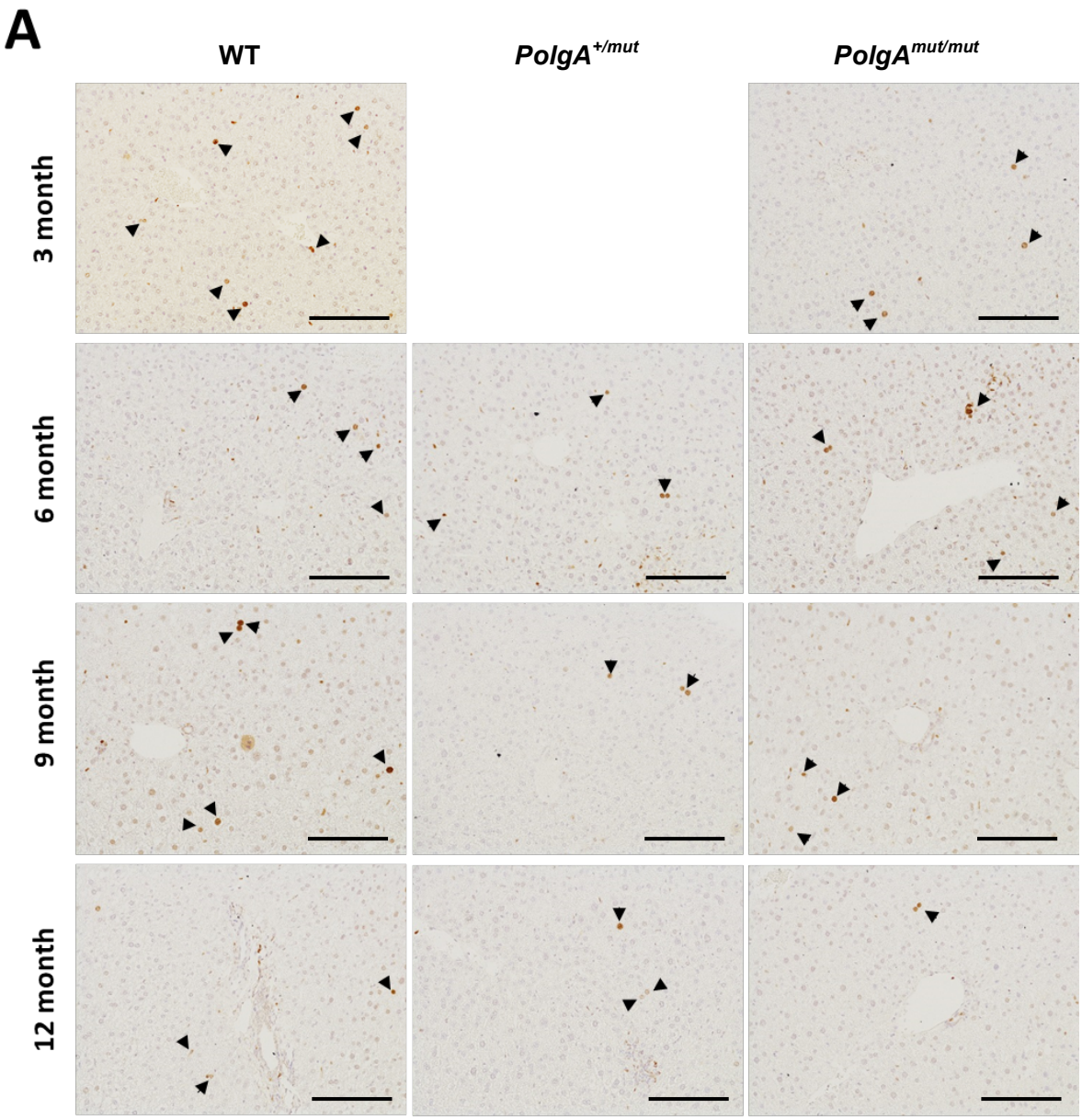

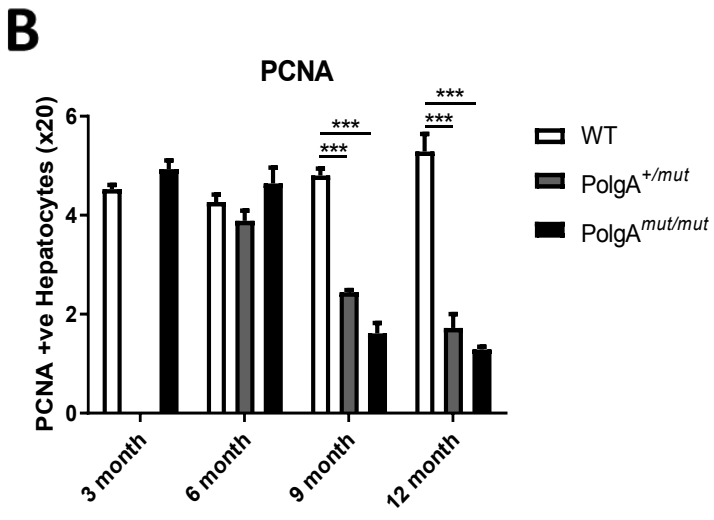

Figure 4-4: Basal proliferation of ageing WT, PolgA$^{+/mut}$ and PolgA$^{mut/mut}$ mice by immunohistological analysis.

*(A) Representative photomicrographs of PCNA staining in WT, PolgA$^{+/mut}$ and PolgA$^{mut/mut}$ mice. Arrow depicts positively stained hepatocytes. Bars 100 µm. (B) Positively stained hepatocytes is significantly reduced in PolgA$^{+/mut}$ and PolgA$^{mut/mut}$ mice (p = 0.05). Positive cells were counted in 15 high power fields at x20 magnification. All P values calculated using a two-way ANOVA. *p=0.05, ***p=0.001. n=3-7 for WTs, n=5 for PolgA$^{+/mut}$ and n=3-7 for PolgA$^{mut/mut}$ mice.*

4.5.2 Increased apoptosis is observed in *PolgA*$^{mut/mut}$ mice

As well as hepatocellular proliferation, liver homeostasis requires the additional regulation of hepatic apoptosis for maintenance, in which termination of parenchymal regeneration, for example, requires small wave apoptosis to correct excess hepatocytes produced during restoration (Sakamoto *et al.*, 1999). Disrupted balance can lead to either hyperplasia and tumour development, or where there is increased apoptosis, hepatocyte cell loss and liver damage. Induction requires the functional role of mitochondria to execute programmed cell death following the cytosolic release of intramembrane space proteins such as cytochrome *c*. In the presence of accumulated mtDNA mutations, correlative links to increased apoptotic levels and subsequent mammalian ageing is derived from early work undertaken on *PolgA*$^{mut/mut}$ mice (Kujoth *et al.*, 2005). Here, similar effects can be observed in the present study, whereby immunohistological analysis for executor caspase 3 in liver sections shows significantly increased levels of caspase 3 positive hepatocytes in *PolgA*$^{mut/mut}$ mice at 6 months ($p<0.05$) and 9-12 months ($p<0.001$), when compared *PolgA*$^{+/mut}$ and WTs (figure 4-5, A,B). Indeed, in previous studies elevated caspases are observed in a number of tissues; our findings across 6-12 months coincide with increased liver apoptosis in *PolgA*$^{mut/mut}$ mice, however, at 3 months of age no significance is seen between *PolgA*$^{mut/mut}$ and WT controls (Kujoth *et al.*, 2005; Hiona *et al.*, 2010).

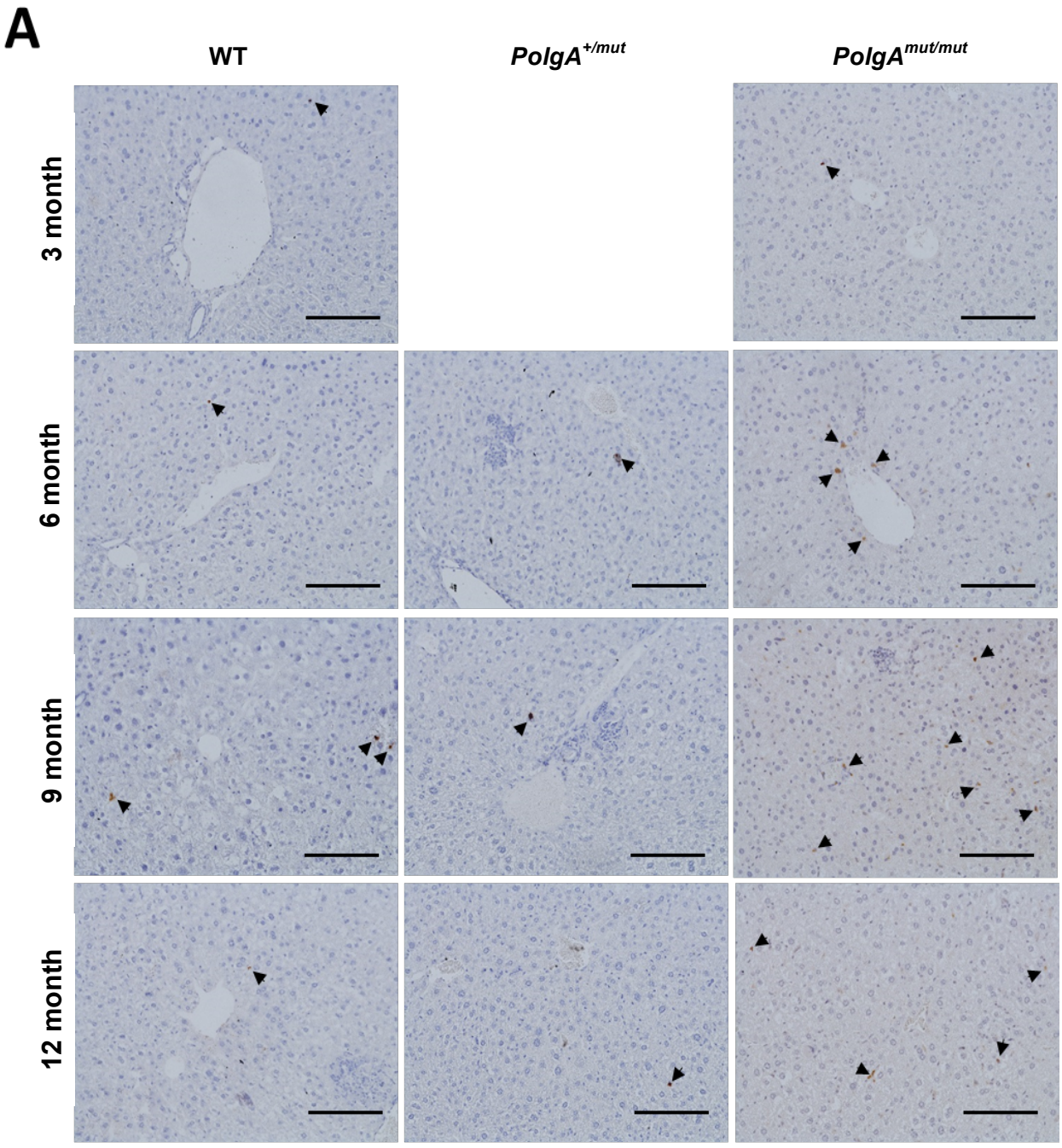

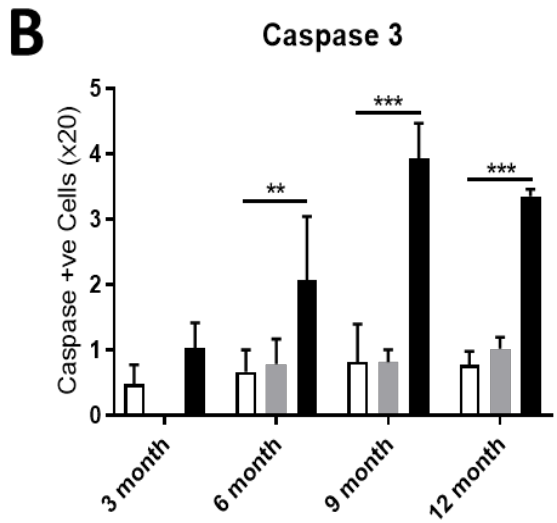

Figure 4-5: Analysis of apoptosis in ageing WT, PolgA$^{+/mut}$ and PolgA$^{mut/mut}$ mice.

*(A) Representative photomicrographs of cleaved caspase-3 staining in WT, PolgA$^{+/mut}$ and PolgA$^{mut/mut}$ mice. Arrows depict caspase-3 positive stained cells. Bars 100 µm. (B) Quantification of caspase-3 positive hepatocytes. Stained hepatocytes were counted in 15 high power fields at x20 magnification. All P values calculated using a two-way ANOVA. *p=0.05, ***p=0.001. n=3-7 for WTs, n=5 for PolgA$^{+/mut}$ and n=3-7 for PolgA$^{mut/mut}$ mice.*

4.6 Respiratory dysfunction and oxidant enzyme expression with age

Numerous studies on propagation of the ageing phenotype in mutator mice predominantly report negligible increases in oxidative damage and stress signals (Trifunovic *et al.*, 2004; Kujoth *et al.*, 2005; Edgar and Trifunovic, 2009; Hiona *et al.*, 2010), whilst other studies report *in vivo* detected levels of peroxide ROS markers and the delay in the onset of ageing following anti-oxidant intervention (Dai *et al.*, 2010; Ahlqvist *et al.*, 2012; Logan *et al.*, 2014). These differences in the literature, however, are most likely attributed to the greater sensitivity of ROS detection methods in later papers over initial *PolgA*$^{mut/mut}$ observational studies. To test whether reduced respiratory capacity was caused by mtDNA mutations that had an effect on oxidative signalling, gene expression for oxidant enzymes were measured in whole liver tissue in 3, 6 and 12 month WT, *PolgA*$^{+/mut}$ and *PolgA*$^{mut/mut}$ mice. Quantification of mRNA levels for glutathione synthase (GSS), glutathione peroxidase (GPx) and superoxide dismutases SOD1 and SOD2 were inconclusive across all age groups and genotypes (figure 4-6, A-D); however, SOD2 expression did show possible indications of increased levels in 12 month *PolgA*$^{mut/mut}$ livers when compared to WT and *PolgA*$^{+/mut}$ mice (figure 4-6, D) but failed to reach significance. This could be explained as SOD2 is an isoform of superoxide dismutase specifically localised at the site of ROS production with the inner mitochondrial matrix. Interestingly, these trends coincided with significant increases in PGC1α (figure 4-7), a transcriptional cofactor, intimately linked to regulation of energy metabolism, including mitochondrial biogenesis and the detoxification of ROS (St-Pierre *et al.*, 2002; St-Pierre *et al.*, 2003; Valle *et al.*, 2005). In 12-month *PolgA*$^{mut/mut}$ mice, PGC1α was shown to be significant when compared to age matched WT and *PolgA*$^{+/mut}$ mice and 3-6 month *PolgA*$^{mut/mut}$ groups.

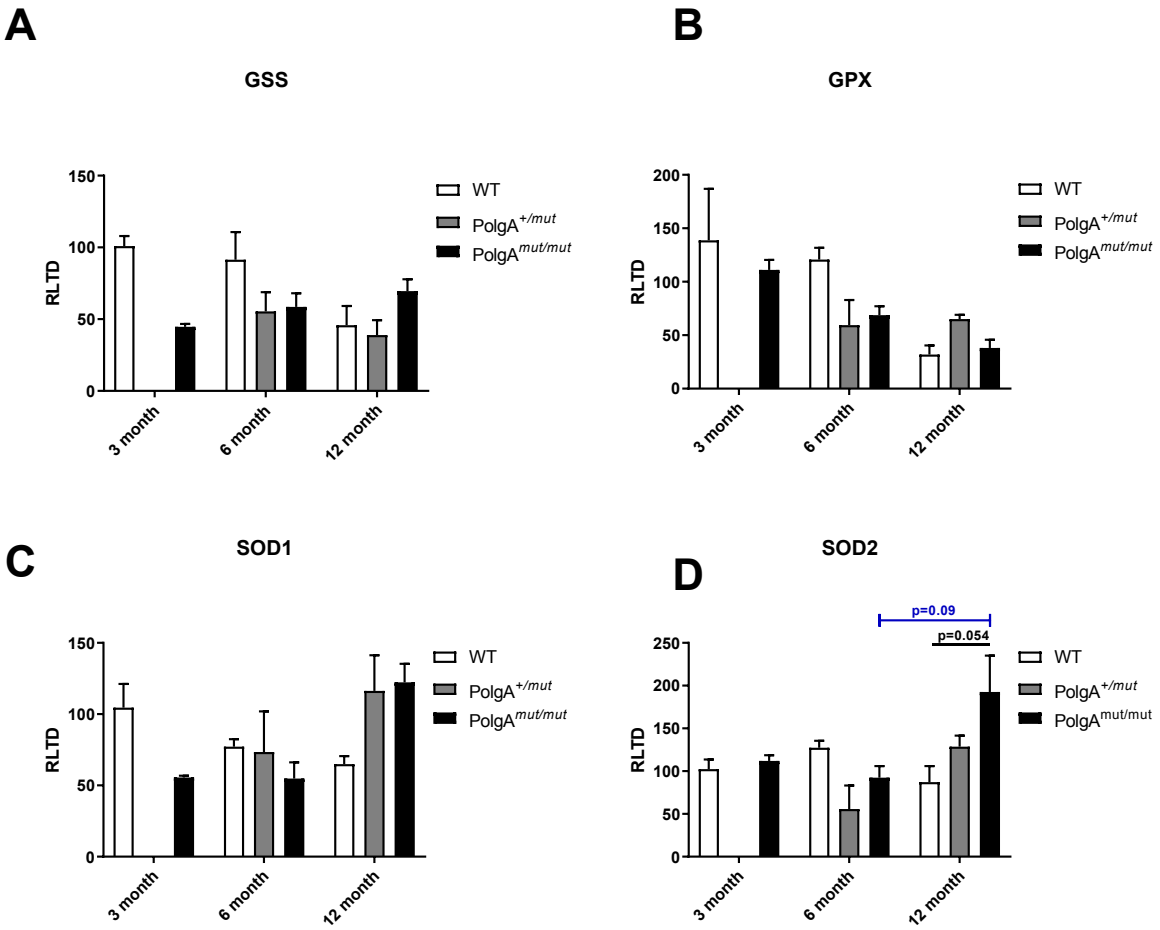

Figure 4-6 (above): mRNA gene expression levels of antioxidant enzymes in 3, 6 and 12-month WT, PolgA$^{+/mut}$ and PolgA$^{mut/mut}$ mice expressed as relative level of transcriptional difference (RLTD) expressed as a mean fold change ± SEM.

(A) mRNA gene expression levels of glutathione synthase (GSS) (B) mRNA gene expression levels of glutathione peroxidase (GPX) (C) mRNA gene expression levels of superoxide dismutase isoform 1 (SOD1) (D) mRNA gene expression levels of SOD2. n=3-5 for WT, PolgA$^{+/mut}$ and PolgA$^{mut/mut}$ mice.

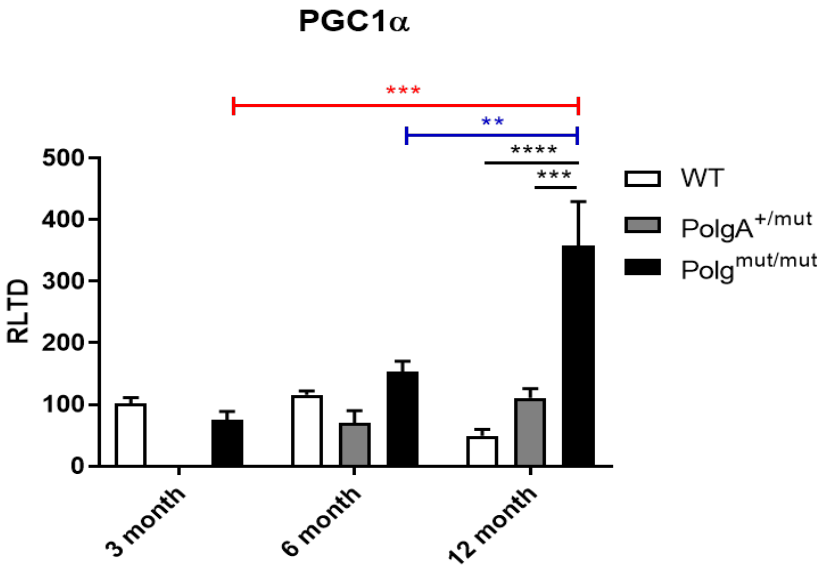

Figure 4-7 (right): mRNA gene expression levels of proliferator-activated receptor γ coactivator-1$^{\alpha}$ (PGC1α). ***p=0.01, ***p=0.001. ****p=0.0001. n=3-5 for WT, PolgA$^{+/mut}$ and PolgA$^{mut/mut}$ mice.*

4.7 Measurement of NAD+/NADH by luciferase reporter

Previous findings indicate that elevated levels of NADH (nicotinamide adenine dinucleotide) and thus augmented NAD+/NADH ratios can delay the proliferative cell cycle and induce senescence (Wiley *et al.,* 2016). Given the catalytic oxidoreductase function of complex I in reducing NADH, NAD+ and NADH levels were measured *via* using the NAD-NADH-Glo^{TM} luciferase reporter assay kit (Promega) to determine if respiratory deficiency in *PolgA$^{mut/mut}$* mouse liver altered these levels when compared to WTs (figure 4-8). No differences were detected in individual NAD+ and NADH levels between both compared genotypes and ages in whole liver tissues (figure 4-8, A,B). Similarly, when comparing NAD+/NADH ratios levels between WTs and *PolgA$^{mut/mut}$* livers, no age-associated alterations were observed (figure 4-8, C). Surprisingly, reductions in basal hepatocellular turnover were not associated with NAD+/NADH control of cell cycle.

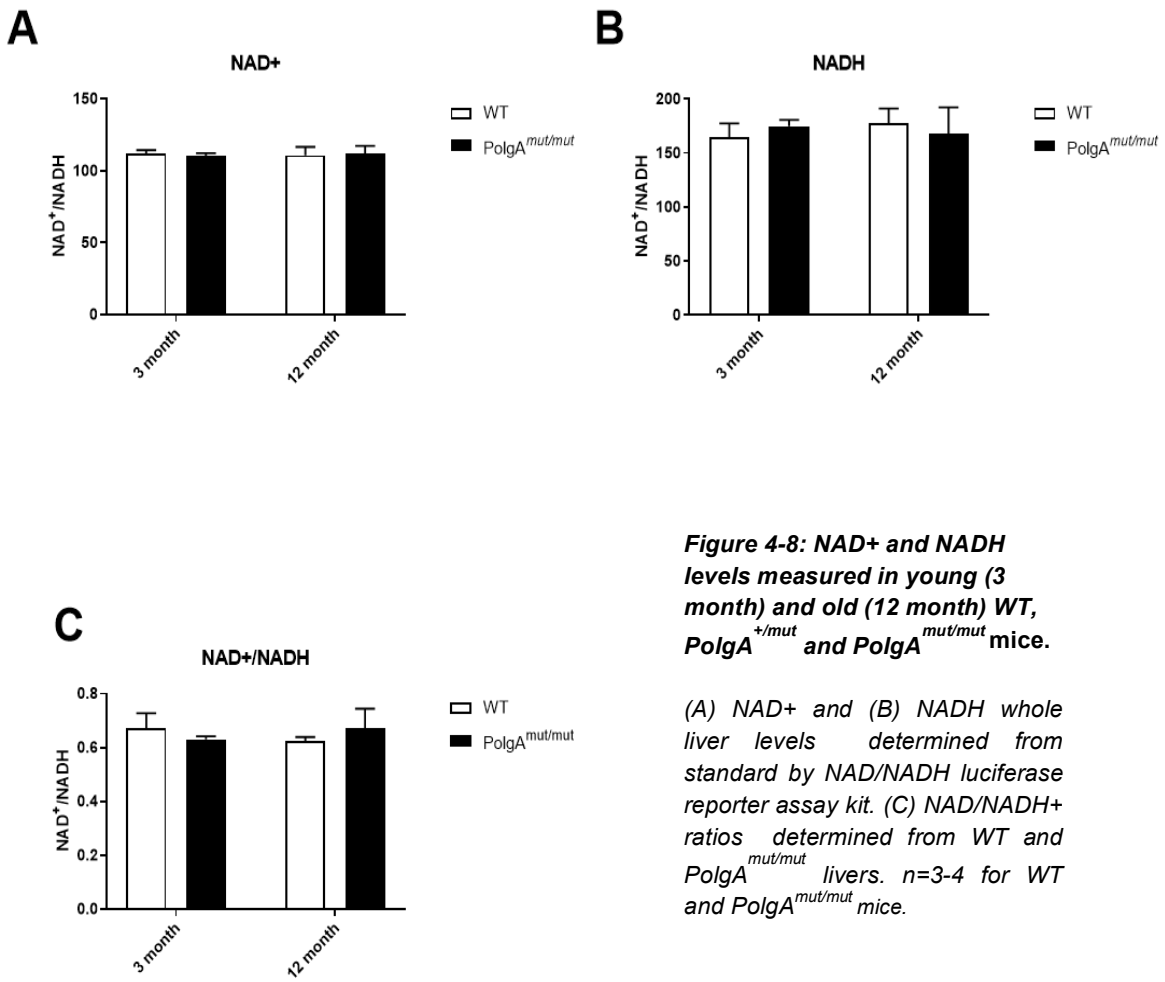

Figure 4-8: NAD+ and NADH levels measured in young (3 month) and old (12 month) WT, PolgA$^{+/mut}$ and PolgA$^{mut/mut}$ mice.

(A) NAD+ and (B) NADH whole liver levels determined from standard by NAD/NADH luciferase reporter assay kit. (C) NAD/NADH+ ratios determined from WT and PolgA$^{mut/mut}$ livers. n=3-4 for WT and PolgA$^{mut/mut}$ mice.

4.8 Characterisation of the effect of the *PolgA* mutation in hepatocytes

4.8.1 Characterisation of primary hepatocyte proliferation

The liver parenchyma is principally composed of hepatocytes, in addition to bile conduits and biliary epithelial cells, whereby hepatocellular proliferation is proposed to undergo a combination of hypertrophy and hyperplasia to maintain cellular mass - dependent on the mode of injury. To test whether basal age-associated proliferative defects observed in whole liver tissues was a hepatocyte defect, hepatocytes were isolated from young (3-4 month) and old (9-12 month) WT, *PolgA*$^{+/mut}$ and *PolgA*$^{mut/mut}$ livers. Once isolated, primary hepatocytes were allowed to adhere to plastic before phenotypic characterisation was analysed in response to proliferative signals. The proliferation of cultured hepatocytes was analysed by BrdU assay: normalised to total protein content and assessed as a fold change compared to WT controls. In response to increasing concentrations of mitogenic factor EGF, old *PolgA*$^{mut/mut}$ mice showed trending reductions in proliferative response when compared to WT and *PolgA*$^{+/mut}$ counterparts; in young hepatocytes across all genotypes, no differences were observed (figure 4-9, B-C). To ensure these observations were not due to altered or decreased viability a resazurin-based alamar Blue assay was used; no differences were detected between WT, *PolgA*$^{+/mut}$ and *PolgA*$^{mut/mut}$ hepatocytes at young and old ages (figure 4-9, D-E). No differences were also observed in levels of cell death marker lactate dehydrogenase (LDH), following initial LDH release due to stresses of hepatocyte isolation methods (figure 4-9, E-F). Instead, observations of photomicrographs show that at both 3-4 and 9-12 months of age, *PolgA*$^{mut/mut}$ hepatocytes show a reduced ability to adhere to the culture flask surface (figure 4-9, A), with 9-12 month *PolgA*$^{mut/mut}$ hepatocytes looking increasingly stressed under culture conditions at 24 hours. Hepatocytes isolated from WT, *PolgA*$^{+/mut}$ and *PolgA*$^{mut/mut}$ mice exhibited comparable levels of viability once they have adhered to plastic at both 3 months and 12 months; however, *PolgA*$^{mut/mut}$ hepatocytes failed to initially adhere and thrive - perhaps due to the greater presence of mitochondrial respiratory deficiency in these mice.

Subsequently, to further characterise and confirm respiratory deficiency within the liver and specifically hepatocytes, protein expression was also analysed in isolated primary hepatocytes *via* western blot. Direct comparisons were made between young and old hepatocytes across all genotypes and found NDUFB8 to have reduced

expression in both *PolgA* mice groups (figure 4-10). Coinciding with whole liver tissue analysis, our results show reduced hepatocellular proliferation specifically coincided with complex I mitochondrial deficiency. Reduced NDUFB8 expression was also observed in 9-12 month old *PolgA*$^{mut/mut}$ hepatocytes. No differences by western blot were observed for other ETC complexes, between genotypes and between ages.

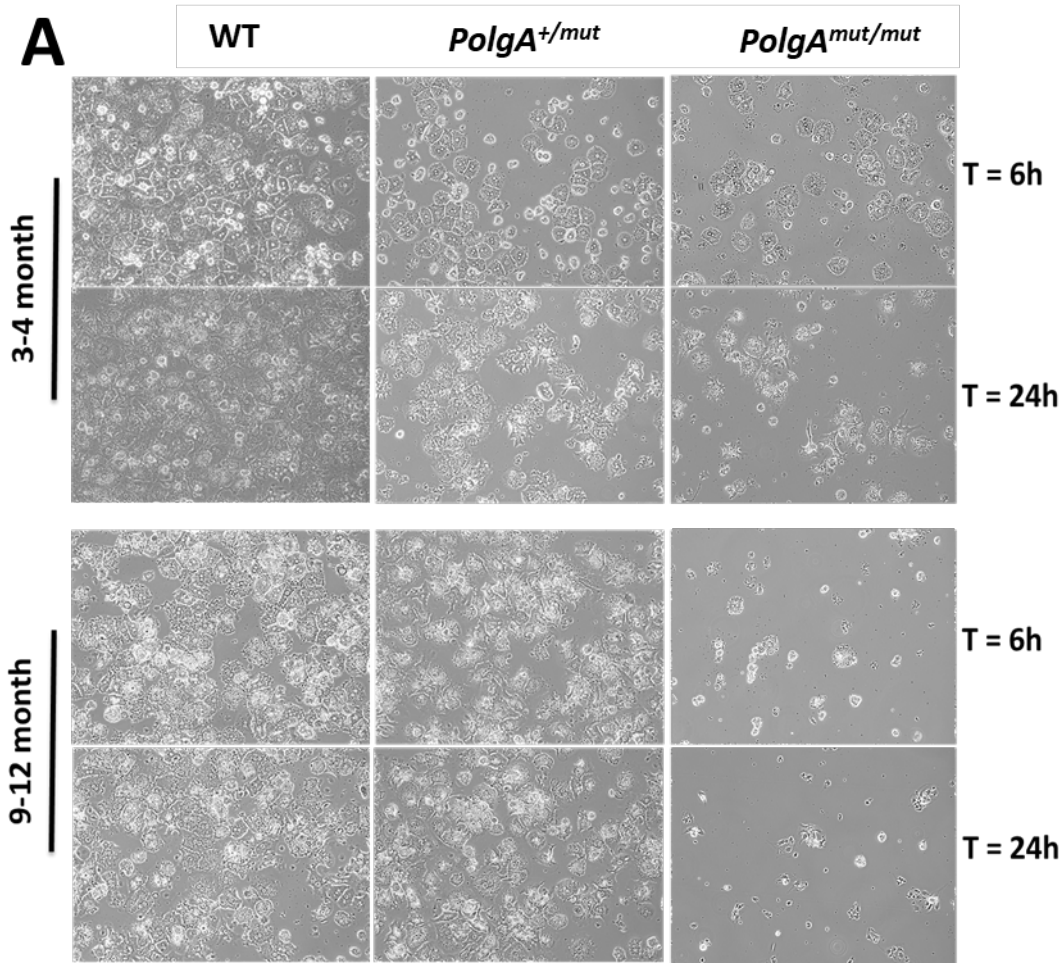

Figure 4-9A: Representative photomicrographs of hepatocytes isolated from PolgA WT, PolgA$^{+/mut}$ and PolgA$^{mut/mut}$ mice.

(A) Representative photomicrographs of cultured hepatocytes isolated from 3-4 month and 9-12 month WT and PolgA mice. Hepatocytes were allowed to adhere for 6 hours, washed and then left for a further 24 hours untreated or stimulated with varying concentrations of epithelial growth factor (EGF) to measure proliferation. N=4 per genotype.

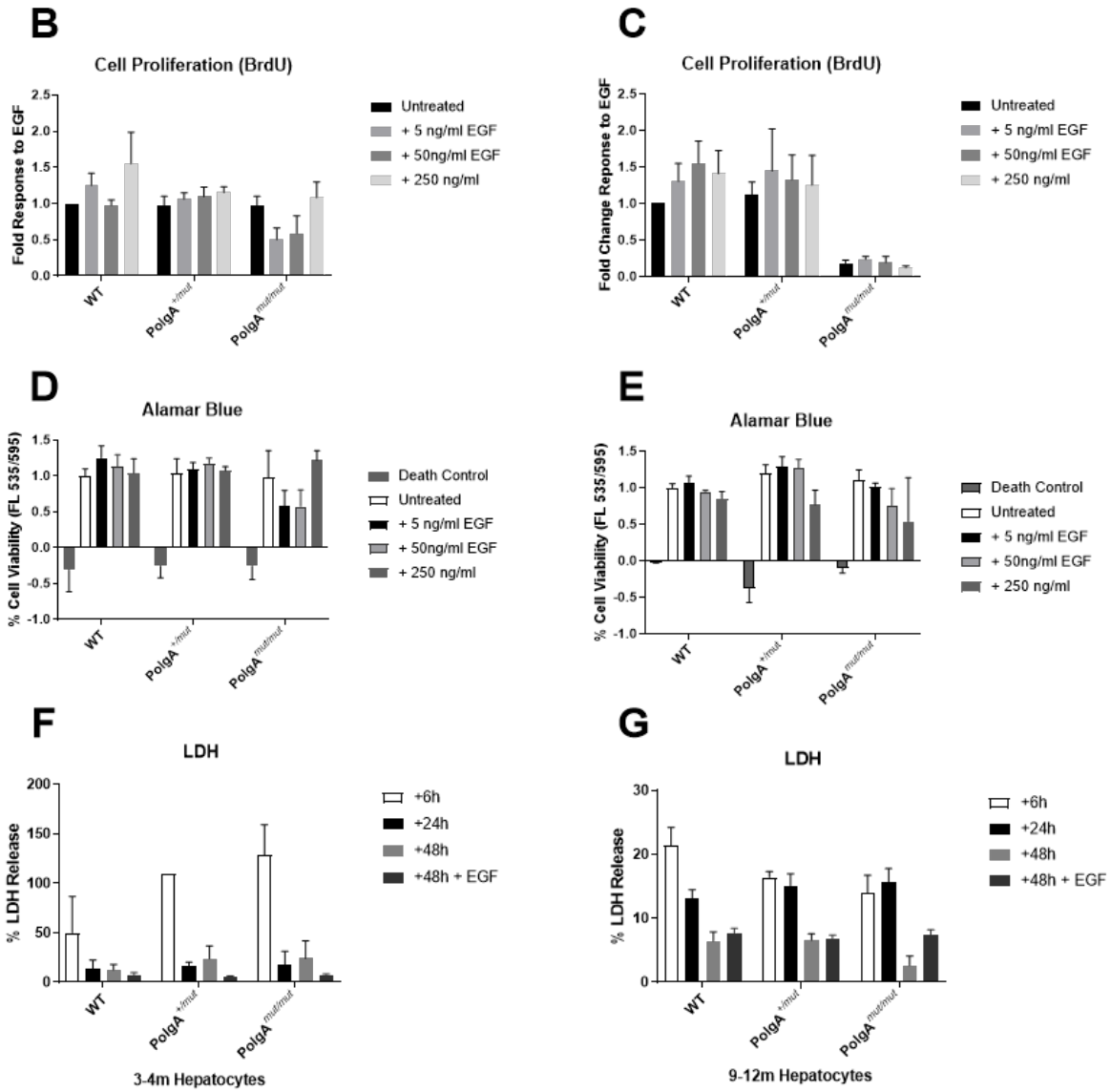

Figures 4-9B to 4-9E: Proliferative and viability assays in isolated hepatocytes from WT, PolgA$^{+/mut}$ and PolgA$^{mut/mut}$ mice.

Isolated PolgA WT, PolgA$^{+/mut}$ and PolgA$^{mut/mut}$ hepatocytes were allowed to adhere for 6 hours, washed and then left for a further 24 hours untreated or stimulated with varying concentrations of epithelial growth factor (EGF) to measure proliferation via (B-C) BrdU proliferation assay. Cell viability and death of hepatocytes were confirmed via (D-E) Alamar Blue and (F-G) lactate dehydrogenase; LDH assay. N=4 for WTs, PolgA$^{+/mut}$ and PolgA$^{mut/mut}$ mice.

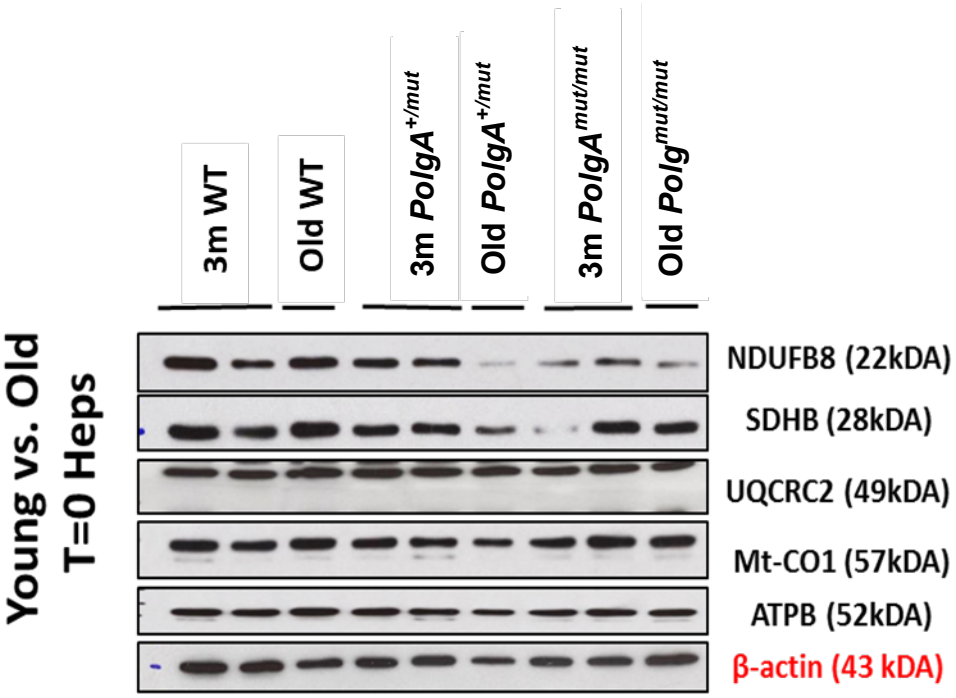

Figure 4-10: Western blot detection of complex I (NDUFB8), complex II (SDHB), complex III (UQCRC2), complex IV (Mt-CO1) and complex V (ATPB) in hepatocytes isolated from young (3 month) and old (12 month) WT, PolgA$^{+/mut}$ and PolgA$^{mut/mut}$ mice livers.

4.8.2 Characterisation of primary hepatocyte apoptosis

In the presence of increased levels of mtDNA mutations, the inability for cultured primary hepatocytes to survive and proliferate could be due to an increase in apoptotic signalling. Mitochondria are known to have an integral role in arbitrating apoptosis, with the presence of mtDNA mutations thought to increase cell death *via* reduced mitochondrial membrane potential that induces dysfunctional release of proapoptotic intermembrane space proteins (Hiona *et al.,* 2010). To characterise whether hepatic mtDNA mutations skew signalling towards a proapoptotic phenotype and consequently diminish hepatocellular survival and proliferation, mRNA expression levels of apoptotic proteins were measured in freshly isolated (T0) primary hepatocytes. Quantification of mRNA gene expression levels show specific trends of augmented proapoptotic Bax protein in both *PolgA*$^{mut/mut}$ and *PolgA*$^{+/mut}$ mice (figure 4-11, C). Comparisons made between genotypes revealed trends of increased levels in old hepatocytes, specifically with greatest expression observed in hepatocytes from old *PolgA*$^{mut/mut}$ mice. Anti-apoptotic protein Bcl_{XL} by contrast is significantly reduced in the presence of mtDNA mutations and specifically in old hepatocytes (figure 4-11, A). Similar trends were observed for anti-apoptotic Bcl-2, but was only significant when comparing young WT and *PolgA*$^{mut/mut}$ hepatocyte mRNA expression (figure 3-11B). Coinciding with this, no obvious changes were shown in proapoptotic Bid gene expression, in which its truncation is shown to play an important role in executing cell death (figure 4-11D).

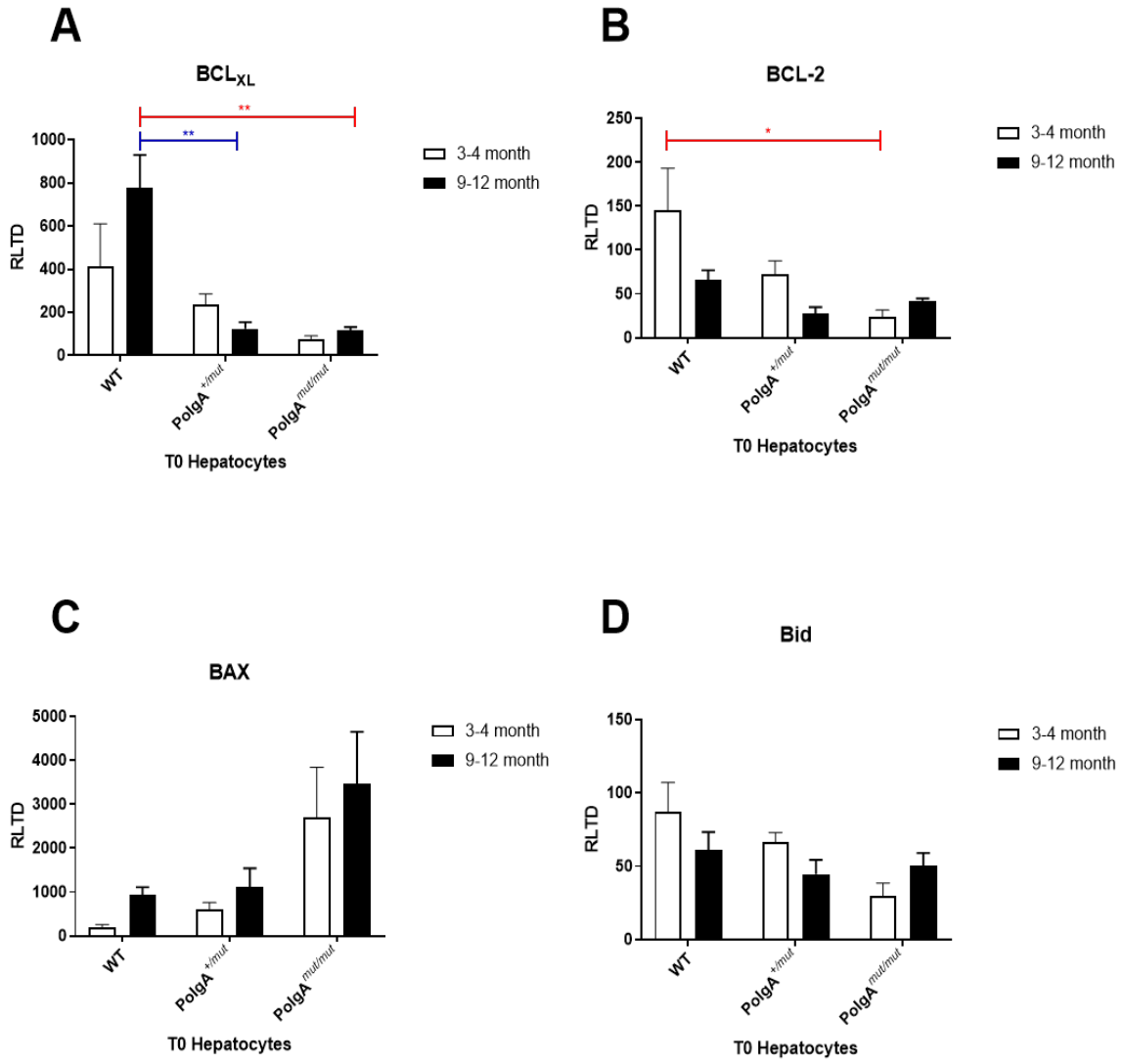

Figure 4-11 mRNA expression of pro- and anti-apoptotic genes in freshly isolated (T0) hepatocytes.

*(A-B) Anti-apoptotic genes BCL$_{xL}$ and BCL-2 expression in young (3-4 month) and old (9-12) month hepatocytes isolated from WT, PolgA$^{+/mut}$ and PolgA$^{mut/mut}$ mice livers, as well as quantification of gene expression for (C) proapoptotic BAX and (D) Bid genes in the presence of mitochondrial dysfunction. All P values calculated using a two-way ANOVA. *p=0.05, **p=0.01. N=4 per WT, PolgA$^{+/mut}$ and PolgA$^{mut/mut}$ genotype groups.*

4.9 Characterisation of inflammation in *PolgA* aged livers

A pervasive feature of normal ageing is inflammageing, a term coined to reflect age-related inflammation, typically encompassing chronic and dysfunctional immune cell signalling. Mitochondria are recognised to play a proinflammatory role that ranges from the activation of the NLRP3 inflammasomes and proinflammatory pathway by mitochondrially-derived DAMPs to intermediary ROS signalling. Mitochondria are a major source of ROS, implicated in ageing as well as a secondary messenger in inflammatory signalling and the subsequent expression of proinflammatory cytokines largely by augmented NF-κB signalling (Ichimura *et al.*, 2003; Amma *et al.*, 2005; Zhou *et al.*, 2011; Jurk *et al.*, 2014). The observed basal proliferative defects and increased apoptosis in *PolgA*$^{mut/mut}$ hepatocytes could therefore be a consequence of ROS and oxidative stress, with ROS implicated in the suppression of cell cycle entry following checkpoints (Shackelford *et al.*, 2000). The increase in *in vivo* mitochondrial ROS within *PolgA*$^{mut/mut}$ is also notably implicated in the activation of proinflammatory and apoptotic signalling pathways (Dai *et al.*, 2010; Logan *et al.*, 2014). Accordingly, exposure of cells to hydrogen peroxide (H_2O_2) has been linked to the cell cycle arrest *via* cyclin D1 targeting (Burch and Heintz, 2005; Pyo *et al.*, 2013).

Taken together, previous work could collectively hypothesise the presence of mitochondrial respiratory function to diminish cell proliferation *via* oxidative signalling. The aim of the following section is to therefore determine if the presence of mtDNA mutations alters proinflammatory signalling and ROS, and reduces *PolgA* hepatocytes capacity for hepatocellular proliferation.

4.9.1 MtDNA mutations cause increased lymphopenia in ageing *PolgA* livers

Common to the feature of ageing are alterations to inflammatory signalling, in which chronic low-grade systemic inflammageing is observed. To test whether the presence of mtDNA mutations altered inflammatory infiltration in the ageing liver, tissue sections were stained for inflammatory markers. Staining with CD45R and CD3 found inflammatory infiltrate of respective B and T cell lymphocytes to be significantly reduced in *PolgA*$^{mut/mut}$ mice at 9 months ($p<0.001$) and 12 months of age ($p<0.001$) (figure 4-12, figure 4-13). Diminished T cell levels were also observed in *PolgA*$^{mut/mut}$ at 6 months ($p<0.001$), though this followed a significant initial increase when

compared to WTs at 3 months of age ($p<0.001$). Similar significance was observed for CD45R stained B cells, whereby elevations in 3 and 6-month *PolgA*$^{mut/mut}$ mice were subsequently followed by T cell lymphopenia (figure 4-13). A stain for monocyte and macrophages marker CD68 showed levels to increase at older age in WT mice; however, such significant increases were not observed in older *PolgA*$^{+/mut}$ and *PolgA*$^{mut/mut}$ livers (figure 4-14). Interestingly, analysis of CD68 staining in *PolgA* mice demonstrates highly significant increases in monocyte/macrophage infiltration at younger ages when compared to WTs – remaining relatively constant at old age.

4.9.2 MtDNA mutations cause increased neutrophilia in *PolgA*$^{mut/mut}$ livers

Livers of *PolgA*$^{mut/mut}$ mice had considerable immune cell infiltration, with tissue staining demonstrating the infiltrate to be predominantly neutrophils, found within the liver in greater numbers than WT and *PolgA*$^{+/mut}$ mice (figure 4-15). Indeed, in manifestations of liver disease, inappropriate activation and homing of neutrophils to the liver is observed, secondary to altered wound healing processes (Theilgaard-Monch *et al.*, 2004). Therefore to understand whether mtDNA mutations promote proinflammatory signalling, quantification of cytokine mRNA expression was undertaken in homogenised whole liver tissue (figure 4-15) from all groups for cytokines CXCL2, TNFα and IL-6: proinflammatory signals known to be chemotactic for neutrophils (figure 4-16, B-E).

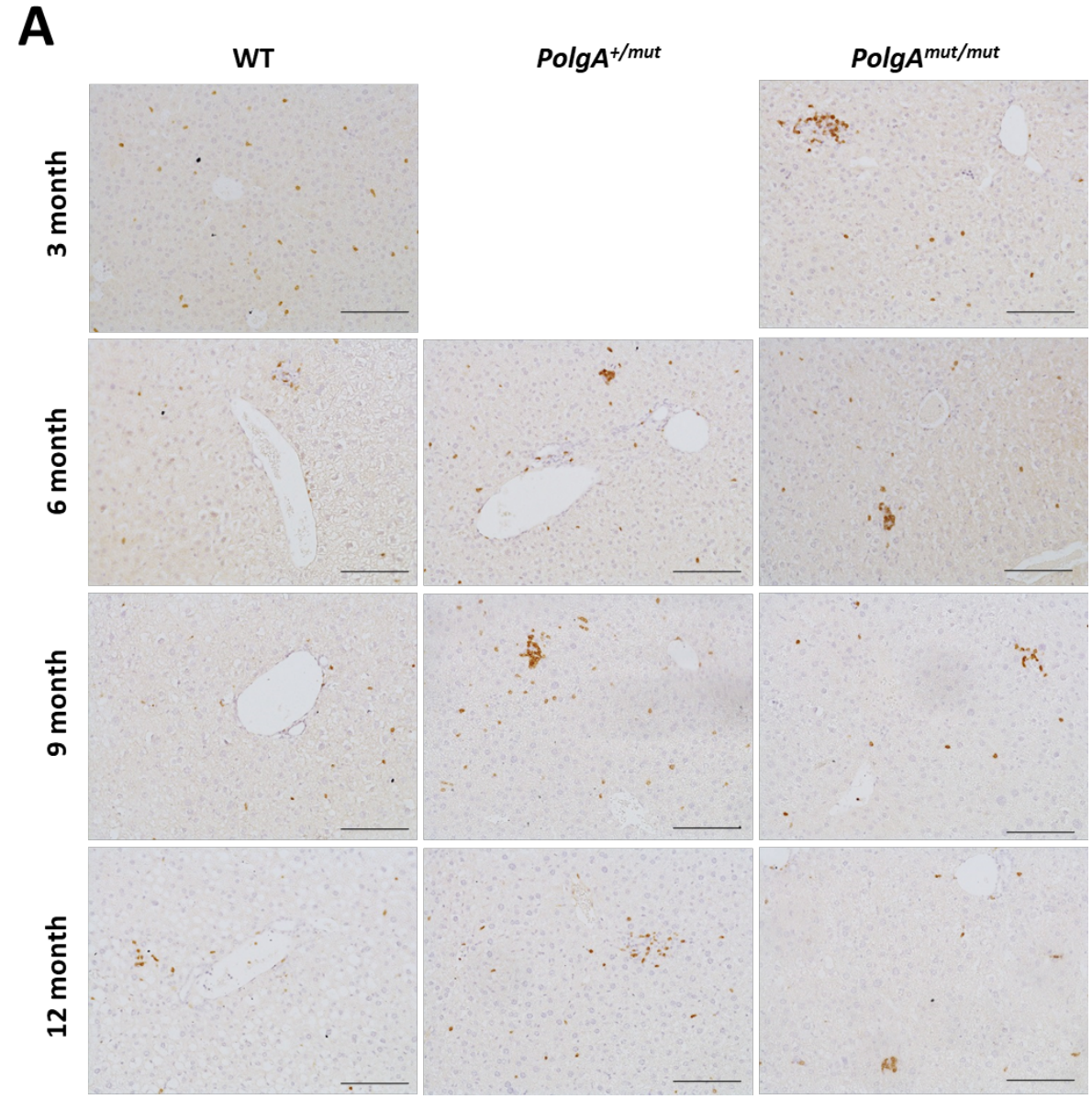

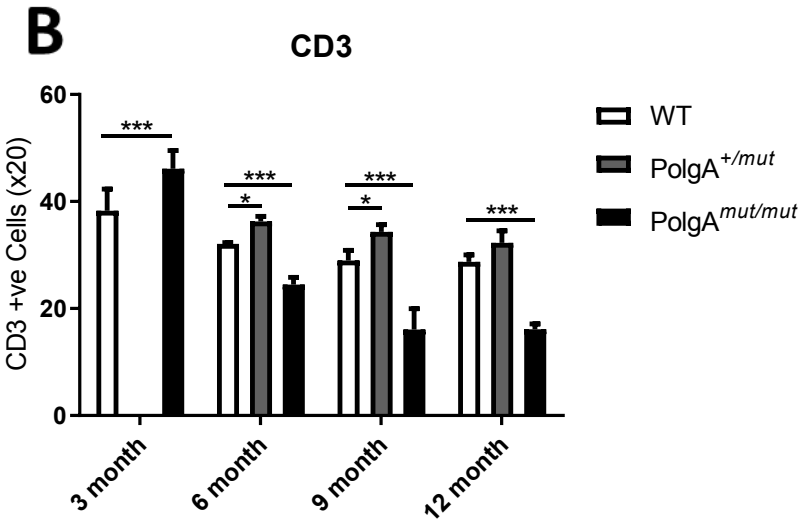

Figure 4-12: Analysis of CD3 staining in ageing WT, PolgA$^{+/mut}$ and PolgA$^{mut/mut}$ livers.

*(A) Representative photomicrographs of CD3 staining in WT, PolgA$^{+/mut}$ and PolgA$^{mut/mut}$ mice. Bars 100 µm. (B) Quantification of CD3 positively stained cells in WT, PolgA$^{+/mut}$ and PolgA$^{mut/mut}$ mice livers at 3, 6, 9 and 12 months of age. Positive cells were counted in 15 fields at x20 magnification. All p values calculated using a two-way ANOVA. *p=0.05, *** p-0.001. n=3-7 for WTs, n=5 for PolgA$^{+/mut}$ and n=3-7 for PolgA$^{mut/mut}$ mice.*

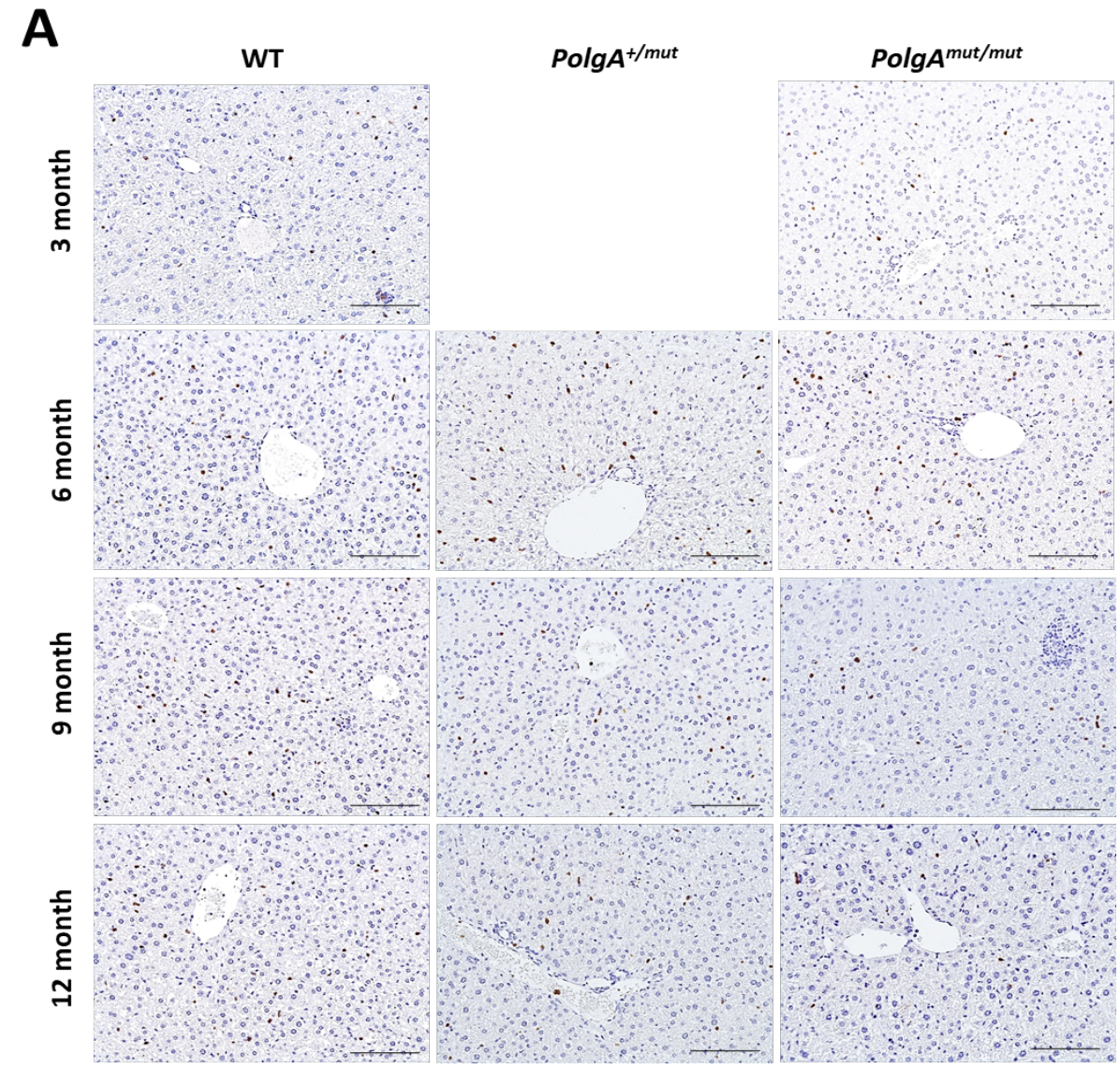

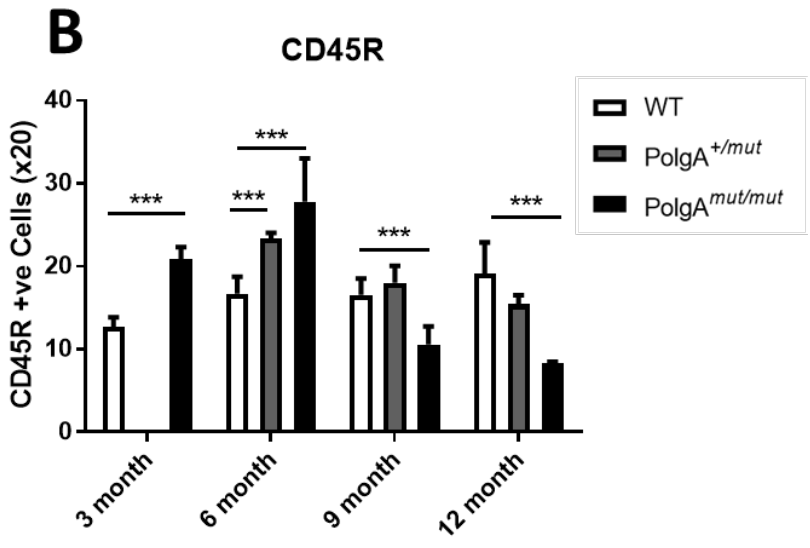

Figure 4-13: Analysis of CD45R staining in ageing WT, PolgA$^{+/mut}$ and PolgA$^{mut/mut}$ livers.

*(A) Representative photomicrographs of CD45R staining in WT, PolgA$^{+/mut}$ and PolgA$^{mut/mut}$ mice. Bars 100 µm. (B) Quantification of CD45R positively stained in WT, PolgA$^{+/mut}$ and PolgA$^{mut/mut}$ mice livers. Positive cells were counted in 15 fields at x20 magnification. All p values calculated using a two-way ANOVA., *** p=0.001. n=3-7 for WTs, n=5 for PolgA$^{+/mut}$ and n=3-7 for PolgA$^{mut/mut}$ mice.*

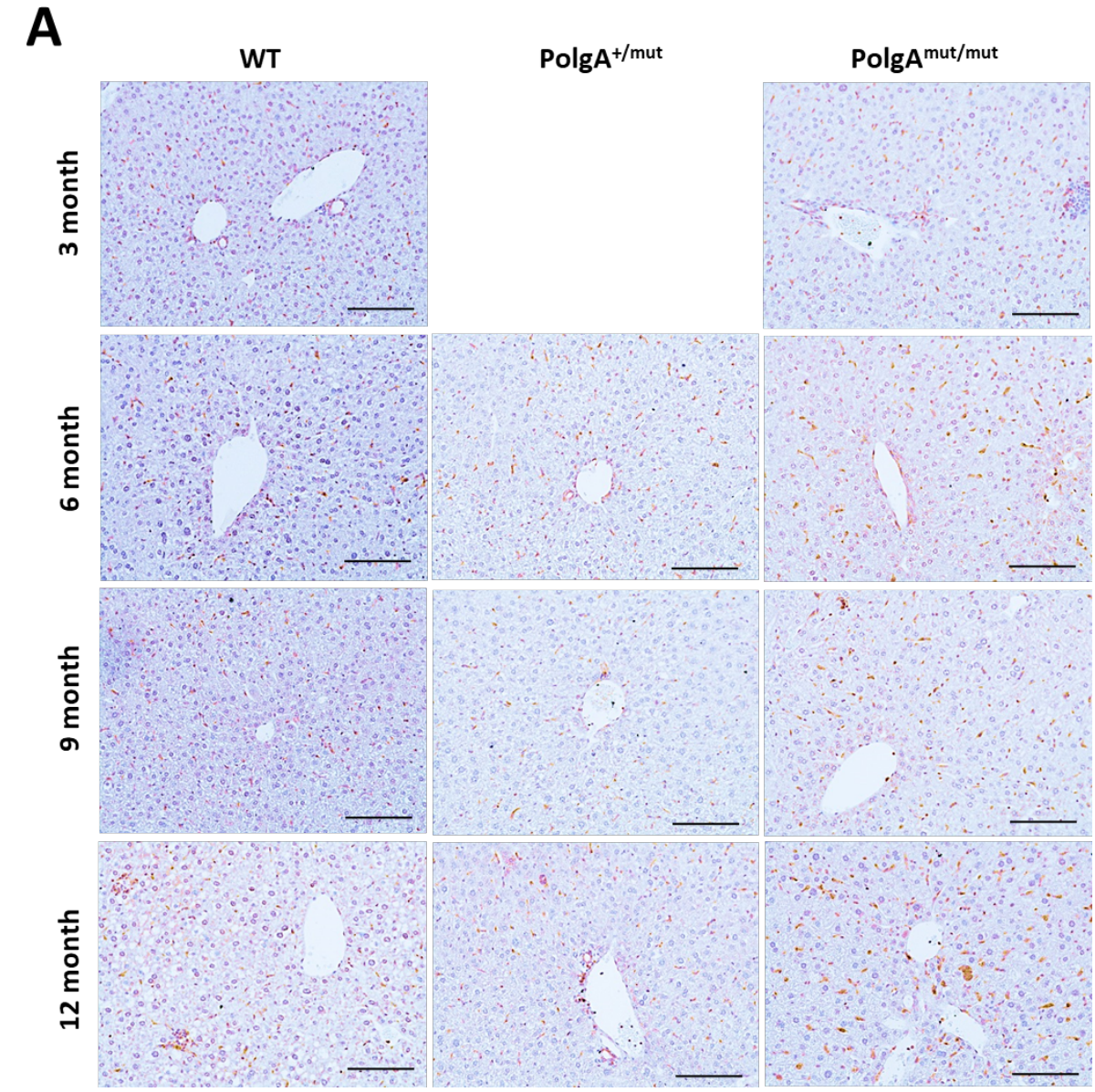

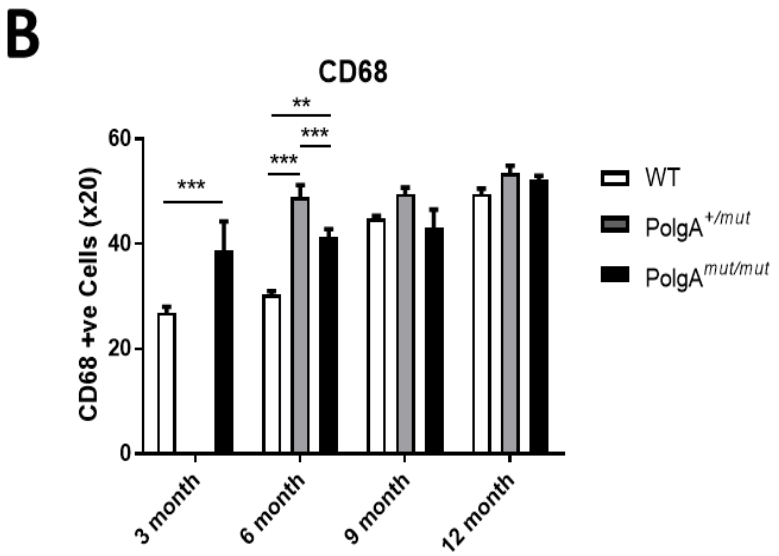

Figure 4-14: Analysis of CD68 staining in ageing WT, PolgA$^{+/mut}$ and PolgA$^{mut/mut}$ livers.

*(A)Representative photomicrographs of CD68 staining in WT, PolgA$^{+/mut}$ and PolgA$^{mut/mut}$ mice. Bars 100 µm. (B) Quantification of CD68 positively stained cells in WT, PolgA$^{+/mut}$ and PolgA$^{mut/mut}$ mice livers at 3, 6, 9 and 12 months of age. Positive cells were counted in 15 fields at x20 magnification. All p values calculated using a two-way ANOVA. **p=0.01, *** p=0.001. n=3-7 for WTs, n=5 for PolgA$^{+/mut}$ and n=3-7 for PolgA$^{mut/mut}$ mice.*

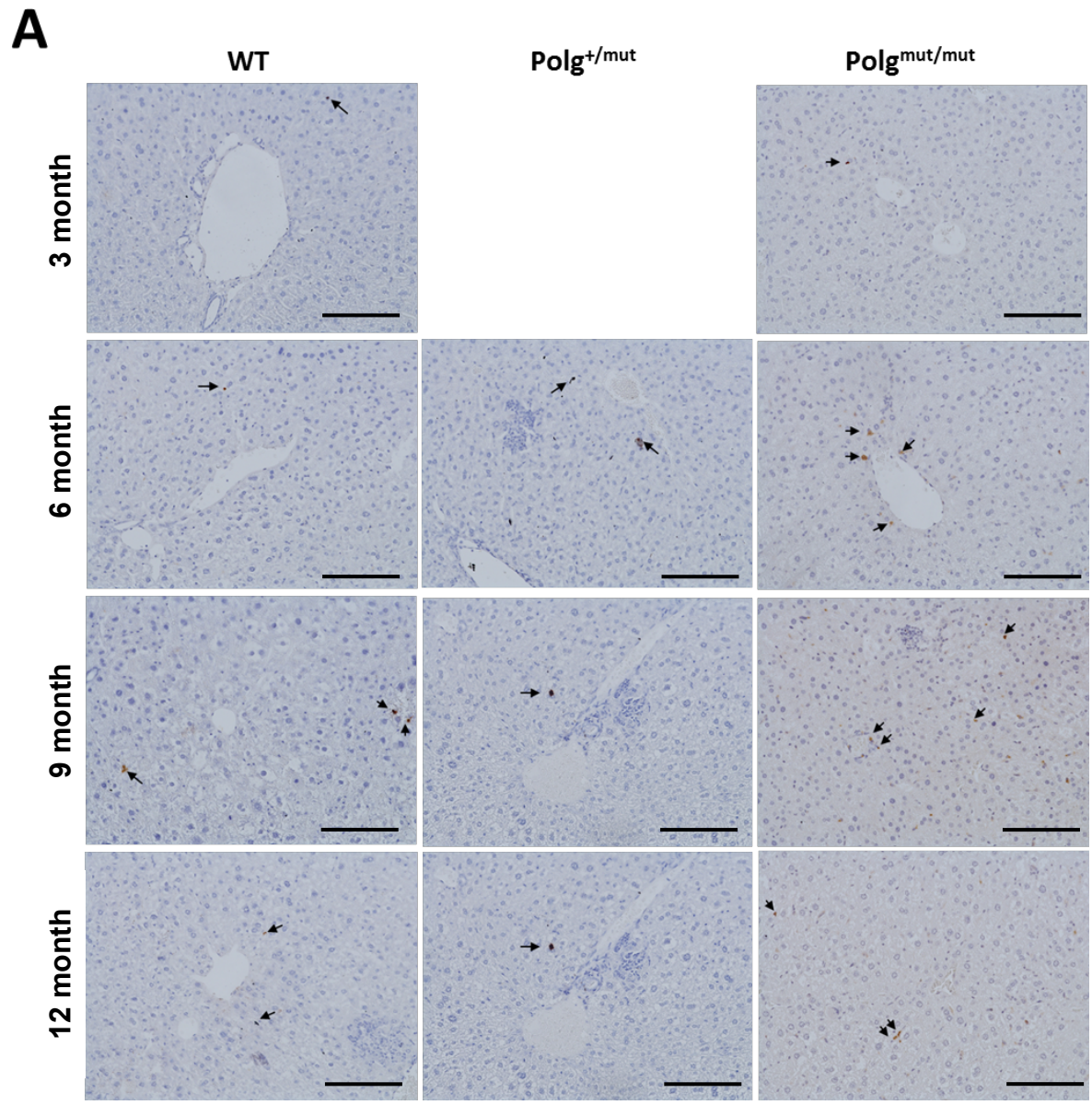

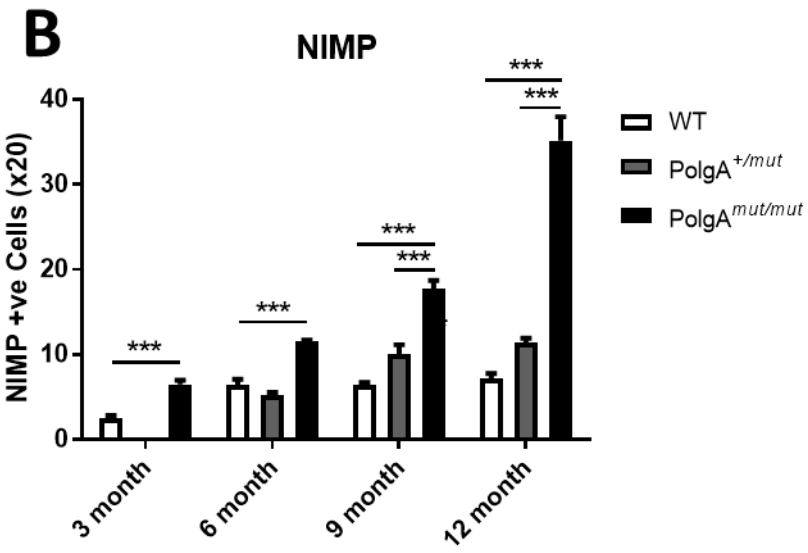

Figure 4-15: Analysis of NIMP staining in ageing WT, PolgA$^{+/mut}$ and PolgA$^{mut/mut}$ livers.

*(A) Representative photomicrographs of NIMP staining in WT, PolgA$^{+/mut}$ and PolgA$^{mut/mut}$ mice. Bars 100 µm. (B) Quantification of NIMP positively stained cells (arrows) are significantly increased with age in PolgA$^{mut/mut}$ mice and at 9-12 months in PolgA$^{+/mut}$ mice. Increases at old age were gene dose-dependent. Positive cells were counted in 15 fields at x20 magnification. All p values calculated using a two-way ANOVA. *** p=0.001. n=3-7 for WTs, n=5 for PolgA$^{+/mut}$ and n=3-7 for PolgA$^{mut/mut}$ mice.*

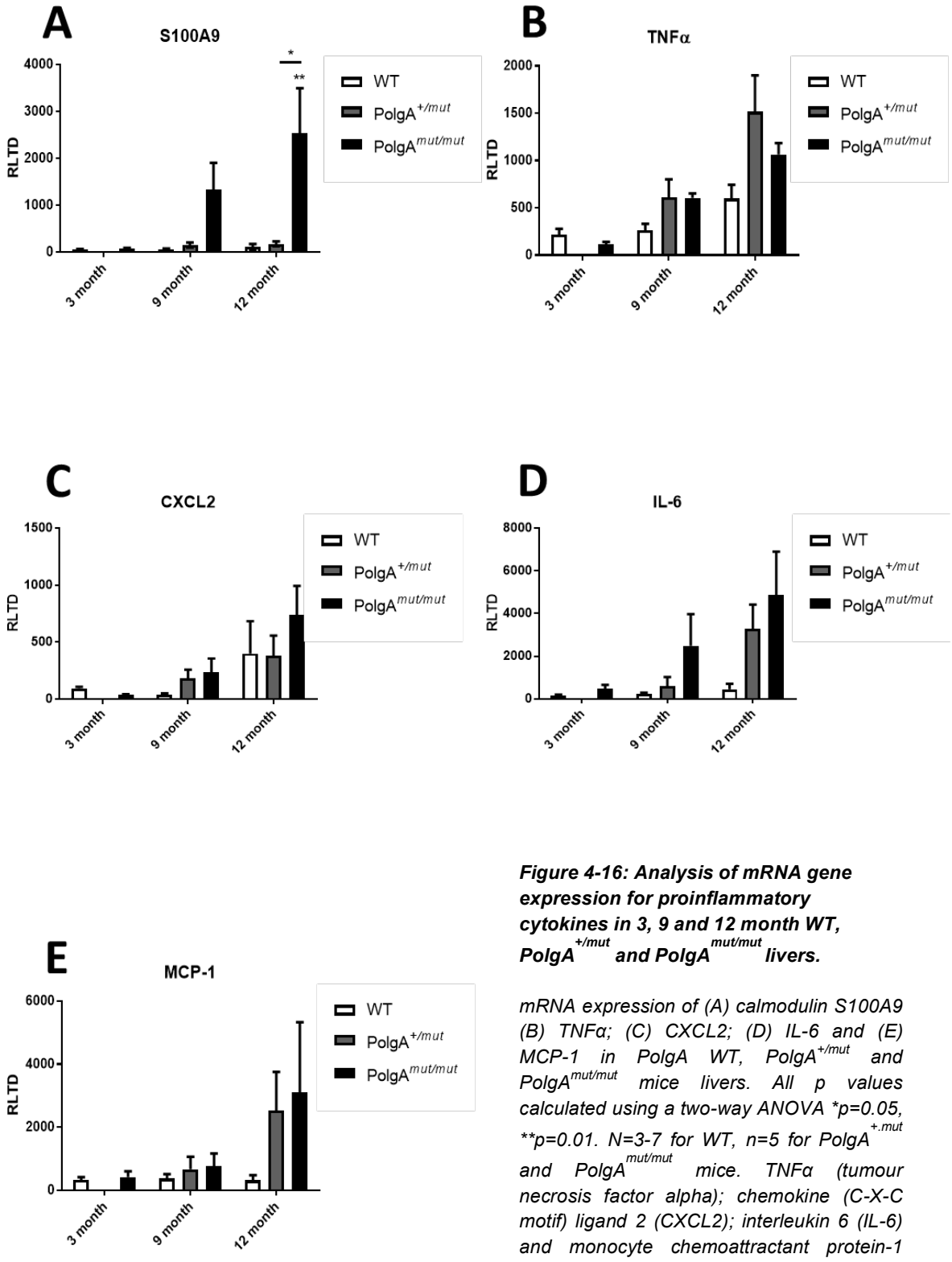

Figure 4-16: Analysis of mRNA gene expression for proinflammatory cytokines in 3, 9 and 12 month WT, PolgA$^{+/mut}$ and PolgA$^{mut/mut}$ livers.

*mRNA expression of (A) calmodulin S100A9 (B) TNFα; (C) CXCL2; (D) IL-6 and (E) MCP-1 in PolgA WT, PolgA$^{+/mut}$ and PolgA$^{mut/mut}$ mice livers. All p values calculated using a two-way ANOVA *p=0.05, **p=0.01. N=3-7 for WT, n=5 for PolgA$^{+.mut}$ and PolgA$^{mut/mut}$ mice. TNFα (tumour necrosis factor alpha); chemokine (C-X-C motif) ligand 2 (CXCL2); interleukin 6 (IL-6) and monocyte chemoattractant protein-1 (MCP-1).*

4.9.3 Serum detection of proinflammatory cytokines

Inflammatory homing to the liver was additionally investigated using MSD multiplex ELISA to detect serum chemotactic factors in WT, *PolgA*$^{+/mut}$ and *PolgA*$^{mut/mut}$ female mice. Coinciding with mRNA expression trends, sera assayed from 3 and 12-month mice found significantly elevated levels of TNFα in older *PolgA*$^{mut/mut}$ mice (n=4) when compared to WTs ($p<0.05$, n=5) and *PolgA*$^{+/mut}$ mice ($p<0.05$, n=4) (figure 4-17, A). A similar finding was observed for IL-6 (figure 4-17, B), with the greatest increase in IL-6 concentration demonstrated between older WT and *PolgA*$^{mut/mut}$ mice ($p<0.001$), in addition to differences noted between sera of 12-month *PolgA*$^{+/mut}$ and *PolgA*$^{mut/mut}$ groups ($p<0.01$). Interestingly, despite previous low levels of CD3 and CD45R staining, increased protein concentrations for lymphocyte chemotactic factor IL-2, were also found in older *PolgA*$^{mut/mut}$ mice (figure 4-17, C). Further examination of cytokine protein levels between ageing cohorts, additionally demonstrated increased levels for IL-6 and IL-2 in both *PolgA*$^{mut/mut}$ groups, which taken together, may indicate presence and accumulation of mtDNA mutations with age to skew inflammatory signalling. No differences were observed for chemokines KC, IL-1β, IL4, IL5, IL-10 and IL-12 across both genotypes and ages (figure 4-17, D-I).

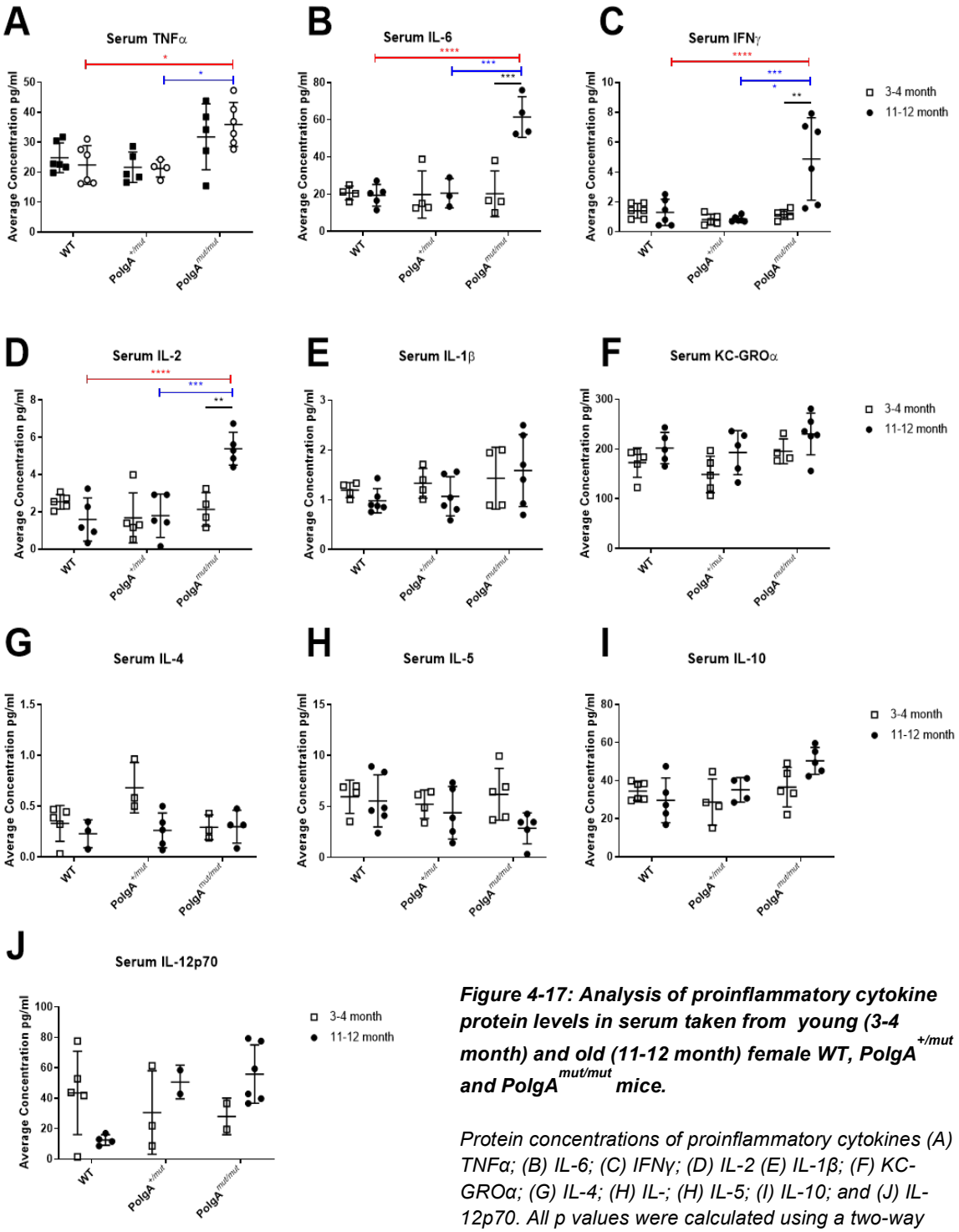

Figure 4-17: Analysis of proinflammatory cytokine protein levels in serum taken from young (3-4 month) and old (11-12 month) female WT, PolgA$^{+/mut}$ and PolgA$^{mut/mut}$ mice.

*Protein concentrations of proinflammatory cytokines (A) TNFα; (B) IL-6; (C) IFNγ; (D) IL-2 (E) IL-1β; (F) KC-GROα; (G) IL-4; (H) IL-; (H) IL-5; (I) IL-10; and (J) IL-12p70. All p values were calculated using a two-way ANOVA *p=0.05, **p=0.01, ***p=0.001, *p=0.0001. n=>5 for WT, PolgA$^{+/mut}$ and PolgA$^{mut/mut}$ mice. Tumour necrosis factor alpha (TNFα); interleukin (IL); keratinocyte chemoattractant) / human growth-related oncogene (KC-GROα); interferon gamma (IFNγ)*

4.10 Neutrophils

4.10.1 Phenotypic characterisation of neutrophils

The liver harbours a diverse range of immune cells that play an integral role in mediating tolerance to self-antigens, as well as typical host defence mechanisms against invading pathogens. Within the steady state liver, neutrophils have relatively low abundance, participating in the clearance of cell debris and initiation of tissue repair/wound healing processes during sterile tissue injury. Interestingly, following the experimental depletion of neutrophils, diminished post-PHx parenchymal restoration is seen as a result of reduced ICAM-1-dependent activation of Kupffer macrophages (Selzner *et al.*, 2003). Therefore, to test whether increased homing of neutrophils to the *PolgA*$^{mut/mut}$ liver was a cell inherent defect, neutrophils from young murine bone marrow were isolated and phenotypically characterised. Responding to chemotactic factors platelet activating factor (PAF) and N-formylmethionyl-leucyl-phenylalanine (FMLP), neutrophils from *PolgA*$^{mut/mut}$ mice were found to have trends of increased chemotaxis over other control groups (figure 4-18, A), though this failed to reach significance. Therefore, no firm conclusion can be made with regards to augmented chemotactic function in the presence of mtDNA mutations. However, isolated *PolgA*$^{mut/mut}$ neutrophils did observe significantly greater uptake of zymogen particles when analysing phagocytic function in relation to the clearance of tissue debris (figure 4-18, B).

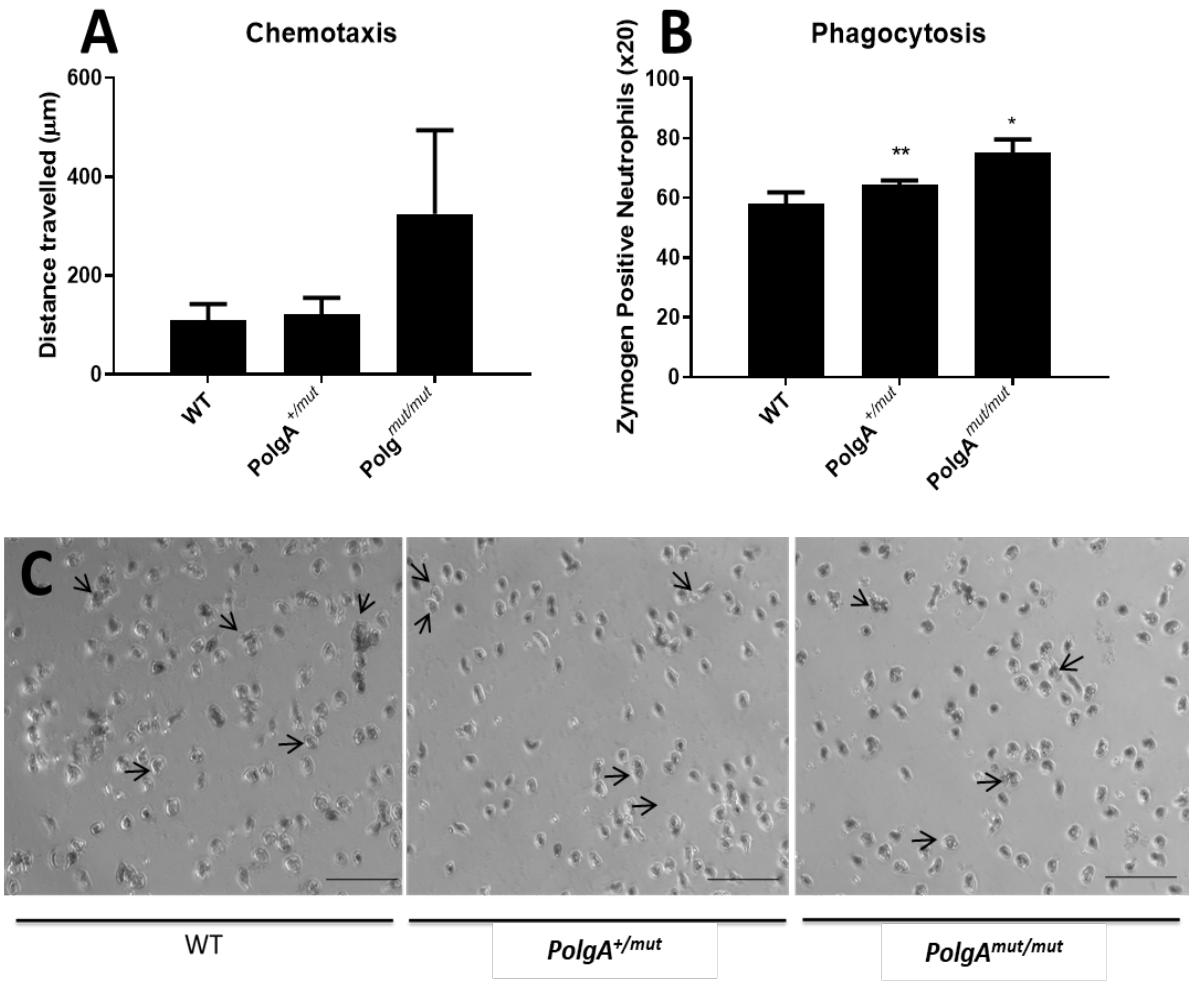

Figure 4-18: Chemotaxis and phagocytosis functional assays of bone marrow isolated neutrophils from WT, PolgA$^{+/mut}$ and PolgA$^{mut/mut}$ mice.

*(A) Distance travelled (µM) by bone marrow isolated neutrophils in response to FMLP and PAF stimulation. (B) Zymogen uptake by bone marrow isolated neutrophils from WT, PolgA$^{+/mut}$ and PolgA$^{mut/mut}$ mice. Uptake of two or more zymogen particles was considered positive for neutrophil phagocytosis neutrophils, arrows show examples of phagocytosed zymogens. Positive cells were counted in 10 fields at x10 magnification (scale bar = 100 µm). All p values calculated using a two-way ANOVA., * p=0.05, **p=0.01. N=4 for WT, PolgA$^{+/mut}$ and PolgA$^{mut/mut}$ mice in all functional assays.*

4.10.2 Quantification of neutrophil reactive oxygen species

Sterile inflammageing and age-related chronic pathologies are characterised by the dysfunctional and low-grade excess release of ROS and proinflammatory cytokines, of which neutrophils are amongst suggested key effectors (Ogawa *et al.*, 2008). Indeed, an inherent neutrophil function is the production of superoxide and other ROS following NAPDH oxidase (NOX2)-dependent phagocytosis, as well neutrophil extracellular traps (NETs) production. NETs are an extrusion of DNA and granular proteins that induce proinflammatory clearance of pathogens and potential self-antigens, and for which ROS and oxidised mtDNA are important mediators (Zhang *et al.*, 2015; Wang, 2018). Consequently, with age, it suggested that neutrophils may contribute to the inflammageing phenotype with failure to clear aged neutrophils resulting in increased NET and ROS production from such cells (Zhang *et al.*, 2015). It was therefore hypothesised that irregular presence and increased numbers of neutrophils in *PolgA*$^{mut/mut}$ livers may contribute to hepatocellular ageing and proinflammatory phenotype through increased ROS production. To test this, neutrophils from young (3-4 month) and old (11-12 month) WT, *PolgA*$^{+/mut}$ and *PolgA*$^{mut/mut}$ mice were isolated from blood and livers and stained fluorogenically for ROS during basal and activated states. Of the 100,000 events measured by flow cytometry, it was found that in 3-4 month blood, fewer neutrophils were present basally in *PolgA*$^{mut/mut}$ and *PolgA*$^{+/mut}$ mice when compared to WT controls and comprised relatively similar levels of ROS - an observation more pronounced with age but failing to reach significance (figure 4-19, A-C). Counts of unstimulated neutrophils and their ROS content were also increased in 11-12 month *PolgA*$^{mut/mut}$ livers when compared to WT controls (figure 4-20, A-C). When activated with PAF and FMLP, hepatic neutrophil counts increased and induced a greater release of ROS in *PolgA*$^{mut/mut}$ livers at 11-12 months of age (figure 4-20, A-C), a change not observed in 3-4 month livers. Similarly, greater ROS levels were detected on activation in blood *PolgA*$^{mut/mut}$ neutrophils (figure 4-19, B, C). Between the aged cohorts, notable increases in 3-4 month *PolgA*$^{mut/mut}$ counts coincided lower levels of ROS, whereas lesser *PolgA*$^{mut/mut}$ blood neutrophils at 11-12 months released a greater amount of ROS when compared to WTs. For *PolgA*$^{+/mut}$ neutrophils in both tissues and age groups a gene-dose effect was observed; however, when analysing DHR staining, ROS levels were often detected to be higher than that released from *PolgA*$^{mut/mut}$ mice.

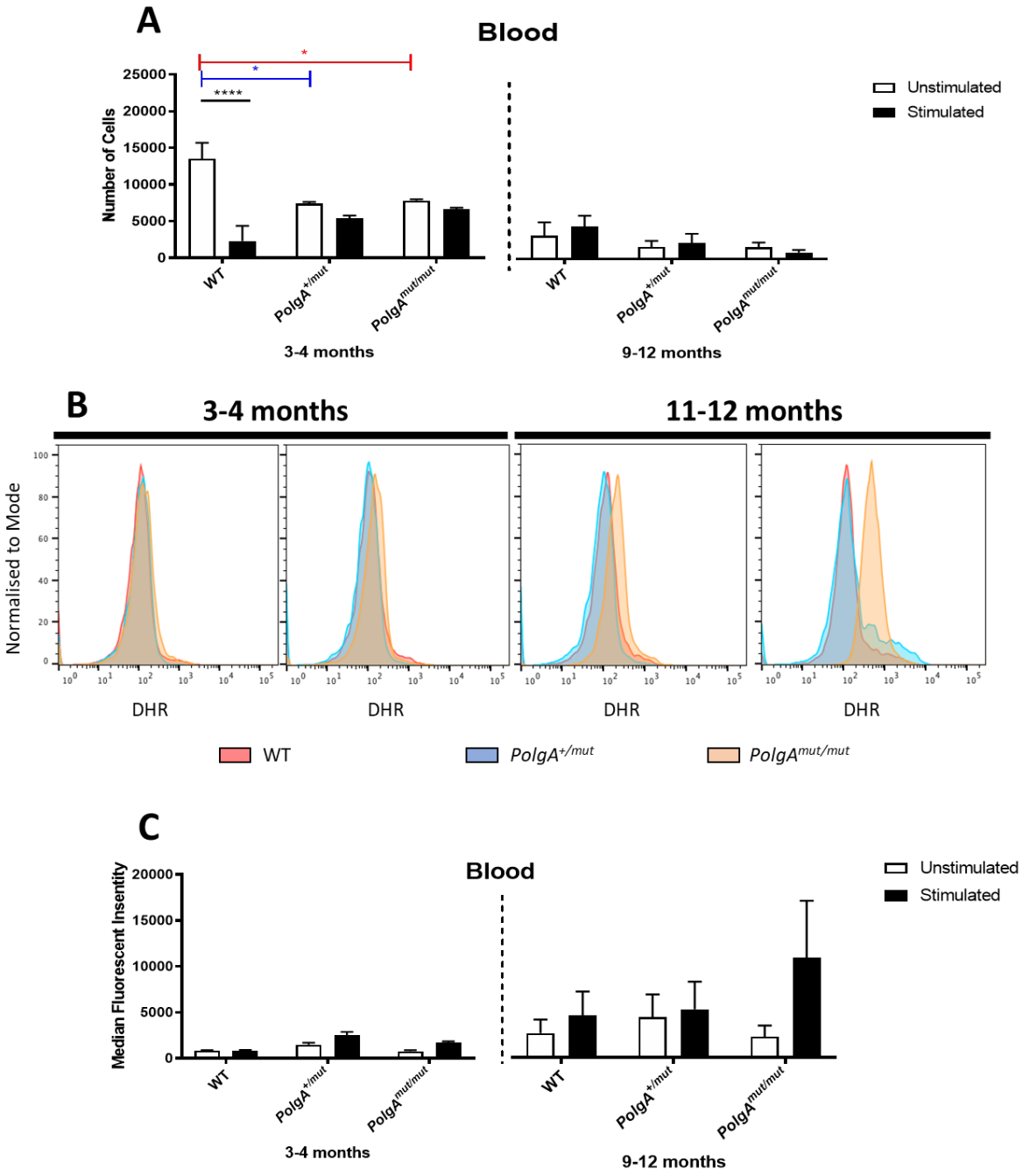

Figure 4-19: Flow cytometry analysis of WT, PolgA$^{+/mut}$ and PolgA$^{mut/mut}$ neutrophils isolated from blood.

*(A) Counts for Ly6G, CD11b positively stained neutrophils isolated from 3-4 month and 9-12 month WT, PolgA$^{+/mut}$ and PolgA$^{mut/mut}$ mice blood. (B-C) Measurement of ROS release from blood isolated neutrophils via detection of DHR expressed as median fluorescent intensity. All p values calculated using a two-way ANOVA., * p=0.05, ****p=0.0001. n=4-6 for WT, PolgA$^{+/mut}$ and PolgA$^{mut/mut}$ mice in all functional assays. N=3 per genotype; Dihydrorhodamine 123 (DHR)*

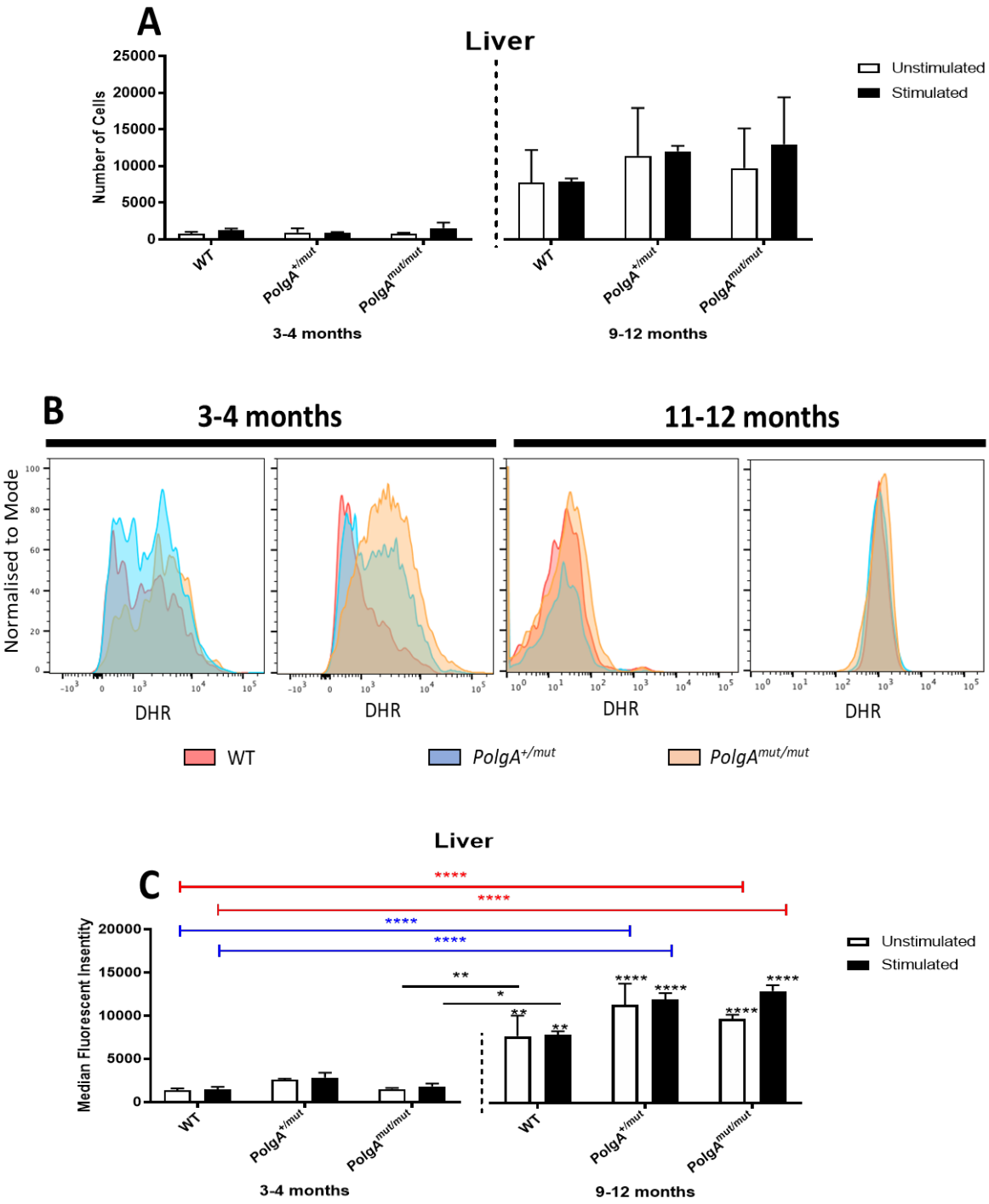

Figure 4-20: Flow cytometry analysis of WT, PolgA$^{+/mut}$ and PolgA$^{mut/mut}$ neutrophils isolated from livers.

*(A) Counts for Ly6G, CD11b positively stained neutrophils isolated from 3-4 month and 9-12 month WT, PolgA$^{+/mut}$ and PolgA$^{mut/mut}$ mice livers. (B-C) Measurement of ROS release from liver isolated neutrophils via detection of DHR expressed as median fluorescent intensity. All p values calculated using a two-way ANOVA., * p=0.05, **p=0.001, ****p=0.0001. n=4-6 for WT, PolgA$^{+/mut}$ and PolgA$^{mut/mut}$ mice in all functional assays. N=3 per genotype. Dihydrorhodamine 123 (DHR)*

4.12 Conclusions

The presence of somatic mtDNA mutations appears to have correlative links to cellular proliferation within the liver. Both *PolgA*$^{+/mut}$ and *PolgA*$^{mut/mut}$ mice displayed significant gene-dose reductions in PCNA between 9 and 12 months when compared to WTs, an observed trend also seen in *PolgA*$^{mut/mut}$ mice hepatocytes during EGF stimulation causing DNA synthesis. Although *PolgA*$^{+/mut}$ and *PolgA*$^{mut/mut}$ livers appeared histologically normal, trends of increased mitochondrial respiratory deficiency observed by COX/SDH staining was demonstrated in *PolgA*$^{mut/mut}$ mice and was significant at older age. It would also appear that qualitatively, deficiency occurs in normal WT ageing, though this was not statistically significant. Further qualitative examination found deficiency to predominantly occur around the portal vein and to extend with age towards the pericentral zones, which may be due to clonal expansion of mtDNA mutations. Previous work investigating normal human hepatic homeostasis displays clonal populations originating periportally, which then undergo unidirectional flux in a hypothesised 'streaming liver' manner (Fellous *et al.*, 2009). Here deficient hepatocytes were found to increase in frequency with age, in line with previous *PolgA* mice studies (Trifunovic *et al.*, 2004; Kujoth *et al.*, 2005). However, no differences were observed in the levels of COX deficiency between young and old *PolgA*$^{mut/mut}$ mice: perhaps ascribed to possibility that the level of respiratory deficient hepatic cells is within the tolerance level and does not demonstrate an observable phenotype in *PolgA*$^{mut/mut}$ *mice*. Subsequently, onset may be ascribed to accumulation and the exacerbation of inflammation and apoptosis that in turn results in an observable reduction in hepatocellular turnover within the ageing liver.

Analysis of ETC complexes confirmed mitochondrial respiratory dysfunction. However, although staining was indicative of mitochondrial COX dysfunction, complex IV (Mt-CO1) protein expression was not downregulated in liver and hepatocytes. Whilst these results cannot exclude the possibility of complex IV loss of protein functionality, instead analysis of specific ETC complexes found that in *PolgA*$^{mut/mut}$ mice deficiencies observed were specific for complex I (NDUFB8) across all ages in both hepatocytes and whole liver, indicating a possible link between complex I respiratory dysfunction and reduced hepatocellular turnover. Indeed, in other work, reduction of complex I by pharmacological inhibition is found to halt cell proliferation *via* induction of G2/M cell cycle arrest as well as provoke apoptosis

(Srivastava and Panda, 2007). Similarly, it was found that hepatocyte cell death was markedly increased in *PolgA*$^{mut/mut}$ mice when compared to other groups and previous findings (Kujoth *et al.*, 2005). In spite of the altered complex I expression, it was found that reduced basal hepatocellular turnover in *PolgA*$^{mut/mut}$ mice was not linked to altered NAD+/NADH ratios, at least utilising the assays available to do so. Despite this, alterations in PGC1α within aged *PolgA*$^{mut/mut}$ mice was observed, in which changes to the redox balance of NAD+/NADH is noted to regulate its transcriptional activity *via* metabolic sensor SIRT1. Although extensively described as a master regulator of mitochondrial biogenesis, the present data cannot conclusively correlate increased PGC1α gene expression with such a role due to the absence of upregulated protein expression of mitochondrial complexes during western blot. Such observations, however, may be ascribed to additional transcriptional and post-translational targets of PCG1α, including the regulation of ROS-detoxifying enzymes (St-Pierre *et al.*, 2002; St-Pierre *et al.*, 2003; Valle *et al.*, 2005). Indeed, the present study shows increased mRNA expression of ROS scavenger SOD2 with age as well as reductions in anti-oxidants GSS and GPx. In turn, PGC1α is shown to be induced by oxidative stress. It is therefore possible that respiratory-associated reductions in cellular proliferation and redox alterations could be allied to mitochondrially-driven oxidative stress, though further work such quantifying ROS within the liver and determining cell cycle markers would be required to confirm and elucidate this. Although interesting, the mutation load of mtDNA in liver was not investigated further to determine thresholds required for the observed phenotypes.

Analysis of neutrophils confirmed greater numbers within the *PolgA*$^{mut/mut}$ liver at old age when compared to WT controls, both basally and when activated, which may be in part due to increased neutrophil priming, recruitment and sensitivity to activation. Although failing to reach significance, functional analysis of *PolgA*$^{mut/mut}$ neutrophils show amplified ability for chemotaxis, which was not further explored in older ages. The role of oxidative stress and signalling is also unclear, with isolated aged liver *PolgA*$^{mut/mut}$ neutrophils showing increased basal levels of ROS, thus raising the question as to whether neutrophils are initially recruited due to excess ROS signalling by liver resident immune cells and/or recruited neutrophils are the source of excess oxidative stress signalling. Both would appear plausible, with initial increases in CD68 positive monocytes and macrophages seen at 3 to 6 months *PolgA*$^{mut/mut}$ mice, whilst higher basal *PolgA*$^{mut/mut}$ neutrophil ROS levels further augment on activation.

Taken together, these observations suggest the presence of mitochondrial dysfunction promotes the proinflammatory recruitment of neutrophils to the liver. These neutrophils are basally more primed for recruitment and galvanisation than WTs and release more ROS when stimulated. Heightened activation may also explain the increased gene-dose dependent phagocytic activity observed in *PolgA* mice. Indeed, it is understood that in the presence of sterile tissue injury, sustained neutrophil recruitment and activation can lead to chronic inflammation and impaired tissue recovery, as well as have some clinical relevance to inflammation in normally aged subjects (Meyer *et al.*, 1998; Ogawa *et al.*, 2008; de Oliveira *et al.*, 2016). Recruitment could be alluded to the dysregulated stimulation of immune cell signalling due to mitochondrial dysfunction, in which downstream production of cytokines are chemotactic for neutrophils. Specifically, in relation to *PolgA*$^{mut/mut}$ mice, it has been previously shown that significant increases in *in vivo* ROS due to age-accumulated mitochondrial dysfunction induces activation of pro-apoptotic and proinflammatory pathways (Logan *et al.*, 2014). Therefore, taken together with the present changes in SOD2, it is therefore likely that the observable proinflammatory phenotype in aged *PolgA*$^{mut/mut}$ mice is ascribed to accumulation of mitochondrial dysfunction and resultant exacerbated ROS. In turn, inciting *via* oxidant-inflammatory signalling pathways, neutrophil recruitment.

With previous work noting the importance of immune cells in liver homeostasis, it is also possible that altered inflammatory signalling in the presence of mitochondrial dysfunction could contribute to the basal proliferative phenotype within the liver (Moiseeva *et al.*, 2009; Jiang and Torok, 2013; Jiang *et al.*, 2013). However, with aged hepatocytes showing trends of reduced proliferative response in culture, any contribution of immune cells in reducing hepatocellular turnover is likely to be secondary. Alternatively, it is possible that inflammation could be an inducer of mitochondrial dysfunction, though this avenue was not explored. Consequently, further work to explore whether the presence of complex I deficiency affects hepatocyte proliferation using models of regeneration in subsequent chapters, will be essential to elucidate the impact of mtDNA mutations in this setting.

Table 4-1: Chapter 4 Summary Table. *ND denotes 'no statistical difference'*

	Regeneration		Mitochondrial Function					Hepatocytes				
	Liver Weight	Histology	Histology	Protein		Gene	Biochemical	Biochemical			Protein	
	Total Liver Weight	PCNA	COX /SDH	NDUFB8 (CI)	Mt-CO1 (CIV)	PGC1α	NAD/NADH	BrDU	Alamar Blue	LDH	NDUFB8 (CI)	Mt-CO1 (CIV)
WT	↓↓↓↓ 12-month WT vs. 12-month *PolgA*$^{mut/mut}$	↑↑↑ 9- & 12-month WT vs. 9- & 12 month *PolgA*$^{+/mut}$ & *PolgA*$^{mut/mut}$	ND	↑↑ 12-month WT vs. 12-month *PolgA*$^{mut/mut}$	ND	↓↓↓↓ 12-month WT vs. 12-month *PolgA*$^{mut/mut}$	ND	ND	ND	ND	↑ 12-month WT vs. 12-month *PolgA*$^{+/mut}$ & 12-month *PolgA*$^{mut/mut}$	ND
***PolgA*$^{+/mut}$**	↓↓↓↓ 12-month *PolgA*$^{+/mut}$ vs. 12-month *PolgA*$^{mut/mut}$	↓↓↓ 9-month *PolgA*$^{+/mut}$ vs. 9-month WT	-	↑ 12-month *PolgA*$^{+/mut}$ vs. 12-month *PolgA*$^{mut/mut}$	ND	↓↓↓12-month *PolgA*$^{+/mut}$ vs. 12-month *PolgA*$^{mut/mut}$	-	ND	ND	ND	↑ 3-month *PolgA*$^{+/mut}$ vs. 12-month *PolgA*$^{mut/mut}$ ↓ 12-month *PolgA*$^{+/mut}$ vs. 12-month WT	ND
***PolgA*$^{mut/mut}$**	↑ 12-month *PolgA*$^{mut/mut}$ vs. 3-month *PolgA*$^{mut/mut}$ ↑↑↑↑ 12-month *PolgA*$^{mut/mut}$ vs. 12-month WT & *PolgA*$^{+/mut}$	↓↓↓ 9- & 12-month *PolgA*$^{mut/mut}$ vs. 9- & 12-month WT	↑↑ 12-month *PolgA*$^{mut/mut}$ vs. 3-month *PolgA*$^{mut/mut}$	↓↓ 12-month *PolgA*$^{mut/mut}$ vs. WT ↓ 12-month *PolgA*$^{+/mut}$	ND	↑↑↑ 12-month *PolgA*$^{mut/mut}$ vs. 3-month *PolgA*$^{mut/mut}$ ↑↑ 12-month *PolgA*$^{mut/mut}$ vs. 6-month *PolgA*$^{mut/mut}$ ↑↑↑ 12-month *PolgA*$^{mut/mut}$ vs. 12-month WT & *PolgA*$^{+/mut}$	ND	ND	ND	ND	↓ 3-month *PolgA*$^{mut/mut}$ vs. 12-month *PolgA*$^{mut/mut}$ ↓ 12-month *PolgA*$^{mut/mut}$ vs. 12-month WT	ND

Table 4-1 Continued: Chapter 4 Summary Table. *ND denotes 'no statistical difference'*

	Apoptosis					Antioxidants				Inflammation					
	Histology	Hepatocyte Apoptosis				Gene				Gene					Protein
	Caspase 3	BAX	Bid	BCL_{XL}	BCL-2	GSS	GPX	SOD1	SOD2	S100A9	TNFα	CXCL1	IL6	MCP--1	MSD
WT	↓↓ 6-month WT vs. 6-month *PolgA*$^{mut/mut}$ ↓↓↓ 9- & 12-month WT vs. 9- & 12-month *PolgA*$^{mut/mut}$	ND	ND	↑↑ 12-month WT vs. 12-month *PolgA*$^{+/mut}$ ↑↑ 12-month WT vs.12-month *PolgA*$^{mut/mut}$	↑ 3-month WT vs. 3-month *PolgA*$^{mut/mut}$	ND	ND	ND	P=0.054 12-month WT vs. 12-month *PolgA*$^{mut/mut}$	↓↓ 12-month WT vs. 12-month *PolgA*$^{mut/mut}$	ND	ND	ND	ND	Lower 12-month WT serum TNFα, IL-6, IFNγ and IL-2 vs. 12-month *PolgA*$^{mut/mut}$
***PolgA*$^{+/mut}$**	↓↓↓ 6-month *PolgA*$^{+/mut}$ vs. 6-month *PolgA*$^{mut/mut}$	ND	ND	↓↓ 12-month *PolgA*$^{+/mut}$ vs. 12-month *PolgA*$^{mut/mut}$	ND	ND	ND	ND	ND	↓12-month *PolgA*$^{+/mut}$ vs. 12-month *PolgA*$^{mut/mut}$	ND	ND	ND	ND	Lower 12-month *PolgA*$^{+/mut}$ serum TNFα, IL-6, IFNγ and IL-2 vs.12-month *PolgA*$^{mut/mut}$
***PolgA*$^{mut/mut}$**	↑↑ 6-month *PolgA*$^{mut/mut}$ vs. 6-month WT ↑↑↑ 9 & 12-month *PolgA*$^{mut/mut}$ vs. 9- & 12-month WT	ND	ND	↓↓ 12-month *PolgA*$^{mut/mut}$ vs. 12-month *PolgA*$^{mut/mut}$	↓ 3-month *PolgA*$^{mut/mut}$ vs. 3-month WT	ND	ND	ND	P=0.054 12-month WT vs. 12-month *PolgA*^{mut}	↑↑ 12-month *PolgA*$^{mut/mut}$ vs. 12-month WT ↑ 12-month *PolgA*$^{mut/mut}$ 12-month *PolgA*$^{+/mut}$	ND	ND	ND	ND	Higher 12-month *PolgA*$^{mut/mut}$ serum TNFα, IL-6, IFNγ and IL-2 vs. 12-month WT & PolgA$^{+/mut}$ Higher 12-month *PolgA*$^{mut/mut}$ serum IL-6, IFNγ and IL-2 vs. 3-month *PolgA*$^{mut/mut}$

Table 4-1 Continued: Chapter 4 Summary Table. *ND denotes 'no statistical difference'*

	Inflammation							
	Histology				BM Neutrophil Assay		Flow Cytometry	
	CD3	CD45R	CD68	NIMP	Chemotaxis	Phagocytosis	Blood	Liver
WT	↓↓↓ 3-month WT vs. *PolgA*$^{mut/mut}$ ↑↑↑ 6-, 9- & 12 month WT vs. 6-, 9- & 12-month *PolgA*$^{mut/mut}$ ↓ 6 & 9-month WT vs. 6 & 9-month *PolgA*$^{+/mut}$	↓↓↓ 3 & 6-month WT vs 3 & 6-month *PolgA*$^{mut/mut}$ ↑↑↑ 9 & 12 month WT vs. 9 & 12-month *PolgA*$^{mut/mut}$ ↓↓↓ 6-month WT vs. 6-month *PolgA*$^{+/mut}$	↓↓↓ 3-month WT vs. 3-month *PolgA*$^{mut/mut}$ ↓↓↓ 6-month WT vs. 6-month *PolgA*$^{+/mut}$ ↓↓ 6-month WT vs. 6-month *PolgA*$^{mut/mut}$	↓↓↓ 3-, 6- 9- & 12-month WT vs. 3-, 6-, 9- & 12-month *PolgA*$^{mut/mut}$ ↓↓↓ 6-month WT vs. 6-month *PolgA*$^{+/mut}$	ND	↓ WT vs. *PolgA*$^{mut/mut}$	Reduced 3-month blood neutrophils unstimulated numbers in *PolgA* mice vs. WT Increased trends of neutrophil ROS release with age	Trends of increased liver neutrophils with age across all genotypes Significantly increased neutrophil ROS release with age across all genotypes
***PolgA*$^{+/mut}$**	↑ 6 & 9-month *PolgA*$^{+/mut}$ vs. 6 & 9-month WT	↑↑↑ 6-month *PolgA*$^{+/mut}$ vs. 6-month WT	↑↑↑ 6-month *PolgA*$^{+/mut}$ vs. 6-month WT ↑↑↑ 6-month *PolgA*$^{+/mut}$ vs. 6-month *PolgA*$^{mut/mut}$	↓↓↓ 9-month *PolgA*$^{+/mut}$ vs. 9-month *PolgA*$^{mut/mut}$	ND	↓↓ *PolgA*$^{+/mut}$ vs. *PolgA*$^{mut/mut}$		
***PolgA*$^{mut/mut}$**	↑↑↑ 3-month *PolgA*$^{mut/mut}$ vs. 3-month WT ↓↓↓ 6-, 9- & 12-month *PolgA*$^{mut/mut}$ vs. 6-, 9- & 12-month WT	↑↑↑ 3 & 6-month *PolgA*$^{mut/mut}$ vs. 3 & 6-month WT ↓↓↓ 9- & 12-month *PolgA*$^{mut/mut}$ vs. 9 & 12-month WT	↑↑↑ 3-month *PolgA*$^{mut/mut}$ vs. 3-month WT ↑↑ 6-month *PolgA*$^{mut/mut}$ vs. 6-month WT ↓↓↓ 6-month *PolgA*$^{mut/mut}$ vs. 6-month *PolgA*$^{+/mut}$	↑↑↑ 3-, 6-, 9- & 12-month *PolgA*$^{mut/mut}$ vs. 3-6-, 9- & 12-month WT ↑↑↑ 9-month *PolgA*$^{mut/mut}$ vs. 9-month *PolgA*$^{+/mut}$	ND	↑ *PolgA*$^{mut/mut}$ vs. WT ↑↑ *PolgA*$^{mut/mut}$ vs. *PolgA*$^{+/mut}$		

4.13 Chapter 4 Key Summary Points

- COX/SDH staining and reduced protein expression of complex I NDUFB8 indicates mitochondrial respiratory dysfunction to increase with age in *PolgA*$^{mut/mut}$ *mice,* which in turn may be correlated with reduced *PolgA*$^{mut/mut}$ hepatocyte proliferative capacity and basal hepatocellular turnover.

- Decreased GSS and GPX, as well as increases in SOD2 expression was observed in ageing *PolgA*$^{mut/mut}$ mice, in which loss of hepatocellular turnover may be ascribed to exacerbated ROS signalling and possible subsequent oxidative damage to the liver tissue.

- *PolgA*$^{mut/mut}$ mice demonstrate changes in immune cell homeostasis with age. Mitochondrial respiratory dysfunction appears to induce a neutrophilic pro-inflammatory environment as seen *via* increased NIMP positive neutrophils and increased detection of cytokines chemotactic for neutrophils.

- Previous studies show ROS to be a potent activator of the innate immune response, whilst exacerbated neutrophil recruitment hinders tissue recovery. Increased mitochondrial respiratory dysfunction may therefore increase ROS-induced neutrophil activation, which in turn may reduce hepatocellular proliferation in ageing *PolgA*$^{mut/mut}$ mice. Aged neutrophils appear to be basally 'more primed' for activation, releasing more ROS basally and are functionally more active, as indicated by greater phagocytosis.

- Caspase-3 positive hepatocytes and reduced expression of anti-apoptotic genes suggests that the presence of mitochondrial dysfunction also induces greater apoptosis with age.

- Absence of reduced hepatocellular turnover in 3-month *PolgA*$^{mut/mut}$ and *PolgA*$^{+/mut}$ mice, despite some mitochondrial respiratory dysfunction, may be due to the ability for these hepatocytes to tolerate the level of mitochondrial respiratory dysfunction present. Onset of reduced basal hepatocellular turnover may be therefore ascribed to much greater levels of mtDNA mutations with age and the exacerbation of aberrant inflammatory, ROS and apoptotic signalling pathways acting in concert.

Chapter 5 | Investigating the Role of Mitochondrial Dysfunction and Ageing on Liver Regeneration

5.1 Introduction

To further assess the implications of defective basal hepatocellular proliferation within ageing respiratory chain deficient *PolgA*$^{mut/mut}$ mice, the surgical model incorporating two-thirds (70%) partial hepatectomy (PHx) was undertaken. As proliferation of existing hepatocytes is key to hyperplasic and hypertrophic regenerative mechanisms and since the progeroid ageing phenotype in *PolgA*$^{mut/mut}$ mice is correlated with accumulated mitochondrial respiratory chain dysfunction over time, partial hepatectomy (PHx) studies were carried out on aged WT and *PolgA*$^{mut/mut}$ mice to assess the role of mitochondrial respiratory chain dysfunction on 'ageing' liver regeneration. Aberrant hepatocellular proliferation is also associated with ageing, with age-associated changes including a basal reduction in liver volume, decreased hepatocyte cell numbers and increased hypertrophy and more specifically, diminished hepatic mitochondrial density and alterations to the mitochondrial ultrastructure observed (Tauchi and Sato, 1968; Ferri *et al.*, 2005; Frith *et al.*, 2008). Diminished liver function as measured by liver clearance and phase I pharmakokinetics is additionally noted in the ageing liver; however, is often less well documented, due to compensatory mechanisms of the liver that include regeneration (Schmucker, 2005; Schmucker and Sanchez, 2011). More clinically relevant is the significant decline in hepatocyte survival following PHx intervention, ascribed to reduced capacity in hepatocellular proliferative mechanisms: including reduction in hepatocyte cell cycle entry, reduced expression of hepatocellular proliferative factors and diminished regenerative signalling (Bucher and Swaffield, 1964; Stocker and Heine, 1971; Miyaoka and Miyajima, 2013; Enkhbold *et al.*, 2015) . In the previous chapter, hepatoproliferative defects observed in the aged *PolgA*$^{mut/mut}$ mice were due to an age-associated accumulation of mitochondrial respiratory dysfunction. Therefore, to assess active liver regeneration with age, PHx surgery removing 70% of the liver mass was performed in *PolgA*$^{+/mut}$ and *PolgA*$^{mut/mut}$ mice at 3 and 6 months of age.

5.2 Aims

To further assess the implications of mitochondrial dysfunction within *PolgA*$^{+/mut}$ heterozygous and *PolgA*$^{mut/mut}$ mice, in the context of ageing liver regeneration, parenchymal recovery was assessed using the classical 70% PHx model. Characterisation of hepatocellular regeneration in the presence of mitochondrial respiratory chain deficiency was undertaken in the present study to:

1. Determine if the presence of mitochondrial respiratory chain dysfunction in the *PolgA*$^{+/mut}$ and *PolgA*$^{mut/mut}$ mice alters hepatocellular regeneration post-PHx in both young (3 month) and aged (6 month) mice.

2. Assess whether age-associated accumulations of mitochondrial respiratory chain dysfunction diminishes post-surgical parenchymal recovery in 6 month old *PolgA*$^{+/mut}$ and *PolgA*$^{mut/mut}$ mice when compared to 3 month controls.

5.3 Partial hepatectomy

Resection of the liver or “partial hepatectomy” is understood to be the most classical model of synchronous liver regeneration involving surgical removal of the liver’s medial and left lateral lobes that equates to 70% of liver mass (Higgins, 1931). Here, removal of liver tissue gives rise to parenchymal recovery of the liver, predominantly by means of hepatocellular hypertrophic and hyperplasic mechanisms that compensate for the loss of hepatocyte cell numbers and function - the process of which involves a complex plethora of growth factors and inflammatory cytokines acting in concert across priming, proliferation and termination of regenerative phases to regulate cellular regrowth and liver size post-injury. Primed by cytokines and complement factors secreted by activated inflammatory cells like Kupffer cells, post-PHx liver regeneration begins with rapid entry of quiescent G_0 hepatocytes into the G_1 phase of cell cycle and by ~24 hours post-surgery, the ‘S phase’ peak in DNA synthesis occurs (Michalopoulos and DeFrances, 1997; Miyaoka *et al.*, 2012; Miyaoka and Miyajima, 2013). By ~3 days, the majority of hepatocellular proliferation and parenchymal hyperplasia by means of G_1 phase transition into mitotic division occurs, carefully mediated by mitogenic factors such as hepatocyte growth factor (HGF) and epithelial growth factor (EGF). Finally, once 2.5 times the normal liver to body weight ratio is restored, entry into the termination phase of liver regeneration occurs, with induction of growth arrest regulated predominantly by tumour necrosis

factor (TGF)β and interleukin 1β (IL-1β) signalling (Tao *et al.*, 2017). Within 5-7 days parenchymal recovery of mass is largely completed, closely followed by a wave of regeneration from non-parenchymal cells; 7-10 days post-PHx, the majority of lost cellular mass (93%) is recovered and by 20 days, liver volume pre-PHx is fully regained (Michalopoulos and DeFrances, 1997; Miyaoka *et al.*, 2012). By contrast, 30% PHx induces hepatic tissue recovery chiefly by sole means of hepatocellular hypertrophy (Miyaoka *et al.*, 2012). The present study was therefore undertaken to determine if age-associated accumulation of mitochondrial respiratory chain dysfunction in *PolgA*$^{+/mut}$ and *PolgA*$^{mut/mut}$ mice alters hepatocellular regeneration following 70% partial liver resection.

5.4 Regenerative response in WT, *PolgA*$^{+/mut}$ and *PolgA*$^{mut/mut}$ mice following partial hepatectomy

5.4.1 Presence of mitochondrial respiratory dysfunction reduces survival following partial liver resection in aged *PolgA*$^{mut/mut}$ *mice*

Presence of complex I respiratory deficiency, as demonstrated in *PolgA*$^{mut/mut}$ mice, appears to be correlated with defective hepatocellular proliferation and survival both basally with age and when hepatocytes are stimulated for DNA synthesis. It was therefore hypothesised that ageing *PolgA*$^{mut/mut}$ mice would have aberrant liver regeneration. Utilising PHx in WT, *PolgA*$^{+/mut}$ and *PolgA*$^{mut/mut}$ mice at 3 and 6 months of age to determine this effect, mice were initially grouped into post-operative survivors and non-survivors. PHx survivors were determined as post-surgical mice at 48 or 72 hours (time points were determined by peak regenerative markers measured following PHx in 8-week WT mice; appendix IV), whilst non-survivors determined as those sacrificed ahead of the set timepoints due to welfare concerns. Here it was found that following surgery at 3 months, all genotypes thrived till their given time points, achieving 100% survival; yet when aged to 6 months, survival in *PolgA*$^{+/mut}$ PHx mice was lowered to 90.1% and in *PolgA*$^{mut/mut}$ mice 70% (figure 5-1, table 5-1). 100% survival was also observed in 6-month WTs, therefore indicating that age-associated presence of mitochondrial dysfunction seen in 6-month *PolgA*$^{+/mut}$ and *PolgA*$^{mut/mut}$ mice reduces survival following partial liver resection.

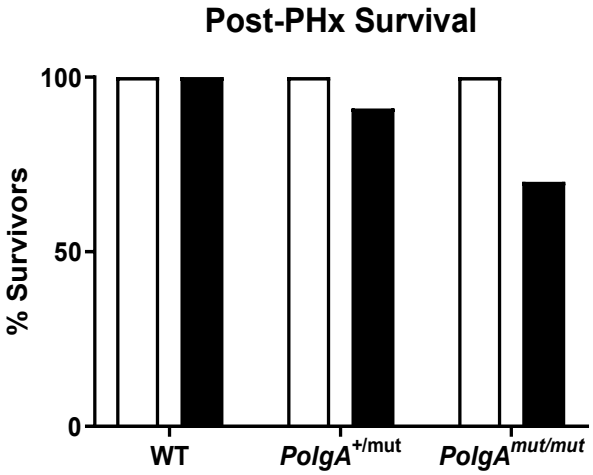

	Survivors	Non-Survivors
WT	10	0
PolgA$^{+/mut}$	10	1
PolgA$^{mut/mut}$	8	4

Figure 5-1: Survival following partial hepatectomy (PHx); Table 5-1: Surviving and non-surviving 6-month WT, PolgA$^{+/mut}$ and PolgA$^{mut/mut}$ mice following PHx.

Survival following post-PHx surgery in WT, PolgA$^{+/mut}$ and PolgA$^{mut/mut}$ mice, expressed as a percentage of total PHx surgeries undertaken. 3-month WT (n=10), PolgA$^{+/mut}$ (n=10) and PolgA$^{mut/mut}$ (n=8) observed 100% survival whilst the percentage survival was reduced to ~91% and 70% in 6-month PolgA$^{+/mut}$ (n=11) and PolgA$^{mut/mut}$ (n=10). Dichotomy of 6-month data into number of survivors and non-survivors for each genotype is shown in table 5-1 (above).

5.4.2 Regenerative capacity of the liver is reduced in the presence of mitochondrial respiratory dysfunction and with age

It is established that following two-thirds liver resection, recovery of lost liver cell mass by means of hyperplasic and hypertrophic mechanisms occurs from pre-existing hepatocytes, subsequently returning to homeostatic levels over time by apoptotic removal of generated excess cells (Miyaoka *et al.*, 2012). As such, when testing by means of liver to body weight ratios whether the presence of mitochondrial respiratory dysfunction affects parenchymal recovery post-PHx, no significant difference between WT, *PolgA*$^{+/mut}$ and *PolgA*$^{mut/mut}$ mice in naïve (median laparotomy only) and hepatectomised groups at 3 months of age was observed (figure 5-2, A). Similarly, in 6-month WT and *PolgA*$^{+/mut}$ mice, liver to body weight ratios of the liver remnant increased with time – reaching statistical significance in 72-hour post-PHx WT mice when compared to naïve laparotomy only controls (figure 5-2, B). No changes were observed in 6-month *PolgA*$^{mut/mut}$ mice, perhaps ascribed to much lower body weights (figure 5-2, C-D), however they did appear to have initially larger livers than other naïve groups. Alternative measures by means of total liver weights were otherwise assessed, noting no significant changes between genotypes in 3-month mice (figure 5-3, A). However, when comparing each 3-month genotype to their naïve controls, significantly increased liver weights were observed post-PHx at 48 hours post-PHx in *PolgA*$^{mut/mut}$ mice, as well as at 72 hours in both *PolgA*$^{+/mut}$ and *PolgA*$^{mut/mut}$ cohorts. Corresponding to liver to body weight ratios, 6-month naïve *PolgA*$^{mut/mut}$ liver weights were also significantly elevated in comparison to WT and *PolgA*$^{+/mut}$ mice - these findings indicating initial hepatic enlargement (figure 5-3, B). Subsequently, PHx surgery was shown to increase liver mass in WT and *PolgA*$^{+/mut}$ mice, reaching significance at 72 hours post-PHx; yet, by contrast in *PolgA*$^{mut/mut}$ livers, hepatic mass was shown to significantly reduce 48-72 hours post-surgery. These results indicate possible failure in the ability to regain liver mass post-PHx.

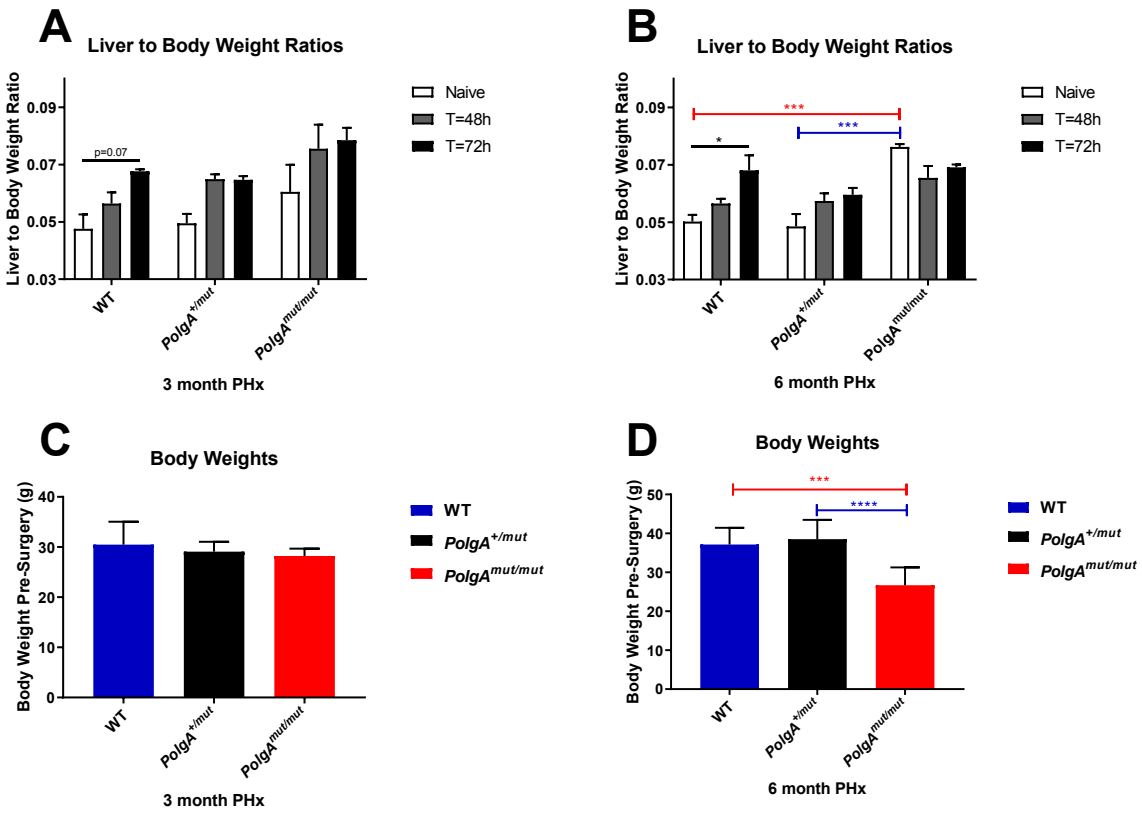

Figure 5-2: Liver to body weight ratios in WT and in the presence of mitochondrial respiratory dysfunction following partial hepatectomy (PHx).

*(A-B) Liver to body weight ratios taken from naïve (median laparotomy only) and 70% PHx WT, PolgA$^{+/mut}$ and PolgA$^{mut/mut}$ mice at 3 and 6 months of age. Ratios expressed as a proportion of total liver weight at 48 and 72 hours post-PHx to body weight at surgery. N=5 per WT and PolgA$^{+/mut}$ naïve and PHx groups, n=3 per PolgA$^{mut/mut}$ naïve and PHx groups. All p values were calculated using a two-way ANOVA *p=0.05, *** p=0.005, **** p =0.001*

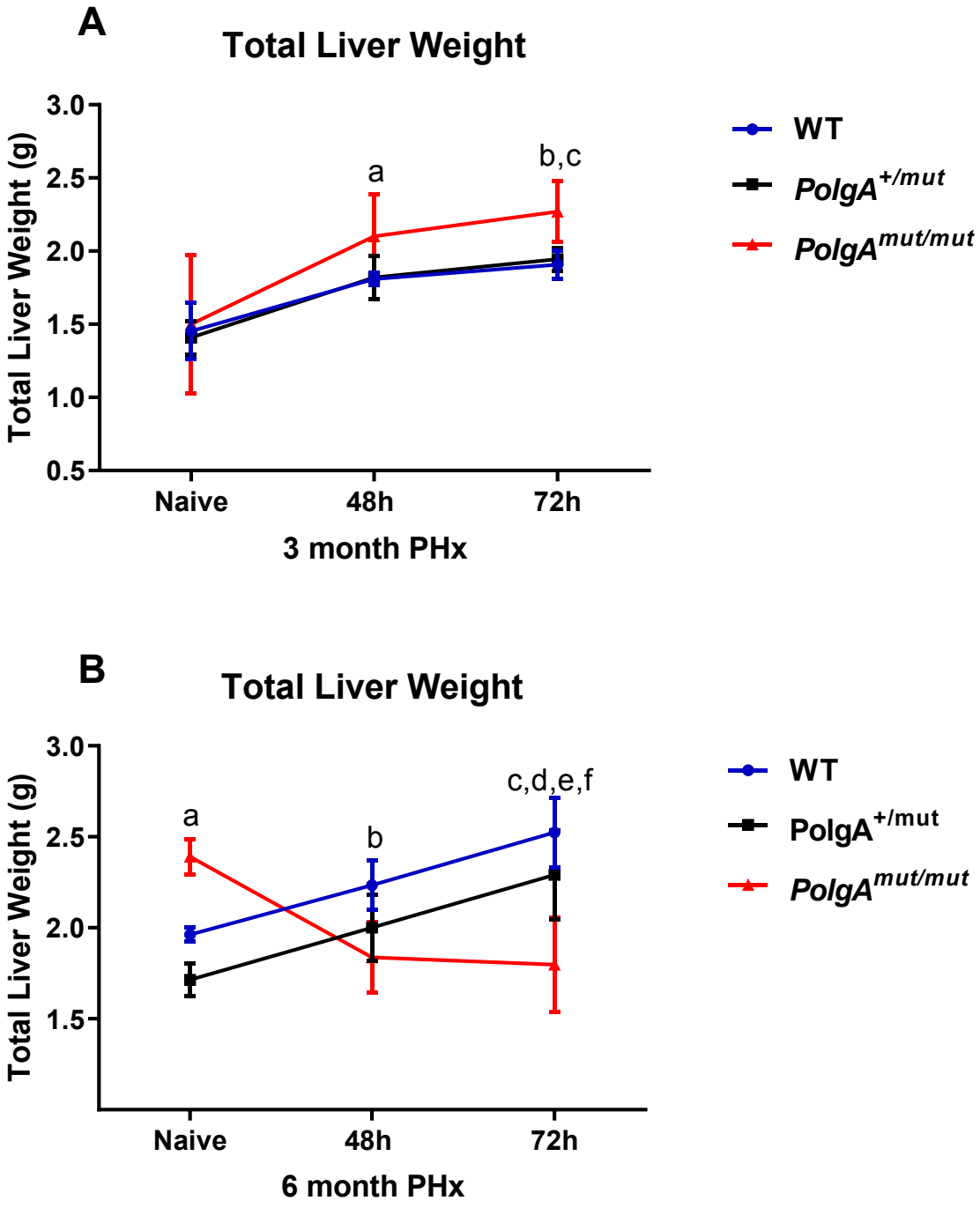

Figure 5-3: Total liver weights in naïve and post-PHx WT, PolgA$^{+/mut}$ and PolgA$^{mut/mut}$ mice.

(A) Total liver weights are shown for 3-month WT, PolgA$^{+/mut}$ and PolgA$^{mut/mut}$ naïve and PHx mice. ***a*** *denotes p<0.05 between naïve and 48 hour post-PHx PolgA$^{mut/mut}$ mice;* ***b*** *denotes p<0.05 between naïve and 72 hour post-PHx heterozygous PolgA$^{+/mut}$ mice;* ***c*** *denotes p<0.01 between naïve and 72 hour post-PHx PolgA$^{mut/mut}$ mice. N=5 per WT and PolgA$^{+/mut}$ naïve and PHx groups, n=3 per PolgA$^{mut/mut}$ naïve and PHx groups.*

(B) Total liver weights are shown for 6-month WT, PolgA$^{+/mut}$ and PolgA$^{mut/mut}$ naïve and PHx mice. ***a*** *denotes p<0.001 between naïve WT and PolgA$^{+/mut}$ to PolgA$^{mut/mut}$ mice;* ***b*** *denotes p<0.05 between naïve and 48 hour post-PHx PolgA$^{mut/mut}$ mice;* ***c*** *denotes p<0.01 between naïve and 72 hour post-PHx WT mice;* ***d*** *denotes p<0.01 between naïve and 72 hour post-PHx PolgA$^{+/mut}$ mice;* ***e*** *denotes p<0.05 reduction between naïve and 72 hour PolgA$^{mut/mut}$ mice;* ***f*** *denotes p<0.01 between 72 hour post-PHx WT and PolgA$^{+/mut}$ to 72 hour PolgA$^{mut/mut}$ mice. N=5 per WT and PolgA$^{+/mut}$ naïve and PHx groups, n=3 per PolgA$^{mut/mut}$ naïve and PHx groups.*

Although no differences in liver to body weight ratios were noted across genotypes in PHx groups, total *PolgA*$^{mut/mut}$ liver weights appeared to correspond to diminished parenchymal regeneration as observed by H&E and PCNA immunohistochemical (IHC) analyses. Measurement of hepatocyte proliferative markers across WT, *PolgA*$^{+/mut}$ and *PolgA*$^{mut/mut}$ livers revealed that PHx in 3-month mice induced a significant elevation in hepatocyte mitotic bodies (MB) and the DNA synthesis marker PCNA when compared to T0 liver tissue. PCNA and MB peak at 48 hours post-PHX and then fall towards baseline levels at 72 hours (figure 5-4, A, B). However, in the *PolgA*$^{+/mut}$ and *PolgA*$^{mut/mut}$, the magnitude of this increase in MBs was significantly less than in WT mice in a gene-dose dependent manner, reaching statistical significance at 72 hours. A similar trend was observed in the PCNA IHC, with 3-month PCNA-positive hepatocytes, also displaying a gene-dose dependent reduction in positively stained cells at 48 hours post-PHx in *PolgA*$^{+/mut}$ and *PolgA*$^{mut/mut}$ livers, when compared to T0 liver tissue (figure 5-5, A-B). Interestingly, whilst reductions in PCNA were additionally observed in *PolgA*$^{+/mut}$ at 72 hours; this was not observed in *PolgA*$^{mut/mut}$ mice – instead, the data trended towards an increase of PCNA positive hepatocytes, possibly indicative of impaired delayed regenerative response in the presence of mitochondrial respiratory dysfunction.

Surgical intervention by PHx in 6-month mice appeared to induce hepatocellular proliferation in a similar manner to the 3-month cohort. However, as with previous studies performed in WT mice, assessment of ageing post-PHx parenchymal recovery in the present study revealed reductions in mitotic and PCNA indices in 6-month mice compared to 3-month PHx mice, indicating that hepatocellular regenerative capacity declines with normal ageing (figure 5-8) (Bucher and Swaffield, 1964; Enkhbold *et al.*, 2015). In 48-hour post-PHx, 6 month WT mice saw a ~3 and ~1.5-fold significant reduction in MBs and PCNA respectively compared to 3-month PHx mice, whilst at 72 hours a ~2-fold reduction in MBs was recognised. Decline in hepatocyte proliferation appeared to be exacerbated by the presence of mitochondrial respiratory dysfunction: 6-month *PolgA*$^{+/mut}$ and *PolgA*$^{mut/mut}$ mice demonstrated reduced MB at 48 hours post-PHx when compared to WTs in a gene-dose dependent manner, as well as at 72 hours (figure 5-6, A-B). By contrast, no reductions in PCNA were seen particularly within 6-month *PolgA*$^{+/mut}$ and *PolgA*$^{mut/mut}$ livers when compared to 3-month cohorts, although at 72 hours post-PHx demonstrated diminished levels when compared to WT mice (figure 5-7, B).

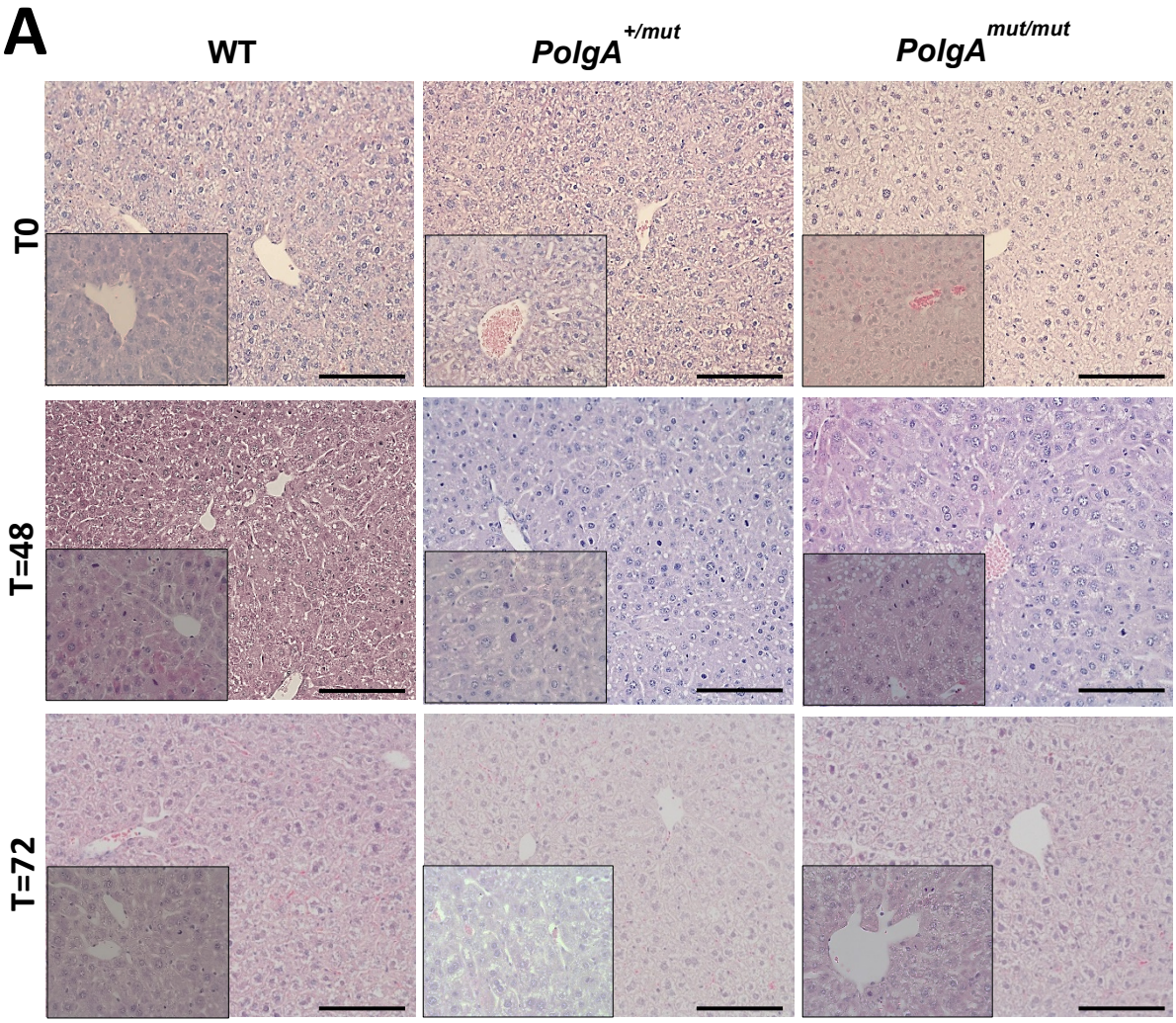

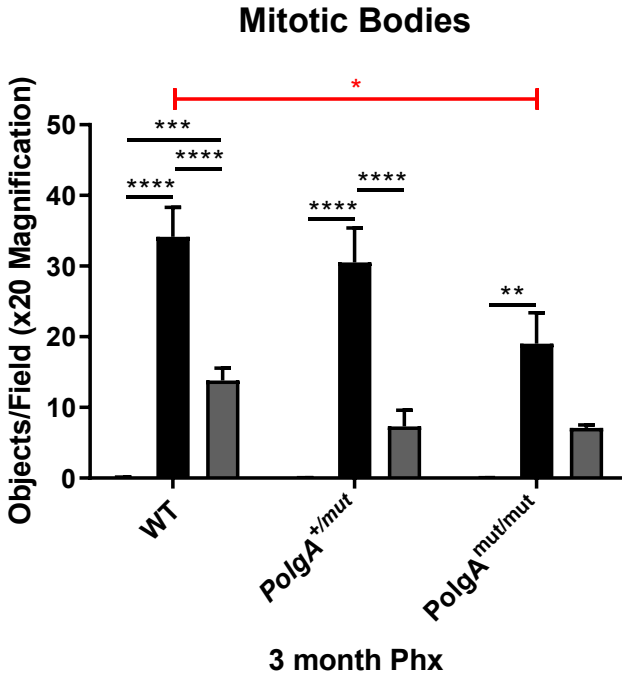

Figure 5-4: Analysis of regenerative mitotic indices following PHx in 3-month WT, PolgA$^{+/mut}$ and PolgA$^{mut/mut}$ mice.

*(A) Representative photomicrographs of H&E staining from 3-month old male WT, PolgA$^{+/mut}$ and PolgA$^{mut/mut}$ PHx mice. Bars 100 µm. (B) Quantification of mitotic bodies in T0, 48 hour and 72 hour post-PHx mice. n=5 per group for WT and PolgA$^{+/mut}$ PHx mice; n=3 per group for PolgA$^{mut/mut}$ PHx mice. All P values were calculated using a two-way ANOVA **p<0.01, ***p<0.001, ****p<0.0001.*

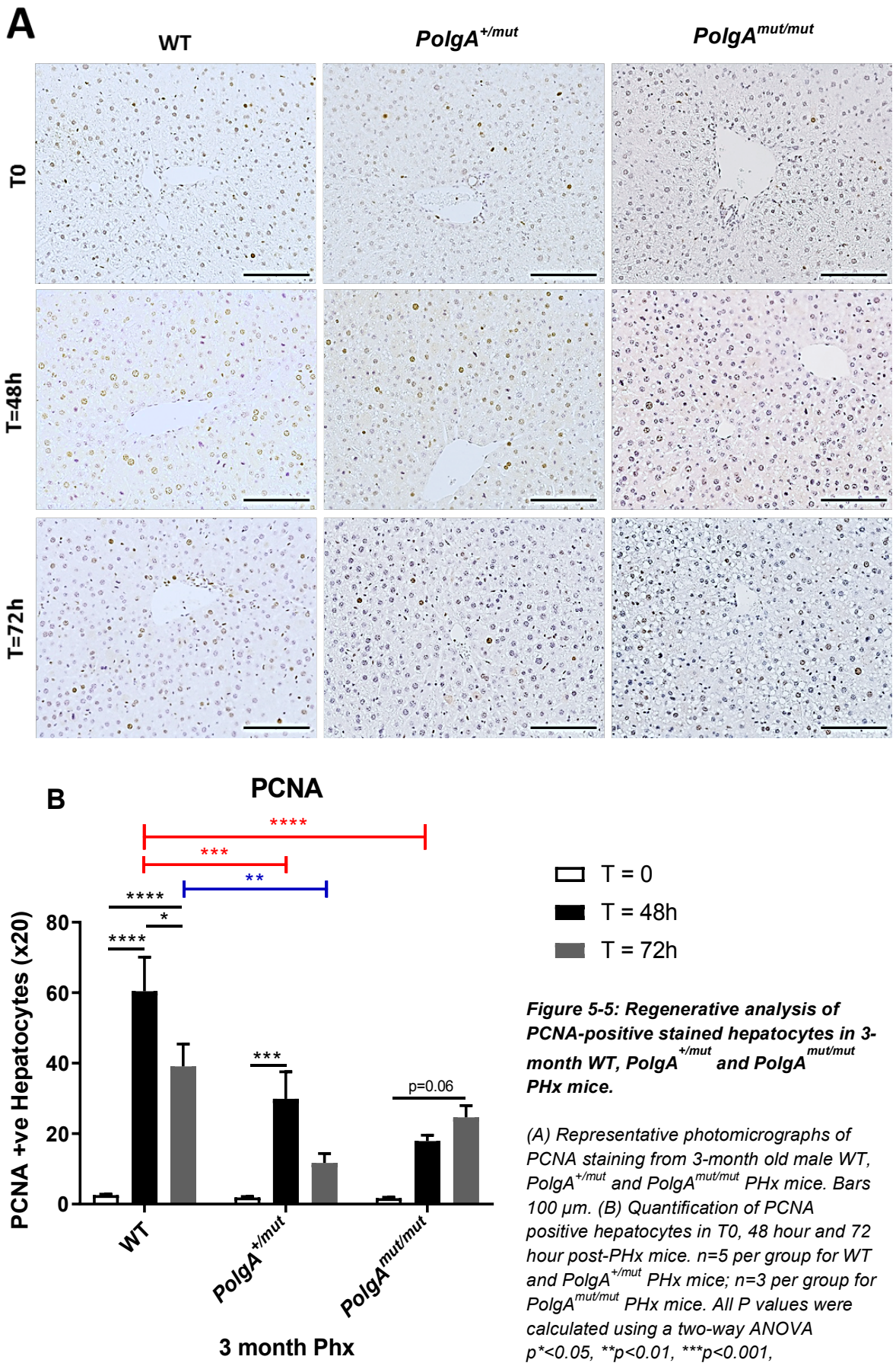

Figure 5-5: Regenerative analysis of PCNA-positive stained hepatocytes in 3-month WT, PolgA$^{+/mut}$ and PolgA$^{mut/mut}$ PHx mice.

(A) Representative photomicrographs of PCNA staining from 3-month old male WT, PolgA$^{+/mut}$ and PolgA$^{mut/mut}$ PHx mice. Bars 100 µm. (B) Quantification of PCNA positive hepatocytes in T0, 48 hour and 72 hour post-PHx mice. n=5 per group for WT and PolgA$^{+/mut}$ PHx mice; n=3 per group for PolgA$^{mut/mut}$ PHx mice. All P values were calculated using a two-way ANOVA p<0.05, **p<0.01, ***p<0.001, ****p<0.0001.*

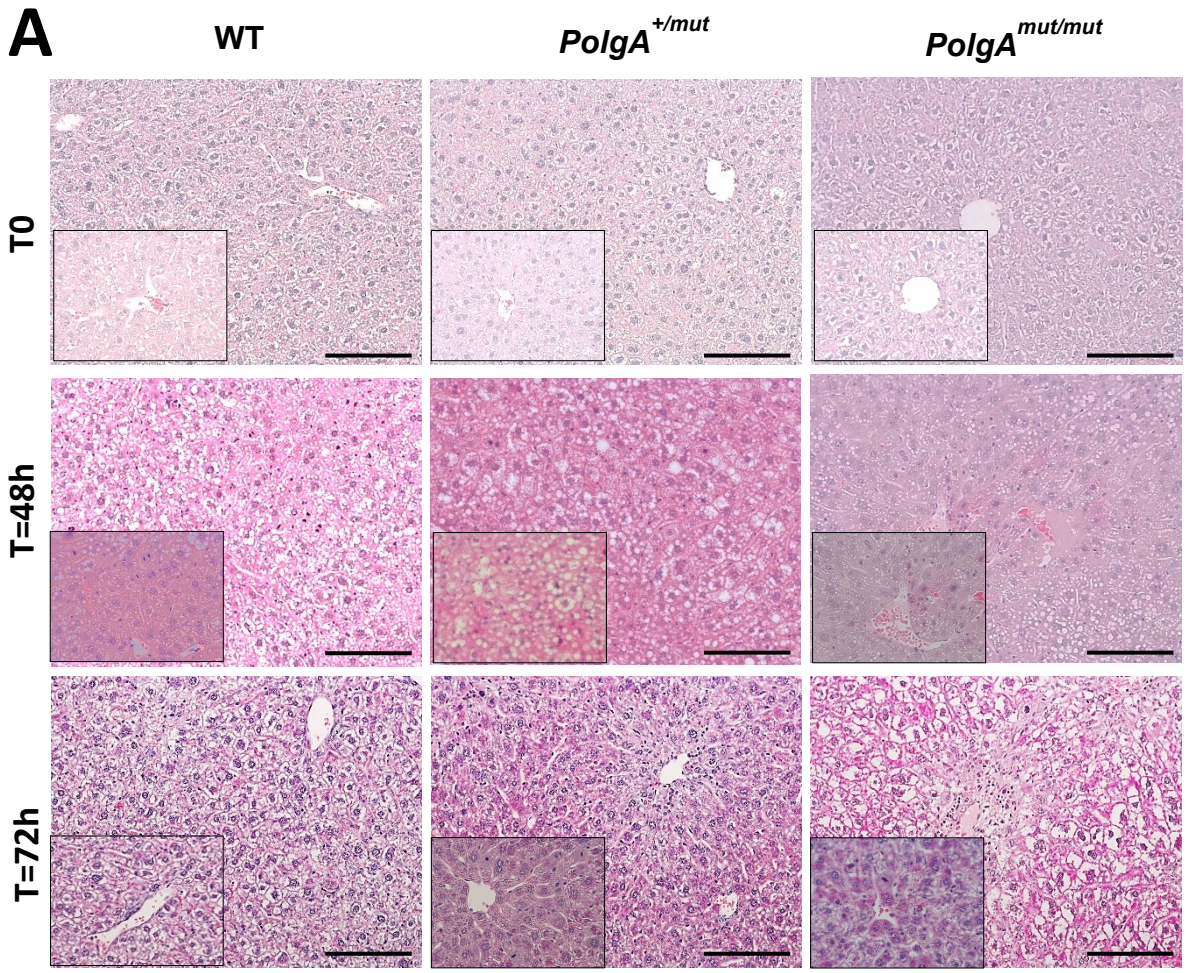

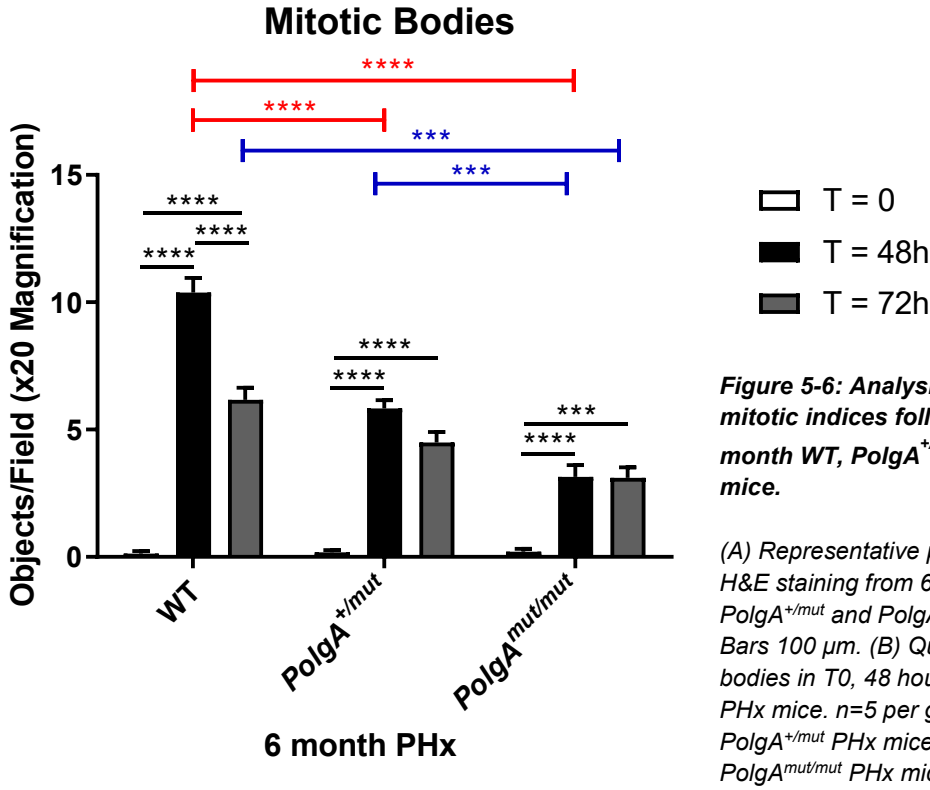

Figure 5-6: Analysis of regenerative mitotic indices following PHx in 6-month WT, PolgA$^{+/mut}$ and PolgA$^{mut/mut}$ mice.

*(A) Representative photomicrographs of H&E staining from 6-month old male WT, PolgA$^{+/mut}$ and PolgA$^{mut/mut}$ PHx mice. Bars 100 µm. (B) Quantification of mitotic bodies in T0, 48 hour and 72 hour post-PHx mice. n=5 per group for WT and PolgA$^{+/mut}$ PHx mice; n=3 per group for PolgA$^{mut/mut}$ PHx mice. All P values were calculated using a two-way ANOVA **p<0.01, ***p<0.001, ****p<0.0001.*

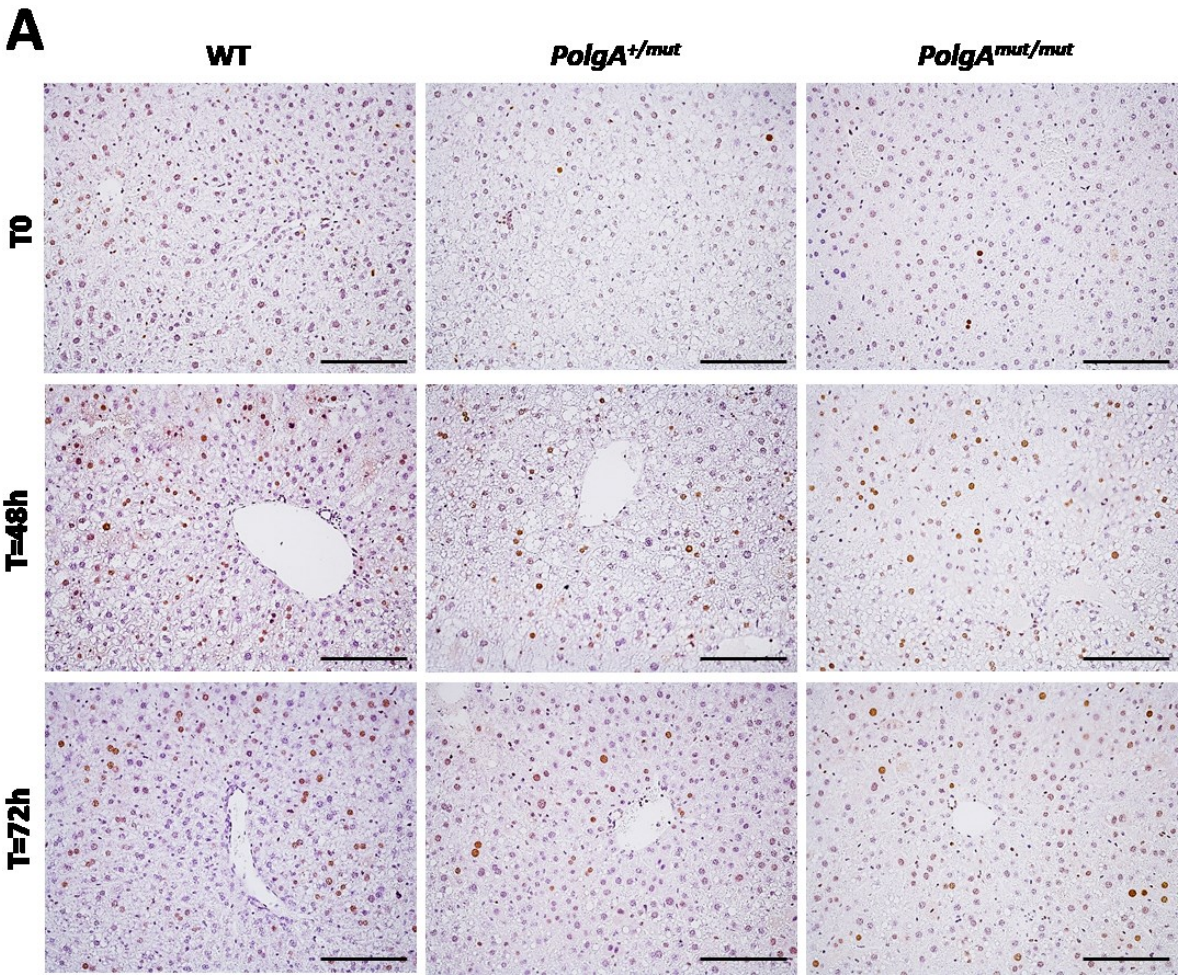

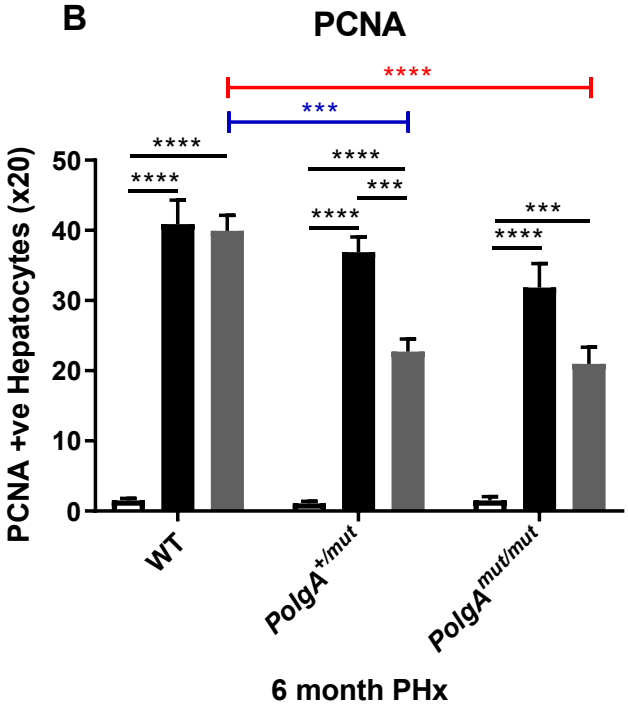

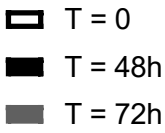

Figure 5-7: Regenerative analysis of PCNA-positive stained hepatocytes in 6-month WT, PolgA$^{+/mut}$ and PolgA$^{mut/mut}$ PHx mice.

*(A) Representative photomicrographs of PCNA staining from 6-month old male WT, PolgA$^{+/mut}$ and PolgA$^{mut/mut}$ PHx mice. Bars 100 µm. (B) Quantification of PCNA positive hepatocytes in T0, 48 hour and 72 hour post-PHx mice. n=5 per group for WT and PolgA$^{+/mut}$ PHx mice; n=3 per group for PolgA$^{mut/mut}$ PHx mice. All P values were calculated using a two-way ANOVA,***p<0.001, ****p<0.0001.*

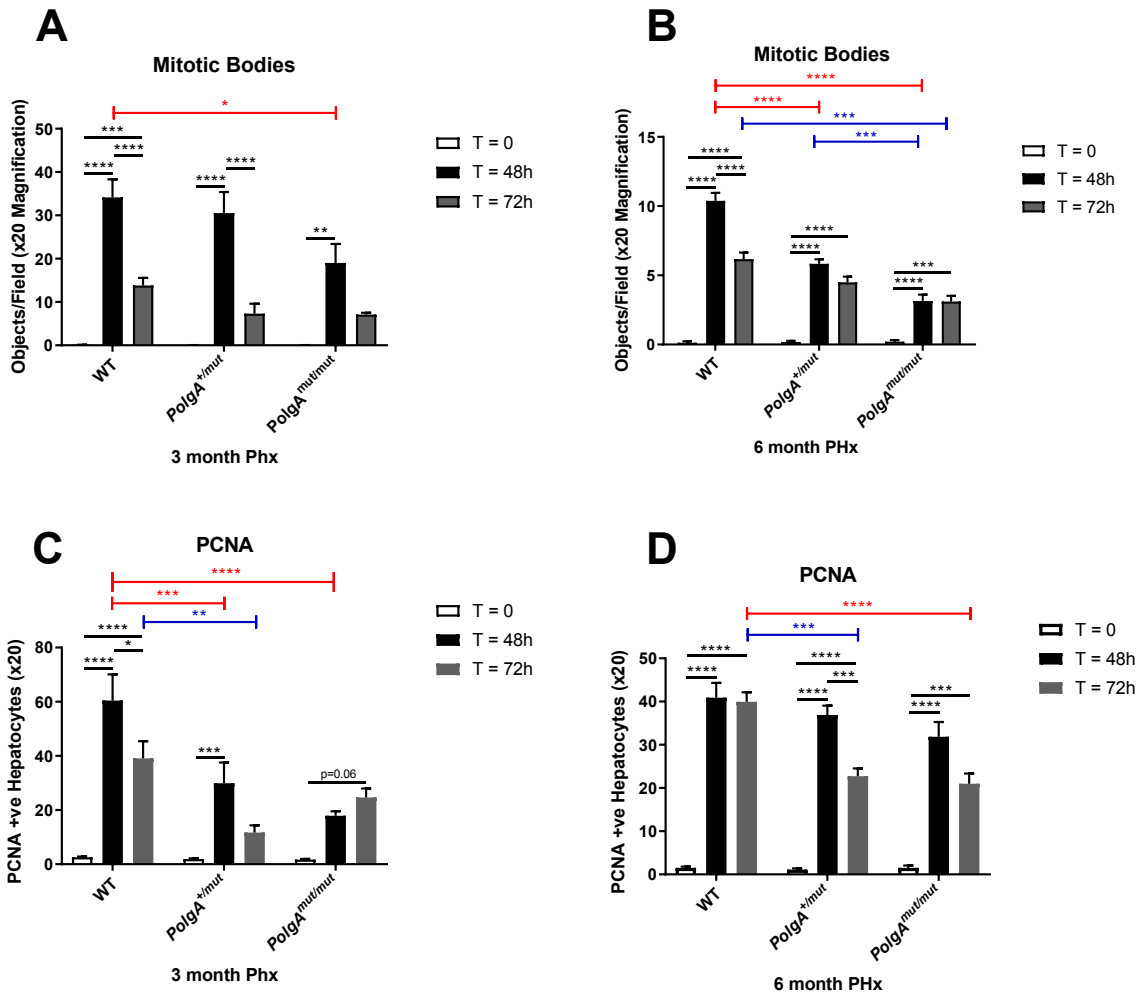

Figure 5-8: Regenerative markers in naïve (median laparotomy only) and partial hepatectomised young (3-month) and aged (6-month) in WT, PolgA$^{+/mut}$ and PolgA$^{mut/mut}$ mice for direct comparison only.

*(A-B) Quantification of mitotic bodies in T0, 48 hour and 72 hours 3-month and 6-month mice (B-C) Quantification of PCNA positive hepatocytes in T0, 48 hour and 72 hour 3-month and 6-month old post-PHx mice. n=5 per group for WT and PolgA$^{+/mut}$ PHx mice; n=3 per group for PolgA$^{mut/mut}$ PHx mice. All P values were calculated using a two-way ANOVA,*p<0.05, **p<0.01, ***p<0.001, ****p<0.0001.*

5.4.3 Hepatoproliferative and growth termination factors following partial liver resection

Parenchymal restoration during liver regeneration is a process mediated by the coordinated pleiotropic effects of priming proinflammatory cytokines, mitogenic and mito-inhibitory factors. Therefore, when assessing gene expression of proliferation-associated proinflammatory cytokines during post-PHx recovery, the present study unsurprisingly observed alterations to hepatoproliferative factors. Such changes were predominantly observed in 6-month cohorts, in which *PolgA*$^{mut/mut}$ T0 livers demonstrates significantly elevated levels of proliferative proinflammatory cytokine TNFα (tumour necrosis factor factor-α) compared with T0 WTs; followed by a significantly marked downregulation at 48-72 hours in response to PHx when compared to WT and *PolgA*$^{+/mut}$ PHx livers (figure 5-9, C). Such findings would appear to correlate with reduced 6-month hepatocellular proliferation markers and inability to recover liver mass post-PHx in these mice. By contrast, WT and *PolgA*$^{+/mut}$ mice demonstrated trends of elevated TNFα expression at 72 hours post-PHx. In addition, 3-month mice did not observe any differences between genotypes, rather TNFα was shown to be significantly upregulated in *PolgA*$^{mut/mut}$ mice at 48 hours in response to PHx and reduced to baseline levels by 72 hours (figure 5-9, A).

By contrast, the termination of liver regeneration is less well investigated, however factors such as transforming growth factor (TGFβ) are well known to be anti-proliferative: mediating apoptotic signalling to correct for excess parenchymal recovery (Sakamoto *et al.*, 1999). Consequently, whilst the mediated effects are noted as only transient, TGFβ receptor II deficient mice are shown to have enhanced hepatocellular proliferation (Oe *et al.*, 2004). Assessing TGFβ in the present study, gene expression was shown to have no obvious changes across all genotypes in 3-month PHx mice, despite the reductions in regenerative markers 48-72 hours post-PHx in *PolgA*$^{+/mut}$ and *PolgA*$^{mut/mut}$ livers (figure 5-9, A). 3-month WT mice appeared to demonstrate downregulated expression of hepatic TGFβ mRNA at 72 hours post-PHx, whilst no obvious changes were observed in corresponding *PolgA*$^{+/mut}$ and *PolgA*$^{mut/mut}$ livers: perhaps reflecting reduced hepatocellular proliferation in these groups. More interestingly, however, in 6-month mice significant upregulation of TGFβ was observed in *PolgA*$^{mut/mut}$ mice at 48-72 hours post-PHx in comparison to corresponding WT and *PolgA*$^{+/mut}$ groups – perhaps causative in the diminution of liver regeneration responses within these mice (figure 5-9, B).

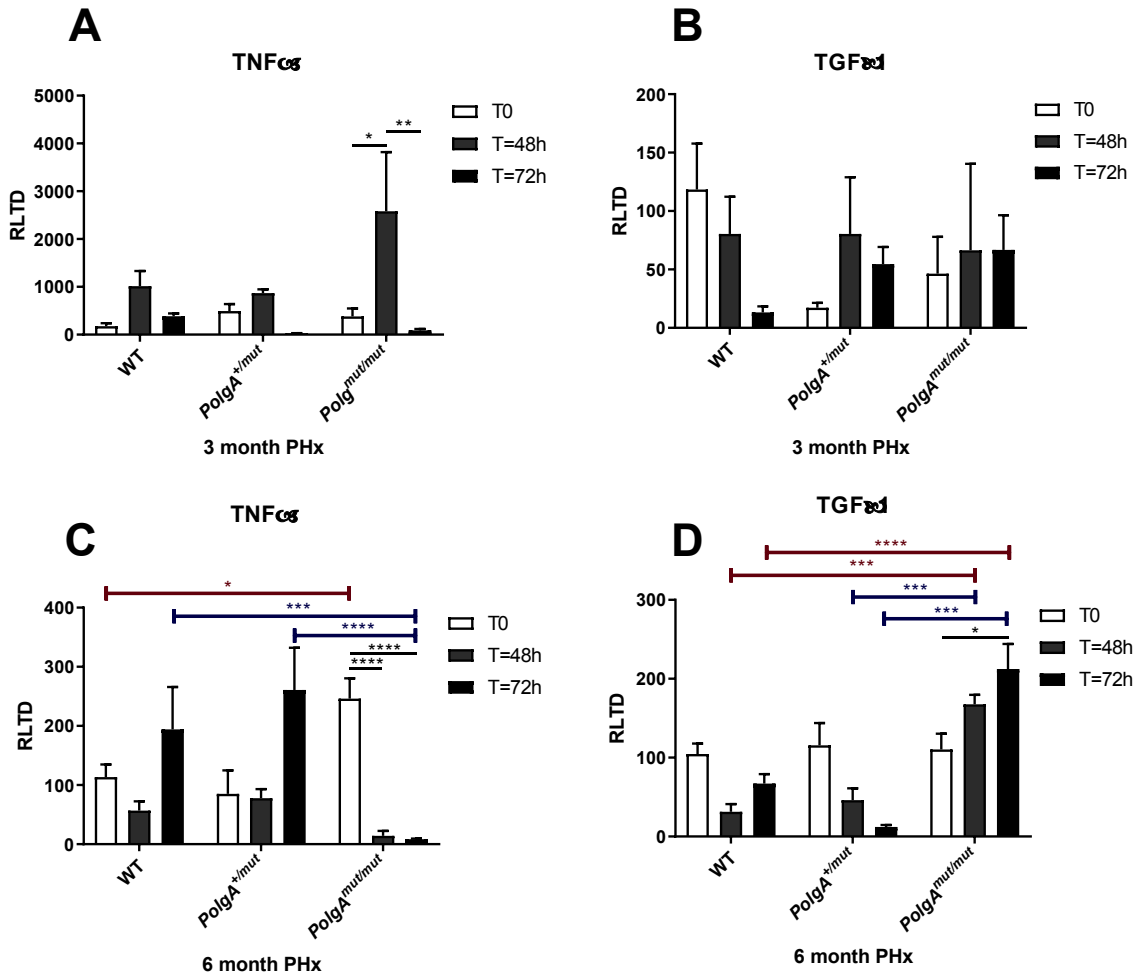

Figure 5-9: Hepatoproliferative and mito-inhibitory factors in 3- and 6-month WT, *PolgA*$^{+/mut}$ and *PolgA*$^{mut/mut}$ T0 and PHx livers.

Hepatoproliferative proinflammatory cytokine tumour necrosis factor-α (TNFα) gene expression was quantified in (A) 3 month and (C) 6 month in T0, 48 and 72 hours post-PHx mice. Mito-inhibitory factor transforming growth factor-β (TGFβ) mRNA levels were quantified in (B) 3 month and (D) 6-month mice. N=5 per group for WT and *PolgA*$^{+/mut}$ PHx mice; n=3 per group for *PolgA*$^{mut/mut}$ PHx mice at both ages. Two-way ANOVA was used to calculate P values, *p<0.05, **p<0.01, ***p<0.001, ****p<0.0001.

5.5 Mitochondrial function WT, *PolgA*$^{+/mut}$ and *PolgA*$^{mut/mut}$ mice following partial hepatectomy

5.5.1 Partial hepatectomy induces changes in mitochondrial respiratory function

Energetic demand is well understood to increase following PHx in order to meet metabolic needs for cellular biosynthesis as the liver regenerates cellular mass and function following loss. Since under homeostatic conditions cellular energy is predominantly provided by the mitochondrial oxidative phosphorylation (OXPHOS) system, liver parenchymal recovery appears to be closely dependent on mitochondrial respiratory function. Increased respiratory and phosphorylation rates, changes in oxidant/redox state and altered activities of respiratory chain complexes have all been shown to occur during liver regeneration (Kamiyama *et al.*, 1976; Inomoto *et al.*, 1994; Hernandez-Munoz *et al.*, 2003). Therefore, since *PolgA*$^{mut/mut}$ mice basal hepatocellular proliferation has been shown in the previous chapter to be defective, it was hypothesised that the presence of age-accumulated mitochondrial respiratory chain dysfunction would result in aberrant active hepatocellular regeneration processes, as tested by PHx in 3 and 6-month WT, *PolgA*$^{+/mut}$ and *PolgA*$^{mut/mut}$ livers.

Mitochondrial respiratory function *via* COX/SDH staining was examined in T0 and post-PHx livers at 3 and 6 months, revealing presence and changes in cytochrome c oxidase (COX) deficiency post-PHx to predominantly occur in previously noted active proliferating periportal regions of the liver (Ferri *et al.*, 2005). At 3 months, photomicrographic indications of possible basal COX deficiency was observed in T0 *PolgA*$^{+/mut}$ and *PolgA*$^{mut/mut}$ livers, though COX/SDH staining was unable to be quantified across the study due to induction of hepatic steatosis on PHx. Parenchymal regeneration at 48 hours post-PHx, coincided with increased COX deficient staining, signifying PHx induces mitochondrial respiratory dysfunction that subsequently returns to approximate T0 levels by 72 hours post-PHx (figure 5-10, A). Interestingly, the presence of mitochondrial respiratory dysfunction in 3-month *PolgA*$^{+/mut}$ and *PolgA*$^{mut/mut}$ appeared to demonstrate the ability to return to T0 levels, although showing some areas of COX deficient staining to remain in a gene-dose dependent manner. These findings were certainly more marked when assessing 6-month mice, with similar inductions of mitochondrial dysfunction on PHx at 48 hours

and in particular, reduced ability to resolve COX deficiency within *PolgA*$^{+/mut}$ and *PolgA*$^{mut/mut}$ mice (figure 5-11, A). Of note, photomicrographs also demonstrated that within 6-month mice, basal T0 levels showed greater COX deficiency than 3 month mice – indicating cumulative mitochondrial respiratory dysfunction with age.

5.5.2 Partial hepatectomy induces protein expression changes in respiratory complexes

The abovementioned changes appeared to reflect alterations in mitochondrial respiratory complexes: specifically, whole liver protein expression of complex I (NDUFB8) and complex IV (Mt-CO1) observed in *PolgA*$^{+/mut}$ and *PolgA*$^{mut/mut}$ mice at 3 and 6 months. Whilst no 3-month changes were observed for complex II (SDHB), complex III (UQCRC2) and complex V (ATPB), diminished NDUFB8 protein expression was observed 48-72 hours in *PolgA*$^{+/mut}$ PHx mice, as well as downregulation of Mt-CO1 expression observed 48-72 hours and at 48 hours in *PolgA*$^{+/mut}$ and *PolgA*$^{mut/mut}$ mice respectively (figure 5-10, B-D). Upregulation of NDUFB8 was also observed 48 hours post-PHx in WTs, demonstrating a seemingly greater upregulation of WT NDUFB8 at this timepoint when compared with 3-month *PolgA*$^{+/mut}$ and *PolgA*$^{mut/mut}$ livers. Testing for respiratory complex proteins in 6-month mice, similar increases in NDUFB8 expression at 48 hours post-PHx was also observed but in WT and *PolgA*$^{+/mut}$ livers only (figure 5-11, B-D) rather *PolgA*$^{mut/mut}$ failed to upregulate NDUFB8 expression following resection – perhaps ascribed to initial complex I deficiencies seen within T0 and basal livers (see chapter 4). In addition, Mt-CO1 also appeared to be decreased post-PHx in 6-month *PolgA*$^{mut/mut}$ livers but not in *PolgA*$^{+/mut}$ mice. No observable changes were observed for SDHB, UQCRC2 and ATPB were detected across the genotypes.

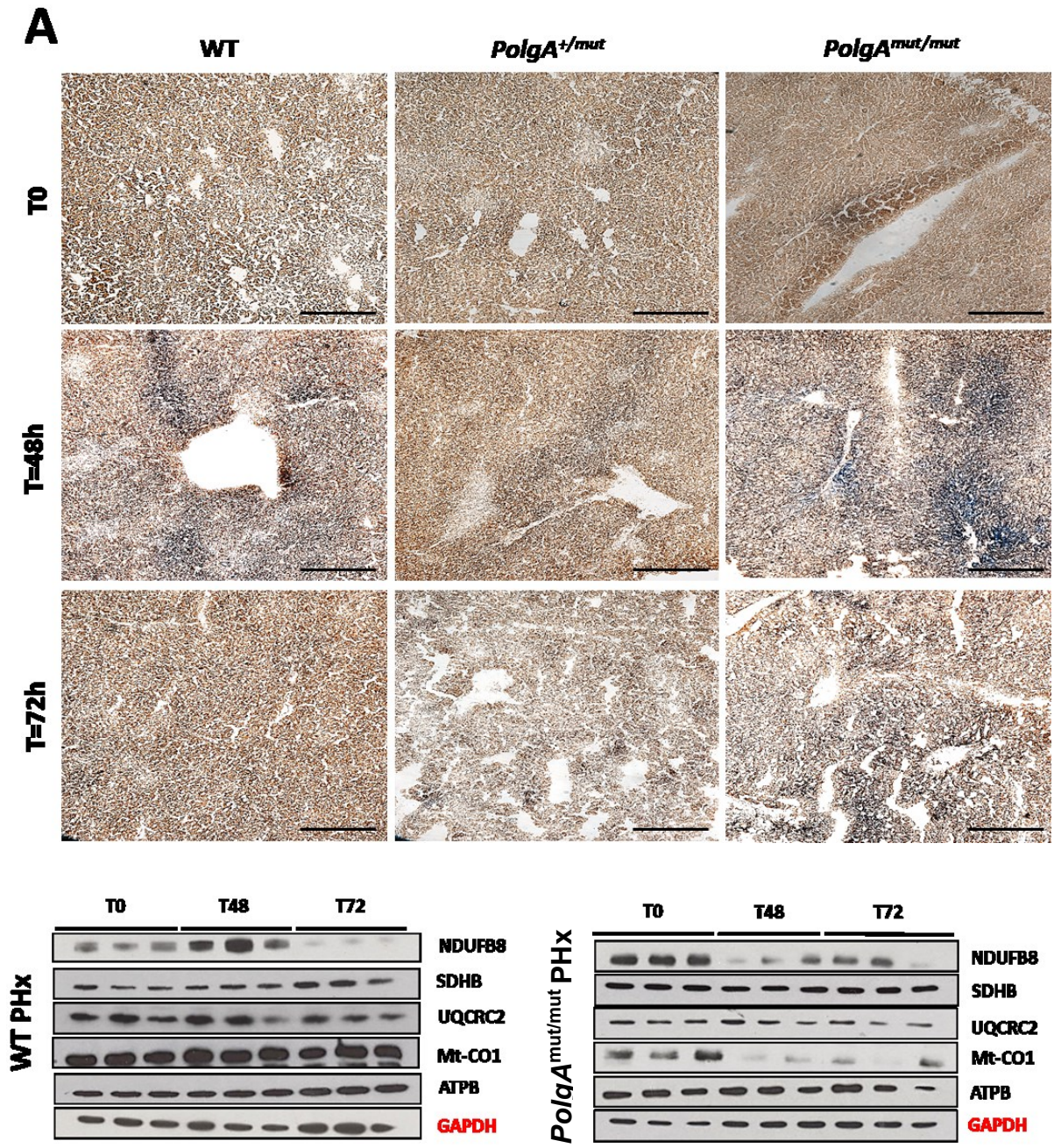

Figure 5-10: Analysis of mitochondrial respiratory function and respiratory complex protein expression in 3-month WT, PolgA$^{+/mut}$ and PolgA$^{mut/mut}$ T0 and PHx livers.

(A) Representative photomicrographs of COX/SDH staining for mitochondrial function from 3-month old male WT, PolgA$^{+/mut}$ and PolgA$^{mut/mut}$ T0 and PHx mice. Bars 100 µm. (B-D) Western blots of mitochondrial respiratory complex subunits protein expression for complex I (NDUFB8), complex II (SDHB), complex III (UQCRC2), complex IV (Mt-CO1) and complex V (ATPB) in 3-month WT, PolgA$^{+/mut}$ and PolgA$^{mut/mut}$ T0, 48 and 72 hours post-PHx mice livers.

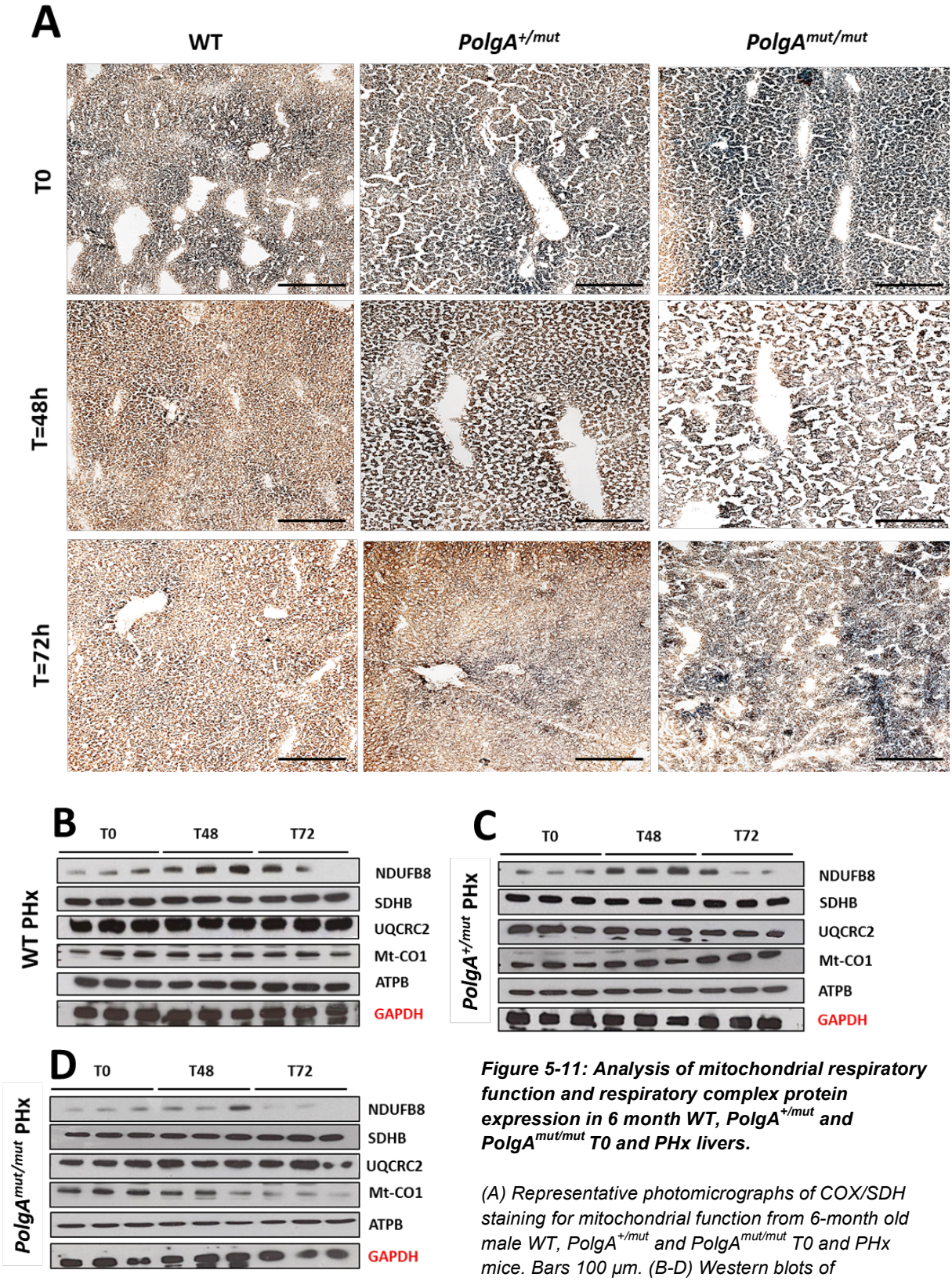

Figure 5-11: Analysis of mitochondrial respiratory function and respiratory complex protein expression in 6 month WT, PolgA$^{+/mut}$ and PolgA$^{mut/mut}$ T0 and PHx livers.

(A) Representative photomicrographs of COX/SDH staining for mitochondrial function from 6-month old male WT, PolgA$^{+/mut}$ and PolgA$^{mut/mut}$ T0 and PHx mice. Bars 100 µm. (B-D) Western blots of mitochondrial respiratory complex subunits protein expression for complex I (NDUFB8), complex II (SDHB), complex III (UQCRC2), complex IV (Mt-CO1) and complex V (ATPB) in 6-month WT, PolgA$^{+/mut}$ and PolgA$^{mut/mut}$ T0, 48 and 72 hours post-PHx mice livers.

5.5.3 Mitochondrial biogenesis during ageing liver regeneration

The co-transcriptional regulatory factor PGC1α (peroxisome proliferator activated receptor gamma coactivator 1-alpha) is integral to the transcriptional control of mitochondrial biogenesis and respiratory chain function (Austin *et al.,* 2012). PGC1α gene expression did not show marked changes in expression in 3-month mice (figure 5-12, A). However, following PHx in 6-month aged WT mice, PGC1α gene expression was elevated at 48 hours, but subsequently returned to approximate baseline T0 levels by 72 hours. These changes in PGC1α, were not statistically significant (figure 5-12, B). Upregulation of PGC1α levels at 48 hours, on the other hand, was significantly raised in WT mice when compared to *PolgA*$^{+/mut}$ and Polg$^{mut/mut}$ groups.

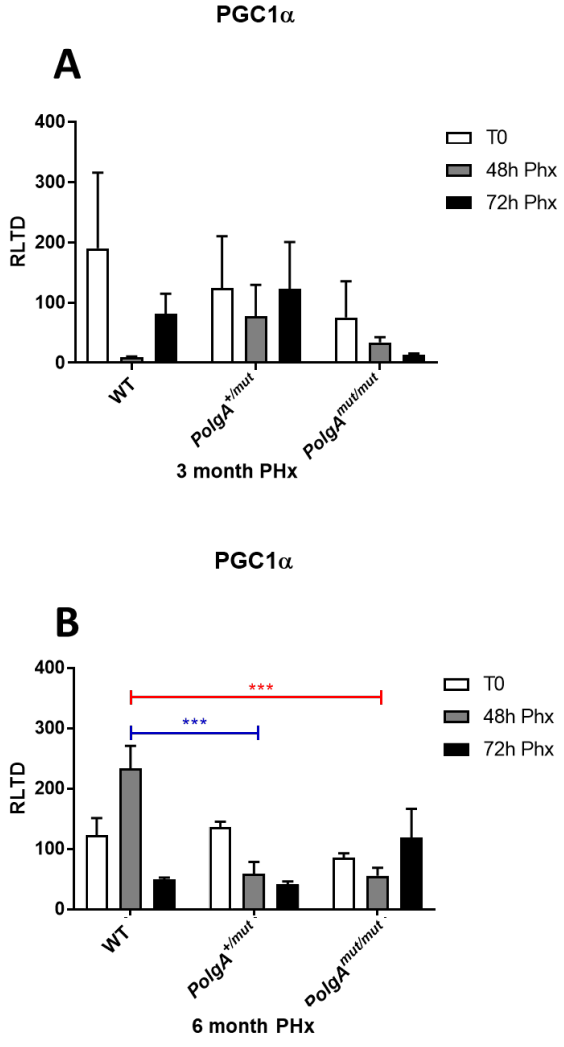

Figure 5-12: Gene expression of mitochondrial biogenesis co-transcriptional regulatory factor PGC1α.

*Gene expression for co-transcriptional regulatory factor for mitochondrial biogenesis, PGC1α (peroxisome proliferator activated receptor gamma coactivator 1-alpha), quantified in (A) 3 month and (B) 6-month WT, PolgA$^{+/mut}$ and PolgA$^{mut/mut}$ mice at T0, 48 and 72 hours post-PHx. N=5 per group for WT and PolgA$^{+/mut}$ PHx mice; n=3 per group for PolgA$^{mut/mut}$ PHx mice at both ages. Two-way ANOVA was used to calculate P values, ***p<0.001*

5.5.4 Partial hepatectomy and alterations in anti-oxidant enzymes in *PolgA*

The formation of reactive oxygen by-products has been reported to increase following PHx as a result of increased OXPHOS energetic demands (Yang *et al.,* 2004), in which detrimental excess reactive oxygen species (ROS) levels are detoxified by anti-oxidant scavenging activity. Amongst observations noted is augmented levels of glutathione (GSH) 24-72 hours after initial decreases (≈24 hours) post-surgery (Huang *et al.*, 1998), yet when assessing mRNA expression of corresponding GSH synthesising enzyme GSS (glutathione synthetase) in the present study, significantly decreased levels were observed at 48-72 hours post-PHx in 3 month mice, when compared to T0 WT tissues (figure 5-13, A). Similar observations were also observed for *PolgA*$^{+/mut}$ mice, but failed to reach statistical significance. Conversely, *PolgA*$^{mut/mut}$ mice showed failure to differentially regulate GSS across all given time points. In addition and also in accordance with previous studies, glutathione peroxidase (GPX) gene expression was also decreased in response to PHx, 48-72 hours in 3-month mice (figure 5-13, B); however, such findings are inconclusive with statistical analysis failing to reach significance (Huang *et al.*, 1998; Yang *et al.*, 2004). Moreover, no significant differences in mRNA levels were demonstrated for superoxide dismutase 1 (SOD1) across all genotypes when compared to T0 controls (figure 5-13, C)

With murine ageing, comparable trends in antioxidant gene expression were observed at 6 months of age when normalised to 6-month T0 WT livers. Quantification of GSS mRNA levels revealed gene-dose dependent increases in baseline T0 *PolgA*$^{+/mut}$ and *PolgA*$^{mut/mut}$ livers, which was significant in the latter. Similar to 3-month PHx mice, GSS mRNA levels were markedly reduced in 6-month mice at 48-72 hours post hepatectomy (figure 5-14, A). Similar findings to 3-month mice were also observed for GPX, in which mRNA levels remained relatively unaltered following surgical resection of the liver in the presence of mitochondrial respiratory chain dysfunction, as in *PolgA*$^{+/mut}$ and *PolgA*$^{mut/mut}$ mice (figure 5-14, B). PHx also appeared to induce SOD1 gene expression at 48 hours post-PHx in 6-month aged WT livers, however, SOD1 expression subsequently returned to T0 levels by 72 hours. Such observations showed significantly reduced expression when compared to *PolgA*$^{mut/mut}$ mice, which on PHx, showed significantly increased SOD1 expression across 48-72 hour time points (figure 5-14, C). No changes were

observed amongst 6-month *PolgA*$^{+/mut}$ groups across all antioxidant gene measurements taken.

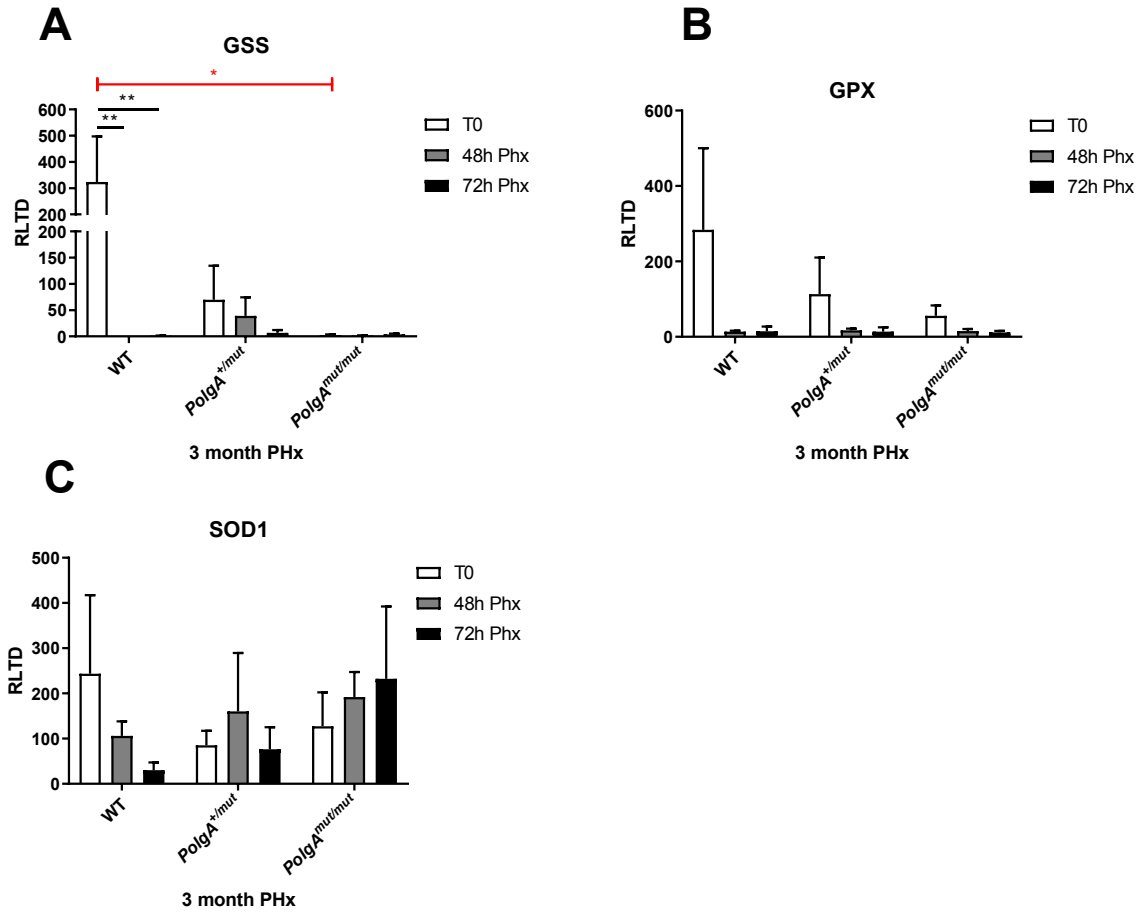

Figure 5-13: Analysis of anti-oxidant enzyme expression in 3-month WT, PolgA$^{+/mut}$ and PolgA$^{mut/mut}$ PHx mice.

*(A) Quantification of glutathione synthetase (GSS), (B) glutathione peroxidase (GPX) and (C) superoxide dismutase 1 (SOD1) gene transcription was analysed in 3-month WT, PolgA$^{+/mut}$ and PolgA$^{mut/mut}$ livers at T0, 48 and 72 hours post-PHx. N=5 per group for WT and PolgA$^{+/mut}$ PHx mice; n=3 per group for PolgA$^{mut/mut}$ PHx mice. Two-way ANOVA was used to calculate P values, *p<0.05, **p<0.01.*

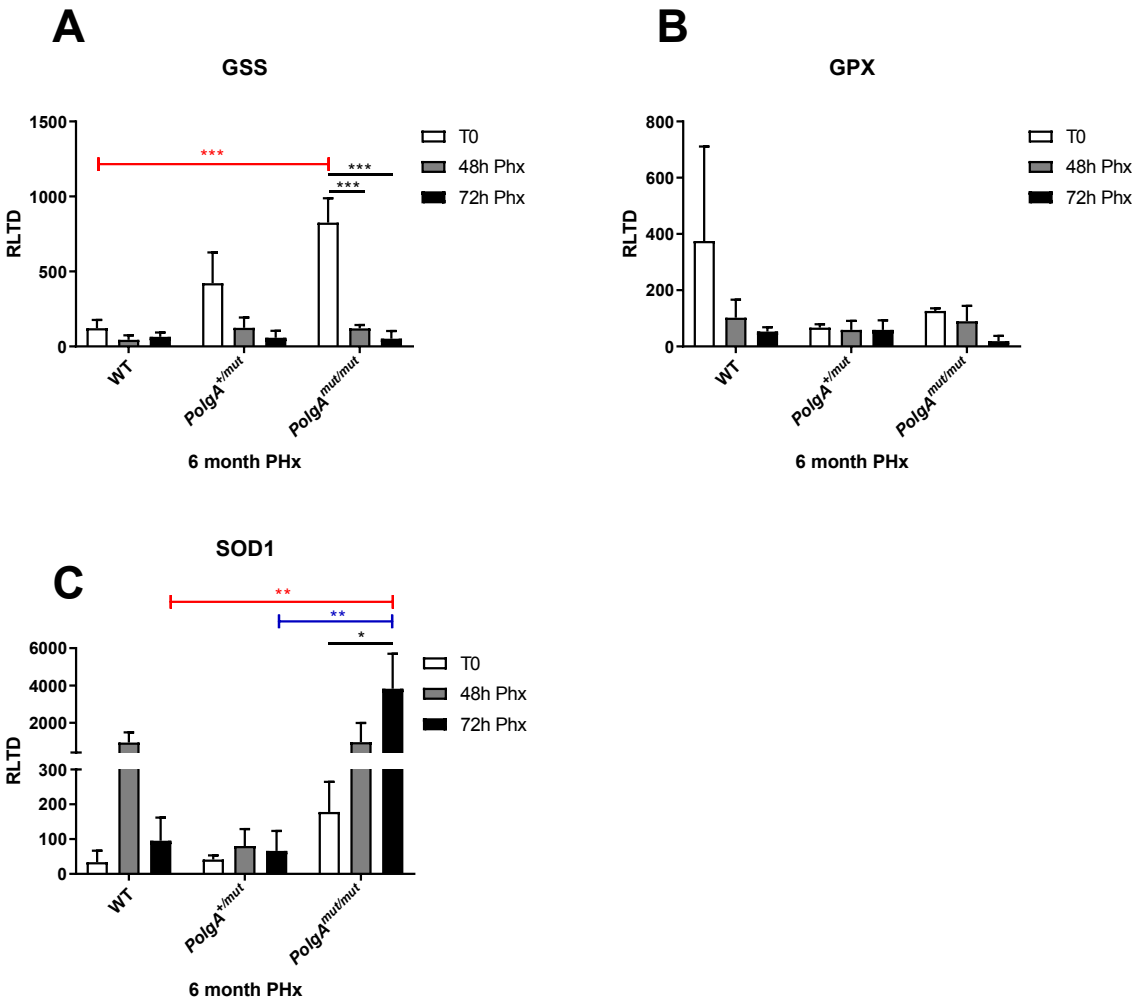

Figure 5-14: Analysis of anti-oxidant enzyme expression in 6-month WT, PolgA$^{+/mut}$ and PolgA$^{mut/mut}$ PHx mice.

*(A) Quantification of glutathione synthetase (GSS), (B) glutathione peroxidase (GPX) and (C) superoxide dismutase 1 (SOD1) gene transcription was analysed in 6-month WT, PolgA$^{+/mut}$ and PolgA$^{mut/mut}$ livers at T0, 48 and 72 hours post-PHx. N=5 per group for WT and PolgA$^{+/mut}$ PHx mice; n=3 per group for PolgA$^{mut/mut}$ PHx mice. Two-way ANOVA was used to calculate P values, *p<0.05, **p<0.01, ***p<0.001.*

5.6 Conclusion

Despite basal age-associated reductions in hepatocellular proliferation and hepatocyte survival associated with complex I respiratory deficiency (see chapter 4), *PolgA*$^{mut/mut}$ mice respond to regenerative stressors from PHx with varying degrees. Whilst 3-month mice trended towards normal post-PHx recovery recognised by pronounced liver to body weight increases and similar liver weights to WT and *PolgA*$^{+/mut}$ mice, diminished post-surgical recovery was an effect more marked in the presence of age-accumulated mitochondrial respiratory chain dysfunction. As a consequence, 100% post-PHx survival across all 3-month genotypes was reduced in a gene-dose dependent manner to ~91% and 70% in 6-month *PolgA*$^{+/mut}$ and *PolgA*$^{mut/mut}$ mice respectively, and coincided with a significant decline in liver mass post-PHx in *PolgA*$^{mut/mut}$ mice - despite initial enlargement observed in naïve *PolgA*$^{mut/mut}$ livers. Such decreases in the presence of respiratory chain dysfunction could be ascribed to reductions in hepatocellular regenerative markers PCNA and mitotic indices; however, in 3-month *PolgA*$^{+/mut}$ and *PolgA*$^{mut/mut}$ mice and 6-month *PolgA*$^{+/mut}$ livers, ability to recover liver mass was not impaired, showing similar recuperation to aged matched WTs. It is therefore possible that where no diminution in hepatic regrowth is observed, the threshold of mtDNA mutations required to induce an aberrant effect on post-PHx recovery is unlikely to have been exceeded. At 3 months of age, it is likely that normal mitochondrial function remains within remaining cells to compensate for respiratory defunct cells, whilst greater mitochondrial dysfunction in 6-month *PolgA*$^{mut/mut}$ induces diminished parenchymal recovery. Certainly, initial studies show that *PolgA*$^{mut/mut}$ mice accumulate mtDNA mutations a rate 3-5 fold greater than WTs within tissues including the liver, whilst further comparisons with *PolgA*$^{+/mut}$ groups show mtDNA mutations in ageing mitotic tissues to accumulate at an accelerated rate in *PolgA*$^{mut/mut}$ tissues only (Trifunovic *et al.*, 2004; Kujoth *et al.*, 2005; Vermulst *et al.*, 2008).

Diminished liver regeneration is present in the ageing liver, with previous WT murine studies showing reduced survival following partial liver resection in older cohorts; this is likely associated with aberrant changes to hepatoproliferative signalling, as well as changes in hepatic ultrastructures (Guerrieri *et al.*, 2002; Ferri *et al.*, 2005; Enkhbold *et al.*, 2015). Whilst no losses in hepatic liver mass and regenerative markers are observed in 3-month WT mice, levels of hepatocyte proliferative indicators are noted

to decrease within the 6-month cohort, exacerbated by the presence of respiratory chain dysfunction. Therefore it was hypothesised that *PolgA*$^{mut/mut}$ mice would show cumulative aberrant effects in regenerative signalling associated with age-accumulated mitochondrial dysfunction and the onset of a progeroid ageing phenotype. Certainly at 3 months of age, *PolgA*$^{+/mut}$ and *PolgA*$^{mut/mut}$ hepatocytes are still able to proliferate to recover lost cell mass, albeit to varying extents when compared to WT livers - ascribed to significant gene-dose reductions at 48 hours post-PHx in DNA synthesis marker PCNA and corresponding mitotic indices in *PolgA*$^{+/mut}$ and *PolgA*$^{mut/mut}$ mice. Such changes appeared to extend to 72 hours post-PHx within *PolgA*$^{mut/mut}$: interestingly denoting increased counts in PCNA positive hepatocytes when compared to T0 control groups. Whether this is indicative of a delayed regenerative response is unclear due to contrasts with corresponding MB counts and no differences in 3 month post-surgical liver mass; however, DNA synthesis during the cell cycle prior to mitosis is understood to be tightly controlled – halted at the G_2/M checkpoint in the presence of DNA damage and incomplete DNA replication *via* predominantly cyclin B-CDK1 mediated mechanisms (Fisher *et al.*, 2012). As such, increased DNA synthesis-associated PCNA levels could be suggestive of halted or delayed entry of *PolgA*$^{mut/mut}$ hepatocytes into mitotic division during liver regeneration. Further work to determine this would no doubt require assessment of cell cycle proteins, as well as the inclusion of additional time points to oversee a delayed regenerated response. Moreover, where age-associated mitochondrial dysfunction is present in 6-month *PolgA*$^{+/mut}$ mice and reduced regenerative markers are observed in the absence of reduced liver mass recovery, other regenerative mechanisms may be sufficient to compensate for proliferative defects. Unfortunately, this avenue was not further investigated; however, further work could be conducted in the future to address such possibilities including, for example exploration of hepatocyte hypertrophy and autophagic regenerative mechanisms.

With reductions in hepatocyte mitosis and PCNA expression present in the post-PHx liver, it was alluded that observed post-surgical hepatocellular changes at both 3 and 6 months may be in part due to changes in hepatoproliferative and mito-inhibitory factors. Carefully orchestrated in concert with other hepatocyte proliferative factors, the proinflammatory cytokine TNFα is a priming factor understood to diminish hepatic regenerative processes, as explored during genetic ablation or inhibition of the

corresponding TNFα receptor (Akerman *et al.*, 1992; Yamada *et al.*, 1997). Despite undergoing reduced hepatocyte mitosis, 3-month *PolgA*$^{mut/mut}$ livers were able to recover mass: showing similar abilities to WT and *PolgA*$^{+/mut}$ mice to upregulate TNFα gene expression 48 hours post-PHx. Whilst previous studies have demonstrated a double-edged sword role for TNFα in cellular apoptosis and survival, in the context of post-PHx recovery, TNFα is shown to a have a hepatoprotective role against Fas-mediated apoptosis following surgery (Takehara *et al.*, 1998; Flusberg and Sorger, 2015). It is therefore possible that in order to achieve liver homeostasis post-PHx in 3-month *PolgA*$^{mut/mut}$ mice, greater upregulation of TNFα may be required to ensure survival of remaining compensatory hepatocytes in the presence of diminished post-surgical hepatocellular proliferation. On the contrary, PHx appears to downregulate TNFα at 48-72 hours in 6-month *PolgA*$^{mut/mut}$ mice when compared to T0 controls and other murine groups, resulting in possible diminished TNFα-mediated hepatoprotection against apoptotic signalling and which may manifest in post-PHx reductions in liver cell mass and survival. Unfortunately, apoptotic signalling was not further explored with PHx; however, accelerated ageing in *PolgA*$^{mut/mut}$ mice ascribed to increased apoptosis observed in the present study (chapter 4) may provide some explanation for greater TNFα expression in 6-month *PolgA*$^{mut/mut}$ T0 livers. Moreover, despite reduced regenerative indicators and smaller decreases in post-surgical survival, TNFα expression in 6-month PHx *PolgA*$^{+/mut}$ mice showed similarities to WTs, further advocating for additional compensatory mechanisms against proliferative defects to ensure recuperation of liver mass following PHx.

Interestingly, a decrease in hepatocellular proliferative response within 3-month PHx *PolgA*$^{+/mut}$ and *PolgA*$^{mut/mut}$ mice did not appear to significantly correlate with the premature termination of liver regeneration, with no overall significant differences observed in TGFβ mRNA levels. Yet, in 6-month *PolgA*$^{mut/mut}$ mice, expression is significantly upregulated over 48-72 hours post-PHx when compared to corresponding WT and *PolgA*$^{+/mut}$ mice. Anti-proliferative effects of TGFβ signalling are transient: demonstrated in previous studies to increase gene expression within 3-4 hours of PHx and peaking at 48 hours; ensuing mito-inhibition occurs in a paracrine manner *via* suppression of DNA synthesis which is then shown to reduce by 72 hours alongside a decreased sensitivity of hepatocytes to TGFβ signalling (Nishikawa *et al.*, 1998). As such, significantly increased TGFβ expression in 72 hour, 6-month

PolgA$^{mut/mut}$ mice may be allied to observed reductions in hepatocyte PCNA and mitosis markers and reductions in liver regeneration *via* mito-inhibitory signalling. Despite a lack of significance, observed trends of gradual downregulated TGFβ expression between T0 and 72 hours post-PHx in both 3 month and 6 month WT and *PolgA*$^{+/mut}$ mice may also be of interest: in that gradual periportal-to-pericentral loss of TGFβ is noted in earlier studies to proceed hepatocyte mitotic division and thus its removal from the hepatic environment is required for completion of normal liver regeneration, as in WTs and *PolgA*$^{+/mut}$ mice (Braun *et al.*, 1988; Jirtle *et al.*, 1991). However, this conflict between results in *PolgA*$^{+/mut}$ and *PolgA*$^{mut/mut}$ mice, together with indices of hepatocellular proliferation and liver mass recovery, means findings remain inconclusive. As such, further work should be carried out to fully complement the current findings, including the characterisation of other priming and mitogenic factors such as IL-6, epidermal growth factor (EGF), hepatocyte growth factor (HGF) and TGF-α, as well as known anti-proliferative factors like activin A and bone morphogenic proteins (BMP).

In previous studies, increases in mitochondrial activated respiration (state 3), respiratory and ATP phosphorylation activities have been observed and as such, it was hypothesised that *PolgA*$^{mut/mut}$ mice have a defective regenerative response, due to additional stress on mitochondrial respiratory capacity as energetic demands and OXPHOS metabolism increase (Hernandez-Munoz *et al.*, 2003; Yang *et al.*, 2004). Following PHx, induction of mitochondrial respiratory chain dysfunction across all genotypes at 48 hours post-PHx, and as seen by COX/SDH staining, occurred around the hepatic periportal areas in 3- and 6-month mice as previously shown (Ferri *et al.*, 2005). These changes were further exacerbated in *PolgA*$^{+/mut}$ and *PolgA*$^{mut/mut}$ mice in a gene-dose dependent manner, with enhanced induction of COX deficiency ascribed to greater baseline presence of mitochondrial respiratory dysfunction within T0 tissues. Subsequently, enhancement appears correlated with observed reduced ability to fully resolve COX deficiency by 72 hour post-PHx to a lesser and gene-dose extent. Taken together these data suggest that the presence of basal mitochondrial respiratory dysfunction may exacerbate any mitochondrial respiratory stresses induced by PHx. Indeed in *PolgA*, enhanced COX deficiency may be ascribed to alterations to respiratory chain complex protein expression following resection, most notably complex I and complex IV, with failure at 3 months to express NDUFB8 and Mt-CO1 in *PolgA*$^{+/mut}$ and *PolgA*$^{mut/mut}$ mice across 48-72

hours post-PHx. Yet, with intact capacity to regenerate liver mass in these mice it is also possible that the threshold amount of respiratory chain deficient cells required to induce a tissue-level phenotype may have not have been exceeded due to respiratory proficient cells able to compensate for changes in mitochondrial complex expression post-PHx. Moreover, where reduced recovery of liver mass is seen in 6-month *PolgA*$^{mut/mut}$ mice, inability to upregulate complex I and IV are similarly observed. In chapter 4, demonstrated changes in respiratory function imply mitochondrial dysfunction increases with time, ascribed by previous studies on the clonal expansion of these respiratory deficient cells, which in turn could impact on basal hepatocellular turnover (Baines *et al.*, 2014; Ma *et al.*, 2018). Loss of hepatocellular proliferation is therefore likely to be linked to the inability to upregulate expression of mitochondrial complex proteins, in particular complex I (NDUFB8) and/or in combination with Mt-CO1 deficiency. The latter of which demonstrates some variability across age groups and genotypes in this study. Methods utilised for observing mitochondrial function were largely qualitative, therefore if permitted more time, quantifiable approaches such as assessing mitochondrial complex gene expression, respiratory control ratios and OXPHOS metabolism would be used to determine a more conclusive mechanism as to how the presence of mitochondrial respiratory dysfunction alters ageing hepatocellular regeneration. This could be achieved by a range of methods, including the use of precision cut liver slices which maintain a liver microenvironment in murine and human models, to address inability of *PolgA*$^{mut/mut}$ hepatocytes to survive *ex vivo* (Olinga and Schuppan, 2013*;* Koch *et al., 2014;* Paish *et al.,* 2019).

Oxidative phosphorylation is known to significantly increase in response to PHx to meet the energetic demands of liver regeneration: with elevated ATP production coupled to increased OXPHOS enzyme activity and mitochondrial DNA content due to increases in mitochondrial biogenesis (Nagino *et al.*, 1989; Yang *et al.*, 2004). Whilst variable and inconclusive changes were found in 3-month PHx mice, 6-month WT livers observed significantly higher PGC1α gene expression levels at 48 hours than *PolgA* mice, indicating upregulated PGC1α-mediated activities 0-48 hours post-PHx, including possible stimulated mitochondrial biogenesis as previously reported by Nagino and colleagues (1989). However, no observed upregulation was seen in the expression profile of mitochondrial protein complexes - postulating changes in PGC1α gene expression could be upstream of alternative transcriptionally targeted

pathways (Lupez-Loch *et al.,* 2009). No significant upregulation of PGC1α gene expression was observed in *PolgA*$^{mut/mut}$ mice, possibly resulting in failure to meet the energetic demands of post-PHx regeneration, exacerbation of mitochondrial COX deficiency and ultimately failure to recover lost cellular mass. Interestingly, within 6-month *PolgA*$^{+/mut}$ mice, increases in PGC1α were also absent despite relatively normal capacity for parenchymal regeneration. This may be ascribed to the use of PGC1α as a marker in the present study, since mitochondrial biogenesis has also been shown to also occur in a PGC1α-independent manner (Wilson *et al.*, 2007). To further ascertain the role of PGC1α in the present study, including mitochondrial biogenesis, would no doubt require additional work, including assessing additional biogenesis markers like nuclear respiratory factor (NRF), TFAM and COX, as well as other PGC1α targets through additional assays.

Alterations to anti-oxidant enzyme gene expression were found in the presence of mitochondrial respiratory dysfunction. Reactive oxygen species (ROS) are a by-product of OXPHOS that are subsequently scavenged to maintain tissue homeostasis, therefore it was hypothesised that exacerbation of existing mitochondrial respiratory dysfunction in *PolgA* mice following PHx was a result of damaging excess ROS and leakage into the surrounding cellular environment. Despite being a first line defence against ensuing superoxide radicals, SOD1 expression in WT, *PolgA*$^{+/mut}$ and *PolgA*$^{mut/mut}$ livers showed no significant difference at 3 months of age. Yet in 6-month mice, resection appeared to exacerbate SOD1 gene expression in WTs and *PolgA*$^{mut/mut}$ livers - indicating a possible upregulation in response to OXPHOS, which may increase ROS production. Interestingly, SOD1 expression remained constitutively and significantly upregulated in *PolgA*$^{mut/mut}$ mice when compared to WTs and *PolgA*$^{+/mut}$ livers, which may be suggestive of greater ROS generation or insufficient ROS scavenging. Indeed, gene expression levels of other anti-oxidant glutathione synthesising and rate-limiting GSS enzyme appears to complement this: increasing in a gene-dose dependent manner within T0 livers at 6 months. Taken together these data suggest that following PHx, surgical intervention enhances respiratory chain dysfunction in *PolgA*$^{mut/mut}$ mice and thus excess ROS levels as a consequence of age-accumulated mtDNA mutations. Interestingly, increased GSS activity is observed prior to DNA synthesis (~12 hours) and diminishes by 24 hours post-PHx (Huang *et al.*, 1998). Therefore, such changes in GSS expression are likely to go unnoticed by the present study's given time points.

Due to the breeding strategy and reduced survival observed following PHx in *PolgA*$^{mut/mut}$ mice, the present study was limited to a small number of mice in each group. If allowed more time, more *PolgA*$^{mut/mut}$ mice would be included in the study to reduce variability and increase statistical power. Nonetheless, this chapter's findings suggest PHx induces transient mitochondrial dysfunction and changes to mitochondrial complex protein activity and anti-oxidant expression, which in the presence of basal mitochondrial respiratory chain dysfunction in heterozygous *PolgA*$^{+/mut}$ and *PolgA*$^{mut/mut}$ mice diminishes hepatocellular proliferation. At 3 months, thresholds for deficiency may have not been exceeded to induce an aberrant phenotype in *PolgA* mice, with enough mitochondrial function remaining to permit normal liver regeneration. Compensatory mechanisms may also contribute to the maintenance of hepatic recovery, including the upregulation of TNFα signalling and mito-inhibitory TGFβ signalling that are altered at 6 months of age. Age-associated accumulation of mitochondrial respiratory dysfunction is therefore likely to diminish post-surgical parenchymal recovery in *PolgA*$^{mut/mut}$ mice with age, due to insufficient mitochondrial respiratory chain capacity to meet the energetic demands of post-PHx liver regeneration. Further work is needed to determine this: including complementary studies on hepatocellular regenerative signalling and cell cycle progression, as well as the inclusion of additional time points.

Table 5-2: Chapter 5 Summary Table. *ND denotes 'no statistical difference'*

	Regeneration			Inflammation		Mitochondrial Function				Antioxidants	
	Liver Weight	Histology		Gene		Histology	Protein		Gene	Gene	
	Total Liver Weight	H&E: Mitotic Bodies	PCNA	TNFα	TGFβ	COX /SDH	NDUFB8 (CI)	Mt-CO1 (CIV)	PGC1α	GSS	SOD1
3 month	48h: ↑ $PolgA^{mut/mut}$ 72h: ↑ $PolgA^{+/mut}$ & ↑ $PolgA^{mut/mut}$	48h: ↓$PolgA^{mut/mut}$	48h: ↓↓↓↓ $PolgA^{mut/mut}$ 72h: ↓↓$Polg^{+/mut}$ vs WT	ND	ND	PHx induces respiratory dysfunction	48h: ↓$PolgA^{+/mut}$	48h: ↓$PolgA^{+/mut}$ & $PolgA^{mut/mut}$ 72h: ↓$PolgA^{+/mut}$ & $PolgA^{mut/mut}$	ND	T0: ↓$PolgA^{mut/mut}$	ND
6 month	Naïve: ↓ $PolgA^{mut/mut}$ & ↓ PolgA 48h: ↓ $PolgA^{mut/mut}$ 72h: ↓ $PolgA^{mut/mut}$, ↓ PolgA, ↓ $PolgA^{mut/mut}$ Vs. ↓ PolgA	48h: ↓↓↓↓ $PolgA^{+/mut}$ & $PolgA^{mut/mut}$ 72h: ↓↓↓ $PolgA^{mut/mut}$	72h: ↓↓↓ $PolgA^{+/mut}$, ↓↓↓↓ $PolgA^{+/mut}$	T0: ↑$PolgA^{mut/mut}$ 72h: ↓↓↓$PolgA^{mut/mut}$	48h: ↑↑↑$PolgA^{mut/mut}$ 72h: ↑↑↑$PolgA^{mut/mut}$	PHx induces respiratory dysfunction	48h: ↓$PolgA^{mut/mut}$ 72h: ↓$PolgA^{mut/mut}$	72h: ↓$PolgA^{+/mut}$ & $PolgA^{mut/mut}$	48h: ↓↓↓$PolgA^{+/mut}$ & ↓↓↓$PolgA^{mut/mut}$	T0: ↑↑↑$PolgA^{mut/mut}$	T0: ↑$PolgA^{mut/mut}$

5.7 Chapter 5 Key Summary Points

- Despite COX deficiency shown periportally and changes in Mt-CO1 protein expression, results from 3-month post-PHx surgery suggests that the threshold required for mtDNA mutation-induced respiratory dysfunction in *PolgA* mice is unlikely to be exceeded, thereby permitting hepatic recovery

- Inability to recover liver mass during 6-month post-PHx hepatocellular regeneration is likely to be ascribed to reduced complex I (NDUFB8) protein expression following age-associated accumulation of mtDNA mutations, as well as changes in hepato-proliferative signalling.

- In 6-month *PolgA*$^{mut/mut}$ mice, alterations to hepato-protective TNFα may increase susceptibility to apoptosis, whilst elevated changes to TGFβ expression may prevent proliferative signalling. Taken together, this may limit liver recovery post-PHx in these mice.

- Surgical intervention appears to exacerbate respiratory chain dysfunction. Changes to anti-oxidant enzyme SOD1 gene expression was found in the presence of homozygous *PolgA*-induced respiratory chain dysfunction, indicating greater ROS production / insufficient ROS scavenging. This may be ascribed to increased energetic demand upon remaining respiratory deficient cells, resulting in excess ROS production post-PHx.

Chapter 6 | Liver Regeneration in Response to Oxidative Stress

6.1 Introduction

Mitochondria are recognised as important arbitrators of reactive oxygen species (ROS) production, highly reactive oxygen-containing molecules well established as oxidative phosphorylation (OXPHOS) by-products that occurs during cellular energy metabolism. Understood to chiefly emanate from complex I and III of the electron transport chain (ETC) and dependent on NADH and coenzyme Q (CoQ) pools, they include for example, superoxide (O_2*), singlet oxygen ($^1O_2$) molecules, hydroxyl (OH^*), hydroperoxyl (HO_2*) and peroxyl (RO_2*) radicals, although work to date has predominantly focused on the peroximal mitochondrial O_2^*, shown within isolated mitochondria to arise from one electron reduction of oxygen (Chance *et al.*, 1979; Murphy, 2009). Controlling the levels of O_2^* and other ROS within cells through defensive antioxidant enzymes such as SOD (superoxide dismutase), catalase and glutathione peroxidase (GPx) provides further evidence for *in vivo* ROS. For example, genetic ablation and conditional knockout of SOD is demonstrated to have curtailed lifespan and pathological effects in mice due to failure in O_2^* dismutation into oxygen and hydrogen peroxide (H_2O_2) (Li *et al.*, 1995; Uchiyama *et al.*, 2006; Watanabe *et al.*, 2013). Such deleterious effects are associated with failure to balance the pro-oxidant environment with antioxidant scavenging, which under normal homeostatic conditions supports a variety of functions like ROS-mediated cell signalling and ROS-inducing phagocytosis by neutrophil and macrophage immune cells. Excess ROS levels and leakage from the mitochondria are therefore understood to result in aberrant redox-induced activation of transcriptional signalling and inflammation, as well as reactivity with cell DNA, protein and lipid macromolecules, leading to damaging oxidative tissue stress (Sharma *et al.*, 2003). As such, cumulative oxidative damage to cellular components has been observed in a number of chronic low grade proinflammatory conditions, including neurological diseases, cancer, cardiovascular disease, diabetes, as well as ageing (Dhalla *et al.*, 2000; Sayre *et al.*, 2001; Jenner, 2003; Dalle-Donne *et al.*, 2006).

Oxidative stress secondary to endogenous excess ROS was first popularised in Harman's mitochondrial free radical theory (of ageing). The degenerative ageing process outlined to share common pathological mechanisms with cancer biology and radiation toxicity, through the generation of deleterious cumulative free radicals

generated from mitochondrial oxygen consumption (Harman, 1956; Harman, 1972; Boveris and Chance, 1973). Dysfunctional mitochondria, in particular, are proposed as less efficient at ATP synthesis yet produce greater levels of ROS and present a possible major source of oxidative imbalance in many chronic and age-associated pathologies, including those of the liver like non-alcoholic fatty liver disease (NAFLD), that also coincides with detected impairment of normal mitochondrial function (Caldwell *et al.*, 1999; Sanyal *et al.*, 2001). Interestingly, when assessing oxidative stress in mitochondria, the mitochondrial genome (mtDNA) that encodes 13 of the genes required for respiratory complex protein subunits, demonstrates a 50-fold greater vulnerability to ROS-induced mutagenesis over nuclear DNA; perhaps unsurprisingly, ascribed to the close proximity of mtDNA molecules' to the ETC oxidative environment. Taken together, the observations invariably lend support towards a 'vicious cycle' hypothesis: ROS targets mtDNA that in turn induces further aberrant mtDNA oxidative damage (Harman, 1956; Harman, 1972). Amongst alterations observed from mtDNA oxidised mutagens, for example, is the loss of mitochondrial membrane potential (ΔΨm), able to affect ETC productivity as well as mitochondrial membrane permeability that can lead to downstream pro-apoptotic signalling; oxidised mtDNA may also act as 'alarmins,' resulting in activation of the NLRP3 inflammasome and proinflammatory IL-1β secretion (Lopez-Armada *et al.*, 2006; Shimada *et al.*, 2012).

In vivo, treatment of aberrant ROS signalling is understood to ameliorate pathogenic onset and survival in a number of conditions; yet, in *PolgA*$^{mut/mut}$ mice, evidence for mitochondrial dysfunction and oxidative stress appears to be conflicting. On one hand, some previous *PolgA*$^{mut/mut}$ mice studies report negligible changes in ROS production or oxidative damage markers despite an age-associated accumulation of mtDNA mutations (Trifunovic *et al.*, 2004; Kujoth *et al.*, 2005; Hiona *et al.*, 2010). Yet advancements of quantifiable PCR and bioanalytical techniques beyond early biochemistry-based methods, has enabled other studies to demonstrate evidence of increased ROS in *PolgA*$^{mut/mut}$ whether it be measured directly or indirectly, *via* antioxidant changes (Vermulst *et al.*, 2008; Logan *et al.*, 2014). In specific, findings by Logan and colleagues (2014) show augmented *in vivo* levels of oxidative stress marker H_2O_2 in ageing *PolgA*$^{mut/mut}$ mice through detection *via* mitochondria-targeted mass spectrometry probe MitoB, suggesting its contribution to progeroid ageing. However, this occurs in the absence of altered and detectable changes in markers of

oxidative markers or *ex vivo* ROS. These findings in older *PolgA*$^{mut/mut}$ mice could therefore suggest that a vicious cycle of mitochondrially disruptive oxidative damage in potentiating the degenerative ageing process. It was therefore hypothesised in the present study, that mitochondrial dysfunction that arises from defective *PolgA* and ensuing mtDNA mutations results in the production of ROS, which in turn contributes to reduced post-injury hepatocellular recovery.

6.2 Aims

The aim of this chapter was to investigate the effects of mitochondrial dysfunction on the *PolgA*$^{+/mut}$ and *PolgA*$^{mut/mut}$ liver repair following acute CCl_4-induced oxidative stress.

6.3 Acute CCl_4 injury induces greater oxidative stress to mitochondria in the presence of respiratory dysfunction

Single dose CCl_4 injection induces a transient acute inflammatory response encompassing hepatocellular apoptosis and necrosis, minimal hepatic stellate cell (HSC) activation, extracellular matrix (ECM) deposition, and the stimulated regeneration of the liver parenchyma around 48 hours post-injury (Weber *et al.*, 2003). Damage follows oxidative stress stimulated by the cytochrome P450 CYP2E1-mediated metabolism of CCl_4 into CCl_3^* and CCl_3OO^* radicals, understood to exert cellular cytotoxicity through lipid peroxidising effects. Since oxidising effects of CCl_4 also include the induction of mitochondrial respiratory dysfunction, we hypothesised that CCl_4-induced chemical stresses on *PolgA*$^{+/mut}$ and *PolgA*$^{mut/mut}$ mice could further reduce the ability for hepatocellular regeneration secondary to additional oxidative damage to mtDNA (Knockaert *et al.*, 2011). Therefore, at 8-12 weeks of age, WT, *PolgA*$^{+/mut}$ and *PolgA*$^{mut/mut}$ mice were injected with a single acute dose of CCl_4 and allowed to recover until sacrificial time points; livers were then harvested and analysed for experimental testing.

6.3.1 Acute CCl_4 induces additional mitochondrial respiratory dysfunction

PolgA$^{mut/mut}$ are characterised by accelerated progeroid ageing with phenotypic onset occurring approximately around 6 months of age and ascribed to somatic mtDNA mutations and respiratory dysfunction accumulated with time (Trifunovic *et al.*, 2004; Kujoth *et al.*, 2005). Interestingly, even in the absence of ageing symptoms, 1-3 month old *PolgA*$^{mut/mut}$ mice observe a 7-11 fold increase in mtDNA mutations (Vermulst *et al.*, 2008). To therefore test whether oxidative stress had a compounding effect on present mitochondrial respiratory dysfunction, harvested CCl_4 and olive oil injected livers were subjected to dual COX/SDH staining. Here, histological examination revealed that even at 8-12 weeks, olive oil control *PolgA*$^{mut/mut}$ mice displayed signs of greater cytochrome c oxidase (COX) deficiency that emanates periportally, when compared to WT and *PolgA*$^{+/mut}$ livers (figure 6-1, A). The acute administration of CCl_4 induced COX deficiency across all genotypes at 48 hours, which failed to varying extents to return to control olive oil levels observed. Such an effect was more pronounced in *PolgA*$^{mut/mut}$ mice, suggesting that the basal presence of respiratory deficiency further perpetuates mitochondrial dysfunction in response to oxidative tissue injury - making it possible that subsequent failure in parenchymal recovery may be secondary to greater respiratory dysfunction. These findings were inconclusive, however, due to the difficulty in quantifying COX deficiency in the presence of necrotic liver damage.

To test for specific mitochondrial respiratory complex deficiencies, protein expression was determined in WT, *PolgA*$^{+/mut}$ and *PolgA*$^{mut/mut}$ liver tissues from olive oil and CCl_4 injected mice *via* western blot. Interestingly, despite observations of complex IV (COX) deficient staining following CCl_4 injection in all genotypes and in olive oil *PolgA*$^{mut/mut}$ mice, no observable differences in Mt-CO1 protein expression could be detected (figure 6-5, B). Similar expression patterns were also observed for complex II (SDHB), complex III (UQCRC2) and complex V (ATPB). Instead, a gene-dose dependent reduction in expression of complex I (NDUFB8) was observed in olive oil *PolgA*$^{+/mut}$ and *PolgA*$^{mut/mut}$ mice, which following CCl_4 intoxication, induced NDUFB8 upregulation at 48 hours across all genotypes (figure 6-1, B). Interestingly, this remained constitutively expressed solely in WT mice at 5 days.

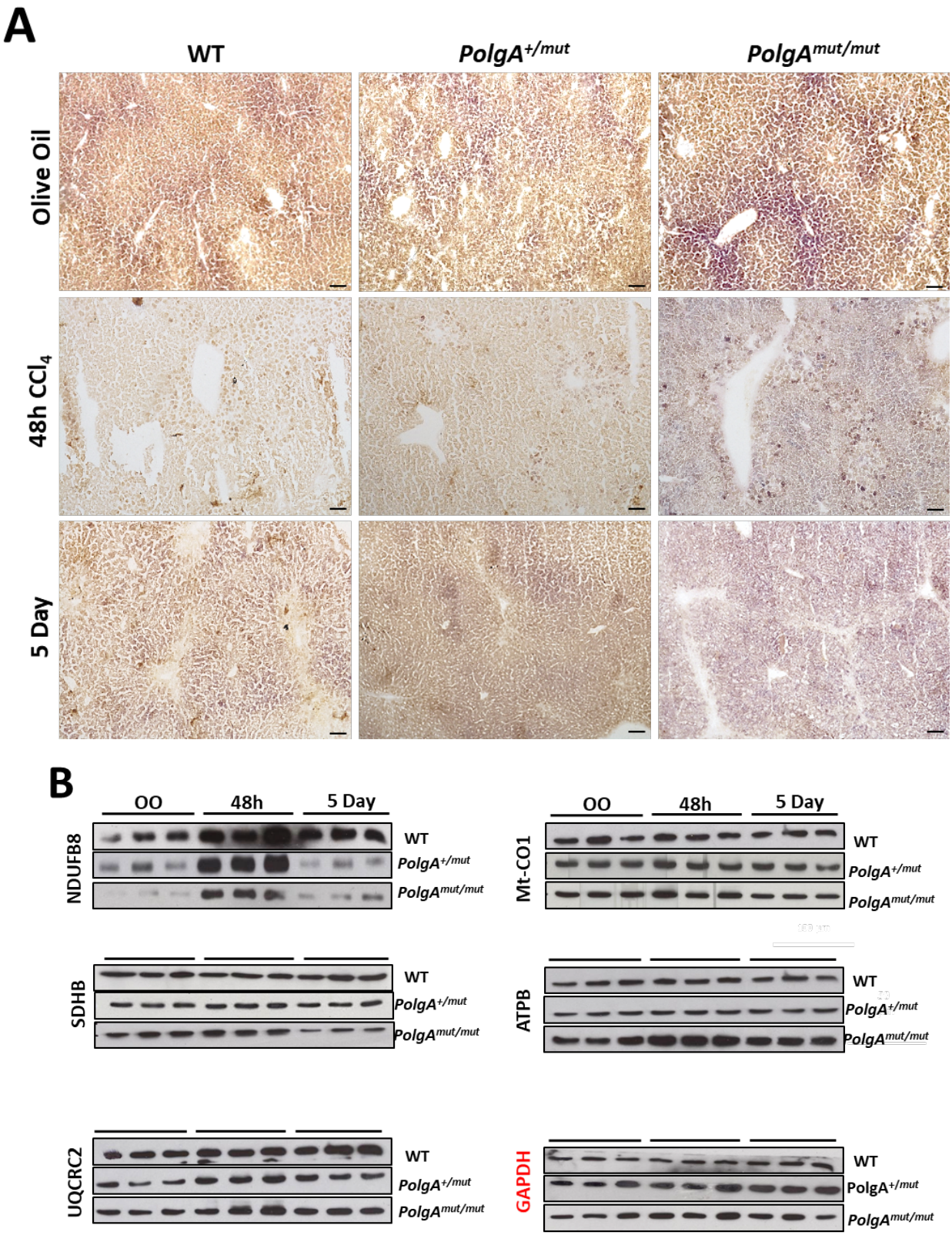

Figure 6-1: Mitochondrial function and protein subunit expression following acute CCl_4 administration.

(A) Representative photomicrographs of COX/SDH stained livers from 8-12 week old male WT, PolgA$^{+/mut}$ and PolgA$^{mut/mut}$ mice. Mice were administered acute dose of CCl_4 at 2 µl/g. Bars 50 µm. Representative of n=5 mice per WT and PolgA$^{+/mut}$ groups and n=4 mice per PolgA$^{mut/mut}$ (B) Protein expression of mitochondrial protein complex I subunit (NDUFB8); complex II (SDHB); complex III (UQCRC2); complex IV (Mt-CO1); and complex V in WT, PolgA$^{+/mut}$ and PolgA$^{mut/mut}$ mice, n=3 mice are shown per genotype at each time point.

Changes in protein expression of mitochondrial complexes appeared to occur alongside changes in mitochondrial subunit gene expression, in which mRNA levels of complex I membrane-anchor subunit ND1 was shown to be significantly upregulated at 48 hours post-CCl_4 injection in WT and *PolgA*$^{+/mut}$ livers, unfortunately failing to reach significance in *PolgA*$^{mut/mut}$ 48 hour groups (figure 6-2, A). By contrast, no differences in gene expression was observed for complex I subunit ND4 (figure 6-2, B), perhaps ascribed to the temporal stages of complex I assembly and its involvement in the latter P module completion stages (Lazarou *et al.*, 2009). For other mitochondrial respiratory complex genes cytochrome b, COX1 and ATP6, day 5 CCl_4 injured *PolgA*$^{mut/mut}$ mice demonstrated greater increases in expression of the markers when compared to olive oil and 48-hour post-injection controls, as well as during comparisons made to corresponding WT and *PolgA*$^{+/mut}$ mice (figure 6-2, C-D, F). Significantly increased mRNA gene expression of COX3 was only observed at 5 days in *PolgA*$^{mut/mut}$ mice when compared to *PolgA*$^{mut/mut}$ olive oil controls (figure 6-2, E).

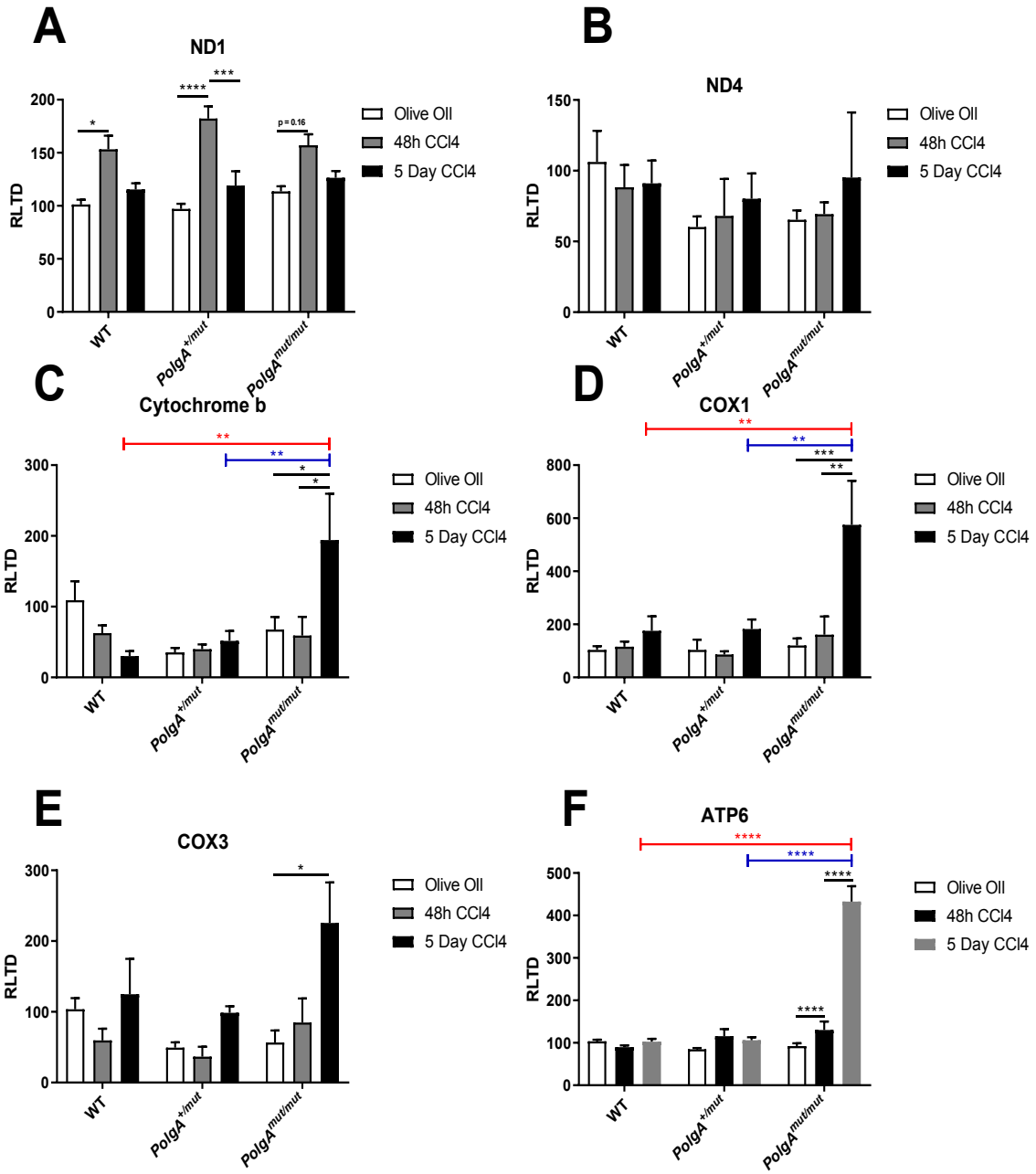

Figure 6-2: Gene expression of mitochondrial respiratory complex subunits.

*Mitochondrial gene expression of (A-B) ND1 and ND4, complex I; (C) cytochrome b, complex III; (D-E) COX1 and COX3, complex IV and (F) ATP6, complex V subunits in olive oil control and acute CCl_4 injected WT (n=5), $PolgA^{+/mut}$ and $PolgA^{mut/mut}$ (n=4 mice per gentoype). All P values were calculated using a two-way ANOVA. * p<0.05, **p<0.01, ***p<0.001 **** p = 0.0001.*

6.3.2 Acute CCl_4 oxidative liver injury induces expression of a subset of antioxidant genes in *PolgA*$^{mut/mut}$ mice

Whilst reports on antioxidant enzyme expression following oxidative cytotoxicity remain inconclusive, the upregulation of endogenous enzymes appears to minimise disease pathology including subsequent decreases of lipid peroxidising effects during CCl_4 administration (Szymonik-Lesiuk *et al.*, 2003; Venugopal *et al.*, 2007; Knockaert *et al.*, 2011). With the induction of mitochondrial respiratory dysfunction in *PolgA*$^{mut/mut}$ mice, gene expression of antioxidant enzymes were assessed for oxidative status following olive oil and acute CCl_4 injury. As with previous rodent studies, CCl_4 administration revealed no significant differences in GPX expression (figure 6-3, B); yet, when determining SOD1 expression, significantly greater levels in WT mice were observed at 5 days following CCl_4 intoxication (Szymonik-Lesiuk *et al.*, 2003). However, this response was impaired in *PolgA*$^{+/mut}$ and *PolgA*$^{mut/mut}$ mice, with *PolgA*$^{+/mut}$ mice presenting with an intermediate phenotype (figure 6-3, C). No differences were observed for mitochondrial SOD2 (figure 6-3, D) Furthermore, acute oxidative injury stimulated increases in glutathione synthetase (GSS) mRNA expression in *PolgA*$^{mut/mut}$ mice, significantly peaking at 48 hours before lowering to significantly elevated levels at 5 days post-administration (figure 6-3, A). Augmented levels were also greatly significant when compared to 48-hour WT and *PolgA*$^{+/mut}$ mice.

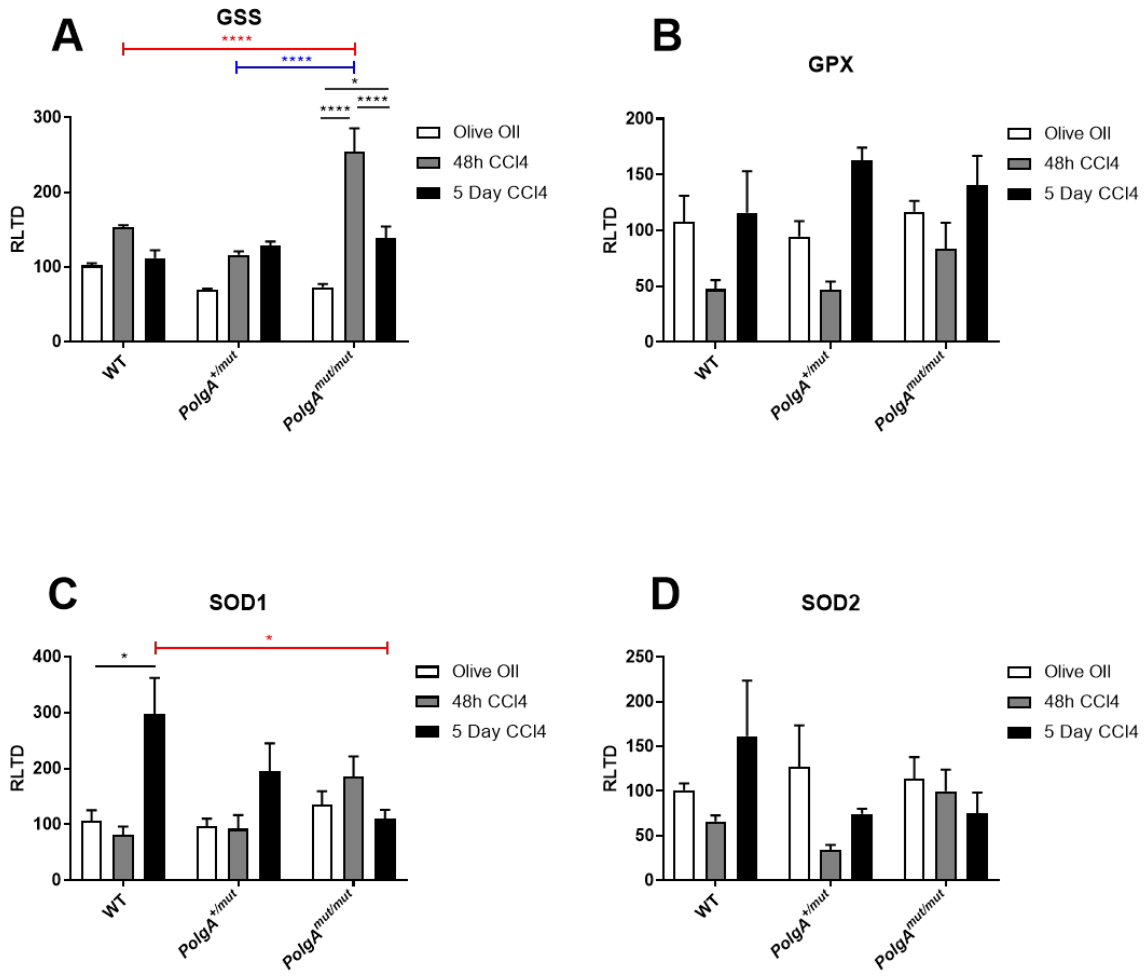

Figure 6-3: Gene expression of antioxidant enzymes (A) GPX; gluthathione peroxidase; (B) SOD1, superoxide dismutase 1; (C) SOD2 and (D) GSS, glutathione synthetase

*qRT-PCR measurement of mRNA expression for antioxidant genes SOD1, SOD2, GSS and GPX in olive oil and acute CCl_4 treated WT, $PolgA^{+/mut}$ and $Polg^{mut/mut}$ livers. N=3 for olive oil groups, n=5 for WT and $PolgA^{+/mut}$ CCl_4 treatment groups, n=4 for $PolgA^{mut/mut}$ CCl_4 treated mice. All P values were calculated using a two-way ANOVA. * p<0.05, **** p = 0.0001.*

6.4 Liver tissue damage and regeneration following acute CCl_4-induced oxidative hepatic injury

6.4.1 Hepatocellular damage and necrosis ensues following acute CCl_4 administration in *PolgA* mice

Liver tissue damage was initially evaluated by macroscopic analysis and H&E staining, revealing acute CCl_4 dosing to induce liver swelling and centrilobular necrosis at 48 hours that resolved to varying extents across all genotypes within 5 days (figure 6-4, figure 6-5). In specific, H&E staining observed hepatocytes to undergo ballooning and tissue injury. As expected, analysis of necrotic liver tissue confirmed that the percentage area of necrotic tissue significantly increased at 48 hours post-injury in WT, *PolgA*$^{+/mut}$ and *PolgA*$^{mut/mut}$ mice. Although no significant differences were recognised between genotypes, at 5 days post-injection, the necrotic tissue area in *PolgA*$^{mut/mut}$ mice remained slightly elevated, suggestive of a delayed wound healing response and failure to fully resolve liver injury (figure 6-5, A-B). Establishing whether possible sustained necrosis was a result of greater recipient tissue damage, the lipid peroxidation marker 4-hydroxynonenal (4HNE) was assessed in livers for oxidative injury. Observed by western blot, 4HNE protein expression was increased at 48 hours post-CCl_4 injection with a seemingly more pronounced detection in *PolgA*$^{+/mut}$ and *PolgA*$^{mut/mut}$ mice: possibly indicating greater CCl_4-induced oxidative tissue injury (figure 6-6). As expected, increased lipid peroxidation coincided with the similar diminution of CYP2E1 protein expression at 48 hours across all genotypes (figure 6-6), in which CCl_4-derived metabolite CCl_3^* is understood to bind to the CYP2E1 active site that subsequently leads to the enzyme's inactivation and degradation (Tierney *et al.*, 1992; Dai and Cederbaum, 1995). Despite observing more tissue necrosis histologically in *PolgA*$^{mut/mut}$ injured mice, evidence for greater oxidative tissue damage remains inconclusive, since serum quantification of the liver damage marker aspartate transaminase (AST) at 24 hour post- CCl_4 injury reveal no significant differences in AST levels in WT, *PolgA*$^{+/mut}$ and *PolgA*$^{mut/mut}$ mice. This indicated that levels of CCl_4-induced liver damage was comparable across all genotypes, suggesting that the failure to fully resolve the injury in *PolgA*$^{mut/mut}$ mice was not due to differences in the initial damage stimulus (figure 6-7).

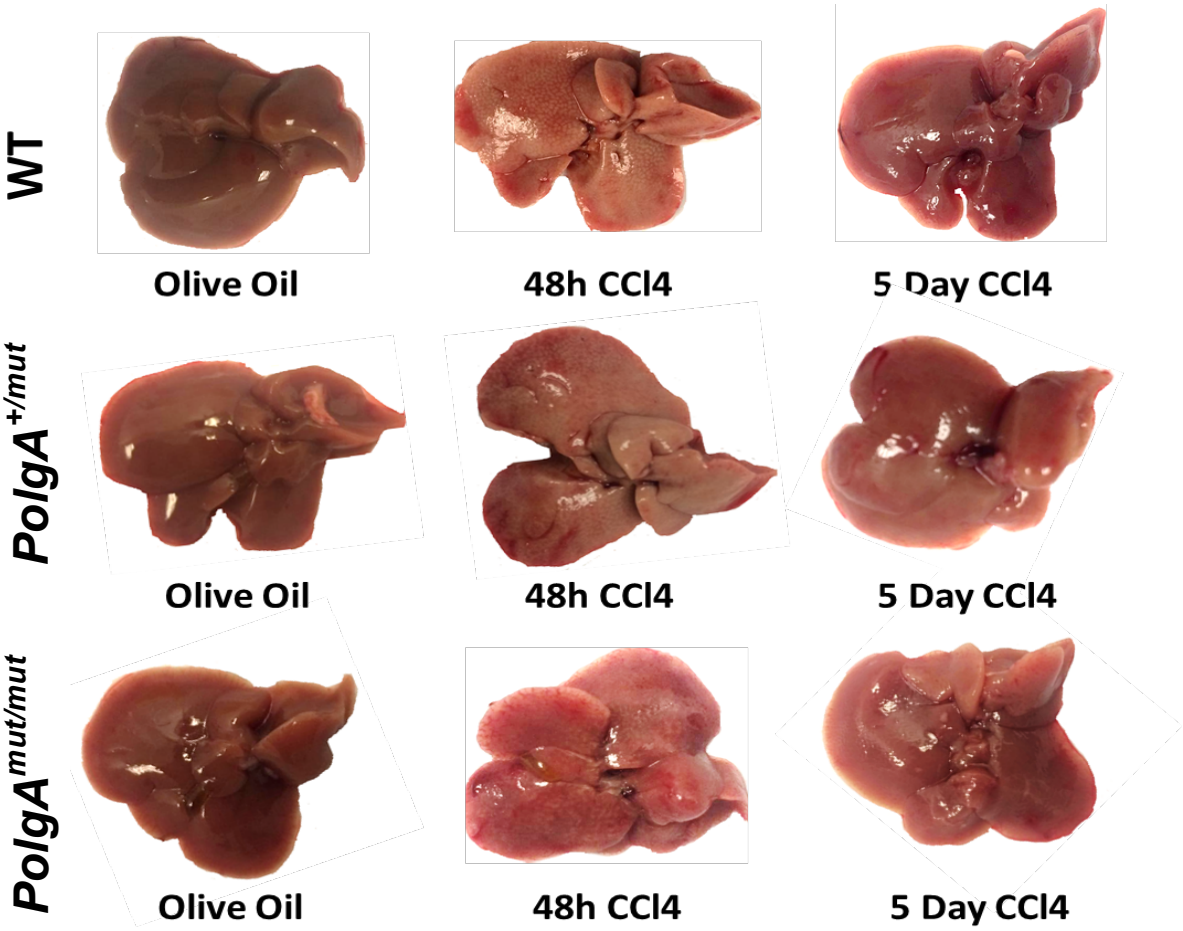

Figure 6-4: Macroscopic images of livers harvested from olive oil, 48 hour (48h) and 5-day post-acute CCl_4 administered WT, $PolgA^{+/mut}$ and $PolgA^{mut/mut}$ mice.

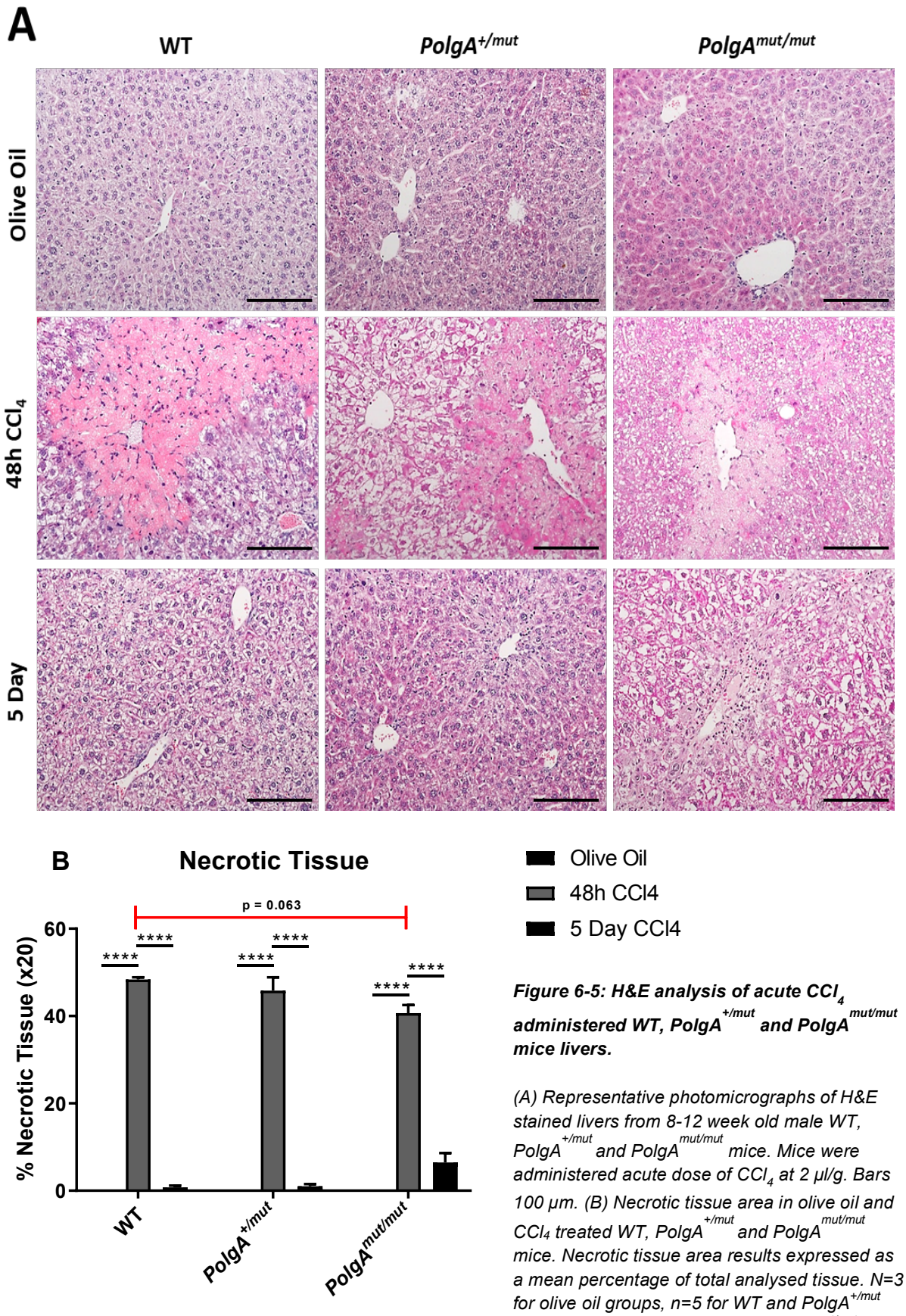

Figure 6-5: H&E analysis of acute CCl_4 administered WT, PolgA$^{+/mut}$ and PolgA$^{mut/mut}$ mice livers.

*(A) Representative photomicrographs of H&E stained livers from 8-12 week old male WT, PolgA$^{+/mut}$ and PolgA$^{mut/mut}$ mice. Mice were administered acute dose of CCl_4 at 2 µl/g. Bars 100 µm. (B) Necrotic tissue area in olive oil and CCl_4 treated WT, PolgA$^{+/mut}$ and PolgA$^{mut/mut}$ mice. Necrotic tissue area results expressed as a mean percentage of total analysed tissue. N=3 for olive oil groups, n=5 for WT and PolgA$^{+/mut}$ CCl_4 treatment groups, n=4 for PolgA$^{mut/mut}$ CCl_4 treated mice. All P values were calculated using a two-way ANOVA. **** p = 0.0001.*

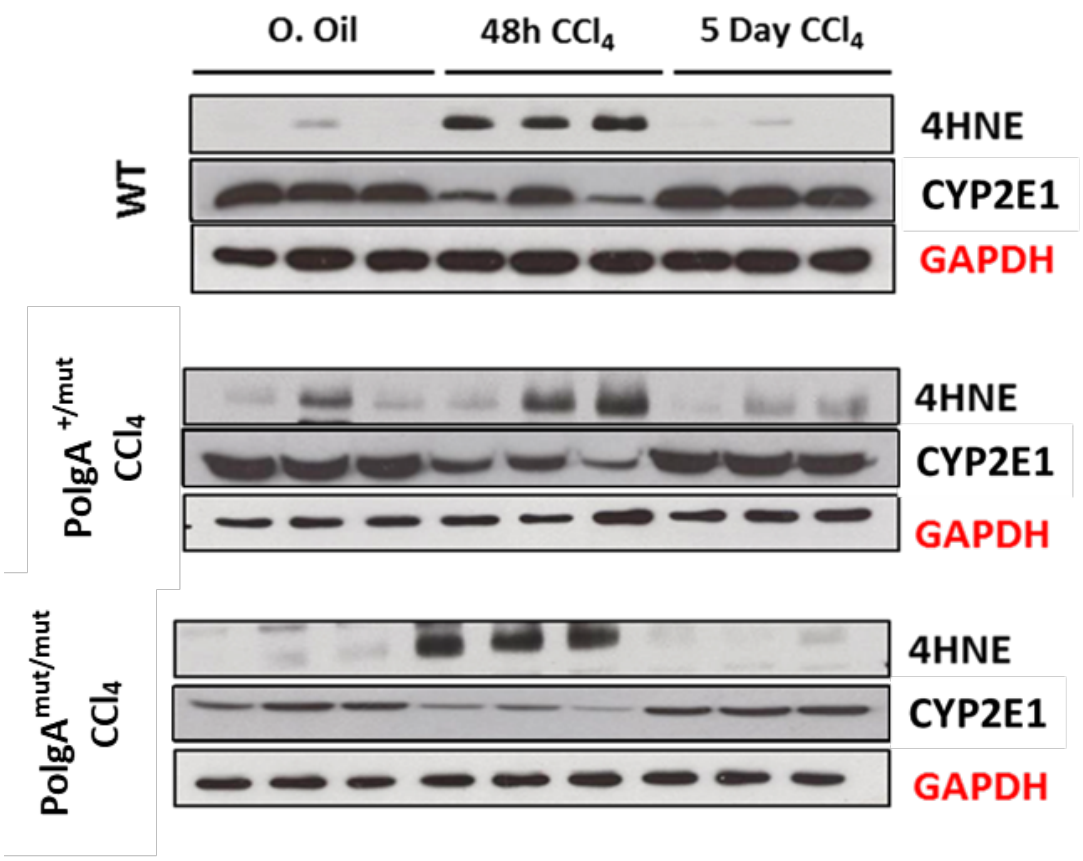

Figure 6-6 (above): Protein expression detecting 4-hydroxynenonal (4HNE) and CCl_4 detoxifying cytochrome P450 enzyme CYP2E1 in olive oil and acute CCl_4 administered WT, PolgA$^{+/mut}$ and PolgA$^{mut/mut}$ mice livers. *Protein expression of lipid peroxidation marker 4HNE and CYP2E1 was detected via Western blot in mice livers; GAPDH used as control marker. N=3 mice shown per genotype, per time point.*

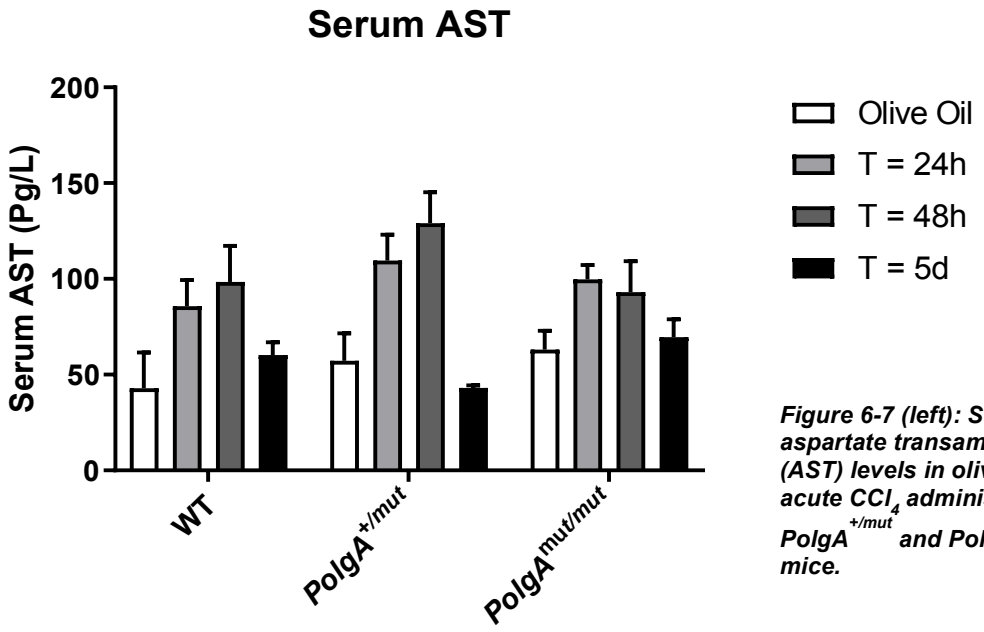

Figure 6-7 (left): Serum aspartate transaminase (AST) levels in olive oil and acute CCl_4 administered WT, PolgA$^{+/mut}$ and PolgA$^{mut/mut}$ mice.

6.4.2 Liver regeneration is delayed in *PolgA*$^{mut/mut}$ mice in response to acute oxidative CCl_4 injury

With the liver's remarkable ability to recover lost cellular mass and function, hepatocyte regeneration ensues in response to tissue injury. Testing if oxidative injury in the context of dysfunctional liver mitochondria hinders parenchymal recovery, indices of hepatocellular regeneration by means of liver to body weight ratios (figure 6-8) appear to indicate no significant difference between WT, *PolgA*$^{+/mut}$ and *PolgA*$^{mut/mut}$ olive oil and CCl_4 groups. This is despite previous likely inability of *PolgA*$^{mut/mut}$ to fully resolve necrotic tissue injury following CCl_4 intoxication (figure 6-5). These findings are similar to the indifferences observed across the liver to body weight ratios seen in WT and *PolgA* following partial hepatectomy (PHx). By contrast, hepatocellular proliferation quantified from H&E staining (figure 6-5, A) reveals that levels of mitotic bodies (MB) peak 48 hours post-injection and return within 5 days to vehicle olive oil levels in WT and *PolgA*$^{+/mut}$ mice (figure 6-9, B). These findings were similar in *PolgA*$^{mut/mut}$ livers; however, mitotic hepatocytes were still present at 5 days, perhaps indicating a delayed regenerative response. Comparable trends were also demonstrated by proliferating cell nuclear antigen (PCNA) IHC, with further analysis indicating a significant decrease in proliferating *PolgA*$^{mut/mut}$ hepatocytes compared to WT livers at 48 hours post-CCl_4 injection (figure 6-9, A, C). The results would therefore suggest that the presence of mitochondrial respiratory deficiency in *PolgA* $^{mut/mut}$ mice diminishes hepatocellular regeneration following further oxidative tissue injury to mitochondria.

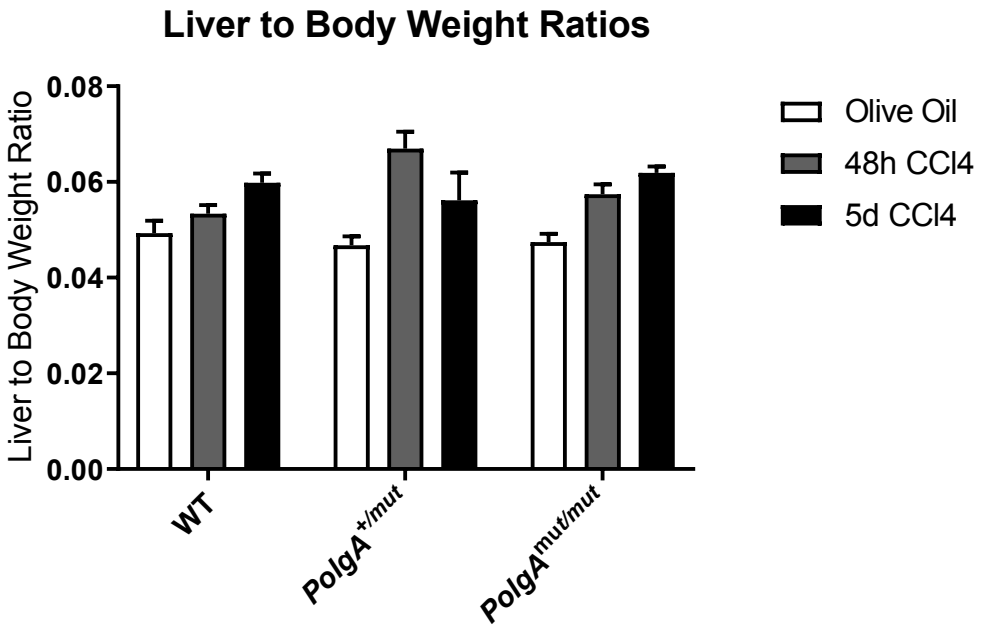

Figure 6-8: Liver to body weight ratio of olive oil and acute CCl_4 treated WT, PolgA$^{+/mut}$ and PolgA$^{mut/mut}$ mice.

Liver to body weight quantified as ratio of excised liver weight at 48 hour or 5d post-CCl_4 to body weight pre-CCl4 injection. N=3 for all olive oil treatment groups, n=5 for WT and PolgA$^{+/mut}$ CCl_4 treatment groups, n=4 for PolgA$^{mut/mut}$ CCl_4 treated mice.

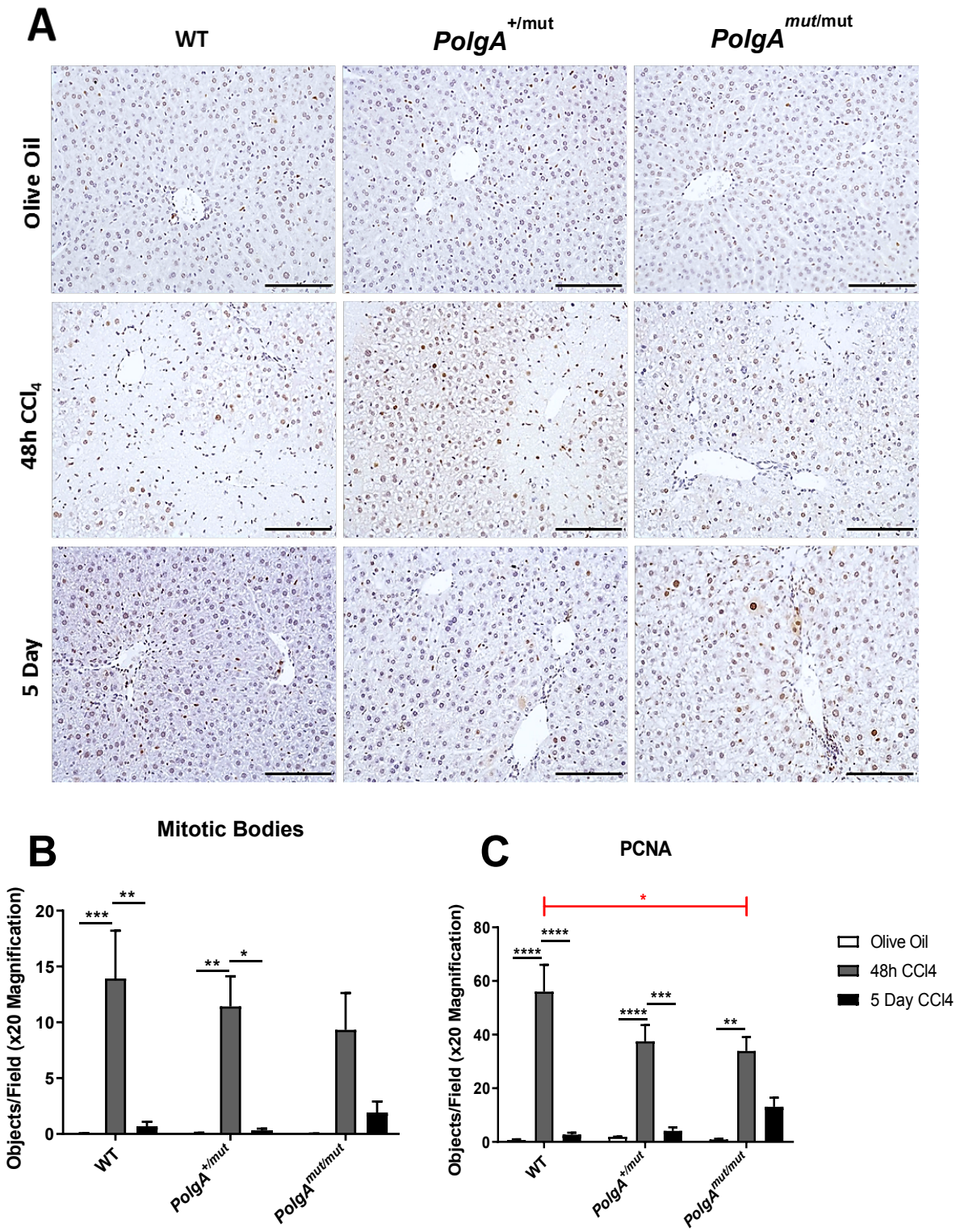

Figure 6-9: Regenerative analysis of livers following olive oil and acute CCl_4 administration in WT, PolgA$^{+/mut}$ and PolgA$^{mut/mut}$ mice.

*Regenerative response following CCl_4 intoxication in control and CCl_4 treated mice was analysed by mitotic bodies quantified from H&E (figure 6-5) and PCNA staining (above). Bars 100 µm. N=3 for all olive oil treatment groups, n=5 for WT and PolgA$^{+/mut}$ CCl_4 treatment groups, n=4 for PolgA$^{mut/mut}$ CCl_4 treated mice. All P values were calculated using a two-way ANOVA, *p<0.05, **p<0.01, ***p<0.001, ****p<0.0001.*

Reductions in liver regeneration could be ascribed to cell cycle arrest which can be detected by quantifying $P16^{INK4a}$ protein levels. $P16^{INK4a}$ is elevated in $PolgA^{mut/mut}$ livers from 48 hours to 5 days following acute CCl_4 injury (figure 6-10, A) and constitutively expressed at 5 days when compared to WT and $PolgA^{+/mut}$ mice. This constitutive expression is likely to limit post-injury hepatocellular proliferation, as initiated by the shift of normally quiescent G_0 hepatocytes into G_1 phase. Specifically, $P16^{INK4a}$ is understood to negatively regulate cyclin D and its interaction with CDK4/6, and as such, is able to halt cell cycle progression at the G_0-G_1 phase transition (Pavletich, 1999; Jeffrey *et al.*, 2000). Across all genotypes, it was also observed that $P16^{INK4a}$ expression was induced at 48 hours and coincided with increased expression of cyclin D1 (G_0/G_1; figure 6-10B). Changes at 48 hours post-CCl_4 were also seen for cyclin A2 (G_2M), E1 (G_1/S) and H (all cell cycle phases) (figure 6-10B). No obvious differences in all expression patterns between the three genotypes were observed for these cyclins, except for the constitutive expression of cyclin H, even at 5 days in $PolgA^{mut/mut}$ CCl_4-injured mice. Less is understood regarding cyclin H and its role in cell cycle, however, as part of the trimeric CDK activating kinase (CAK) complex, cyclin H assists in the activation of CDKs including during the phosphorylation of G1 phase CDK6 following association with its relevant cyclin (Lolli and Johnson, 2005). During cell cycle, cyclin H concentration and activity of its corresponding kinase CDK7 also remains invariant; however the return to cellular quiescence reduces levels – reflecting observations seen in 5-day CCl_4 WT and $PolgA^{+/mut}$ mice (Lolli and Johnson, 2005). Taken together, it is therefore plausible that in mitochondrially deficient $PolgA^{mut/mut}$ mice, oxidative CCl_4 injury further compounds hepatocellular regeneration by halting entry of quiescent state hepatocytes into the cell cycle *via* $P16^{INK4a}$-mediated signalling. This leads to a reduction in cellular proliferation, therefore hindering liver recovery following oxidative CCl_4-induced chemical injury.

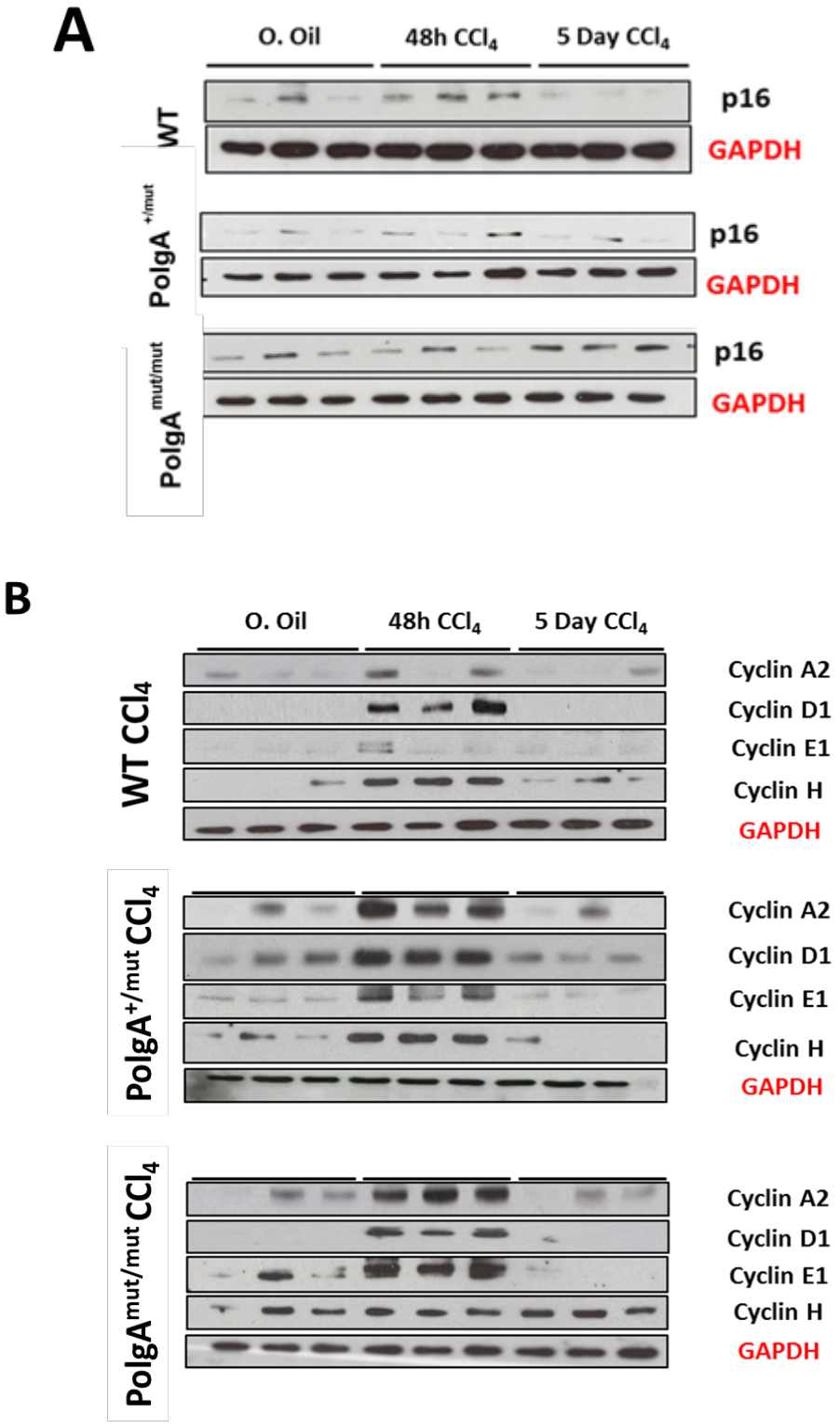

Figure 6-10: Western blot analysis of $P16^{INK4a}$ and cyclins A2, D1, E1 and H protein expression in WT, $PolgA^{+/mut}$ and $PolgA^{mut/mut}$ mice livers following CCl_4 injury.

Changes in protein expression observed at 48 and 72 hour time points post-CCl_4 intoxication for: (A) $P16^{INK4a}$ expression in olive oil and CCl_4 treated WT, $PolgA^{+/mut}$ and $PolgA^{mut/mut}$ mice (B) Acute CCl_4 induced changes in cyclin A2, D1, E1 and H in WT, $PolgA^{+/mut}$ and $PolgA^{mut/mut}$ mice. N=3 mice per genotype, per time point.

6.4.3 Acute CCl_4 liver injury induces proapoptotic signalling in PolgA$^{mut/mut}$ livers

Small wave apoptosis is typically required to correct excess hepatocytes produced during liver restoration: failure to incite apoptosis can lead to excess hyperplasia or tumorigenesis, whilst excessive apoptosis can lead to hepatocyte cell loss and liver damage (Sakamoto *et al.*, 1999). In the present study, it was suggested that alterations to the homeostatic balance between cell survival and programmed cell death signalling is altered during post-CCl_4 parenchymal recovery, with delays at 5 day post-CCl_4 injection coinciding with upregulated changes in mRNA expression of anti-apoptotic and pro-apoptotic genes. Indeed, *PolgA*$^{mut/mut}$ mice demonstrated significant elevations in anti-apoptotic genes Bcl-2 and Bcl_{XL} at 5 days post-CCl_4 intoxication when compared to other treatment groups, yet no significance was observed between genotypes (figure 6-11, A-B). No differences between genotypes were also observed for pro-apoptotic gene Bid, in which expression was significantly downregulated in response to CCl_4 administration as Bid truncates to assist with proapoptotic signalling figure (6-11, C). Instead, when assessing pro-apoptotic gene expression, BAX observed a 500-fold increase in 5 day *PolgA*$^{mut/mut}$ livers, greatly significant when comparing expression from other treatment groups and WT and *PolgA*$^{+/mut}$ genotypes (figure 6-11, D). Taken together, the results could therefore suggest alterations to the anti-apoptotic/pro-apoptotic signalling balance in favour of the latter, corroborating with failure to resolve pro-necrotic tissue damage as a result of CCl_4-induced oxidative stress.

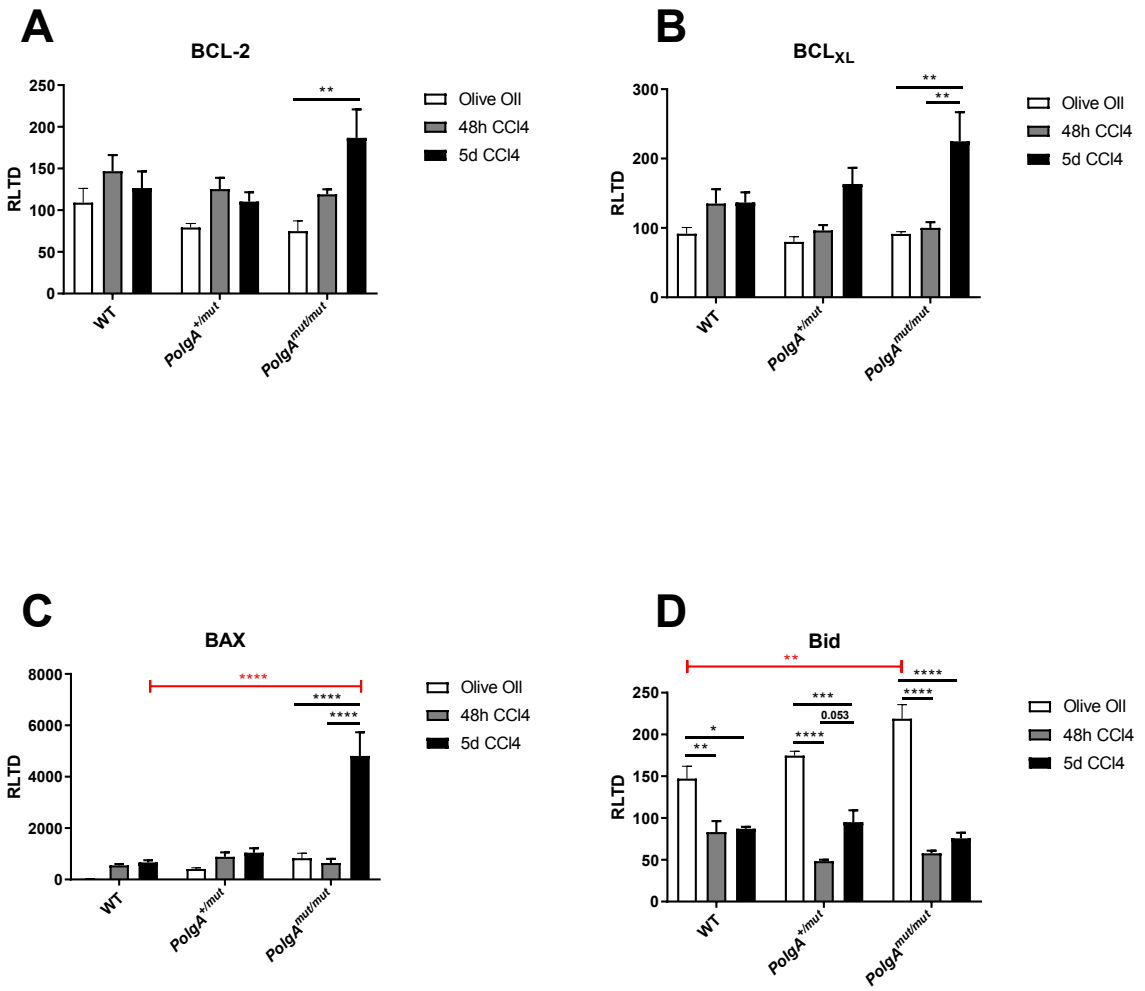

Figure 6-11: Apoptotic gene expression in WT, PolgA$^{+/mut}$ and PolgA$^{mut/mut}$ mice livers treated with olive oil and acute CCl_4 intoxication.

*CCl_4 injection induced alterations in anti-apoptotic Bcl-2 and BCL_{XL} and pro-apoptotic BAX and Bid genes in olive oil and CCl_4 treated WT, PolgA$^{+/mut}$ and PolgA$^{mut/mut}$ mice. N=3 for all olive oil treatment groups, n=5 for WT and PolgA$^{+/mut}$ CCl_4 treatment groups, n=4 for PolgA$^{mut/mut}$ CCl_4 treated mice. All P values were calculated using a two-way ANOVA, *p<0.05, **p<0.01, ***p<0.001, ****p<0.0001.*

6.5 Inflammatory cell infiltration in response to acute CCl_4 oxidative injury

With clear failure to resolve proinflammatory liver necrosis and a diminished hepatocellular regenerative response following acute CCl_4 intoxication in *PolgA*$^{mut/mut}$ mice, IHC staining for immune cells markers CD68 and NIMP were utilised to assess proinflammatory status within the oxidatively stressed liver. Staining with CD68 and NIMP indeed found proinflammatory infiltration following CCl_4 injury, of which the infiltrate was a mixture of monocyte, macrophages and neutrophils. Present in significantly greater numbers than olive oil controls, CD68 staining positively identified, following injury, increased liver monocyte and macrophages at 48 hours in *PolgA*$^{mut/mut}$ mice, as well as at 5 days in WT and *PolgA* groups (figure 6-12, A-B). These changes appeared to be typical of downstream proinflammatory immune cell recruitment following injury; however, no significant differences were observed between the different genotypes. In addition, proinflammatory neutrophil recruitment was also reflected through significantly greater levels of NIMP positive cells at 48 hours post-injection in WT, *PolgA*$^{+/mut}$ and *PolgA*$^{mut/mut}$ mice, which in the latter then failed to return to control olive oil levels at 5 days post injection (figure 6-13, A-B).

The recruitment of such immune cells appears to be downstream of proinflammatory signalling. CCl_4 injection induces gene expression of chemokine (C-X-C motif) ligand 2 (CXCL2) and tumour necrosis factor alpha (TNFα) in all genotypes within 48 hours and at 5 days. In addition, there were significantly higher expression of these cytokines in *PolgA*$^{mut/mut}$ mice when compared to WT and *PolgA*$^{+/mut}$ groups (figure 6-14, B-C). CXCL2 and TNFα are identified as chemotactic factors for neutrophils (Wolpe *et al.*, 1989; Colletti *et al.*, 1996). Gene expression for neutrophil chemotactic factor CXCL1 was also elevated at 5 days post-injection, reaching significance only in *PolgA*$^{mut/mut}$ mice when compared to olive oil controls and other genotypes (figure 6-14, A). By contrast, no obvious differences were observed between genotypes when assessing predominantly monocyte recruiting cytokines, monocyte chemoattractant protein-1 (MCP-1) and RANTES (C-C motif chemokine ligand 5), with peak gene expression at 48 hours and at 5 days post-injection respectively in WT, *PolgA*$^{+/mut}$ and *PolgA*$^{mut/mut}$ mice (figure 6-14, D-E). Taken together, these results suggest that CCl_4-induced oxidative stress, could stimulate a greater proinflammatory phenotype in the presence of greater mitochondrial respiratory dysfunction, which subsequently may perpetuate acute oxidative tissue injury and diminish parenchymal regeneration, as seen in *PolgA*$^{mut/mut}$ mice.

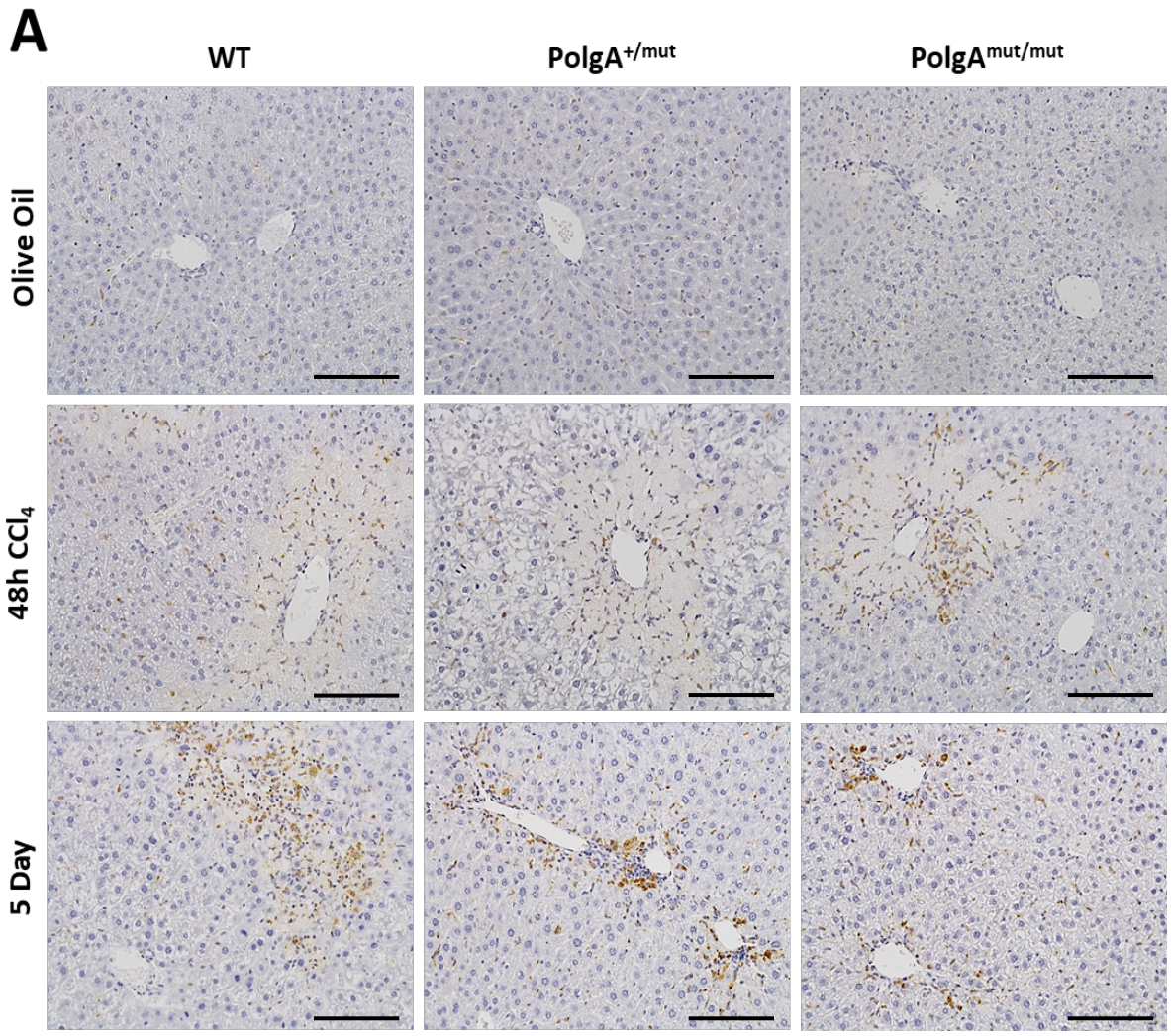

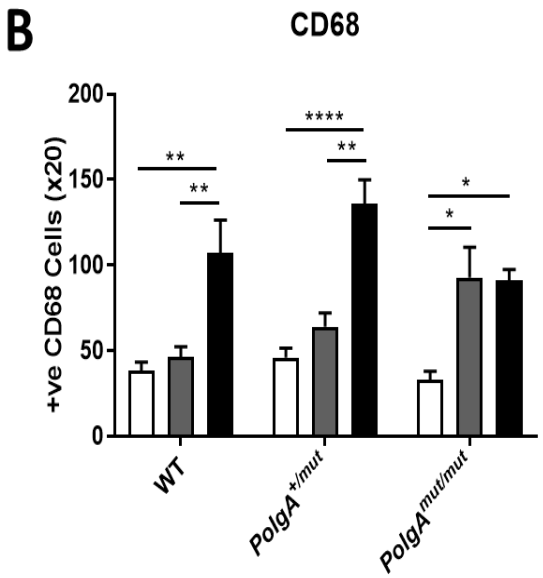

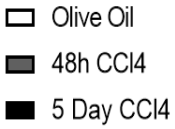

Figure 6-12: CD68 immunohistochemistry of acute CCl_4 administered WT, PolgA$^{+/mut}$ and PolgA$^{mut/mut}$ mice livers.

*(A) Representative photomicrographs of CD68 immunohistochemistry on livers from 8-12 week old male WT, PolgA$^{+/mut}$ and PolgA$^{mut/mut}$ mice. Mice were administered acute dose of CCl_4 at 2 µl/g. Bars 100 µm. (B) Quantification of CD68 positive cells in olive oil controls and in mice 48 hours and 5 days post-CCl_4 administration. CD68 positively stained cells were counted in 15 HPF at x20 magnification. N=3 for all olive oil treatment groups, n=5 for WT and PolgA$^{+/mut}$ CCl_4 treatment groups, n=4 for PolgA$^{mut/mut}$ CCl_4 treated mice. All p values were calculated using a two-way ANOVA *p<0.05, ** = 0.01, **** p = 0.0001.*

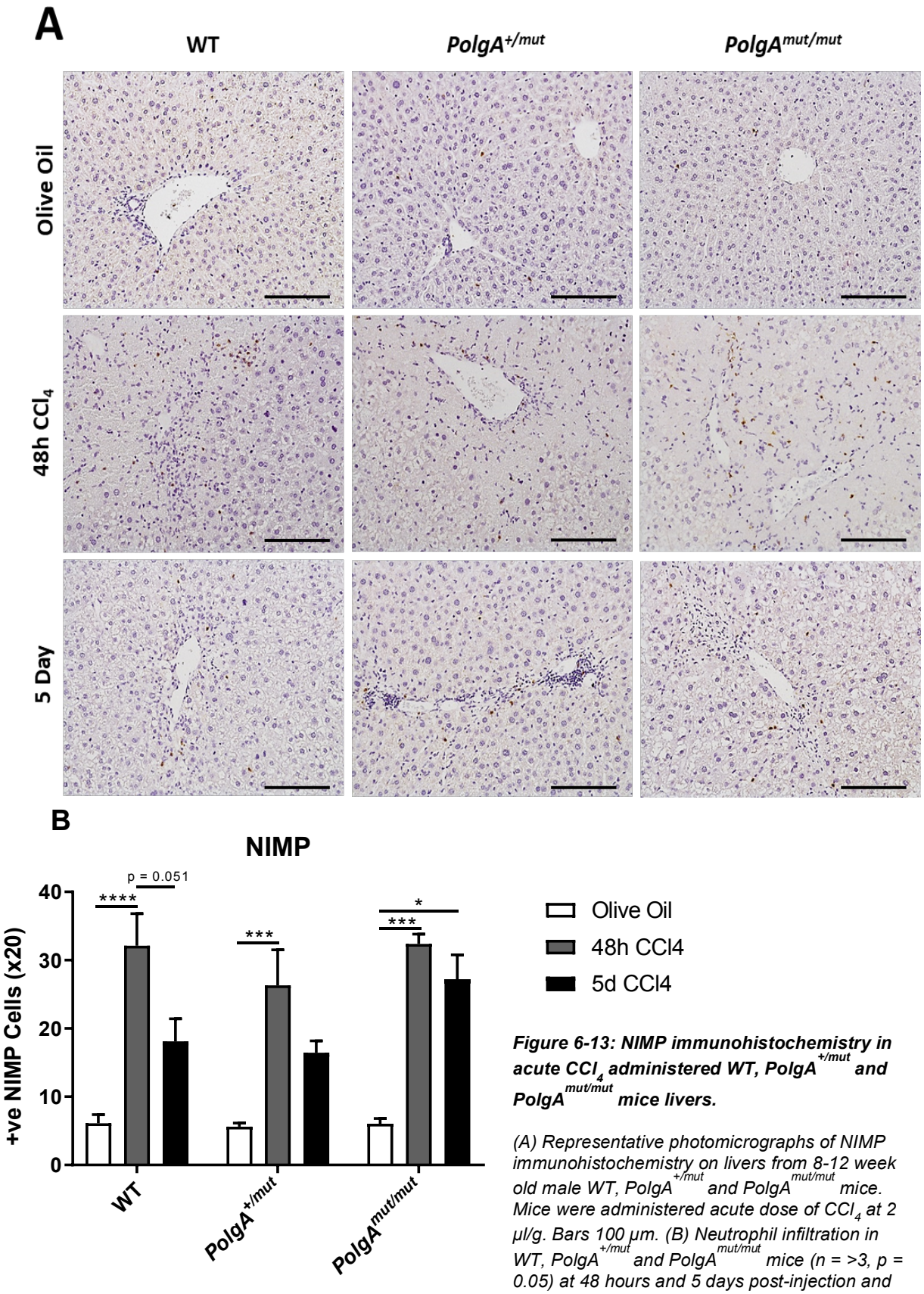

Figure 6-13: NIMP immunohistochemistry in acute CCl_4 administered WT, PolgA$^{+/mut}$ and PolgA$^{mut/mut}$ mice livers.

*(A) Representative photomicrographs of NIMP immunohistochemistry on livers from 8-12 week old male WT, PolgA$^{+/mut}$ and PolgA$^{mut/mut}$ mice. Mice were administered acute dose of CCl_4 at 2 µl/g. Bars 100 µm. (B) Neutrophil infiltration in WT, PolgA$^{+/mut}$ and PolgA$^{mut/mut}$ mice (n = >3, p = 0.05) at 48 hours and 5 days post-injection and in olive oil controls. NIMP positive neutrophils were counted in 15 HPF at x20 magnification. N=3 for all olive oil treatment groups, n=5 for WT and PolgA$^{+/mut}$ CCl_4 treatment groups, n=4 for PolgA$^{mut/mut}$ CCl_4 treated mice. All p values were calculated using a two-way ANOVA *p<0.05, *** = 0.005, **** p = 0.001.*

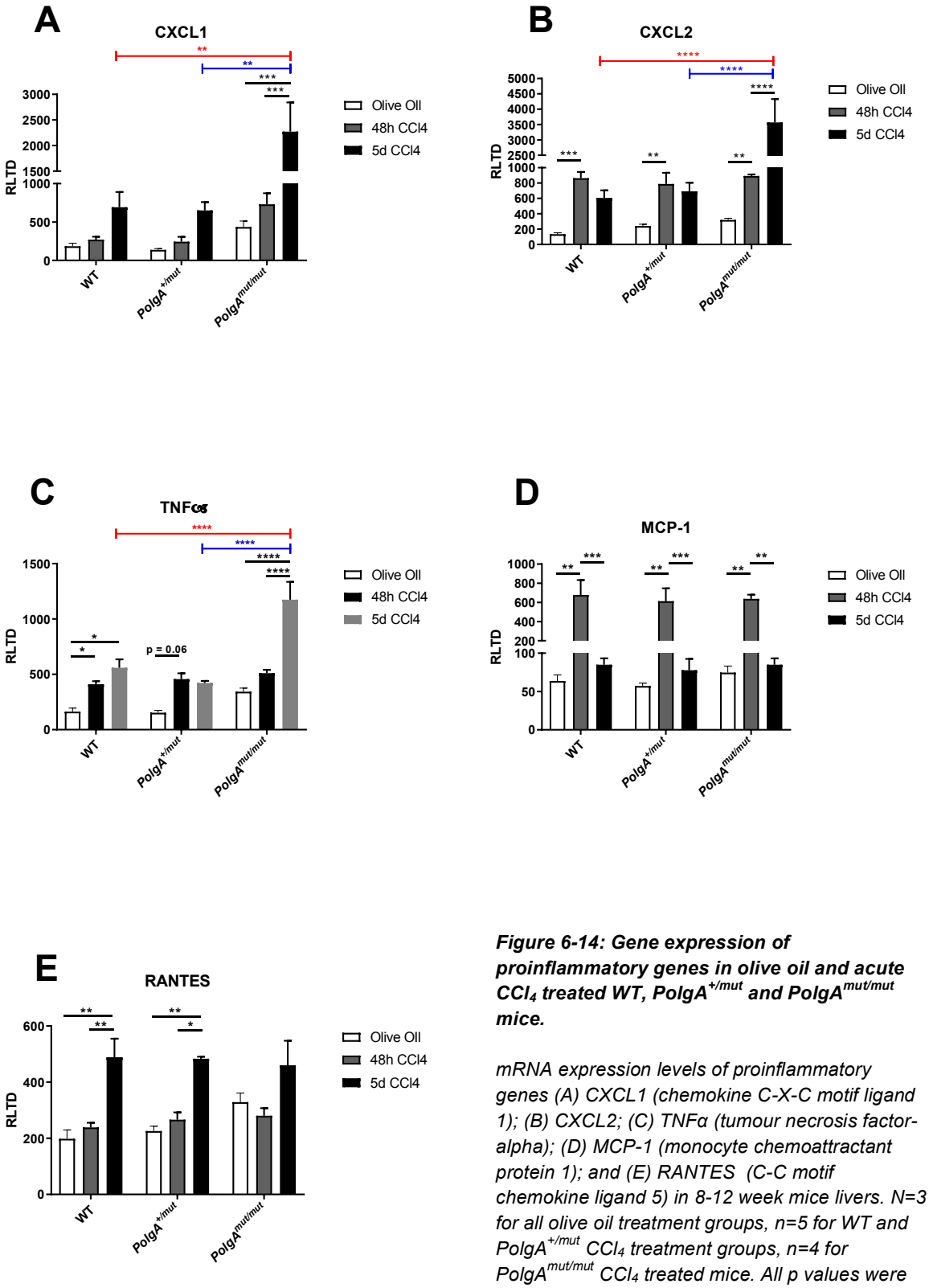

Figure 6-14: Gene expression of proinflammatory genes in olive oil and acute CCl_4 treated WT, PolgA$^{+/mut}$ and PolgA$^{mut/mut}$ mice.

*mRNA expression levels of proinflammatory genes (A) CXCL1 (chemokine C-X-C motif ligand 1); (B) CXCL2; (C) TNFα (tumour necrosis factor-alpha); (D) MCP-1 (monocyte chemoattractant protein 1); and (E) RANTES (C-C motif chemokine ligand 5) in 8-12 week mice livers. N=3 for all olive oil treatment groups, n=5 for WT and PolgA$^{+/mut}$ CCl_4 treatment groups, n=4 for PolgA$^{mut/mut}$ CCl_4 treated mice. All p values were calculated using a two-way ANOVA *p<0.05, **=0.01, *** = 0.005, **** p = 0.001.*

6.6 Fibrogenic activation in *PolgA*$^{mut/mut}$ mice

Liver regeneration and repair encompass highly coordinated and complex wound healing processes that are key to resuming tissue homeostasis following physical stress and toxic injury to the liver parenchyma. Specifically, the term regeneration applies to compensatory hypertrophy and hyperplasia with no lasting damage on tissue morphology, often observed during partial liver resection. Tissues that cannot undergo regeneration undertake repair mechanisms that frequently lead to tissue fibrosis, characterised by ensuing ECM deposition during scar formation (Pinzani and Rombouts, 2004; Pellicoro *et al.*, 2014). Within the liver, fibrosis leads to deposition of non-functional ECM by activated HSCs in place of healthy parenchymal tissue (Pinzani and Rombouts, 2004; Pellicoro *et al.*, 2014). Whether liver regeneration or profibrotic repair mechanisms take place, depend on the burden of injury: larger, chronic and irreparable injuries often lead to fibrosis that can impair organ function whereas acute or smaller injuries result in the return of normal tissue function.

Key to the re-establishment of tissue homeostasis is the complex coordination of haemostatic factors and proinflammatory immune cell recruitment with downstream activation of normally quiescent resident HSCs, cells essential in liver repair processes. Activated in response to proinflammatory cytokines like IL-1 and TGFβ, as well as growth factors such as platelet derived growth factor (PDGF) and connective tissue growth factor (CTGF), activated HSCs or ‘myofibroblasts’ support post-injury cell repopulation *via* the establishment of a temporary organ scaffold, generated by myofibroblastic secretion of ECM (Baiocchini *et al.*, 2016). Once repopulated under normal reparative conditions, myofibroblasts typically undergo removal from the liver by apoptosis; they may also secrete metalloproteinases (MMPs) that break down formed granulation tissue and crosslink collagenous fibres to strengthen any scar tissue permanently deposited (Iredale *et al.*, 1998; Wright *et al.*, 2001). Indeed following acute liver injury, repair processes are transient and result in the rapid resolution of proinflammatory cell signalling and hepatic tissue vasculature to re-establish homeostasis. However, where failure to remove the causal insult exists, such repair processes can become dysregulated, resulting in chronic tissue damage, inflammation, sustained HSC activation and ultimately the imbalance of tissue repair and excess myofibroblast ECM scar formation that contribute to disease pathogenesis. As such, to determine whether the presence of mitochondrial respiratory dysfunction dysregulates hepatocellular regeneration and

repair mechanisms in response to oxidative injury, fibrotic status was assessed in olive oil and acute CCl_4-injured WT, *PolgA*$^{+/mut}$ and *PolgA*$^{mut/mut}$ mice.

6.6.1 Presence of mitochondrial respiratory dysfunction promotes persistent HSC activation following acute CCl_4 oxidative damage

Activation of liver fibroblastic HSCs following injury results in the switching from a normally quiescent, retinoid storing state into an active myofibroblast characterised immunophenotypically by expression of ECM and fibrosis-associated genes such as tissue inhibitor of metalloproteinase (TIMP), α-smooth muscle actin (αSMA) and type I collagens (COL1A1) (Higashi *et al.*, 2017). Following acute oxidative CCl_4 injury, myofibroblast populations in the WT, *PolgA*$^{+/mut}$ and *PolgA*$^{mut/mut}$ livers were visualised with αSMA immunohistochemistry. Corresponding to the induction of parenchymal necrosis by CCl_4, αSMA positive staining showed significantly more activated myofibroblasts at 48 hours post-injury across all genotypes when compared to olive oil controls and 5 day groups (figure 6-15, A, B). Subsequently, levels of CCl_4 activated αSMA-positive myofibroblasts observed reductions in parallel with the resolution of necrotic tissue injury within 5 days post-intoxication, limiting cell positivity solely to endothelial cells lining hepatic blood vessels in WT and *PolgA*$^{+/mut}$ mice. Whereas, αSMA positive cells were significantly increased in 48 hours CCl_4 *PolgA*$^{mut/mut}$ mice compared to olive oil *PolgA*$^{mut/mut}$ and remain elevated at 5 days post-injury. It is therefore plausible to suggest that the presence of mitochondrial respiratory dysfunction further compounds hepatocellular regeneration and repair following oxidative tissue injury *via* persistent profibrotic activity. Where comparisons were made between WT, *PolgA*$^{+/mut}$ and *PolgA*$^{mut/mut}$ mice, observations failed to reach significance. The persistence of αSMA-positive myofibroblasts in *PolgA*$^{mut/mut}$ mice was confirmed by western blot. Figure 6-16 shows constitutive αSMA protein expression in CCl_4 injured *PolgA*$^{mut/mut}$ mice when compared to WT and *PolgA*$^{+/mut}$ controls, indicating sustained myofibroblast activation even after cessation of acute CCl_4 injury.

To therefore test if diminished liver regeneration and repair processes were a result of dysregulated fibrogenic response, mRNA expression of fibrosis-associated genes were measured and the fold change quantified. Expectedly, αSMA gene expression was upregulated across all genotypes at 48 hours as reflected in prior immunohistological staining, with significantly elevated levels in *PolgA*$^{+/mut}$ mice when

compared to other experimental groups (figure 6-17, A). The quantification of αSMA mRNA also revealed αSMA expression to be significantly upregulated in 5-day CCl_4 *PolgA*$^{mut/mut}$ mice when compared to WT and *PolgA*$^{+/mut}$ controls, consistent with the constitutive *PolgA*$^{mut/mut}$ αSMA protein expression seen *via* western blot and IHC. In line with a sustained fibrogenic response in *PolgA*$^{mut/mut}$ mice, mRNA expression of profibrogenic genes COL1A1 and TIMP1 were also elevated in 5 day CCl_4 *PolgA*$^{mut/mut}$ mice compared to WT and *PolgA*$^{+/mut}$ controls (figure 6-17, B-C). By contrast no differences were observed between genotypes for myofibroblast activating factor TGFβ following CCl_4 injury, albeit stimulated expression at 48 hours across all genotypes (6-17, D). Observations of these profibrogenic genes would therefore appear to indicate the persistence of myofibroblastic activation which in turn could hinder parenchymal recovery in response to oxidative stress.

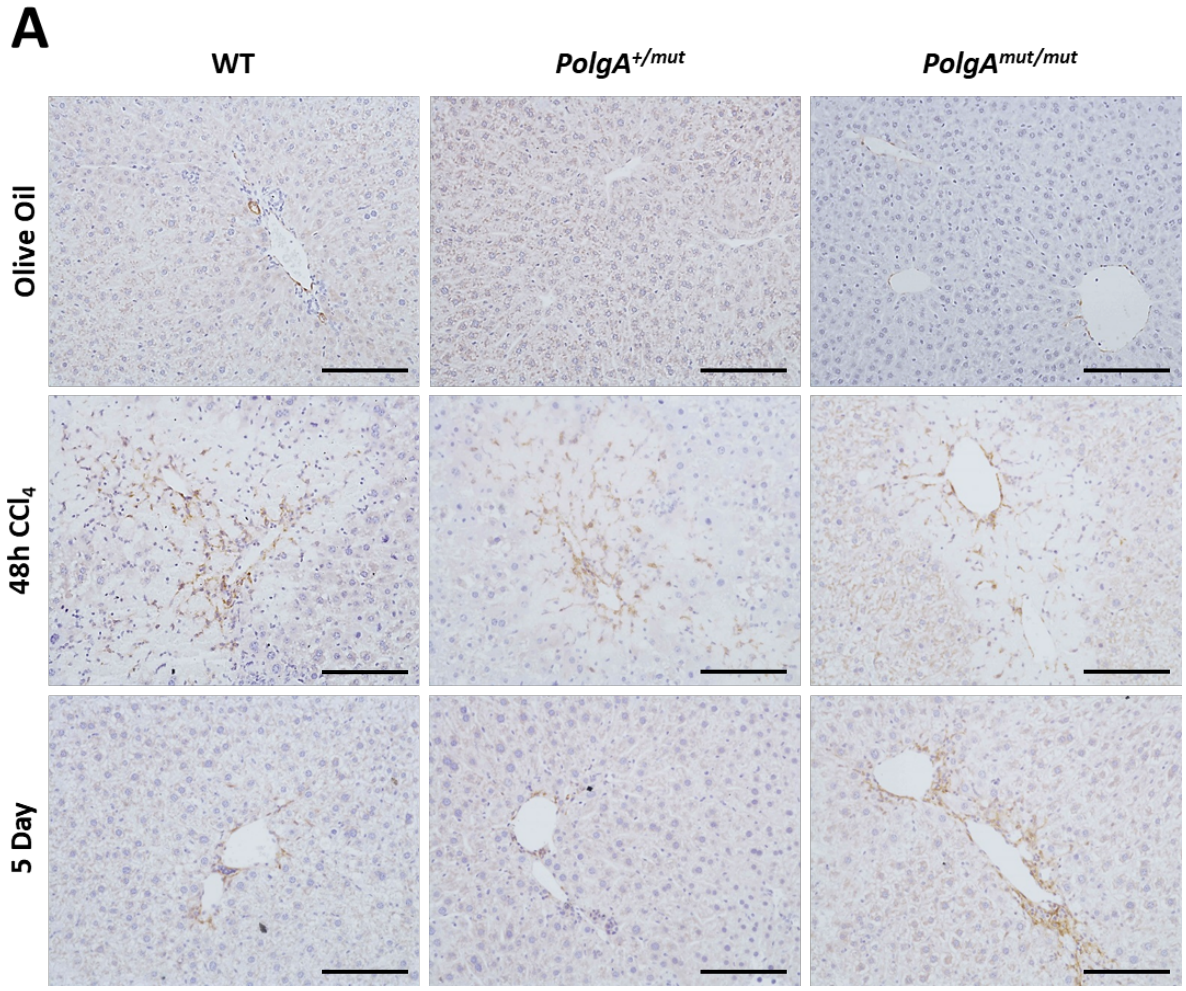

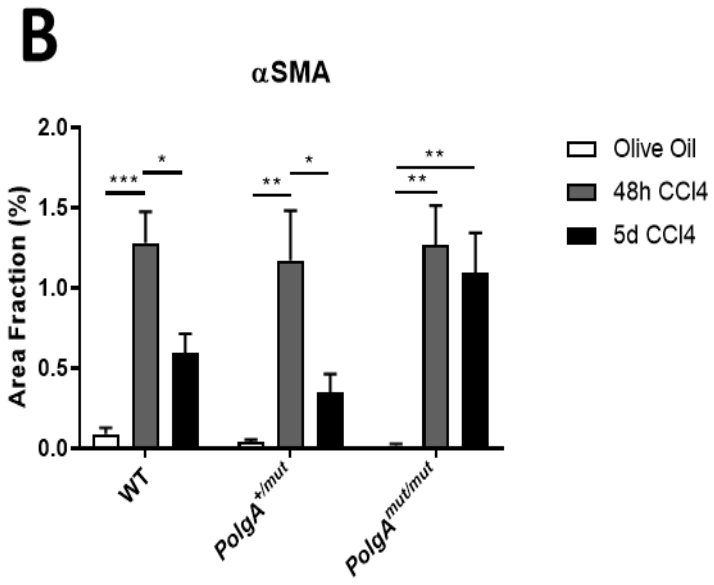

Figure 6-15: αSMA immunohistochemistry in acute CCl_4 administered WT, PolgA$^{+/mut}$ and PolgA$^{mut/mut}$ mice livers.

*(A) Representative photomicrographs of α-smooth muscle actin (αSMA) immunohistochemistry on livers from 8-12 week old male WT, PolgA$^{+/mut}$ and PolgA$^{mut/mut}$ mice. Mice were administered acute dose of CCl_4 at 2 µl/g. Bars 100 µm. (B) Quantification of αSMA positive staining as a percentage of total tissue area at x20 magnification. N=3 for all olive oil treatment groups, n=5 for WT and PolgA$^{+/mut}$ CCl_4 treatment groups, n=4 for PolgA$^{mut/mut}$ CCl_4 treated mice. All p values were calculated using a two-way ANOVA *p<0.05, *** = 0.005, **** p = 0.001.*

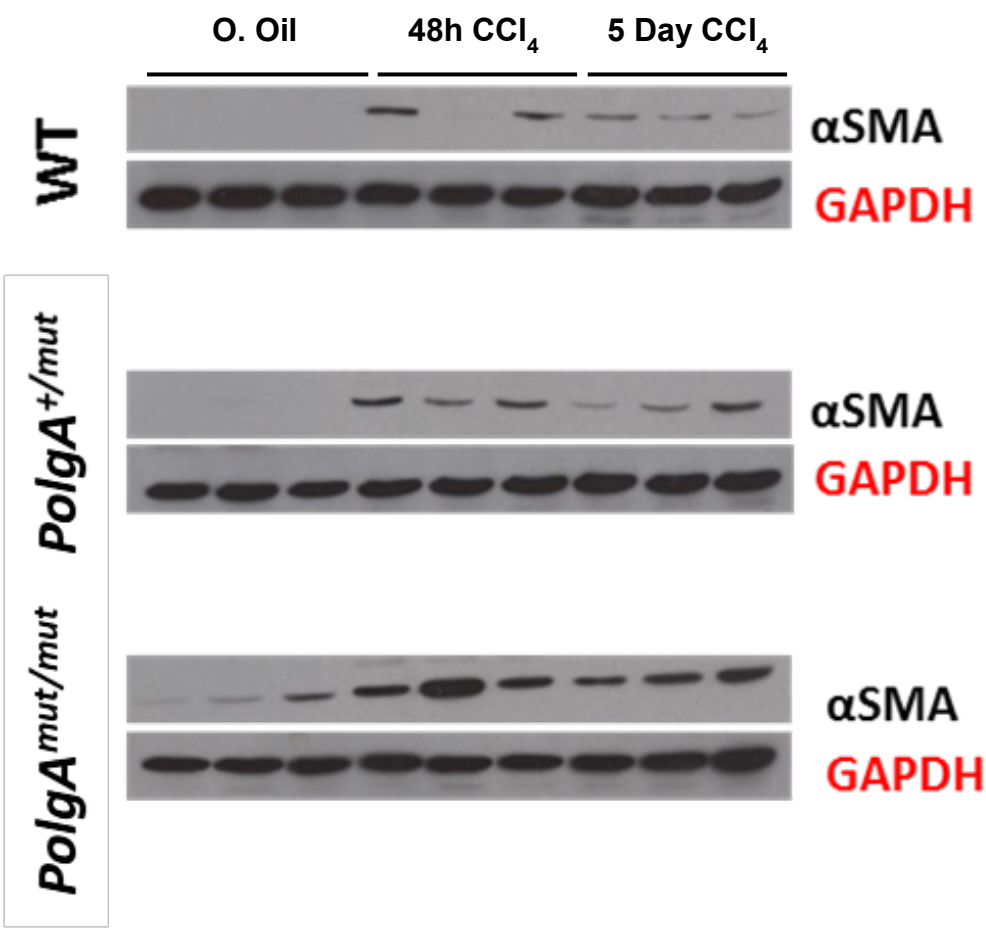

Figure 6-16: α-smooth muscle actin (αSMA) protein expression in livers of olive oil and acute CCl_4 administered WT, PolgA$^{+/mut}$ and PolgA$^{mut/mut}$ mice.

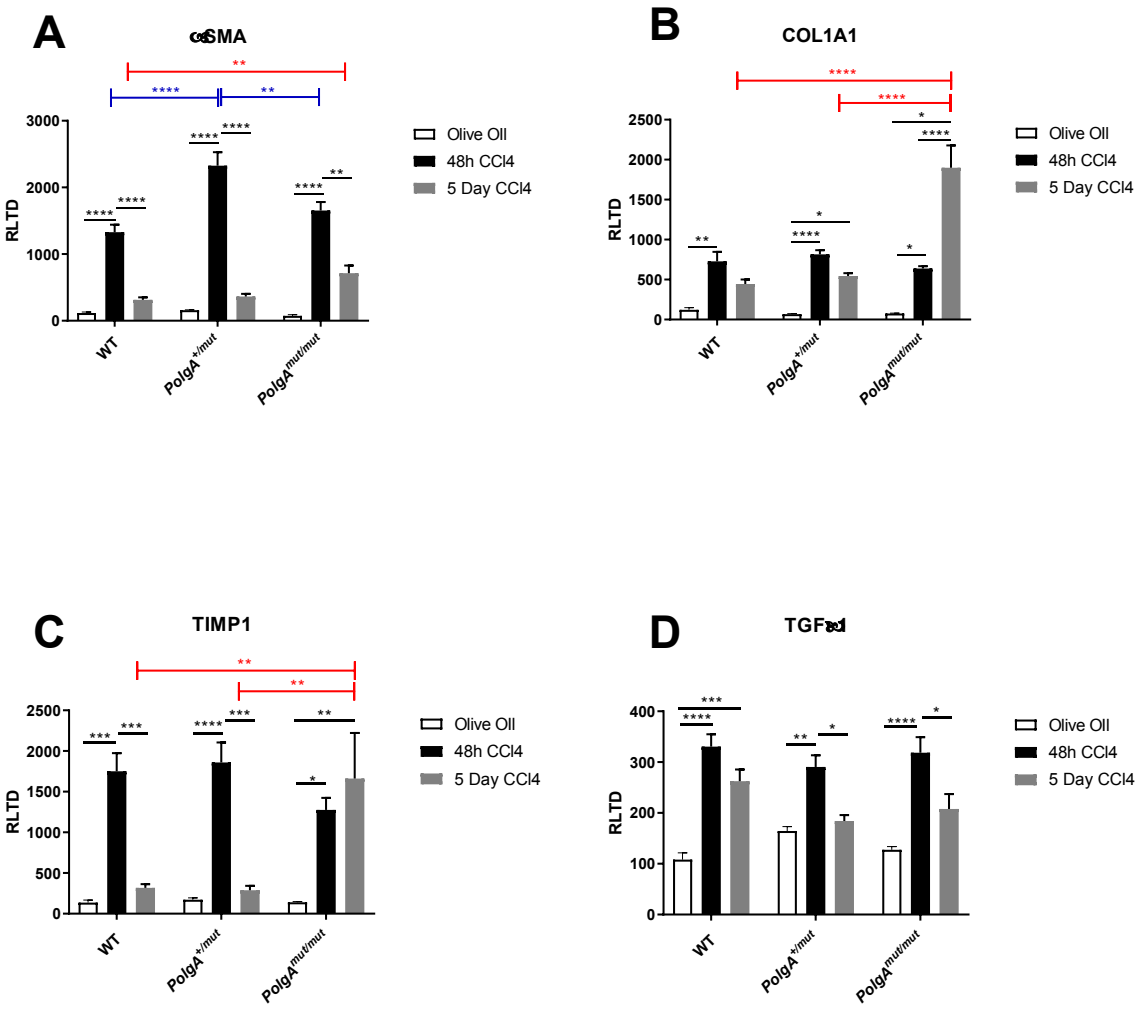

Figure 6-17: Fibrogenic gene expression in livers of olive oil and acute CCl_4 administered WT, PolgA$^{+/mut}$ and PolgA$^{mut/mut}$ mice.

*Quantification of mRNA expression of (A) alpha smooth muscle actin (αSMA); (B) collagen type I alpha chain (COL1A1); (C) tissue inhibitor of metalloproteinase 1 (TIMP1); and (C) tumour growth factor beta (TGFβ) at 48 hour and 5 days following acute CCl_4 administration in WT, PolgA$^{+/mut}$ and PolgA$^{mut/mut}$ mice. N=3 for all olive oil treatment groups, n=5 for WT and PolgA$^{+/mut}$ CCl_4 treatment groups, n=4 for PolgA$^{mut/mut}$ CCl_4 treated mice. All p values calculated using a two-way ANOVA; *p=0.05, **p=0.01, ***p=0.005, ****p=0.001.*

6.6.2 Activation of hepatic stellate cells

Whereas previous results show an inability for *PolgA*$^{mut/mut}$ hepatocytes to survive in culture, no similar defects were observed for isolated HSCs. In similarity to WT controls, transdifferentiation of quiescent HSC into hepatic myofibroblasts ensued around day 3; however, *PolgA*$^{mut/mut}$ HSCs appeared to undergo fibroblastic activation in greater numbers between day 3 and day 7 than in WTs when examined by cell microscopy (figure 6-19). Although this observation is interesting, no conclusive remarks can be generated from simple cell cultures with regards to sustained myofibroblastic activation and persistent fibrogenic activity. To determine whether the profibrogenic phenotype of *PolgA* mice is increased relative to control cells will require further work in isolated HSCs including the biochemical assessment of basal and activated phenotypic characteristics such as expression of fibrogenic genes, secretion of fibrotic ECM and cellular proliferation rates.

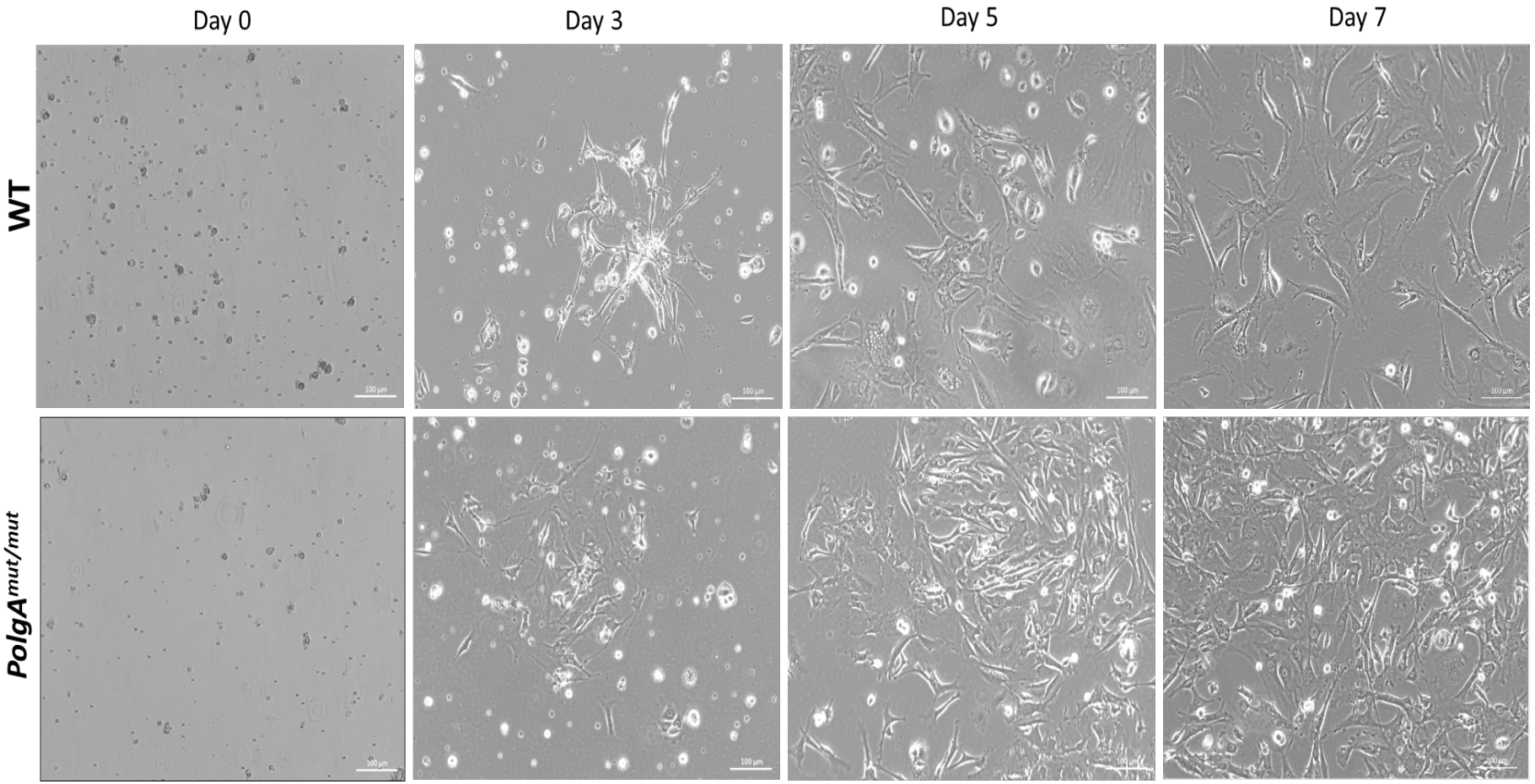

Figure 6-18: In vitro culture micrographs of hepatic stellate cells (HSCs) isolated from WT and PolgA$^{mut/mut}$ mice livers.

6.7 Conclusion

Even at 8-12 weeks of age, *PolgA*$^{mut/mut}$ display alterations to normal mitochondrial function, characterised by deficient COX staining and the decreased expression of complex I NDUFB8 proteins in the absence of any acute CCl_4 insult. Despite absence of any obvious pathologies, previous findings show that 1-3 month old *PolgA*$^{mut/mut}$ mice possess somatic mtDNA mutations 7-11 fold higher than WT and *PolgA*$^{+/mut}$ tissues (Vermulst *et al.*, 2008). Interestingly, when challenged by CCl_4-induced oxidative stress, *PolgA*$^{mut/mut}$ livers were found to harbour greater levels of COX deficiency than 48 hour CCl_4 injured WT and *PolgA*$^{+/mut}$ mice and had a lesser ability to resolve CCl_4-induced respiratory deficiency within 5 days. Such findings could be attributed to *PolgA*$^{mut/mut}$ failure in the upregulation of complex I ND1 gene expression at 48 hours, albeit no differences were observed between genotypes. Rather, induced respiratory deficiency following intoxication did lead to the significant upregulation of mitochondrial genes cytochrome b, COX1, COX3 and ATP6 in 5 day CCl_4 *PolgA*$^{mut/mut}$ mice - perhaps indicative of compensatory mechanisms associated with respiratory complex I deficiency. Indeed in *PolgA*$^{mut/mut}$ livers, inability to significantly upregulate ND1 coincided with failure to constitutively activate NDUFB8 protein expression at 5 days post-CCl_4 intoxication when compared to WTs. Whether this is associated with the observed diminished response in resolving CCl_4-induced tissue injury is unclear, since NDUFB8 was similarly expressed in the 5-day *PolgA*$^{+/mut}$ group as to the *PolgA*$^{mut/mut}$ mice.

Alterations to mitochondrial function also coincided with the significant upregulation of antioxidant gluthathione synthesising enzyme GSS and elevations of SOD1 at 48 hours in *PolgA*$^{mut/mut}$ mice, enzymes understood to be involved in the scavenging of O_2^* and other ROS. In specific, glutathione has been shown to indirectly stabilise redox imbalance following formation of lipid oxy-radicals *via* reduction of ER-associated dehyroascorbic acid (Mehlhorn, 1991; Espinosa-Diez *et al.*, 2015). At 5-day post-CCl_4 SOD1 levels were observed to be decreased in a gene-dose dependent manner in *PolgA*$^{+/mut}$ and significantly so in *PolgA*$^{mut/mut}$ mice. It is therefore plausible that the presence of mitochondrial respiratory dysfunction increases susceptibility to oxidative lipid peroxidation stress, which in turn could further induce mtDNA mutagenesis that drives greater mitochondrial respiratory dysfunction, ROS production and possible tissue damage in a vicious cycle.

Certainly, in *PolgA*$^{+/mut}$ and *PolgA*$^{mut/mut}$ mice, 4HNE expression appears to indicate greater levels of lipid peroxidation, however, whether this is correlated to susceptibility *via* mitochondrial respiratory dysfunction is unclear, since mitochondrial assays conducted were unquantifiable. It would therefore be useful to assess other assays and parameters of mitochondrial function, including mtDNA mutation load and mitochondrial ROS, as well as alternative markers of oxidative damage such as malondialdehyde and 8-OHdG.

In the present study it was hypothesised that CCl_4-induced oxidative stress in *PolgA*$^{+/mut}$ and *PolgA*$^{mut/mut}$ could further compound any hepatocellular recovery secondary to mtDNA oxidative damage. The greater presence of mitochondrial respiratory deficiency coincided with diminished recovery in post-CCl_4 *PolgA*$^{mut/mut}$ mice from necrotic tissue damage and significantly decreased parenchymal regeneration, despite no differences in liver to body weight ratios across genotypes and experimental treatment groups. Whether delay in liver regeneration could be attributed in some part to failure in meeting any energetic demands would require additional experimentation; however, it is possible that findings in *PolgA*$^{mut/mut}$ mice could attribute loss of recovery to P16^{INK4a}-induced cell cycle arrest at G_0/G_1 phase transition, with constitutive expression observed at 48 hours to 5 days post-CCl_4 intoxication. Failure to enter cell cycle at G_1 phase would inevitably limit regenerative response; however, no obvious effects on the majority of cyclin protein expression profiles such as cyclin D1 and E1 were observed across genotypes, albeit persistent expression of cyclin H in olive oil and CCl_4 treated *PolgA*$^{mut/mut}$ mice. To date, little is understood regarding cyclin H in the literature, except its participatory role in cell cycle proliferation *via* its part in the CAK complex. Alternatively, P16^{INK4a} upregulation is also typically associated with cellular senescence, in which previous acute CCl_4 studies show induction of HSC senescence to limit fibrogenic response to acute tissue damage under normal liver repair mechanisms (Krizhanovsky *et al.*, 2008). In the present study, persistent activation of αSMA-positive myofibroblasts in *PolgA*$^{mut/mut}$ livers was accompanied by the significant upregulation of profibrogenic genes αSMA at 48 hours, as well as the ECM-associated genes COL1A1 and TIMP1 at 5 days post-CCl_4 administration, when compared to WT and *PolgA*$^{+/mut}$ mice. It is therefore plausible that the presence of mitochondrial respiratory dysfunction could otherwise diminish hepatocellular recovery *via* sustained lipid peroxidising tissue damage and dysregulated fibrogenic response. To attribute diminished hepatocellular

recovery in the presence of mitochondrial respiratory dysfunction to either the $P16^{INK4a}$-induced inhibition of cell cycle proliferation or chronic liver repair mechanisms would no doubt require additional work; necessitating further assessment of corresponding cyclin dependent kinases (CDKs) and other INK4, Cip/Kip family of cell cycle inhibitors, as well as additional markers of cellular senescence and tissue oxidative tissue damage at both tissue and cellular level.

Failure to fully regenerate and sustained necrotic tissue injury in the presence of mitochondrial respiratory dysfunction appears to be inflammatory driven, with *PolgA*$^{mut/mut}$ mice showing persistent inflammatory cell infiltration and signalling within the liver. Specifically, the continued levels of NIMP positive neutrophils during *PolgA*$^{mut/mut}$ parenchymal regeneration even after 5 days coincided with the upregulated gene expression of proinflammatory cytokines CXCL1, CXCL2 and TNFα, all known to be chemotactic for neutrophils. The prolonged presence of neutrophils in these mice supports growing evidence that persistent inflammation diminishes normal hepatic wound healing and repair processes, ascribed to the promotion of a pro-oxidant environment *via* neutrophil ROS production which in turn further amplifies inflammatory status and diminishes parenchymal recovery (Theilgaard-Monch *et al.*, 2004). It is therefore likely that failure to resolve necrotic tissue injury is linked to inflammatory cell infiltration, although augmented tissue necrosis and increased lipid peroxidation can also incite additional neutrophilic infiltration *via* ROS-mediated processes or complement activation from DAMPs (Marriott *et al.*, 2008; Wera *et al.*, 2016). When assessing whether sustained necrosis in *PolgA*$^{mut/mut}$ livers was a result of greater recipient tissue damage from acute CCl_4 intoxication, no differences in serum AST levels between genotypes were observed - subsequently indicating no differences in the tissue damage received and perhaps indicating that failure to recover from oxidative tissue injury is due to inflammation. Moreover, secondary to this inflammation is stimulation of fibrogenic and proapoptotic responses by proinflammatory cytokines released during post-CCl_4 repair mechanisms - in which cytokine release leads to the activation of HSCs into ECM synthesising myofibroblasts.

Under irreparable tissue damage such as observed failure to clear necrotic liver tissue and upregulated gene expression of the pro-apoptotic signalling protein BAX, functional liver parenchyma is replaced with non-functional scar forming ECM. With

sustained proinflammatory neutrophil infiltration, *PolgA*$^{mut/mut}$ livers also demonstrated dyregulated myofibroblast activation and profibrogenic signalling. Taken together, the observations would appear to suggest that diminished hepatocellular regeneration could be a consequence of dysregulated neutrophil driven profibrogenic wound healing responses. Therefore, determining whether increased presence of mitochondrial respiratory deficiency and the subsequent heightened sensitivity to oxidative tissue damage and ROS production lends itself to altered repair mechanisms would require further work - perhaps including the separate and co-culture cell based assays of neutrophils, hepatocytes and HSCs to determine if cell inherent defects are present. Initial steps have already been taken to show that basally cultured *PolgA*$^{mut/mut}$ HSCs, although smaller, appeared to readily undergo fibroblastic activation in greater numbers than in WT cells. However, these findings remain inconclusive, particularly in the absence of work that determines mitochondrial function, gene and protein complex expression, cell cycle/senescence, inflammatory and ROS signalling as well as fibrogenic responses in these cells both basally and in the presence of acute CCl_4 oxidative stress.

Observations in response to acute CCl_4 oxidative damage in WT, *PolgA*$^{+/mut}$ and *PolgA*$^{mut/mut}$ mice would appear to suggest that in the liver, greater presence of mitochondrial deficiencies appears to reduce ability for the liver to regenerate and could induce further respiratory dysfunction. A key onset effect following CCl_4 intoxication is the reduction in the extent of hepatocellular regeneration that appears following stimulation of profibrogenic tissue repair responses, secondary to dysregulated proinflammatory signalling. Certainly, failure to resolve oxidative injury in the *PolgA*$^{mut/mut}$ liver parenchyma would appear to support a dysfunctional wound healing response, whereby neutrophils recruited to the site are a rich source of ROS and proinflammatory cytokines, which when released into the damaged environment, can activate myofibroblastic activity. Alternatively, where failure to resolve injury results in prolonged wound healing and fibrotic scar formation, fibroblasts may also become senescent and further contribute to disease pathogenesis and the oxidative microenvironment through further ROS production, though this was an avenue not further explored (Campisi, 1996; Krizhanovsky *et al.*, 2008; Kim *et al.*, 2013). Consequently, if allowed more time much further work would be required to discern if the presence of mitochondrial respiratory deficiency affects hepatocellular regeneration post-oxidative injury through dysregulated inflammatory and pro-

apoptotic signalling, including assessing *in vitro* effects of oxidative stress on mitochondria and the mimicking of the oxidative microenvironment during post-CCl_4 injury through methods such as organotypic precision cut tissue slices.

Table 6-1: Chapter 6 summary table. *ND denotes 'no statistical difference'*

	Tissue Injury			Fibrosis						Mitochondrial Function					
	Histo	Serum	Protein	Histo	Protein	Gene			Cells	Histo	Protein		Gene		
	H&E: Necrosis	AST	4HNE	αSMA	αSMA	αSMA	COL1A1	TIMP1	HSCs	COX /SDH	NDUFB8 (CI)	Mt-CO-1 (CIV)	Cytochrome b (CIII)	COX1 (CIV)	ATPB (CV)
WT	↑48h ↓5d	ND	↑48h ↓5d	↑48h ↓72h	↑48h ↓5d	↑48h ↓5d	↑48h	↑48h ↓5d	Normal Activation	Resolution	↑48h ↑5d	ND	ND	ND	ND
PolgA$^{+/mut}$	↑48h ↓5d	ND	↑↑48h ↓5d	↑48h ↓5d	↑48h ↓5d	↑48h ↓5d	↑48h	↑48h ↓5d		Resolution	↑48h ↓5d	ND	ND	ND	ND
PolgA$^{mut/mut}$	↑48h* ↓5d	ND	↑↑↑48h ↓5d	↑48h ↑↑5d vs OO	↑48h & 5d	↑5d vs WT	↑48h ↑↑↑↑5d vs WT & Polg$^{+/mut}$	↑48h ↑↑5d	Premature Activation	↓Resolution	↑48h ↓5d	ND	↑↑5d vs WT & Polg$^{+/mut}$	↑↑5d vs WT & Polg$^{+/mut}$	↑↑5d vs WT & Polg$^{+/mut}$

Table 6-1 continued: Chapter 6 summary table. *ND denotes 'no statistical difference'*

	Antioxidant		Regeneration				Inflammation				Apoptosis	
	Gene		Histo	Protein			Histo	Gene			Gene	
	SOD1	GSS	PCNA	p16	Cyclin A2	Cyclin H	NIMP1	CXCL1	CXCL2	TNFα	Bcl_{xL}	BAX
WT	↑5d	ND	↑48h ↓5d	ND	↑48h ↓5d	↑48h ↓5d	↑48h ↓5d	ND	↑48h	↑48h ↑5d	ND	ND
$PolgA^{+/mut}$	ND	ND	↑48h ↓5d	ND	↑↑48h ↓5d	↑48h ↓5d	↑48h ↓5d	ND	↑48h	ND	ND	ND
$PolgA^{mut/mut}$	↓5d	↑↑48h ↓5d	↓48h vs 48h WT ↓5d	↑5d	↑↑48h ↓5d	↑48h ↑5d	↑48h ↑5d vs OO	↑↑5d vs WT & $Polg^{+/mut}$	↑48h ↑↑↑↑5d vs WT & $Polg^{+/mut}$	↑↑↑↑5d vs WT & $Polg^{+/mut}$	↑↑5d vs OO	↑↑↑↑5d vs WT

6.8 Chapter 6 Key Summary Points

- When challenged by acute CCl_4-induced liver injury, *PolgA*$^{mut/mut}$ mice appear to harbour greater levels of COX deficiency and a lesser ability to resolve induced respiratory deficiency and tissue damage within 5 days. This is likely to be attributed, in some way, to failure in the ability to upregulate complex I gene (ND1) and protein (NDUFB8) expression.

- Alterations in 4HNE protein expression suggest that in the presence of greater respiratory dysfunction, *PolgA*$^{mut/mut}$ mice have greater susceptibility to the lipid peroxidising effects of CCl_4 injury.

- Decreased changes in antioxidant enzyme SOD1 was observed and could also indicate increased lipid peroxidation stress. This in turn could induce more mtDNA mutations, respiratory dysfunction, ROS production and tissue damage.

- Loss of post-CCl_4 tissue recovery in *PolgA*$^{mut/mut}$ mice may also be attributed to halting of cell cycle due to constitutive $P16^{INK4a}$.

- Liver tissue damage and recovery is accompanied by greater profibrogenic signalling in *PolgA*$^{mut/mut}$ mice and leads to stellate cell activation, potentially sustaining acute CCl_4-induced tissue injury.

- Sustained necrotic tissue in Polg$^{mut/mut}$ mice appears to be inflammatory driven as seen by persistent inflammatory NIMP positive neutrophil infiltrations and cytokine signalling in the liver. This may be augmented by lipid peroxidation stress which can incite additional inflammatory cell recruitment.

- Results taken together support dysfunctional wound healing processes in *PolgA*$^{mut/mut}$ mice following acute CCl_4 injury. In a vicious cycle, it is possible that greater lipid peroxidation stress following CCl_4 leads to ROS and recruitment of proinflammatory cytokine-rich neutrophils, which when released promotes profibrogenic myofibroblastic activation and signalling and prolongs wound healing of the liver.

Chapter 7 | Discussion

The link between the inexorable decline of liver homeostasis and increased mitochondrial dysfunction with age is clear. Greater morbidity, mortality and hallmark mitochondrial dysfunction is observed in aged patients for human chronic liver diseases whilst increased mitochondrial DNA (mtDNA) mutagenesis is also recognised to be linked to accelerated ageing. Such observations are yet to be fully elucidated mechanistically as mutually inclusive; however, at a functional level, the liver's demanding roles are widely acknowledged to be supported by the hepatocytes' abundant mitochondria, for example, mitochondria have a functional role in apoptosis, ROS and calcium signalling, glucose metabolism and fatty acid β-oxidation (Grattagliano *et al.*, 2011). It is therefore unsurprising that any molecular changes associated with mitochondrial dysfunction such as loss of mitochondrial membrane potential, reduced transportation of mitochondrial metabolites or changes to oxidative phosphorylation (OXPHOS) can lead to deleterious cellular effects, including, the depletion of ATP production, leakage of reactive oxygen species (ROS) as well as excess lipid storage within the mitochondria (Auger *et al.*, 2015; Salazar-Roa and Malumbres, 2017). Perturbation of mitochondrial function may also be considered an impeding factor: diminishing bioenergetic supply channelled towards compensatory hepatocellular regeneration that often follows hepatic injury and pathogenesis (Salazar-Roa and Malumbres, 2017). As such, mitochondrial dysfunction and mtDNA mutagenesis observed typically with normal organismal ageing, is suggested to lend itself to the development of liver disease such as NAFLD, steatohepatitis, fibrosis and cirrhosis and hepatocellular carcinoma (HCC) due to reduced regenerative capacity of the aged liver (Auger *et al.*, 2015). It was therefore in the present study that the role of mitochondrial dysfunction was examined in the context of ageing liver regeneration.

7.1 Mitochondrial dysfunction appears to reduce hepatocellular turnover and ageing liver regeneration

Liver regeneration is an important hepatocellular process that allows the liver to maintain organ homeostasis, as well as recover cellular mass and function following tissue injury. Regeneration is a highly complex and coordinated process, in which hepatic integrity appears to be maintained through mechanisms involving expansion and differentiation of stem / progenitor cells portions during basal homeostasis, whilst

larger tissue injuries appear to result in the hypertrophy and proliferation of pre-existing hepatocytes with minor input from progenitor cells (Kuwahara *et al.*, 2008; Fellous *et al.*, 2009; Furuyama *et al.*, 2011; Tarlow *et al.*, 2014). Critical to liver regeneration is the tight coordination of cell signalling, that involves the release of tissue growth factors and proinflammatory cytokines by several cell types, such as inflammatory cells. If dysregulated, this can lead to disrupted liver regeneration and even the exacerbation of hepatic tissue injury. The decline of normal liver homeostasis, for example, is widely implicated during the ageing process, enhancing an organism's vulnerability to liver injury and disease. Significantly, models of regeneration utilising partial hepatectomy (PHx) have shown reduced survival in aged subjects, ascribed to lower hepatocyte response to proliferative and cell cycle signalling with age (Huh *et al.*, 2004; Enkhbold *et al.*, 2015).

Underpinning the pathogenesis of age-associated decline in liver homeostasis is the complex interplay of molecular mechanisms that contribute to the ageing process; several common hallmarks acting in concert towards an organism's progressive decline. Amongst them, mitochondrial dysfunction is a potential critical factor for age-associated reduction in hepatic regenerative capacity, with earlier studies showing decline in mtDNA copy and organelle numbers, changes to the mitochondrial ultrastructure and significant reduction in respiratory capacity observed within livers of ageing humans and rodent models (Tauchi and Sato, 1968; Herbener, 1976; Stocco *et al.*, 1977; Stocco and Hutson, 1978; Yen *et al.*, 1989). Meanwhile, in pathologies of the liver, such as non-alcoholic steatohepatitis (NASH) and chronic viral hepatitis infection, increased mitochondrial dysfunction appears to be correlated with disease stage progression (Auger *et al.,* 2015).

Evidence notably reports mitochondrial dysfunction to primarily affect tissues with high energetic demand (Gonzalez-Freire *et al.*, 2015). Within the liver, normal mitochondrial function is critical within the energy intensive process of liver regeneration: playing important roles in the control of respiratory and phosphorylation rates, as well as distinguished responsibilities in mediating functional metabolism and heterogeneity of hepatocytes following PHx (Yang *et al.*, 2004; Ferri *et al.*, 2005). In humans and rodent models, however, clonal expansion of respiratory chain deficient cytochrome c oxidase (COX)-deficient hepatocytes has been observed with growing occurrence (McDonald *et al.*, 2008; Fellous *et al.*, 2009). The increasing presence of

respiratory dysfunction, particularly within replicating cell populations is noted to have an attenuative and proapoptotic outcome on cell proliferation, ascribed in a study to the deleterious effects by age-accumulated mtDNA mutations (Nooteboom *et al.*, 2010). Elucidating the role of mitochondrial dysfunction in tissue ageing is therefore critical in order to identify how age-acquired mtDNA mutations may negatively contribute to liver injury and disease.

The reduction in proliferating cell nuclear antigen (PCNA) markers of regeneration appeared to be associated with mitochondrial dysfunction, with significant increases in mitochondrial COX deficient areas and reduced expression of complex I NDUFB8 concurrent with PCNA marker reductions in 12-month aged *PolgA*$^{mut/mut}$ mice. In line with previous human liver studies, the incidence of increasing mitochondrial defects also occurs during normal murine ageing, with deficiency originating in all mice groups around the periportal area and expanding in the direction of liver's sinusoidal blood flow with age, in support of the 'streaming' hypothesis for hepatocellular turnover (Muller-Hocker *et al.*, 1997; Fellous *et al.*, 2009; Furuyama *et al.*, 2011). Specific to *PolgA*$^{mut/mut}$ mice, defective mitochondrial patches are shown immunohistochemically to be approximately four to eight times larger than patches within age-matched WT controls. The greater occurrence of these deficient areas are likely attributed to the accelerated age-associated accumulation of mtDNA mutations within tissues of aged *PolgA*$^{mut/mut}$ mice, including the liver, that is noted to undelie the model's premature development of ageing (Trifunovic *et al.*, 2004; Kujoth *et al.*, 2005; Vermulst *et al.*, 2007). Taken together, these data suggest that greater levels of mitochondrial dysfunction, including deficiencies of complex I, appear to be a contributing factor in the reduction of basal hepatocellular turnover within older *PolgA*$^{mut/mut}$ mice.

The present study documents for the first time the role of age-acquired mtDNA mutations and resultant mitochondrial dysfunction in active liver regeneration, showing that the increased presence of mitochondrial dysfunction appears to have a deleterious effect on hepatic recovery, including the reduction in PCNA and mitotic body (MB) regenerative observed in both 70% partial hepatectomy (PHx) and CCl_4 oxidative injuries. Focussing on the former, specific failure to recover lost hepatic mass post-PHx was apparent in older *PolgA*$^{mut/mut}$ mice, supported by a reduction in MB and PCNA markers of regeneration. Analyses of regeneration markers, however,

also appeared to show that a certain threshold of mitochondrial dysfunction is required to attenuate post-PHx recovery: despite some reductions in *PolgA*$^{mut/mut}$ MB and PCNA at younger ages. Interestingly, young *PolgA*$^{mut/mut}$ mice have been shown previously to withstand a 500-fold higher mtDNA mutation frequency burden without the onset of ageing features (Vermulst *et al.*, 2007). Therefore at younger ages, enough normal mitochondrial function is likely to remain within *PolgA*$^{mut/mut}$ mice to permit normal liver regeneration. This may be additional aided by the significantly increased expression of cytokine signalling molecule tumour necrosis factor α (TNFα) within *PolgA*$^{mut/mut}$ mice, which even under normal circumstances ensues following PHx. Acting in a compensatory manner, overexpression of TNFα, for example, is noted in one study to induce activation of anti-apoptotic pathways (Kubota *et al.*, 2001).

7.2 Defective liver regeneration due to mitochondrial dysfunction could be associated with cell cycle arrest

There is growing evidence to show that mitochondrial function is intimately linked with cellular proliferation and cell cycle progression (Salazar-Roa and Malumbres, 2017). For example, cyclin D1 is shown to modulate *in vivo* mitochondrial activity during oxidative glycolysis; accumulation of cyclin E is linked with formation of a hyperfused ATP-synthesising mitochondrial network at the G1-S phase transition; whilst inhibition of mitochondrial OXPHOS activity is found to halt cell proliferation *via* cell cycle arrest and apoptosis (Sakamaki *et al.*, 2006; Wang *et al.*, 2006; Srivastava and Panda, 2007; Taguchi *et al.*, 2007; Mitra *et al.*, 2009; Wang *et al.*, 2014). In the present study, a consistent loss of complex I NDUFB8 expression is described within aged *PolgA*$^{mut/mut}$ hepatocytes and during defective *PolgA*$^{mut/mut}$ hepatocellular turnover and regeneration and alludes to a possible critical role for complex I in attenuating liver regeneration. Prior studies by Wang and colleagues (2014), for example, note the inability to phosphorylate complex I subunits and results in the arrest of cell proliferation at the G2/M of the cell cycle, whilst disruption of complex I by genetic ablation or inhibitory means is described to retard cell cycle during G1-S transition (Srivastava and Panda, 2007; Owusu-Ansah *et al.*, 2008; Wang *et al.*, 2014). Therefore, our results suggest that mitochondrial dysfunction arises primarily from complex I deficiency in *PolgA*$^{mut/mut}$ mice and could have a mechanistic role in preventing normal liver regeneration *via* cell cycle arrest within these mice. The present data is unable to conclude, however, the role of complex IV COX deficiency

in the observed *PolgA*$^{mut/mut}$ phenotype due to inconsistent protein detection despite histological COX-negative detection.

An additional supporting explanation for mitochondrial deficiency-mediated cell cycle arrest is the expression of p16^{INK4A} and cyclin H (figure 6-11) during CCl_4 oxidative injury that coincides with failure to resolve necrotic tissue injury within PolgA$^{mut/mut}$ mice. Specifically, p16^{INK4A} is understood to inhibit the cyclin D1/ cyclin dependent kinase (CDK) 4/6 complex that prevents phosphorylation of the retinoblastoma (Rb) protein, resulting in the blockage of G1-S phase transition during cell cycle (Bruce *et al.*, 2000). However, inability to detect differences in cyclin D1 expression makes it unlikely for p16^{INK4A}-induced arrest to be mediated in this manner: P16^{INK4A} is noted alternatively in one study to associate with the RNA polymerase II C-terminal domain (CTD) and general transcription factor TFIIH, of which cyclin H forms a subunit, to regulate gene transcription during cell cycle at G1 phase (Serizawa, 1998). Therefore, since constitutive expression of cyclin H was observed in the present study in *Polg*$^{mut/mut}$ whole livers, failure to recover from oxidative hepatic stress could be ascribed to cell cycle arrest at G1-S phase transition *via* P16^{INKA}-mediated inhibition of CTD phosphorylation by TFIIH. In order to definitively assess whether a p16^{INK4A}-cyclin H mechanism plays a cell cycle arresting role during liver ageing and hepatocellular regeneration, measurements of cyclin protein expression would be consequently extended to hepatectomised and basally ageing models used within the present study. Moreover, since little difference in expression was observed between checkpoint cyclins following CCl_4 injury, a future possibility would be to alternatively determine expression levels of cyclin kinases like CDK4/6 and other cyclin-dependent kinase inhibitors (CKIs) including p21 and p27 of the CIP/KIP family.

In addition, to determine if induction of hepatocyte cell cycle arrest arises from increased mitochondrial complex I respiratory deficiency, a natural progression would be to measure these cell cycle proteins in WT, *PolgA*$^{+/mut}$ and *PolgA*$^{mut/mut}$ hepatocytes. Difficulty in establishing and maintaining *PolgA*$^{mut/mut}$ hepatocyte cell viability was experienced in the present study and consequently was not an avenue further explored. Future possibilities could include measuring these parameters in hepatocyte model involving pharmacological inhibition or siRNA knock-down of

complex I in WT hepatocytes, as previously demonstrated (Fato *et al.*, 2009; He *et al.*, 2013).

7.3 Mitochondrial dysfunction is an inducer of apoptosis

Mitochondria are widely acknowledged to regulate apoptosis, with alterations to typical mitochondrial function and dynamics noted to accompany the release of signalling factors during activated pathways of cell death (Otera and Mihara, 2012). Complex I has been specifically identified as an important substrate for caspase 3, in which p75 nicotinamide adenine dinucleotide (NADH) dehydrogenase (ubiquinone Fe-S protein I) complex I subunit is cleaved and complex I inhibited, resulting in the collapse of the mitochondrial transmembrane potential ($\Delta\Psi_{M}$) and increase in reactive oxygen species (ROS) production (Ricci *et al.*, 2004). Chemical inhibition of complex I by rotenone is also understood to produce a similar response (Li *et al.*, 2003). Therefore, in response to deficiency of complex I with age, *PolgA*$^{mut/mut}$ mice may exhibit a similar phenotype that results in the downstream activation of apoptotic signalling. Immunohistological analyses of caspase-3 within basally aged tissues indeed demonstrates increasingly elevated levels of hepatocyte apoptosis correlate with age-associated increases in mitochondrial dysfunction. These data are supported by mRNA gene expression in favour of pro-apoptotic signalling activation in basally aged *PolgA*$^{mut/mut}$ mice (figure 4-1; figure 4-11). As such, these findings appear to reaffirm the well-established relationship between mitochondrial function and apoptosis, whilst suggesting a more detailed role for complex I deficiency within the activation of apoptotic cell death.

Enhanced apoptosis is shown to delay liver regeneration (Yamada *et al.*, 1998; Kovalovich *et al.*, 2000; López-Fontal *et al.*, 2010). Therefore, mitochondrial deficiency-induced cell death may be a critical driver in reduced *PolgA*$^{+/mut}$ *and* *Polg*$^{mut/mut}$ liver regeneration where hepatocellular proliferation is attenuated; the regulation of intrinsic mitochondrially mediated apoptosis carefully balanced by BCL-2 protein family members – namely by anti-apoptotic BCL-2 and proapoptotic BAX proteins (Dai *et al.*, 2018). BCL-2 and pro-apoptotic BCL_{XL} are noted in the early priming phase of hepatic recovery to increase in expression levels and inhibit proapoptotic cytochrome *c* release: changes that are somewhat reflected in trends within the present study during the recovery period that follows CCl_4 oxidative injury (Fausto, 2000; Su *et al.*, 2002; Jiang *et al.*, 2004; Chung *et al.*, 2005). Whilst, Bax

signalling induces apoptosis through insertion into the mitochondrial outer membrane to mediate the release of apoptotic factors. Gene expression analyses of 5-day CCl_4 injected *PolgA*$^{mut/mut}$ mice reveals a 500-fold increase in BAX (figure 6-12), as well as enhanced levels with normal *PolgA*$^{mut/mut}$ ageing that is concurrent with significant increases in caspase-3 positive hepatocytes. Together these data suggest biological skewing of apoptotic signalling with age-accumulated mitochondrial dysfunction, in favour of cell death. In agreement, significant increases in the BAX/BCL-2 ratio and expression of cleaved caspase-3 has been shown to be an indicator for the initiation of apoptosis (Dai *et al.*, 2018).

It is likely that accumulation of mitochondrial respiratory chain dysfunction with age is a critical contributor in the activation of pro-apoptotic signalling. However, unfortunately due to the time limitations of the study, were unable to extend direct measurements of apoptotic gene expression to PHx in WT and *PolgA* mice. However, the prediction would be that the effect of mitochondrial dysfunction in *PolgA* mice would result in exacerbated pro-apoptotic signalling due tto significant tumour growth factor beta (TGFβ1) upregulation post-PHx. TGFβ1 is widely understood to exert anti-proliferative effects under normal conditions *via* the induction of apoptosis to correct excess parenchymal recovery (Sakamoto *et al.*, 1999). It is therefore possible that failure to recover lost cellular mass in 6-month *PolgA*$^{mut/mut}$ mice may be alluded to the induction of apoptosis. In the post-PHx setting, 6 month TNFα expression was also downregulated, minimising its known effect on preventing apoptotic signalling (Takehara *et al.*, 1998; Flusberg and Sorger, 2015).

Apoptosis is one of several outcomes that can follow cell cycle arrest, in which previous literature frequently establishes transcription factor p53 activity to be a critical decider of cell fate (Hafner *et al.*, 2019). The expression of pro-apoptotic BCL-2 and BAX genes, in particular, are understood to be under transcriptional control of p53; in which both are demonstrated here to be significantly upregulated in basally aged and CCl_4-injured *PolgA*$^{mut/mut}$ mice. Evidence suggests that the levels of p53 are correlated with the induction of apoptosis: higher levels resulting in activation of apoptotic processes, whilst cell cycle arrest is induced at lower concentrations – despite inconsistencies between the onset of apoptosis, p53 levels and apoptotic gene promoter binding (Chen *et al.*, 1996; Kapoor and Lozano, 1998; Appella and Anderson, 2001; Lavin and Gueven, 2006). Alternatively, p53-regulated cell fate is

proposed to be mediated through repressive functions: cyclin B1 for example is repressed following partial binding of p53 dimers to promoter CCBN1's head-to-tail element (Lipski *et al.*, 2012).

Despite this critical role, p53 activity was not assayed in the present study, and if allowed more time would be assessed to determine a possible mechanistic link between mitochondrial respiratory dysfunction and the induction of apoptosis, as apparent within ageing *PolgA*$^{mut/mut}$ mice and *PolgA*$^{mut/mut}$ liver regeneration. Conversely the p16^{INK4A} signalling pathway is understood to play an overlapping role with p53 in cell cycle arrest, with initial emerging data showing p16^{INK4a} to negatively regulate p53 through prevention of MDM2-mediated degradation of p53 (Al-Khalaf and Aboussekhra, 2018). More notably P14^{ARF}, also encoded by the same CDKN2A gene, is well established in the disruption between inhibitory MDM2 and its substrate p53 (Zhang *et al.*, 1998; Vivo *et al.*, 2015). Inhibition results in transcriptionally active p53 accumulation, able to direct cell fate towards either arrest or apoptosis. Taken together, our results could indicate that constitutive expression of p16^{INK4a} in *PolgA*$^{mut/mut}$ mice, as seen following CCl_4 intoxication, may lead to cross-talk inhibition of MDM2, resulting in p53-mediated apoptosis. Confirmation of such a hypothesis thereby requiring measurements of p53 expression.

7.3.1 Apoptosis could be additionally stimulated by increased ROS which together drives reduced liver regeneration in ageing *PolgA*$^{mut/mut}$ mice

Excess ROS production is hypothesised to be a major contributing factor to the ageing process, ascribed to the cumulative effect of increased oxidative tissue injury (Harman, 1972; Lopez-Otin *et al.*, 2013). Through Harman's well-established Theory of Ageing, age-associated biological decline is understood to arise from oxidative free radical reactions by reactive oxygen species (ROS), formed from the leakage of electrons from the mitochondrial respiratory electron transport chain (ETC) (Harman, 1972). In progeroid *PolgA*$^{mut/mut}$ mice, earlier studies demonstrate a lack of oxidative tissue damage despite presence of mitochondrial respiratory dysfunction; however, more recent methodologies involving *in vivo* ROS measurements of redox signalling molecule H_2O_2 (hydrogen peroxide) appears to coincide with abnormal activation of pro-apoptotic and pro-inflammatory signalling pathways (Logan *et al.*, 2014). An observation seemingly consistent with reductions in anti-oxidant genes glutathione synthetase (GSS) and glutathione peroxidase (GPx) and increases in mitochondrial

ROS scavenger superoxide dismutase 2 (SOD2) and peroxisome proliferator activated receptor gamma coactivator 1 alpha (PGC1α), that is concurrent with increased cell death observed within *PolgA*$^{mut/mut}$ primary hepatocytes and ageing livers (St-Pierre *et al.*, 2003; Valle *et al.*, 2005; St-Pierre *et al.*, 2006). In line with this, deficiency of oxidant-catalysing enzymes GPx and GSS are understood to increase ROS-induced oxidative stress, whilst ablation of SOD2 in homozygous and heterozygous mice exhibit reduced mitochondrial respiration and heightened sensitivity to apoptosis, due to increased predilection of MPTP (mitochondrial permeability transition pore) transition in response to superoxide (O_2^*) species (Kokoszka *et al.*, 2001; Espinosa-Diez *et al.*, 2015). Indeed, depolarisation of the mitochondrial membrane leads to uncoupling of the respiratory chain, mitochondrial swelling and rupture, and ultimately, release of apoptosis-inducing factors such as cytochrome *c*, endonuclease G and apoptosis inducing factor (AIF) (Low, 2003; Alexandris *et al.*, 2004; Wang and Youle, 2009). Taken together, results in the present study could therefore similarly indicate abnormal activation of a ROS-apoptotic pathway in *PolgA*$^{mut/mut}$ mice, as seen by Logan and colleagues (2014), ultimately contributing to the observable reduction in basal hepatocellular turnover seen with age.

Oxidant homeostasis plays a critical protective role within the liver against oxidative stress: particularly given the organ's normal physiological exposure to a variety of endogenous and environmental stressors. Hepatocytes protect the liver from harmful oxidants, including ROS, predominantly through capacity to produce anti-oxidant glutathione (GSH), which undergoes reductive and oxidative redox reactions catalysed GPx and glutathione disulphide (GSSG) respectively to achieve anti-oxidant function (Lu, 2009). Alterations to GSH homeostasis can result in oxidative damage, of which hepato-pathophysiological changes can occur: such as hepatic steatosis, hepatic inflammation leading to fibrosis, and liver failure due to dysregulation of lipid metabolism, inflammatory and apoptotic pathways respectively (Mansouri *et al.*, 2018). Such changes may also manifest into disease including non-alcoholic fatty liver disease (NASH), alcoholic and drug-induced liver diseases. Prior studies show that active liver regeneration influences the oxidative state within the normal and pathological liver (Huang *et al.*, 1998; Alexandris *et al.*, 2004; Yang *et al.*, 2004). GSH is noted to immediately decrease following surgical PHx and oxidative CCl_4 injury, with decreased levels recovering soon thereafter (Nishida *et al.*,

1996; Huang *et al.*, 1998). Such findings appear consistent with the present PHx study, in which glutathione synthesising enzyme, glutathione synthetase (GSS), decreases in 6-month *PolgA* mice in the periods following injury. These levels, however, fail to recover post-injury - indicating a possibility for the presence of mitochondrial dysfunction to have a deleterious role in GSH production.

Of particular interest, is the noted reduced ability to produce GSH in disorders that affect mitochondrial respiratory function, which may explain limited detection of GSS in partial hepatectomised 3-month *PolgA*$^{mut/mut}$ mice (Atkuri *et al.*, 2009). Yet in 6-month T0 livers, GSS is significantly raised compared to WT T0 controls. It is therefore plausible that in *PolgA*$^{mut/mut}$ mice, the accumulation of mitochondrial dysfunction with age results in greater oxidative stress from generated ROS and likely lends itself minimisation of oxidant tissue damage *via* GSS-mediated GSH synthesis. This could be additionally supported by increases in ROS scavenger SOD1 post-PHx which increases in 6-month *PolgA*$^{mut/mut}$ mice, whilst such claims may be further substantiated by analyses of liver regeneration following oxidative stress, in which CCl_4 oxidative injury significantly induces GSS production. Given the additive level of oxidative stress to this model, it is therefore possible that defence mechanisms of *PolgA*$^{mut/mut}$ mice in response to greater levels of ROS requires a threshold of oxidative injury to stimulate antioxidant processes, that include GSH production.

The present data does not confirm whether dysfunctional mitochondria are a source of endogenous ROS nor directly results in observable age-associated oxidative tissue damage in *PolgA* mice. Regrettably neither *in vivo* ROS concentrations nor direct measures of oxidative tissue damage, such as malonadialdehyde (MDA), 4HNE (4-hydroxy-2-nonenal) and 8-OHdG (8-hydroxy-2-deoxyguanosine), were further investigated in *PolgA* mice, but if allowed more time would be undertaken. Indirect measures of COX negative areas, however, imply greater mitochondrial dysfunction and abnormal release of electrons at 12 months of age, as inferred biochemically by the reduction of electron acceptor nitroblue tetrazolium (NBT) in the absence of complex I NDUFB8 expression (Ross, 2011). This could therefore support a role within PolgA$^{mut/mut}$ mice for mitochondrially-produced ROS in the abnormal stimulation of apoptotic signalling, that in turn reduces hepatocellular turnover. Such claims for activation of ROS-induced apoptosis in the presence of

increased mitochondrial dysfunction is the concurrent alterations of anti-oxidant and pro-apoptotic markers alongside harboured levels of COX deficiency and reduced complex I expression in PHx and CCl_4-injured *PolgA*$^{mut/mut}$ mice. Given the reduced ability of these models to recover lost cellular mass and normal tissue physiology respectively, the data suggests that the presence of mitochondrial dysfunction in *PolgA*$^{mut/mut}$ mice results increased ROS production, which in turn leads to activation of apoptotic signalling and reduced hepatoregenerative capacity following injury.

7.4 Mitochondrial ROS plays a critical role in proinflammatory and apoptotic signalling in ageing liver regeneration

Whilst accelerated *PolgA*$^{mut/mut}$ ageing is presently suggested to increase oxidative stress and ROS-mediated stimulation of apoptosis, a further explanation could be attributed to the additional activation of pro-inflammatory signalling. Certainly, apoptosis and inflammation are widely understood to be intricately linked, and in Logan's study (2014) age-associated increases in ROS in *PolgA*$^{mut/mut}$ mice was shown to induce elevated serum cytokine levels concurrent with activation of pro-apoptotic pathways. A finding that corroborated data in aged *Polg*$^{mut/mut}$ mice in the present study, where both elevations of serum cytokines and mRNA expression of inflammatory genes are observed in conjunction with alterations in anti-oxidant gene expression and markers of cell death.

ROS are acknowledged to exert their effects across of plethora of pro-inflammatory signalling modules including the NLRP3 (nod-like receptor family pyrin domain containing 3) inflammasome and the redox-sensitive transcription factor nuclear factor κB (NF-κB), both of which are also known to partake in the regulation of cell death (Morgan and Liu, 2011; Abais *et al.*, 2015). In both systems H_2O_2, as well as other ROS such as peroxynitrite (ONOO-) that are likely to arise from age-associated mitochondrial electron leakage, are well documented to be inducing factors of these signalling modules (Bai *et al.*, 2015). The NLRP3 inflammasome has been shown, for example, to be activated by mitochondrial ROS during ETC complex I and III disruption, and able to translocate to the mitochondria on ROS-induced stimulation (Bulua *et al.*, 2011; Zhou *et al.*, 2011; Abais *et al.*, 2015). Activation occurs in a two-step signalling mechanism that ultimately converges on the NF-κB-dependent maturation of cytokine interleukin-1β (IL-1β) and the proteolytic cleavage of pro-apoptotic procaspase-1, yet inconsistently no increases to serum IL-1β were

observed (Abais *et al.*, 2015). On this basis, NLRP3 involvement could be lacking in the suggested ROS-apoptotic proinflammatory axis; however, it is important to note that inability to serologically detect changes could be ascribed to IL-1β's short half-life (Kudo *et al.*, 1990). Therefore to fully exclude its involvement, additional quantification of IL-1β and indicators of NLRP3 signalling may therefore be required: including IL-1β mRNA expression, as well as protein-level or histological detection of caspase-1 functions.

On the other hand, NF-κB is shown previously to undergo a series of direct and indirect H_2O_2-induced phosphorylative modifications that help present NF-κB as a redox-sensitive factor: most likely involved in serving activation of both pro-inflammatory and apoptotic pathways within this study (Schoonbroodt and Piette, 2000; Takada *et al.*, 2003). Apoptotic signalling is particularly understood to arise from NF- κB's mediatory role in transcribing a number of pro-apoptotic inflammatory cytokines, including TNFα and IL-6 (Hayden and Ghosh, 2014). Both cytokines are noted in the present *PolgA*$^{mut/mut}$ study to show increases basally and in response to CCl_4-induced liver regeneration both serologically and at a gene expression level (figure 4-16, 6-15), therefore proposing a possible role for NF-κB signalling in the activation of the apoptotic-proinflammatory pathway axis as suggested within the presence of *PolgA*-induced mitochondrial dysfunction (Logan *et al.*, 2014).

As well as regulating inflammatory pathways, there is a clear link between NF-κB and the potentiating role it plays in anti-oxidant activity (Morgan and Liu, 2011). Targets include a diverse array of anti-oxidant proteins, including targeting of the SOD2 promoter binding site by translocated p50 and p65 NF-κB subunits following TNFα stimulation, as well as the presence of NF-κB binding sites in SOD1 (Jones *et al.*, 1997; Maehara *et al.*, 2000; Morgan and Liu, 2011). Whilst NF-κB remains to be further investigated, in this context it is possible to suggest that induction of proinflammatory cytokines TNFα and IL-6, stimulates anti-oxidant gene transcription. SOD2 appears to show trends of increasing expression with age concurrent with significantly increased serological levels and expression of proinflammatory cytokines within 12-month *PolgA*$^{mut/mut}$ mice. Such rises in anti-oxidants are likely an attempt to minimise effects of inflammation and pro-apoptotic oxidative stress due to increased ROS during mitochondrial dysfunction. Certainly this is plausible with ablation and knockdown of SOD2, for example, having been shown previously to increase cellular

sensitivity to apoptotic signalling, as well as induce inflammation in response to oxidative stress (Ishihara *et al.*, 2015).

By contrast, similarities were not observed in response to liver injury, with variety in the correlation between inflammatory and anti-oxidant signalling likely to arise from complex regulatory molecular mechanisms that control these pathways (Hayden and Ghosh, 2014). Notably TNFα is a key regulator of NF-κB *via* inhibitor of kappa-B (IκB), in which expression terminates NF-κB, as well as TNF-dependent responses (Brown *et al.*, 1993; de Martin *et al.*, 1993; Sun *et al.*, 1993; Klement *et al.*, 1996). It is therefore possible that during CCl_4 injury, the inability to detect changes in SOD2 may be ascribed to the *PolgA*$^{mut/mut}$ mice having a ~2.3 fold increase in TNFα, in the period following intoxication. Significantly increased TNFα expression could, in turn, provide a negative feedback loop which represses NF-κB-induced SOD2 expression. Conversely within partial hepatectomised mice, changes in SOD1 appeared to oppositely mirror elevations in TNFα. These expression patterns may be alluded to the previously reviewed poor response of the SOD1 promoter NF-κB binding site to external stimuli; however, could also result from the antagonising regulatory effect of SOD1 upon TNFα expression (Afonso *et al.*, 2006; Dimayuga *et al.*, 2007; Miao and St Clair, 2009). Nonetheless, the present analyses highlights a relationship between the activation of inflammatory pathways and the induction of apoptosis and anti-oxidant signalling, ascribed to the abnormal release of ROS during age-accumulated mitochondrial respiratory dysfunction.

7.5 Mitochondrial respiratory dysfunction and oxidative stress play key roles in the activation of liver cell senescence

Biologically, mitochondria play a number of key tightly regulated roles across a plethora of cellular processes that include cell cycle regulation, apoptosis, and energy production *via* ATP biosynthesis (Nunnari and Suomalainen, 2012). Alterations to normal function unsurprisingly results in pathophysiological manifestations, including abnormal activation of ROS signalling, cell death and inflammatory pathways as alluded above, as well as the development of disease and organismal age-associated decline (Nunnari and Suomalainen, 2012).

Amongst other findings, cumulative evidence shows that mitochondrial dysfunction can induce cellular senescence, one of several key hallmarks of ageing

characterised by incessant cell cycle arrest and a biological programme of changes including increased β-galactosidase activity and chronic low-grade inflammation (Lopez-Armada *et al.*, 2013; Chapman *et al.*, 2019). Thought to be a mechanistic pathway evolved to evade cellular replication in the presence of DNA damage, senescent cells feature mitochondrial alterations: including increases in mitochondrial mass and hyperfusion, decreased membrane potential and the resultant increase in ROS production and proton leakage (Passos *et al.*, 2007; Moiseeva *et al.*, 2009; Passos *et al.*, 2010). Moreover, the selective removal of dysfunctional mitochondria from senescent cells was shown to ameliorate the senescent phenotype (Correia-Melo *et al.*, 2016). To this end, analyses of the present data could suggest a mediatory role for mitochondrial dysfunction in ageing liver regeneration - *via* activation of hepatocyte senescent cell cycle arrest.

An induction of cellular senescence may be subsequently ascribed to its onset in response to oxidative stress, in which earlier steps undertaken to minimise mitochondrial ROS species are shown to delay oxidative DNA damage-induced cellular senescence and increase replicative lifespan (Packer and Fuehr, 1977; Chen *et al.*, 1995). Increased SOD2 gene expression, concurrent with reductions in hepatoproliferative markers within basally 12-month aged *PolgA*$^{mut/mut}$ mice could likely be a consequence of senescent cell cycle arrest due to exacerbated ROS production due to age-accumulated mtDNA mutations. In this context, excessive pro-oxidants from mitochondrial dysfunction may be a contributory factor as a combination of increased production and the inability to scavenge these eletron transport chain (ETC) by-products: both of which are features observed elsewhere (Passos *et al.*, 2007). The confirmation of senescent induction would however require further investigation of cell cycle mediators to confirm arrest, involving the profiling of proteins like cell cyclins, CDKs and cell cycle regulatory factors such as p16, p21 and p53.

Further establishment of ROS involvement in senescence also suggests a capacity for oxidant signalling in potentiating downstream senescent effector pathways *via* stabilisation of induced cell cycle arrest. Supporting this is the prominent feature of ROS generation following activation of senescence-associated pathways that include p16, p21 and p53 cell cycle mediators (Macip *et al.*, 2002; Macip *et al.*, 2003; Takahashi *et al.*, 2006). Whilst there is considerable overlap between these

pathways, constitutive expression of arresting $p16^{INK4A}$ was noted alongside reduced post-CCl_4 hepatic regeneration in *PolgA*$^{mut/mut}$ mice. The acutely damaging hepatotoxin which allows for clear pathophysiological liver necrosis following cytochrome P450-mediated metabolism into lipid reactive radicals, as well as induce dysfunctional changes within hepatocyte mitochondria, appeared to have changes in line with typical findings. These include histological necrosis, inflammation and increased expression of lipid peroxidation 4HNE and cytochrome CYP2E1 markers at 48 hours post-CCl_4 intoxication (Knockaert *et al.*, 2011). However, unlike PHx and basally aged *Polg*$^{mut/mut}$ mice, alterations in superoxide dismutase (SOD) levels did not accompany putative $p16^{INK4A}$-cyclin H cell cycle arrest, as perhaps alluded to the abovementioned repression of SOD2 gene expression by increased TNFα. Despite this, CCl_4 intoxication did show significantly greater GSS expression at 48 hours within *PolgA*$^{mut/mut}$ mice, alternatively suggesting the presence of glutathione anti-oxidant defence mechanisms to combat CCl_4-induced oxidative injury. Elevations in GSS also proceeded consistent $p16^{INK4A}$ expression at 5 days, therefore the present data suggests that the presence of mitochondrial dysfunction increases liver senescence following the inability to combat oxidative stress – ultimately impacting on the livers ability to regenerate.

Senescence is also shown to involve other signalling pathways including the DNA damage stress response as a consequence of excessive ROS (Chen *et al.*, 1995). Telomeric regions of DNA chromosomes, for example, are shown to be highly sensitive to the oxidising effects of ROS, with mitochondrial ROS, in particular, shown to induce telomere DNA dysfunction and stimulate premature senescence (Petersen *et al.*, 1998; Passos *et al.*, 2007; Hewitt *et al.*, 2012). The manipulation of SOD2 is likewise shown to increase the likelihood of inducing age-dependent telomere dysfunction, whilst steps to minimise production including antioxidant scavenging with MitoQ and partial ETC uncoupling are demonstrated as preventative measures (Saretzki *et al.*, 2003). Regrettably, ROS-induced effects of DNA damage was not an avenue further explored, especially given the contribution of ROS in reinforcing senescent cell cycle arrest *via* persistent activation of damage responses. Assays may include looking at damage foci markers such as γH2.AX and TAF, which would be investigated if allowed more time (Jurk *et al.*, 2014).

7.5.1 Mitochondrial respiratory dysfunction potentiates the senescent inflammatory phenotype

As previously mentioned, chronic low-grade inflammation forms as part of the senescent-associated secretory phenotype (SASP) that accompanies cellular senescence. A hallmark of physiological ageing, the SASP is thought to contribute to age-related deterioration through intensification of senescent cell accumulation, driven by NF-κB mediated bystander processes (Birch and Passos, 2017; Nelson *et al.*, 2018). Subsequent removal of senescent cells ameliorates this secretory phenotype (Baker *et al.*, 2011; Baker *et al.*, 2016). To this end, age-accumulation of mitochondrial complex I dysfunction in basally aged *PolgA*$^{mut/mut}$ mice appears to potentially elicit ROS-induced senescence, in which these mice results in significantly increased levels of cytokines TNFα and IL-6, which are primarily associated with the SASP. Accordingly, *PolgA*$^{mut/mut}$ mice have been previously shown to demonstrate an increased level of senescent cells within tissues, in which Willey and colleagues (2016) propose induction and accumulation of senescent cells *in vivo* in response to the PolgA D257A mutation.

Evidence also shows that the SASP appears to be mediated at a number other levels, including stabilisation of the arrested state in an autocrine manner (Malaquin *et al.*, 2019). Consequently, mitochondrial-dysfunction-induced senescence may be a significant cause of further putative cellular senescence and proinflammatory SASP in *PolgA*$^{mut/mut}$ mice. Activation of the DNA damage response in senescent cells, for example, causes senescence-associated mitochondrial dysfunction characterised by depolarisation of the mitochondrial membrane and exacerbated ROS production (Passos *et al.*, 2007; Passos *et al.*, 2010). The removal of dysfunctional mitochondria, as alluded to previously in studies by Correria-Melo and colleagues (2017), was shown to alleviate pro-oxidative senescent associated stress. Likely induced by initial mitochondrial ROS signalling, senescent-associated mitochondrial dysfunction is shown to be a critical driver of ROS production in vicious cyclical manner within this context. Within this, senescent-associated mitochondrial dysfunction establishes cellular senescence in an autocrine manner *via* exacerbated ROS formation, whilst ROS as part of the inflammatory senescent programme further contributes to senescent cell cycle arrest in surrounding bystander cells through NF-κB processes (Nelson *et al.*, 2012; Nelson *et al.*, 2018).

7.5.2 Mitochondrial respiratory dysfunction perturbs recovery from oxidative liver injury due to activation and senescent activity of stellate cells

As previously highlighted, senescence is critical in preventing replication of old or damaged cells. Its induction is also noted to limit tissue fibrogenesis by hepatic stellate cells (HSCs) on CCl_4 injury, following DNA damaging formation of adducts between cellular DNA and lipid peroxidation by CCl_3OO^* (Krizhanovsky *et al.*, 2008; Knockaert *et al.*, 2011; Scholten *et al.*, 2015) . The constitutive expression of $p16^{INK4A}$ following CCl_4 injury in *PolgA*$^{mut/mut}$ mice may therefore be attributed to activated scar forming hepatic stellate cells (HSCs), in which upregulation of p16 and senescence coincides within chronic CCl_4-induced fibrotic extracellular matrix (ECM) deposits (Krizhanovsky *et al.*, 2008). Activation of HSCs typically follows an induced programme of inflammatory signalling that recruits immune cells to the site of injury. During the inflammatory phase of liver recovery, 0-48 hours post-CCl_4 intoxication, WT and *PolgA* mice demonstrated significant increases in innate proinflammatory NIMP positive neutrophils and increased expression of potent HSC activating cytokine TGFβ1, as well as ECM-associated markers tissue inhibitor of metalloproteinase (TIMP) and α-smooth muscle actin (αSMA), analysed through histological and molecular techniques. Such changes in markers are associated with the transition of HSCs into hepatic myofibroblasts (HM), which include innate immune cell-mediated activation *via* TLR (toll-like receptor) and DAMP (damage-associated molecular pattern) signalling, as well as downstream TGFβ effector pathways like SMAD are noted to be involved (Hellerbrand *et al.*, 1999; Breitkopf *et al.*, 2006; Pellicoro *et al.*, 2014; Tsuchida and Friedman, 2017). However, the data demonstrates no extensive differences in these markers associated with HSC activation at 48 hours post-CCl_4 between WT and *PolgA* genotypes.

Taken together, these data show that during acute CCl_4 toxic injury, activation of HSCs does not significantly differ between WT, *PolgA*$^{+/mut}$ and *PolgA*$^{mut/mut}$ mice. The data does not confirm that the inability to recover from oxidative CCl_4-induced stress is due to greater HSC fibrogenic activation. Failure to resolve CCl_4 tissue injury observed in *PolgA*$^{mut/mut}$ mice, however, may be ascribed to constitutively active HSC activity further potentiated by the inability to clear neutrophils at 5 days, due to increases in chemoattractants CXCL1/2 (C-X-C chemokine ligand) expression and MCP-1 (monocyte chemoattractant protein-1) mediated CD68 inflammatory cell infiltration. Macrophages and neutrophils produce a plethora of cytokines and chemokines that mediate HSC activation, including IL-1β and TNFα, which promotes

HSC survival through NF-κB activation (Pradere *et al.*, 2013; Pellicoro *et al.*, 2014). To this end, the inability to recover from oxidative tissue injury in *PolgA*$^{mut/mut}$ mice may be ascribed to persistent inflammatory-induced activity in the presence of greater mitochondrial dysfunction.

Evidence suggests that in the wider context, HSC senescence is a mechanism undertaken to re-establish the quiescent hepatocellular environment. Senescence is noted to limit fibrotic activity through downregulated ECM production, as well as upregulation of immunomodulatory genes thought to mark senescent cells for apoptotic clearance by immune cells (Schnabl *et al.*, 2003; Krizhanovsky *et al.*, 2008). Pro-apoptotic BAX expression is certainly observed in *PolgA*$^{mut/mut}$ mice at significantly greater levels alongside p16^{INK4A} expression at 5 days, yet the data cannot exclude the possibility of spontaneous liver cell apoptosis elsewhere in response to oxidative stress. Especially given the increased susceptibility to apoptosis in the presence of mitochondrial dysfunction observed in *PolgA* mice. Moreover, HSC-secreted ECM genes TIMP1 and COL1A1 were significantly upregulated at 5 days post-CCl_4 injury within *PolgA*$^{mut/mut}$ mice. This expression could therefore suggest that constitutive p16^{INK4A} liver senescence is alternatively due to hepatocytes, not HSCs, and could also be ascribed to the observed reductions in PCNA and MB markers of regeneration. This could be partially tested through measurement of senescent markers including p16^{INK4A} following acute CCl_4 injury in hepatocytes isolated from *PolgA*$^{mut/mut}$ mice; however, the ability to culture these hepatocytes would require further optimisation given the difficulty of these cells to thrive *in vitro.* Alternatively, inhibitors of mitochondrial complex function in WT hepatocytes could be utilised (Heinz *et al.*, 2017). Drawing these results together, greater mitochondrial dysfunction in *PolgA*$^{mut/mut}$ mice results in the inability to recover from a vicious cycle of CCl_4 induced oxidative injury, most likely ascribed to the persistent inflammatory-induced activity of HSCs and cell cycle arrest of proliferative hepatocytes (figure 7-1).

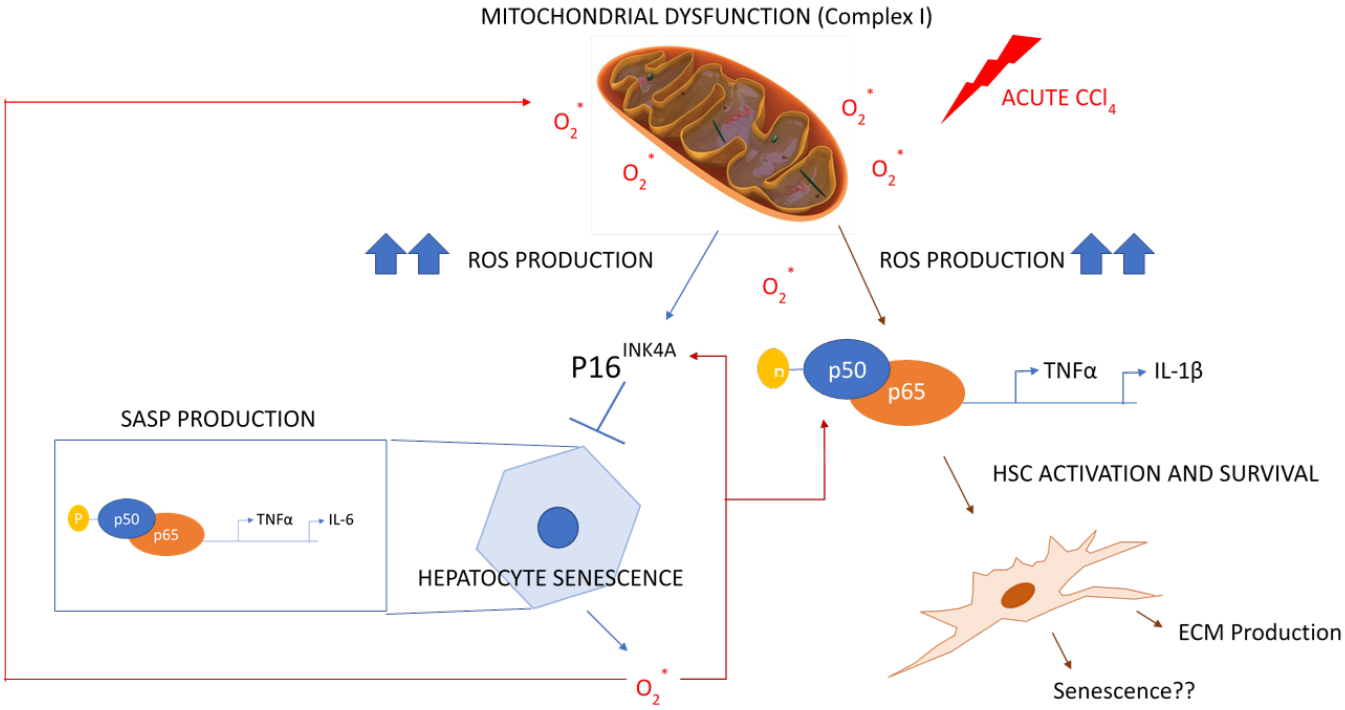

Figure 7-1: Schematic showing the role of mitochondrial dysfunction in response to CCl_4 toxic injury. *CCl_4 injury induces oxidative stress and increases ROS production, which in turn elicits cellular senescence in hepatocytes alongside its senescent-associated secretory phenotype (SASP) comprising proinflammatory cytokine TNFα and IL-6 production and ROS. Meanwhile, inability to repair and resolve the necrotic tissue injury is likely ascribed to hepatic stellate cell (HSC) activation due to ROS-induced stimulation of NF-κB and it's downstream-mediated expression of proinflammatory cytokines TNFα and IL-1β that promote HSC survival and their profibrogenic ECM functional programme. In a vicious cycle ROS produced from the senescent phenotype may further exacerbate mitochondrial dysfunction and mitochondrial ROS production.*

7.6 Mitochondrial respiratory dysfunction is a critical mediator of immune cell homeostasis

Elimination of damaged mitochondria has been shown to alleviate chronic inflammatory disease, including pathology of the liver, and implicates mitochondrial dysfunction in the activation of proinflammatory signalling (Zhong *et al.*, 2016). Whilst the present study alludes to possible aberrant ROS-mediated induced senescence that leads to proinflammatory secretions, the data cannot exclude the possible direct correlation of dysregulated immune cell signalling to age-accumulated complex I mitochondrial dysfunction, exclusive of senescent cell cycle arrest. Specifically, histological, serological and gene expression analyses demonstrate a proinflammatory environment, reflected in significant increases in TNFα, IL-6, and S100A9, as well as greater levels of NIMP positive neutrophils within the *PolgA*$^{mut/mut}$ ageing liver and during post-oxidative CCl_4 injury. These changes are highly suggestive of an activated neutrophilic innate immune response, which during tissue damage are rapidly mobilised to the site of injury and can activate or downregulate both innate and adaptive immunity through the active release of chemotactic factors (Rosales *et al.*, 2017). Interestingly, basally aged *PolgA*$^{mut/mut}$ mice did show an age-associated reduction in the number of positively stained adaptive CD3 T cells and CD45R B immune cells. This may be more in line with previous human and murine ageing models that demonstrate lymphopenic phenotypes, especially given the progeroid features of this model (Dennis *et al.*, 1998; Montella *et al.*, 2003; Nikolich-Žugich, 2014). On the other hand, CD68 histological analyses showed no differences – indicating mitochondrial dysfunction and exacerbated ROS has no significant effect on monocyte and macrophage recruitment. This may be somewhat addressed by their resistance to oxidative stress factors by cytoprotective nitric oxide-catalase mechanisms (Yoshioka *et al.*, 2006). Taken together, these data suggest that mitochondrial dysfunction is likely to result in dysregulated immune cell signalling; however, is likely to require a certain threshold of mtDNA mutations as highlighted by the gene-dose dependent phenotype observed in NIMP-positive neutrophils within the PolgA$^{+/mut}$ liver in the absence of significant changes to cytokine gene expression.

Perturbations in mitochondrial physiology are understood to be able to stimulate inflammatory and innate immune responses through the release of mitochondrial damage-associated molecular patterns (mDAMPs) (Dela Cruz and Kang, 2018). Aberrant mtDNA release, for example, is able to elicit TLR9 signalling pathways *via*

its molecular non-methylated DNA (CpG motifs) similarities to typical bacterial TLR9-binding substrates (Bao *et al.*, 2016). In turn, inducing downstream NF-κB activation and the expression of proinflammatory cytokines like TNFα, IL-6, S100A9, in line with increased 12-month aged PolgA$^{mut/mut}$ neutrophilic expression patterns.

As alluded to previously, evidence suggests that ROS plays an emerging central role in physiological cell signalling, with considerable overlap in the mediation of apoptosis and innate immune signalling (Chen *et al.*, 2018). Activation of proinflammatory and apoptotic signalling pathways in response to aberrant mitochondrial ROS production appears to be similarly reflected in past and present PolgA data, proposing mitochondrial ROS as a core signalling factor in eliciting not only apoptosis but dysfunctional immune cell signalling as a result of age-associated accumulation of mitochondrial dysfunction (Logan *et al.*, 2014). The putative involvement of NF-κB in both pathways also suggests that the primary contribution of mitochondrial ROS to the overall reduction of liver regeneration is *via* its dysregulated activation of NF-κB and its downstream proinflammatory and apoptotic pathways. As with senescence, emerging data also shows that NF-κB potentiates the SASP through additional effector pathways, including p38 MAPK (mitogen-activated protein kinase) and RIG-1 (retinoic acid-inducible gene I); the induction of p16^{INK4A} is shown to have an inhibitory effect (Salminen *et al.*, 2012). Taken together these data highlight the requirement to further delineate whether the observed reduction in the proliferative markers during basal hepatocellular turnover and models of regeneration within *PolgA$^{mut/mut}$* mice is due to increased inflammation and apoptosis or cell cycle arrest, and its mechanistic basis.

7.7 *PolgA$^{mut/mut}$* neutrophils exacerbate oxidative stress and contribute to the inflammatory environment

Neutrophils have been long appreciated in their role within the innate immune response, responding to myriad of perturbations, including mtDNA and ROS, to ensure removal of pathogens and cellular debris released within the host. Within this, neutrophils are primarily recruited to the site of injury or infection and undergo phagocytic and apoptotic processes to ensure removal of the injury stimulus. These processes are well established to involve NF-κB signalling and NADPH oxidase 2 (NOX2) stimulated production of superoxide and other ROS during neutrophil oxidative burst (Winterbourn *et al.*, 2016). Neutrophils also form a key part of tissue injury and repair, yet whilst neutropenia and inhibitions of neutrophil chemotaxis is

shown to delay liver regeneration following insult, persistent activation of neutrophils are also generally thought to exacerbate tissue injury and promote hepatic pathophysiology (Selzner *et al.*, 2003; Slaba *et al.*, 2015). Despite this, there is limited evidence to date outlining mitochondrial relevance for normal functioning of neutrophils beyond provision of activatory signals. Accordingly, stimulation of formyl peptide receptors, on neutrophils, for example, increases mitochondrial membrane potential and ATP production to elicit metabolic switching and the activation of downstream oxidative burst and phagocytic processes by autocrine purinergic signalling (Bao *et al.*, 2014). The presence of a neutrophil proinflammatory environment within the *PolgA*$^{mut/mut}$ model was therefore postulated to have a limiting effect upon basal hepatocellular turnover and hepatic repair. We also present for the first time, data showing *in vivo PolgA*-induced age-accumulated mitochondrial dysfunction as a critical regulator of neutrophil activation.

During basal ageing, stimulation of chemotaxis appeared to be amplified within *PolgA*$^{mut/mut}$ neutrophils, whilst also demonstrating significantly greater ability to phagocytose zymogen particles when compared to WT and *Polg*$^{+/mut}$ neutrophils. These differences may account for greater activated neutrophils presented within the liver, as recruited by neutrophilic chemotactic factors, as well as the greater numbers that remain in the liver following CCl_4 injury. Elsewhere, however, loss of enzymatic ETC function through *PolgA* neutrophil specific deletion and complex I inhibition is shown is shown to negatively impact on neutrophil motility through NF-κB accumulation (Zmijewski *et al.*, 2008; Zhou *et al.*, 2018). A phenotype that appears to be rescued by SOD1 and SOD2 overexpression (Zhou *et al.*, 2018). Differences in these findings could be ascribed to the study of neutrophil functionality within different settings: that is observations following murine lung injury as well as within zebrafish. It must be also noted that isolation of neutrophils from the bone marrow, independent of stimulation is still able to induce neutrophil activation and could be accountable for greater zymogen uptake. Whilst our findings point to a pro-neutrophilic environment, to fully elucidate whether greater neutrophil chemotaxis is an observable phenotype within *PolgA*$^{mut/mut}$ mice, further study involving more subject numbers will be required.

Although not well characterised, activation of neutrophils by N-formylmethionine-leucyl-phenylalanin (FMLP) is shown to be induced *via* the effects of the NF-κB

pathway in previous studies, that could result in functional ROS production (McDonald *et al.*, 1997). However, when ROS production is exacerbated, neutrophils can elicit deleterious effects on the host (Mittal *et al.*, 2014). The present data shows that ROS levels produced by blood and liver-isolated *PolgA*$^{mut/mut}$ neutrophils increased with age basally and production intensified when exposed to platelet activating factor (PAF) and FMLP stimuli. Neutrophils numbers were also greater in the liver when compared the blood. These data suggest that *PolgA*$^{mut/mut}$ neutrophils are basally more primed for tissue recruitment and galvinisation than WTs and subsequently produce more ROS when activated. The increase in intracellular superoxide has been demonstrated to activate NF-κB, inducing proinflammatory cytokine expression and therefore provides one possible explanation for the *PolgA*$^{mut/mut}$ liver's neutrophilic environment (Zmijewski *et al.*, 2008). To put into context, the data could suggest that greater mitochondrial dysfunction is highly likely to promote recruitment of actively 'primed' neutrophils to the liver, either by means of ROS or DAMP signalling, whereby activation releases more ROS and promotes cyclical immune cell recruitment *via* NF-κB-mediated activation of proinflammatory and apoptotic signalling. Neutrophils are therefore key contributors to the oxidative pro-inflammatory observed within *PolgA*$^{mut/mut}$ (figure 7-2). To support this, further work is likely required including the confirmation of the *PolgA*$^{mut/mut}$ susceptible phenotype and immune cell recruitment from the blood into the liver. One possibility could include neutrophil tracking, in which isolated *PolgA*$^{mut/mut}$ neutrophils could be tagged and tracked *in vivo* by a fluorescent and bioluminescent imaging system following adoptive transfer into recipient WT and *PolgA* mice, and vice versa. By doing, would provide further rigour to the data.

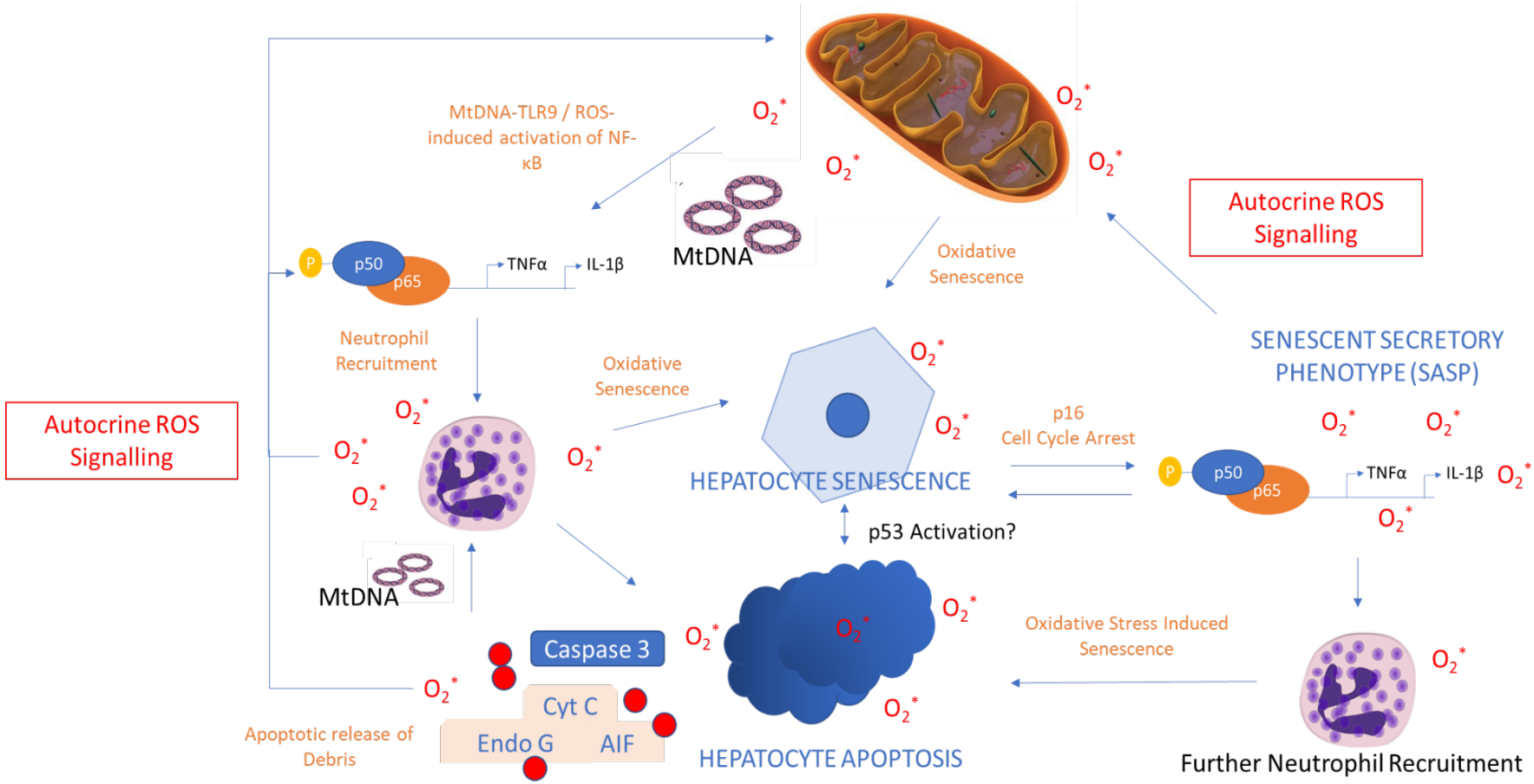

Figure 7-2: Contribution of neutrophil signalling to the proinflammatory environment in the presence of age-accumulated mitochondrial dysfunction. *Within PolgA$^{mut/mut}$ mice, hepatocyte mitochondrial complex I dysfunction results in aberrant mitochondrial ROS production and possible mtDNA release. This elicits NF-κB-mediated proinflammatory gene expression. Cytokines produced are chemotactic for neutrophils, recruiting basally primed neutrophils to the liver that when activated release further ROS. This oxidative environment is able to elicit either or both hepatocyte senescence and apoptosis, putatively potentiated by p53 stress mediator Increased senescent and apoptosis are likely to result in age-associated reduction in hepatocellular regenerative capacity. Whilst p16^{INK4A} senescence is established via SASP, apoptosis is able to additionally feedback into the vicious cycle by release of cellular debris and further oxidants into the extracellular environment. This in turn is able to activate proinflammatory signalling pathways, including that for neutrophil recruitment.*

7.8 Use of murine models to study ageing liver regeneration

The use of animal models in elucidating the physiological effect of mitochondrial dysfunction, specifically in liver regeneration is critical. However, as with most murine models there are inherent limitations particularly when attempting to capture features typical of human ageing. As such, results derived from these murine studies must be interpreted with careful attention.

The classical use of two-thirds PHx is widely used for studying liver regeneration, in which 70% removal of the liver results in the restoration of original liver mass through growth of the remnant liver. PHx is also undertaken within humans; however, it is typically elective in a tumorigenic setting and therefore not typical of the insult potentially experienced by the human liver. Moreover, in mice that are genetically-modified, like *PolgA* D257A, higher mortality rates may be increased especially given the highly energetic demands on mitochondria from the regenerative process (Nevzorova *et al.*, 2015). Since mtDNA mutations accumulate with age in *PolgA*$^{mut/mut}$, we were not able to undertake PHx within 12-month aged mice due to mortality burden, making it difficult to accrue the proinflammatory phenotype observed in basally aged *PolgA*$^{mut/mut}$ mice to 6-month PHx mice.

Similarly in the present study, lack of confirmatory evidence between Mt-CO1 western blotting and COX deficiency during COX/SDH staining was observed in *PolgA*$^{mut/mut}$ mice, admittedly providing some difficulty in corroborating the mechanistic link between *PolgA*$^{mut/mut}$ complex I deficiency with reduced liver regeneration. Certainly, such discrepancies may be ascribed to the differences between the use of western blot antibody detection for protein complexes versus histochemical staining of complex IV activity; yet highlights the future need for further supportive evidence. Of those suggested is the additional characterisation of respiratory chain function and mitochondrial ATP production (MAPR) by biochemical means previously outlined to indeed confirm the mechanistic involvement of complex I and IV in the present study (Wibom *et al.,* 2002; Trifunovic *et al.,* 2005). Furthermore, whilst PCR and gel electrophoresis were used to confirm the genotypes of WT and mutant *PolgA* mice alike (appendix I), mutational burden assays was an avenue not further explored here. In this setting, quantifying mutational burden may also provide additional support in corroborating the present data, should accumulated mutations be shown to occur time. Indeed, previous *PolgA* studies outline increased

mutational burdens within the complex I and IV-encoded gene locus', providing some mechanistic basis for our findings in corroborating complex I deficiencies with reduced liver regeneration (Vermulst *et al.,* 2008; Kim *et al.,* 2019).

Lastly, the *PolgA*$^{mut/mut}$ mice model exhibits several ageing phenotypes ascribed to stimulation of apoptotic pathways and ROS production *via* accumulated mtDNA mutations (Trifunovic *et al.*, 2004; Kujoth *et al.*, 2005; Hiona *et al.*, 2010; Logan *et al.*, 2014). These mice, however, are shown to carry a significantly higher mtDNA mutation burden over WTs, exhibited from 2 months of age and significantly increases to detectable levels only once the observable ageing phenotype arises due to accumulation of mitochondrial dysfunction (Trifunovic *et al.*, 2004; Vermulst *et al.*, 2007). The speed at which mitochondrial dysfunction is accumulated in *PolgA* and the type of mutations may not be necessarily reflective on normal ageing (Williams *et al.*, 2010). Indeed, heterozygous *PolgA*$^{+/mut}$ show an absence of the progeroid phenotype and in this study, signs of reduced liver regeneration despite a higher mutation load than WT mice (Vermulst *et al.*, 2007). This difference as alluded to earlier may suggest the presence of a threshold that is required to be superseded before any aberrant changes are observed.

7.9 Conclusion

The role of mitochondrial dysfunction in reduced hepatocellular regeneration is complex, facilitated by a plethora of interconnected signalling pathways, each of which appear to be potentiated in some part by mitochondrial function. Mitochondria are critical for a number of biological functions, ranging from ATP production and apoptotic cell death to inducing senescent cell cycle arrest; dysfunction of these tightly regulated pathways are unsurprisingly widely documented to result in pathophysiological development. Underpinning the reduction in liver regeneration seen in *PolgA*$^{mut/mut}$ mice is the production of mitochondrial ROS due to age-associated accumulation of mitochondrial dysfunction, specifically complex I. Enzymatic ETC loss and subsequent aberrant ROS production appears to elicit a number of downstream effects that can impinge on liver regeneration both basally and in response to injury: these include, the induction of cell cycle arrest and apoptosis, as well as dysregulated immune cell signalling. Contribution of exacerbated inflammation is further hindered by dysregulated innate immune signalling, specifically increased levels of neutrophils, which further contributes to the

pro-inflammatory oxidative phenotype through further ROS production. I therefore present this vicious cyclical effect following *PolgA*-induced mitochondrial dysfunction simply as follows: age-associated accumulation of mtDNA mutations and resultant complex I mitochondrial dysfunction appears to be highly correlated with the reduction of liver regeneration, in which resultant mitochondrial ROS from ETC leakage induces activation of cell cycle arrest and a proinflammatory-pro-apoptotic axis, which in turn appears to accelerate the ageing and reduced proliferative phenotype through putative autocrine ROS signalling.

Appendix I: *PolgA Genotyping*

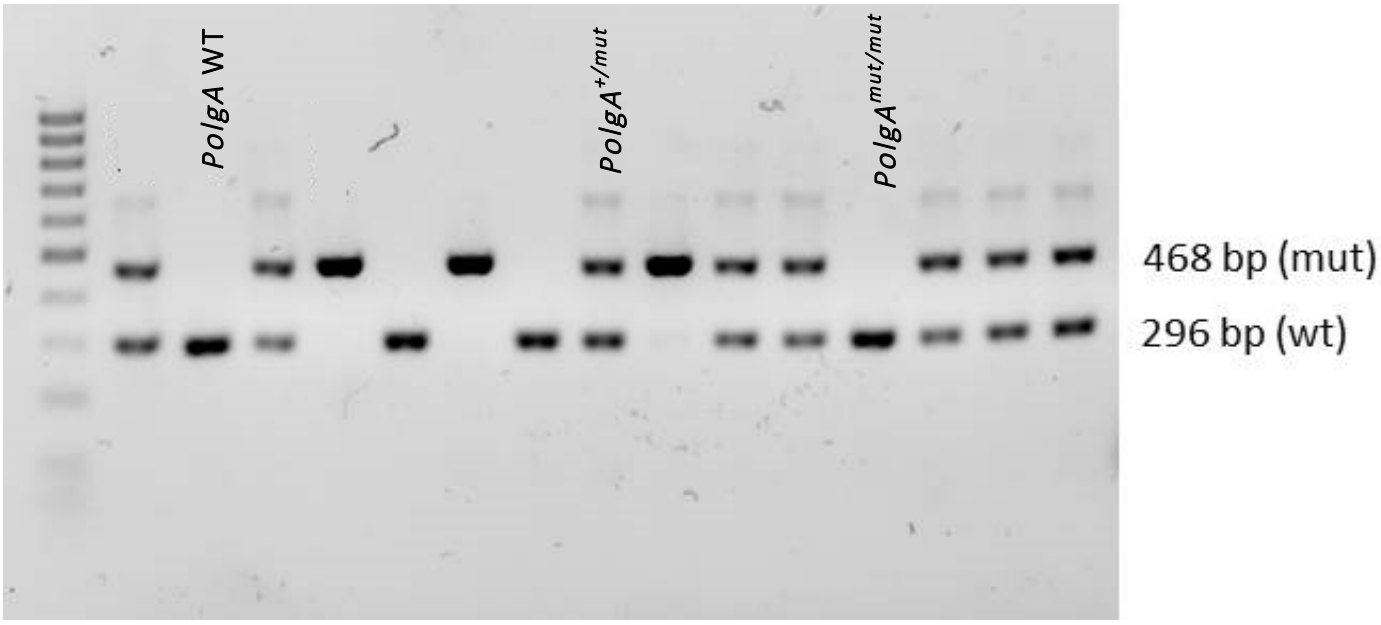

Appendix I: Representative gel showing genotyping of PolgA$^{+/+}$ (WT), PolgA$^{+/mut}$ and PolgA$^{mut/mut}$mice. PCR products separated on a 2% agarose gel. Expected band sizes for WT (296 bp) and homozygous mutant alleles (268 bp) were observed.

Appendix III: HEPES Buffer Recipe

Final Concentration:

1M HEPES 238g
2.7mM KCl 200mg
135mM NaCl 8g
250µM HNa_2 PO_4 0.033g
Made up to 500 ml with dH_2O

To make HEPES $CaCl_2$ buffer:

- Prepare stock of $CaCl_2$ 7.5g in 20ml dH_2O
- Take 50ml HEPES and add 200µl $CaCl_2$ to it

Appendix III: RIPA Buffer Recipe

Final concentration:
150mM NaCl (Sigma)
50mM Tris pH 7.5 (Sigma)
0.1% SDS
1% Triton x-100
0.5% Deoxycholic acid
Phosphatase inhibitor 10µl/ml
Protease inhibitor 1 tablet per 50ml

To make 50ml:

- Weigh out 2.5g Deoxycholic acid and dissolve in 25ml nanopure water by vortexing until clear
- Add 1.5ml 5M NaCl
- Then add 2.5ml 1M Tris pH 7.5
- Dissolve 1 protease inhibitor tablet in 1ml nanopure water and add to mixture
- Add 0.5ml of 10% SDS
- Add 0.5ml Triton x-100
- Add 500µl Protease inhibitor
- Make up to 50ml with nanopure water
- Vortex to mix
- Aliquot into eppendorfs and freeze at -20^{o}C

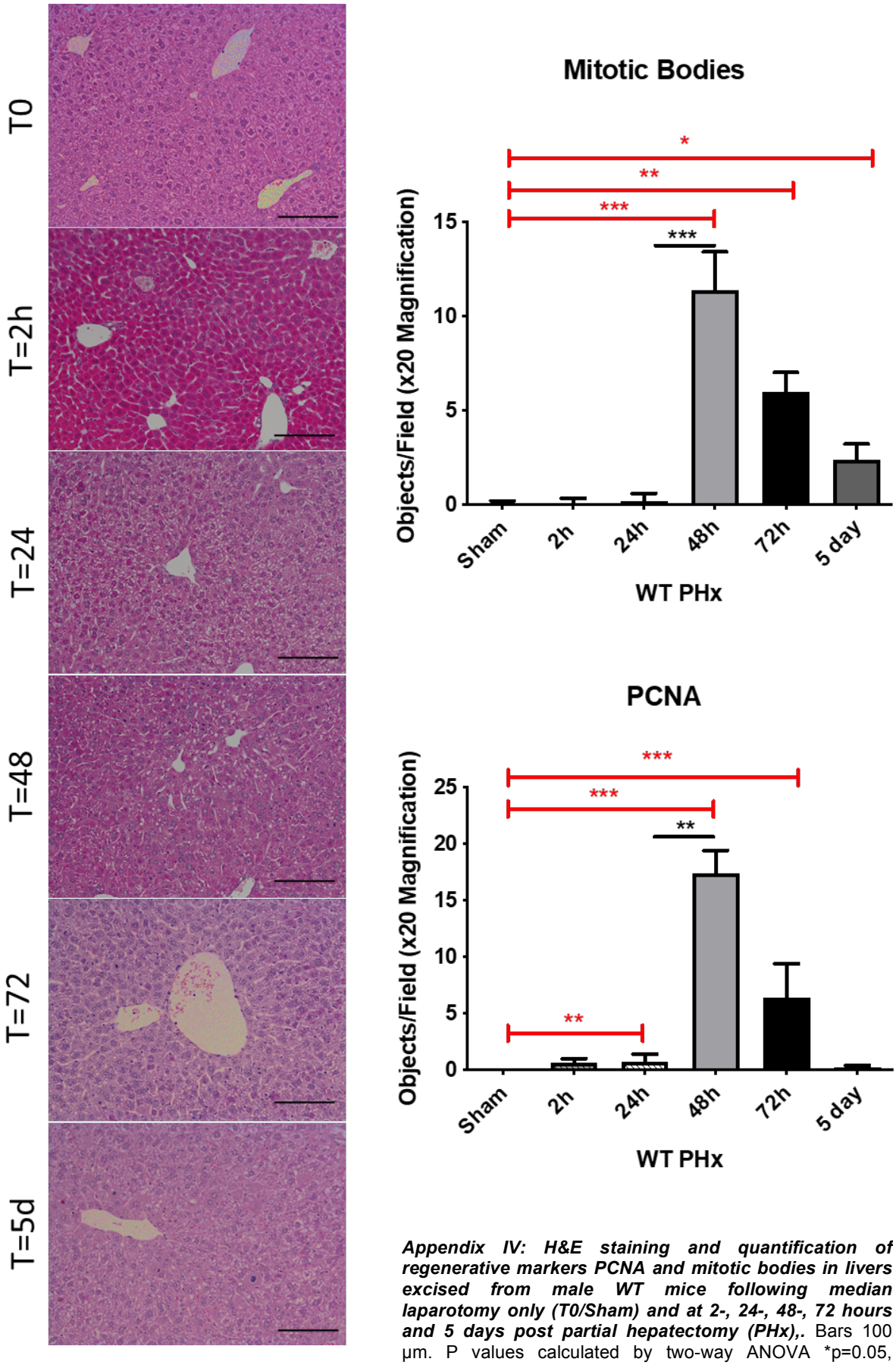

Appendix IV: H&E staining and quantification of regenerative markers PCNA and mitotic bodies in livers excised from male WT mice following median laparotomy only (T0/Sham) and at 2-, 24-, 48-, 72 hours and 5 days post partial hepatectomy (PHx),. Bars 100 µm. P values calculated by two-way ANOVA *p=0.05, **p=0.01, ***p=0.005, **p=0.0001. N=4 per time point.

| References

Abais, J.M., Xia, M., Zhang, Y., Boini, K.M. and Li, P.L. (2015) 'Redox regulation of NLRP3 inflammasomes: ROS as trigger or effector?', *Antioxid Redox Signal*, 22(13), pp. 1111-29.

Abu Rmilah, A., Zhou, W., Nelson, E., Lin, L., Amiot, B. and Nyberg, S.L. (2019) 'Understanding the marvels behind liver regeneration', *Wiley Interdiscip Rev Dev Biol*, 8(3), p. e340.

Afonso, V., Santos, G., Collin, P., Khatib, A.-M., Mitrovic, D.R., Lomri, N., Leitman, D.C. and Lomri, A. (2006) 'Tumor necrosis factor-α down-regulates human Cu/Zn superoxide dismutase 1 promoter via JNK/AP-1 signaling pathway', *Free Radical Biology and Medicine*, 41(5), pp. 709-721.

Aguilera-Aguirre, L., Bacsi, A., Saavedra-Molina, A., Kurosky, A., Sur, S. and Boldogh, I. (2009) 'Mitochondrial dysfunction increases allergic airway inflammation', *J Immunol*, 183(8), pp. 5379-87.

Ahlqvist, K.J., Hamalainen, R.H., Yatsuga, S., Uutela, M., Terzioglu, M., Gotz, A., Forsstrom, S., Salven, P., Angers-Loustau, A., Kopra, O.H., Tyynismaa, H., Larsson, N.G., Wartiovaara, K., Prolla, T., Trifunovic, A. and Suomalainen, A. (2012) 'Somatic progenitor cell vulnerability to mitochondrial DNA mutagenesis underlies progeroid phenotypes in Polg mutator mice', *Cell Metab*, 15(1), pp. 100-9.

Akabane, S., Ueda, T., Nierhaus, K.H. and Takeuchi, N. (2014) 'Ribosome rescue and translation termination at non-standard stop codons by ICT1 in mammalian mitochondria', *PLoS Genet*, 10(9), p. e1004616.

Akerman, P., Cote, P., Yang, S.Q., McClain, C., Nelson, S., Bagby, G.J. and Diehl, A.M. (1992) 'Antibodies to tumor necrosis factor-alpha inhibit liver regeneration after partial hepatectomy', *Am J Physiol*, 263(4 Pt 1), pp. G579-85.

Alani, R.M., Young, A.Z. and Shifflett, C.B. (2001) 'Id1 regulation of cellular senescence through transcriptional repression of p16/Ink4a', *Proc Natl Acad Sci U S A*, 98(14), pp. 7812-6.

Alberts, B., Johnsonm, A., Lewis, J., Martin, R., Roberts, K. and Walter, P. (2002) *Molecular Biology of the Cell*. 4th Edition edn. New York: Garland Science.

Alcorta, D.A., Xiong, Y., Phelps, D., Hannon, G., Beach, D. and Barrett, J.C. (1996) 'Involvement of the cyclin-dependent kinase inhibitor p16 (INK4a) in replicative senescence of normal human fibroblasts', *Proc Natl Acad Sci U S A*, 93(24), pp. 13742-7.

Alexandris, I.H., Assimakopoulos, S.F., Vagianos, C.E., Patsoukis, N., Georgiou, C., Nikolopoulou, V. and Scopa, C.D. (2004) 'Oxidative state in intestine and liver after partial hepatectomy in rats. Effect of bombesin and neurotensin', *Clin Biochem*, 37(5), pp. 350-6.

Ameur, A., Stewart, J.B., Freyer, C., Hagstrom, E., Ingman, M., Larsson, N.G. and Gyllensten, U. (2011) 'Ultra-deep sequencing of mouse mitochondrial DNA: mutational patterns and their origins', *PLoS Genet*, 7(3), p. e1002028.

Amma, H., Naruse, K., Ishiguro, N. and Sokabe, M. (2005) 'Involvement of reactive oxygen species in cyclic stretch-induced NF-kappaB activation in human fibroblast cells', *Br J Pharmacol*, 145(3), pp. 364-73.

Amores-Iniesta, J., Barbera-Cremades, M., Martinez, C.M., Pons, J.A., Revilla-Nuin, B., Martinez-Alarcon, L., Di Virgilio, F., Parrilla, P., Baroja-Mazo, A. and Pelegrin, P. (2017) 'Extracellular ATP Activates the NLRP3 Inflammasome and Is an Early Danger Signal of Skin Allograft Rejection', *Cell Rep*, 21(12), pp. 3414-3426.

Amunts, A., Brown, A., Toots, J., Scheres, S.H.W. and Ramakrishnan, V. (2015) 'Ribosome. The structure of the human mitochondrial ribosome', *Science*, 348(6230), pp. 95-98.

Anderson, S., Bankier, A.T., Barrell, B.G., de Bruijn, M.H.L., Coulson, A.R., Drouin, J., Eperon, I.C., Nierlich, D.P., Roe, B.A., Sanger, F., Schreier, P.H., Smith, A.J.H., Staden, R. and Young, I.G. (1981) 'Sequence and organization of the human mitochondrial genome', *Nature*, 290(5806), pp. 457-465.

Andrews, R.M., Kubacka, I., Chinnery, P.F., Lightowlers, R.N., Turnbull, D.M. and Howell, N. (1999) 'Reanalysis and revision of the Cambridge reference sequence for human mitochondrial DNA', *Nat Genet*, 23(2), p. 147.

Appella, E. and Anderson, C.W. (2001) 'Post-translational modifications and activation of p53 by genotoxic stresses', *Eur J Biochem*, 268(10), pp. 2764-72.

Asin-Cayuela, J., Helm, M. and Attardi, G. (2004) 'A monomer-to-trimer transition of the human mitochondrial transcription termination factor (mTERF) is associated with a loss of in vitro activity', *J Biol Chem*, 279(15), pp. 15670-7.

Atkuri, K.R., Cowan, T.M., Kwan, T., Ng, A., Herzenberg, L.A., Herzenberg, L.A. and Enns, G.M. (2009) 'Inherited disorders affecting mitochondrial function are associated with glutathione deficiency and hypocitrullinemia', *Proceedings of the National Academy of Sciences*, 106(10), pp. 3941-3945.

Auger, C., Alhasawi, A., Contavadoo, M. and Appanna, V.D. (2015) 'Dysfunctional mitochondrial bioenergetics and the pathogenesis of hepatic disorders', *Front Cell Dev Biol*, 3, p. 40.

Bai, P., Nagy, L., Fodor, T., Liaudet, L. and Pacher, P. (2015) 'Poly(ADP-ribose) polymerases as modulators of mitochondrial activity', *Trends Endocrinol Metab*, 26(2), pp. 75-83.

Baines, H.L. (2014) 'Using mouse models to learn about mitochondrial DNA point mutations in ageing and disease'.

Baines, H.L., Stewart, J.B., Stamp, C., Zupanic, A., Kirkwood, T.B., Larsson, N.G., Turnbull, D.M. and Greaves, L.C. (2014) 'Similar patterns of clonally expanded somatic mtDNA mutations in the colon of heterozygous mtDNA mutator mice and ageing humans', *Mech Ageing Dev*, 139, pp. 22-30.

Baiocchini, A., Montaldo, C., Conigliaro, A., Grimaldi, A., Correani, V., Mura, F., Ciccosanti, F., Rotiroti, N., Brenna, A., Montalbano, M., D'Offizi, G., Capobianchi, M.R., Alessandro, R., Piacentini, M., Schininà, M.E., Maras, B., Del Nonno, F., Tripodi, M. and Mancone, C. (2016) 'Extracellular Matrix Molecular Remodeling in Human Liver Fibrosis Evolution', *PLOS ONE*, 11(3), p. e0151736.

Baker, D.J., Childs, B.G., Durik, M., Wijers, M.E., Sieben, C.J., Zhong, J., Saltness, R.A., Jeganathan, K.B., Verzosa, G.C., Pezeshki, A., Khazaie, K., Miller, J.D. and van Deursen, J.M. (2016) 'Naturally occurring p16(Ink4a)-positive cells shorten healthy lifespan', *Nature*, 530(7589), pp. 184-9.

Baker, D.J., Wijshake, T., Tchkonia, T., LeBrasseur, N.K., Childs, B.G., van de Sluis, B., Kirkland, J.L. and van Deursen, J.M. (2011) 'Clearance of p16Ink4a-positive senescent cells delays ageing-associated disorders', *Nature*, 479(7372), pp. 232-6.

Bakiri, L., Lallemand, D., Bossy-Wetzel, E. and Yaniv, M. (2000) 'Cell cycle-dependent variations in c-Jun and JunB phosphorylation: a role in the control of cyclin D1 expression', *Embo j*, 19(9), pp. 2056-68.

Bao, W., Xia, H., Liang, Y., Ye, Y., Lu, Y., Xu, X., Duan, A., He, J., Chen, Z., Wu, Y., Wang, X., Zheng, C., Liu, Z. and Shi, S. (2016) 'Toll-like Receptor 9 Can be Activated by Endogenous Mitochondrial DNA to Induce Podocyte Apoptosis', *Scientific Reports*, 6, p. 22579.

Bao, Y., Ledderose, C., Seier, T., Graf, A.F., Brix, B., Chong, E. and Junger, W.G. (2014) 'Mitochondria regulate neutrophil activation by generating ATP for autocrine purinergic signaling', *J Biol Chem*, 289(39), pp. 26794-803.

Barja, G., Cadenas, S., Rojas, C., Perez-Campo, R. and Lopez-Torres, M. (1994) 'Low mitochondrial free radical production per unit O2 consumption can explain the simultaneous presence of high longevity and high aerobic metabolic rate in birds', *Free Radic Res*, 21(5), pp. 317-27.

Barnum, K.J. and O'Connell, M.J. (2014) 'Cell cycle regulation by checkpoints', *Methods Mol Biol*, 1170, pp. 29-40.

Barrell, B.G., Anderson, S., Bankier, A.T., De Bruijn, M.H.L., Chen, E., Coulson, A.R., Drouin, J., Eperon, I.C., Nierlich, D.P., Roe, B., Sanger, F., Schreier, P.H., Smith, A.J.H., Staden, R. and Young, I.G. (1980) *Biological Chemistry of Organelle Formation*. Berlin, Heidelberg, 1980//. Springer Berlin Heidelberg.

Beach, D., Durkacz, B. and Nurse, P. (1982) 'Functionally homologous cell cycle control genes in budding and fission yeast', *Nature*, 300(5894), pp. 706-9.

Benhamouche, S., Decaens, T., Godard, C., Chambrey, R., Rickman, D.S., Moinard, C., Vasseur-Cognet, M., Kuo, C.J., Kahn, A., Perret, C. and Colnot, S. (2006) 'Apc tumor suppressor gene is the "zonation-keeper" of mouse liver', *Dev Cell*, 10(6), pp. 759-70.

Bhargava, K. and Spremulli, L.L. (2005) 'Role of the N- and C-terminal extensions on the activity of mammalian mitochondrial translational initiation factor 3', *Nucleic Acids Res*, 33(22), pp. 7011-8.

Bibb, M.J., Van Etten, R.A., Wright, C.T., Walberg, M.W. and Clayton, D.A. (1981) 'Sequence and gene organization of mouse mitochondrial DNA', *Cell*, 26(2 Pt 2), pp. 167-80.

Birch, J. and Passos, J.F. (2017) 'Targeting the SASP to combat ageing: Mitochondria as possible intracellular allies?', *Bioessays*, 39(5).

Blindenbacher, A., Wang, X., Langer, I., Savino, R., Terracciano, L. and Heim, M.H. (2003) 'Interleukin 6 is important for survival after partial hepatectomy in mice', *Hepatology*, 38(3), pp. 674-82.

Boehm, E., Zaganelli, S., Maundrell, K., Jourdain, A.A., Thore, S. and Martinou, J.C. (2017) 'FASTKD1 and FASTKD4 have opposite effects on expression of specific mitochondrial RNAs, depending upon their endonuclease-like RAP domain', *Nucleic Acids Res*, 45(10), pp. 6135-6146.

Boesch, P., Weber-Lotfi, F., Ibrahim, N., Tarasenko, V., Cosset, A., Paulus, F., Lightowlers, R.N. and Dietrich, A. (2011) 'DNA repair in organelles: Pathways, organization, regulation, relevance in disease and aging', *Biochim Biophys Acta*, 1813(1), pp. 186-200.

Bogenhagen, D. and Clayton, D.A. (1977) 'Mouse L cell mitochondrial DNA molecules are selected randomly for replication throughout the cell cycle', *Cell*, 11(4), pp. 719-27.

Bogenhagen, D.F. (2012) 'Mitochondrial DNA nucleoid structure', *Biochim Biophys Acta*, 1819(9-10), pp. 914-20.

Borowiak, M., Garratt, A.N., Wustefeld, T., Strehle, M., Trautwein, C. and Birchmeier, C. (2004) 'Met provides essential signals for liver regeneration', *Proc Natl Acad Sci U S A*, 101(29), pp. 10608-13.

Boulet, L., Karpati, G. and Shoubridge, E.A. (1992) 'Distribution and threshold expression of the tRNA(Lys) mutation in skeletal muscle of patients with myoclonic epilepsy and ragged-red fibers (MERRF)', *Am J Hum Genet*, 51(6), pp. 1187-200.

Boveris, A. and Chance, B. (1973) 'The mitochondrial generation of hydrogen peroxide. General properties and effect of hyperbaric oxygen', *Biochem J*, 134(3), pp. 707-16.

Bowmaker, M., Yang, M.Y., Yasukawa, T., Reyes, A., Jacobs, H.T., Huberman, J.A. and Holt, I.J. (2003) 'Mammalian mitochondrial DNA replicates bidirectionally from an initiation zone', *J Biol Chem*, 278(51), pp. 50961-9.

Bratic, A. and Larsson, N.G. (2013) 'The role of mitochondria in aging', *J Clin Invest*, 123(3), pp. 951-7.

Braun, L., Mead, J.E., Panzica, M., Mikumo, R., Bell, G.I. and Fausto, N. (1988) 'Transforming growth factor beta mRNA increases during liver regeneration: a possible paracrine mechanism of growth regulation', *Proc Natl Acad Sci U S A*, 85(5), pp. 1539-43.

Breitkopf, K., Godoy, P., Ciuclan, L., Singer, M.V. and Dooley, S. (2006) 'TGF-beta/Smad signaling in the injured liver', *Z Gastroenterol*, 44(1), pp. 57-66.

Brierley, E.J., Johnson, M.A., Lightowlers, R.N., James, O.F. and Turnbull, D.M. (1998) 'Role of mitochondrial DNA mutations in human aging: implications for the central nervous system and muscle', *Ann Neurol*, 43(2), pp. 217-23.

Brown, K., Park, S., Kanno, T., Franzoso, G. and Siebenlist, U. (1993) 'Mutual regulation of the transcriptional activator NF-kappa B and its inhibitor, I kappa B-alpha', *Proc Natl Acad Sci U S A*, 90(6), pp. 2532-6.

Brown, T.A., Cecconi, C., Tkachuk, A.N., Bustamante, C. and Clayton, D.A. (2005) 'Replication of mitochondrial DNA occurs by strand displacement with alternative light-strand origins, not via a strand-coupled mechanism', *Genes Dev*, 19(20), pp. 2466-76.

Bruce, J.L., Hurford, R.K., Jr., Classon, M., Koh, J. and Dyson, N. (2000) 'Requirements for cell cycle arrest by p16INK4a', *Mol Cell*, 6(3), pp. 737-42.

Brzezniak, L.K., Bijata, M., Szczesny, R.J. and Stepien, P.P. (2011) 'Involvement of human ELAC2 gene product in 3' end processing of mitochondrial tRNAs', *RNA Biol*, 8(4), pp. 616-26.

Bua, E., Johnson, J., Herbst, A., Delong, B., McKenzie, D., Salamat, S. and Aiken, J.M. (2006) 'Mitochondrial DNA-deletion mutations accumulate intracellularly to detrimental levels in aged human skeletal muscle fibers', *Am J Hum Genet*, 79(3), pp. 469-80.

Bucher, N.L., Patel, U. and Cohen, S. (1977) 'Hormonal factors concerned with liver regeneration', *Ciba Found Symp*, (55), pp. 95-107.

Bucher, N.L. and Swaffield, M.N. (1964) 'THE RATE OF INCORPORATION OF LABELED THYMIDINE INTO THE DEOXYRIBONUCLEIC ACID OF REGENERATING RAT LIVER IN RELATION TO THE AMOUNT OF LIVER EXCISED', *Cancer Res*, 24, pp. 1611-25.

Bulua, A.C., Simon, A., Maddipati, R., Pelletier, M., Park, H., Kim, K.Y., Sack, M.N., Kastner, D.L. and Siegel, R.M. (2011) 'Mitochondrial reactive oxygen species promote production of proinflammatory cytokines and are elevated in TNFR1-associated periodic syndrome (TRAPS)', *J Exp Med*, 208(3), pp. 519-33.

Burch, P.M. and Heintz, N.H. (2005) 'Redox regulation of cell-cycle re-entry: cyclin D1 as a primary target for the mitogenic effects of reactive oxygen and nitrogen species', *Antioxid Redox Signal*, 7(5-6), pp. 741-51.

Burke, Z.D., Reed, K.R., Phesse, T.J., Sansom, O.J., Clarke, A.R. and Tosh, D. (2009) 'Liver zonation occurs through a beta-catenin-dependent, c-Myc-independent mechanism', *Gastroenterology*, 136(7), pp. 2316-2324.e1-3.

Caldwell, S.H., Swerdlow, R.H., Khan, E.M., Iezzoni, J.C., Hespenheide, E.E., Parks, J.K. and Parker, W.D., Jr. (1999) 'Mitochondrial abnormalities in non-alcoholic steatohepatitis', *J Hepatol*, 31(3), pp. 430-4.

Campisi, J. (1996) 'Replicative senescence: an old lives' tale?', *Cell*, 84(4), pp. 497-500.

Cao, Z., Wanagat, J., McKiernan, S.H. and Aiken, J.M. (2001) 'Mitochondrial DNA deletion mutations are concomitant with ragged red regions of individual, aged muscle fibers: analysis by laser-capture microdissection', *Nucleic Acids Res*, 29(21), pp. 4502-8.

Carpentier, R., Suner, R.E., van Hul, N., Kopp, J.L., Beaudry, J.B., Cordi, S., Antoniou, A., Raynaud, P., Lepreux, S., Jacquemin, P., Leclercq, I.A., Sander, M. and Lemaigre, F.P. (2011) 'Embryonic ductal plate cells give rise to cholangiocytes, periportal hepatocytes, and adult liver progenitor cells', *Gastroenterology*, 141(4), pp. 1432-8, 1438.e1-4.

Chaisson, M.L., Brooling, J.T., Ladiges, W., Tsai, S. and Fausto, N. (2002) 'Hepatocyte-specific inhibition of NF-kappaB leads to apoptosis after TNF treatment, but not after partial hepatectomy', *J Clin Invest*, 110(2), pp. 193-202.

Chakraborty, J.B., Oakley, F. and Walsh, M.J. (2012) 'Mechanisms and biomarkers of apoptosis in liver disease and fibrosis', *Int J Hepatol*, 2012, p. 648915.

Chance, B., Sies, H. and Boveris, A. (1979) 'Hydroperoxide metabolism in mammalian organs', *Physiol Rev*, 59(3), pp. 527-605.

Chance, B. and Williams, G.R. (1955) 'Respiratory enzymes in oxidative phosphorylation. I. Kinetics of oxygen utilization', *J Biol Chem*, 217(1), pp. 383-93.

Chance, B. and Williams, G.R. (1956) 'Respiratory enzymes in oxidative phosphorylation. VI. The effects of adenosine diphosphate on azide-treated mitochondria', *J Biol Chem*, 221(1), pp. 477-89.

Chapman, J., Fielder, E. and Passos, J.F. (2019) 'Mitochondrial dysfunction and cell senescence: deciphering a complex relationship', *FEBS Lett*, 593(13), pp. 1566-1579.

Chavin, K.D., Yang, S., Lin, H.Z., Chatham, J., Chacko, V.P., Hoek, J.B., Walajtys-Rode, E., Rashid, A., Chen, C.H., Huang, C.C., Wu, T.C., Lane, M.D. and Diehl, A.M. (1999) 'Obesity induces expression of uncoupling protein-2 in hepatocytes and promotes liver ATP depletion', *J Biol Chem*, 274(9), pp. 5692-700.

Chen, L., Zhang, W., Liang, H.-f., Zhou, Q.-d., Ding, Z.-y., Yang, H.-q., Liu, W.-b., Wu, Y.-h., Man, Q., Zhang, B.-x. and Chen, X.-p. (2014) 'Activin A induces growth arrest through a SMAD- dependent pathway in hepatic progenitor cells', *Cell Communication and Signaling*, 12(1), p. 18.

Chen, Q., Fischer, A., Reagan, J.D., Yan, L.J. and Ames, B.N. (1995) 'Oxidative DNA damage and senescence of human diploid fibroblast cells', *Proc Natl Acad Sci U S A*, 92(10), pp. 4337-41.

Chen, Q., Vazquez, E.J., Moghaddas, S., Hoppel, C.L. and Lesnefsky, E.J. (2003) 'Production of reactive oxygen species by mitochondria: central role of complex III', *J Biol Chem*, 278(38), pp. 36027-31.

Chen, W., Kang, J., Xia, J., Li, Y., Yang, B., Chen, B., Sun, W., Song, X., Xiang, W., Wang, X., Wang, F., Wan, Y. and Bi, Z. (2008) 'p53-related apoptosis resistance and tumor suppression activity in UVB-induced premature senescent human skin fibroblasts', *Int J Mol Med*, 21(5), pp. 645-53.

Chen, X., Ko, L.J., Jayaraman, L. and Prives, C. (1996) 'p53 levels, functional domains, and DNA damage determine the extent of the apoptotic response of tumor cells', *Genes Dev*, 10(19), pp. 2438-51.

Chen, X.H., Zhao, Y.P., Xue, M., Ji, C.B., Gao, C.L., Zhu, J.G., Qin, D.N., Kou, C.Z., Qin, X.H., Tong, M.L. and Guo, X.R. (2010) 'TNF-alpha induces mitochondrial dysfunction in 3T3-L1 adipocytes', *Mol Cell Endocrinol*, 328(1-2), pp. 63-9.

Chen, Y., Zhou, Z. and Min, W. (2018) 'Mitochondria, Oxidative Stress and Innate Immunity', *Front Physiol*, 9, p. 1487.

Childs, B.G., Baker, D.J., Wijshake, T., Conover, C.A., Campisi, J. and van Deursen, J.M. (2016) 'Senescent intimal foam cells are deleterious at all stages of atherosclerosis', *Science*, 354(6311), pp. 472-477.

Childs, B.G., Durik, M., Baker, D.J. and van Deursen, J.M. (2015) 'Cellular senescence in aging and age-related disease: from mechanisms to therapy', *Nat Med*, 21(12), pp. 1424-35.
Choi, J. (2016) 'An Evolutionary Understanding of Aging', *Arch Plast Surg*, 43(3), pp. 306-8.
Chomyn, A., Martinuzzi, A., Yoneda, M., Daga, A., Hurko, O., Johns, D., Lai, S.T., Nonaka, I., Angelini, C. and Attardi, G. (1992) 'MELAS mutation in mtDNA binding site for transcription termination factor causes defects in protein synthesis and in respiration but no change in levels of upstream and downstream mature transcripts', *Proc Natl Acad Sci U S A*, 89(10), pp. 4221-5.
Chrzanowska-Lightowlers, Z.M. and Lightowlers, R.N. (2015) 'Response to "Ribosome Rescue and Translation Termination at Non-standard Stop Codons by ICT1 in Mammalian Mitochondria"', *PLoS Genet*, 11(6), p. e1005227.
Chrzanowska-Lightowlers, Z.M., Pajak, A. and Lightowlers, R.N. (2011) 'Termination of protein synthesis in mammalian mitochondria', *J Biol Chem*, 286(40), pp. 34479-85.
Chung, H., Hong, D.P., Jung, J.Y., Kim, H.J., Jang, K.S., Sheen, Y.Y., Ahn, J.I., Lee, Y.S. and Kong, G. (2005) 'Comprehensive analysis of differential gene expression profiles on carbon tetrachloride-induced rat liver injury and regeneration', *Toxicol Appl Pharmacol*, 206(1), pp. 27-42.
Chung, H.Y., Cesari, M., Anton, S., Marzetti, E., Giovannini, S., Seo, A.Y., Carter, C., Yu, B.P. and Leeuwenburgh, C. (2009) 'Molecular inflammation: underpinnings of aging and age-related diseases', *Ageing Res Rev*, 8(1), pp. 18-30.
Clayton, D.A. (1991) 'Replication and transcription of vertebrate mitochondrial DNA', *Annu Rev Cell Biol*, 7, pp. 453-78.
Clayton, D.A. (1992) 'Transcription and replication of animal mitochondrial DNAs', *Int Rev Cytol*, 141, pp. 217-32.
Cleaver, J.E., Brennan-Minnella, A.M., Swanson, R.A., Fong, K.W., Chen, J., Chou, K.M., Chen, Y.W., Revet, I. and Bezrookove, V. (2014) 'Mitochondrial reactive oxygen species are scavenged by Cockayne syndrome B protein in human fibroblasts without nuclear DNA damage', *Proc Natl Acad Sci U S A*, 111(37), pp. 13487-92.
Coller, H.A., Khrapko, K., Bodyak, N.D., Nekhaeva, E., Herrero-Jimenez, P. and Thilly, W.G. (2001) 'High frequency of homoplasmic mitochondrial DNA mutations in human tumors can be explained without selection', *Nature Genetics*, 28(2), pp. 147-150.
Coller, H.A., Khrapko, K., Herrero-Jimenez, P., Vatland, J.A., Li-Sucholeiki, X.C. and Thilly, W.G. (2005) 'Clustering of mutant mitochondrial DNA copies suggests stem cells are common in human bronchial epithelium', *Mutat Res*, 578(1-2), pp. 256-71.
Colletti, L.M., Kunkel, S.L., Green, M., Burdick, M. and Strieter, R.M. (1996) 'Hepatic inflammation following 70% hepatectomy may be related to up-regulation of epithelial neutrophil activating protein-78', *Shock*, 6(6), pp. 397-402.

Coppe, J.P., Desprez, P.Y., Krtolica, A. and Campisi, J. (2010) 'The senescence-associated secretory phenotype: the dark side of tumor suppression', *Annu Rev Pathol*, 5, pp. 99-118.
Corral-Debrinski, M., Horton, T., Lott, M.T., Shoffner, J.M., Beal, M.F. and Wallace, D.C. (1992) 'Mitochondrial DNA deletions in human brain: regional variability and increase with advanced age', *Nat Genet*, 2(4), pp. 324-9.
Correia-Melo, C., Marques, F.D., Anderson, R., Hewitt, G., Hewitt, R., Cole, J., Carroll, B.M., Miwa, S., Birch, J., Merz, A., Rushton, M.D., Charles, M., Jurk, D., Tait, S.W., Czapiewski, R., Greaves, L., Nelson, G., Bohlooly-Y, M., Rodriguez-Cuenca, S., Vidal-Puig, A., Mann, D., Saretzki, G., Quarato, G., Green, D.R., Adams, P.D., von Zglinicki, T., Korolchuk, V.I. and Passos, J.F. (2016) 'Mitochondria are required for pro-ageing features of the senescent phenotype', *The EMBO Journal*, 35(7), pp. 724-742.
Cortez-Pinto, H., Chatham, J., Chacko, V.P., Arnold, C., Rashid, A. and Diehl, A.M. (1999) 'Alterations in liver ATP homeostasis in human nonalcoholic steatohepatitis: a pilot study', *Jama*, 282(17), pp. 1659-64.
Cortopassi, G.A. and Arnheim, N. (1990) 'Detection of a specific mitochondrial DNA deletion in tissues of older humans', *Nucleic Acids Res*, 18(23), pp. 6927-33.
Cortopassi, G.A., Shibata, D., Soong, N.W. and Arnheim, N. (1992) 'A pattern of accumulation of a somatic deletion of mitochondrial DNA in aging human tissues', *Proc Natl Acad Sci U S A*, 89(16), pp. 7370-4.
Cottrell, D.A., Blakely, E.L., Johnson, M.A., Ince, P.G., Borthwick, G.M. and Turnbull, D.M. (2001) 'Cytochrome c oxidase deficient cells accumulate in the hippocampus and choroid plexus with age', *Neurobiol Aging*, 22(2), pp. 265-72.
Cressman, D.E., Greenbaum, L.E., Haber, B.A. and Taub, R. (1994) 'Rapid activation of post-hepatectomy factor/nuclear factor kappa B in hepatocytes, a primary response in the regenerating liver', *J Biol Chem*, 269(48), pp. 30429-35.
Croce, A.C., De Simone, U., Freitas, I., Boncompagni, E., Neri, D., Cillo, U. and Bottiroli, G. (2010) 'Human liver autofluorescence: An intrinsic tissue parameter discriminating normal and diseased conditions', *Lasers in Surgery and Medicine*, 42(5), pp. 371-378.
D'Souza, A.R. and Minczuk, M. (2018) 'Mitochondrial transcription and translation: overview', *Essays Biochem*, 62(3), pp. 309-320.
Dai, C., Xiao, X., Li, D., Tun, S., Wang, Y., Velkov, T. and Tang, S. (2018) 'Chloroquine ameliorates carbon tetrachloride-induced acute liver injury in mice via the concomitant inhibition of inflammation and induction of apoptosis', *Cell Death & Disease*, 9(12), p. 1164.
Dai, D.F., Chen, T., Wanagat, J., Laflamme, M., Marcinek, D.J., Emond, M.J., Ngo, C.P., Prolla, T.A. and Rabinovitch, P.S. (2010) 'Age-dependent cardiomyopathy in mitochondrial mutator mice is attenuated by overexpression of catalase targeted to mitochondria', *Aging Cell*, 9(4), pp. 536-44.

Dai, Y. and Cederbaum, A.I. (1995) 'Inactivation and degradation of human cytochrome P4502E1 by CCl4 in a transfected HepG2 cell line', *J Pharmacol Exp Ther*, 275(3), pp. 1614-22.
Dalle-Donne, I., Rossi, R., Colombo, R., Giustarini, D. and Milzani, A. (2006) 'Biomarkers of oxidative damage in human disease', *Clin Chem*, 52(4), pp. 601-23.
de Lau, W., Peng, W.C., Gros, P. and Clevers, H. (2014) 'The R-spondin/Lgr5/Rnf43 module: regulator of Wnt signal strength', *Genes Dev*, 28(4), pp. 305-16.
de Martin, R., Vanhove, B., Cheng, Q., Hofer, E., Csizmadia, V., Winkler, H. and Bach, F.H. (1993) 'Cytokine-inducible expression in endothelial cells of an I kappa B alpha-like gene is regulated by NF kappa B', *Embo j*, 12(7), pp. 2773-9.
de Oliveira, S., Rosowski, E.E. and Huttenlocher, A. (2016) 'Neutrophil migration in infection and wound repair: going forward in reverse', *Nat Rev Immunol*, 16(6), pp. 378-91.
de Souza-Pinto, N.C., Mason, P.A., Hashiguchi, K., Weissman, L., Tian, J., Guay, D., Lebel, M., Stevnsner, T.V., Rasmussen, L.J. and Bohr, V.A. (2009) 'Novel DNA mismatch-repair activity involving YB-1 in human mitochondria', *DNA Repair (Amst)*, 8(6), pp. 704-19.
DeBalsi, K.L., Hoff, K.E. and Copeland, W.C. (2017) 'Role of the mitochondrial DNA replication machinery in mitochondrial DNA mutagenesis, aging and age-related diseases', *Ageing Res Rev*, 33, pp. 89-104.
Deepa, S.S., Unnikrishnan, A., Matyi, S., Hadad, N. and Richardson, A. (2018) 'Necroptosis increases with age and is reduced by dietary restriction', *Aging Cell*, 17(4), p. e12770.
Dela Cruz, C.S. and Kang, M.J. (2018) 'Mitochondrial dysfunction and damage associated molecular patterns (DAMPs) in chronic inflammatory diseases', *Mitochondrion*, 41, pp. 37-44.
Demaria, M., Ohtani, N., Youssef, S.A., Rodier, F., Toussaint, W., Mitchell, J.R., Laberge, R.M., Vijg, J., Van Steeg, H., Dolle, M.E., Hoeijmakers, J.H., de Bruin, A., Hara, E. and Campisi, J. (2014) 'An essential role for senescent cells in optimal wound healing through secretion of PDGF-AA', *Dev Cell*, 31(6), pp. 722-33.
Dennis, M.S., Nicolson, A., Lehmann, A.B., Junaid, O., Byrne, E.J. and Hopkinson, N. (1998) 'Clinical associations of lymphopenia in elderly persons admitted to acute medical and psychiatric wards', *Gerontology*, 44(3), pp. 168-71.
Dhalla, N.S., Temsah, R.M. and Netticadan, T. (2000) 'Role of oxidative stress in cardiovascular diseases', *J Hypertens*, 18(6), pp. 655-73.
DiLoreto, R. and Murphy, C.T. (2015) 'The cell biology of aging', *Mol Biol Cell*, 26(25), pp. 4524-31.
Dimayuga, F.O., Wang, C., Clark, J.M., Dimayuga, E.R., Dimayuga, V.M. and Bruce-Keller, A.J. (2007) 'SOD1 overexpression alters ROS production and reduces neurotoxic inflammatory signaling in microglial cells', *Journal of Neuroimmunology*, 182(1), pp. 89-99.

Dimri, G.P., Lee, X., Basile, G., Acosta, M., Scott, G., Roskelley, C., Medrano, E.E., Linskens, M., Rubelj, I., Pereira-Smith, O. and et al. (1995) 'A biomarker that identifies senescent human cells in culture and in aging skin in vivo', *Proc Natl Acad Sci U S A*, 92(20), pp. 9363-7.

Doolittle, D.J., Muller, G. and Scribner, H.E. (1987) 'Relationship between hepatotoxicity and induction of replicative DNA synthesis following single or multiple doses of carbon tetrachloride', *J Toxicol Environ Health*, 22(1), pp. 63-78.

Durham, S.E., Brown, D.T., Turnbull, D.M. and Chinnery, P.F. (2006) 'Progressive depletion of mtDNA in mitochondrial myopathy', *Neurology*, 67(3), pp. 502-4.

Edgar, D. and Trifunovic, A. (2009) 'The mtDNA mutator mouse: Dissecting mitochondrial involvement in aging', *Aging (Albany NY)*, 1(12), pp. 1028-32.

Edwards, M.J., Keller, B.J., Kauffman, F.C. and Thurman, R.G. (1993) 'The involvement of Kupffer cells in carbon tetrachloride toxicity', *Toxicol Appl Pharmacol*, 119(2), pp. 275-9.

Elmore, S. (2007) 'Apoptosis: a review of programmed cell death', *Toxicol Pathol*, 35(4), pp. 495-516.

Elson, J.L., Samuels, D.C., Turnbull, D.M. and Chinnery, P.F. (2001) 'Random intracellular drift explains the clonal expansion of mitochondrial DNA mutations with age', *Am J Hum Genet*, 68(3), pp. 802-6.

Enkhbold, C., Morine, Y., Utsunomiya, T., Imura, S., Ikemoto, T., Arakawa, Y., Saito, Y., Yamada, S., Ishikawa, D. and Shimada, M. (2015) 'Dysfunction of liver regeneration in aged liver after partial hepatectomy', *J Gastroenterol Hepatol*, 30(7), pp. 1217-24.

Espinosa-Diez, C., Miguel, V., Mennerich, D., Kietzmann, T., Sanchez-Perez, P., Cadenas, S. and Lamas, S. (2015) 'Antioxidant responses and cellular adjustments to oxidative stress', *Redox Biol*, 6, pp. 183-197.

Evans, T., Rosenthal, E.T., Youngblom, J., Distel, D. and Hunt, T. (1983) 'Cyclin: a protein specified by maternal mRNA in sea urchin eggs that is destroyed at each cleavage division', *Cell*, 33(2), pp. 389-96.

Factor, V.M., Seo, D., Ishikawa, T., Kaposi-Novak, P., Marquardt, J.U., Andersen, J.B., Conner, E.A. and Thorgeirsson, S.S. (2010) 'Loss of c-Met Disrupts Gene Expression Program Required for G2/M Progression during Liver Regeneration in Mice', *PLOS ONE*, 5(9), p. e12739.

Falkenberg, M., Gaspari, M., Rantanen, A., Trifunovic, A., Larsson, N.G. and Gustafsson, C.M. (2002) 'Mitochondrial transcription factors B1 and B2 activate transcription of human mtDNA', *Nat Genet*, 31(3), pp. 289-94.

Fato, R., Bergamini, C., Bortolus, M., Maniero, A.L., Leoni, S., Ohnishi, T. and Lenaz, G. (2009) 'Differential effects of mitochondrial Complex I inhibitors on production of reactive oxygen species', *Biochim Biophys Acta*, 1787(5), pp. 384-92.

Fausto, N. (2000) 'Liver regeneration', *J Hepatol*, 32(1 Suppl), pp. 19-31.

Fausto, N., Campbell, J.S. and Riehle, K.J. (2006) 'Liver regeneration', *Hepatology*, 43(2 Suppl 1), pp. S45-53.

Fellous, T.G., Islam, S., Tadrous, P.J., Elia, G., Kocher, H.M., Bhattacharya, S., Mears, L., Turnbull, D.M., Taylor, R.W., Greaves, L.C., Chinnery, P.F., Taylor, G., McDonald, S.A.C., Wright, N.A. and Alison, M.R. (2009) 'Locating the stem cell niche and tracing hepatocyte lineages in human liver', *Hepatology*, 49(5), pp. 1655-1663.

Ferri, D., Moro, L., Mastrodonato, M., Capuano, F., Marra, E., Liquori, G.E. and Greco, M. (2005) 'Ultrastructural zonal heterogeneity of hepatocytes and mitochondria within the hepatic acinus during liver regeneration after partial hepatectomy', *Biol Cell*, 97(4), pp. 277-88.

Finch, C.E. and Tanzi, R.E. (1997) 'Genetics of aging', *Science*, 278(5337), pp. 407-11.

Fisher, D., Krasinska, L., Coudreuse, D. and Novák, B. (2012) 'Phosphorylation network dynamics in the control of cell cycle transitions', *Journal of Cell Science*, 125(20), pp. 4703-4711.

Flusberg, D.A. and Sorger, P.K. (2015) 'Surviving apoptosis: life-death signaling in single cells', *Trends Cell Biol*, 25(8), pp. 446-58.

Forner, F., Foster, L.J., Campanaro, S., Valle, G. and Mann, M. (2006) 'Quantitative proteomic comparison of rat mitochondria from muscle, heart, and liver', *Mol Cell Proteomics*, 5(4), pp. 608-19.

Fortner, J.G. and Lincer, R.M. (1990) 'Hepatic resection in the elderly', *Ann Surg*, 211(2), pp. 141-5.

Franceschi, C. and Campisi, J. (2014) 'Chronic inflammation (inflammaging) and its potential contribution to age-associated diseases', *J Gerontol A Biol Sci Med Sci*, 69 Suppl 1, pp. S4-9.

Frey, T.G. and Mannella, C.A. (2000) 'The internal structure of mitochondria', *Trends Biochem Sci*, 25(7), pp. 319-24.

Frith, J., Jones, D. and Newton, J.L. (2008) 'Chronic liver disease in an ageing population', *Age and Ageing*, 38(1), pp. 11-18.

Frith, J., Jones, D. and Newton, J.L. (2009) 'Chronic liver disease in an ageing population', *Age Ageing*, 38(1), pp. 11-8.

Fu, Z., Malureanu, L., Huang, J., Wang, W., Li, H., van Deursen, J.M., Tindall, D.J. and Chen, J. (2008) 'Plk1-dependent phosphorylation of FoxM1 regulates a transcriptional programme required for mitotic progression', *Nat Cell Biol*, 10(9), pp. 1076-82.

Furchtgott, L.A., Chow, C.C. and Periwal, V. (2009) 'A model of liver regeneration', *Biophys J*, 96(10), pp. 3926-35.

Furuyama, K., Kawaguchi, Y., Akiyama, H., Horiguchi, M., Kodama, S., Kuhara, T., Hosokawa, S., Elbahrawy, A., Soeda, T., Koizumi, M., Masui, T., Kawaguchi, M., Takaori, K., Doi, R., Nishi, E., Kakinoki, R., Deng, J.M., Behringer, R.R., Nakamura, T. and Uemoto, S. (2011) 'Continuous cell supply from a Sox9-expressing progenitor zone in adult liver, exocrine pancreas and intestine', *Nat Genet*, 43(1), pp. 34-41.

Gan, L., Chitturi, S. and Farrell, G.C. (2011) 'Mechanisms and Implications of Age-Related Changes in the Liver: Nonalcoholic Fatty Liver Disease in the Elderly', *Current Gerontology and Geriatrics Research*, 2011, p. 12.

Gavrilov, L.A. and Gavrilova, N.S. (2002) 'Evolutionary theories of aging and longevity', *ScientificWorldJournal*, 2, pp. 339-56.

Gebhardt, R. and Hovhannisyan, A. (2010) 'Organ patterning in the adult stage: the role of Wnt/beta-catenin signaling in liver zonation and beyond', *Dev Dyn*, 239(1), pp. 45-55.

Gieling, R.G., Elsharkawy, A.M., Caamano, J.H., Cowie, D.E., Wright, M.C., Ebrahimkhani, M.R., Mann, J., Raychaudhuri, P., Liou, H.C., Oakley, F., Mann, D.A. (2010) 'The c-Rel subunit of nuclear factor kappaB regulates murine liver inflammation, wound-healing, and hepatocyte proliferation', *Hepatology*, 51 (3), pp.922-31.

Gomez, C.R., Karavitis, J., Palmer, J.L., Faunce, D.E., Ramirez, L., Nomellini, V. and Kovacs, E.J. (2010) 'Interleukin-6 Contributes to Age-Related Alteration of Cytokine Production by Macrophages', *Mediators of Inflammation*, 2010, p. 7.

Gonzalez-Freire, M., de Cabo, R., Bernier, M., Sollott, S.J., Fabbri, E., Navas, P. and Ferrucci, L. (2015) 'Reconsidering the Role of Mitochondria in Aging', *J Gerontol A Biol Sci Med Sci*, 70(11), pp. 1334-42.

Grattagliano, I., Russmann, S., Diogo, C., Bonfrate, L., Oliveira, P.J., Wang, D.Q. and Portincasa, P. (2011) 'Mitochondria in chronic liver disease', *Curr Drug Targets*, 12(6), pp. 879-93.

Greaves, L.C., Nooteboom, M., Elson, J.L., Tuppen, H.A., Taylor, G.A., Commane, D.M., Arasaradnam, R.P., Khrapko, K., Taylor, R.W., Kirkwood, T.B., Mathers, J.C. and Turnbull, D.M. (2014) 'Clonal expansion of early to mid-life mitochondrial DNA point mutations drives mitochondrial dysfunction during human ageing', *PLoS Genet*, 10(9), p. e1004620.

Greaves, L.C. and Turnbull, D.M. (2009) 'Mitochondrial DNA mutations and ageing', *Biochim Biophys Acta*, 1790(10), pp. 1015-20.

Greber, B.J., Bieri, P., Leibundgut, M., Leitner, A., Aebersold, R., Boehringer, D. and Ban, N. (2015) 'Ribosome. The complete structure of the 55S mammalian mitochondrial ribosome', *Science*, 348(6232), pp. 303-8.

Greber, B.J., Boehringer, D., Leitner, A., Bieri, P., Voigts-Hoffmann, F., Erzberger, J.P., Leibundgut, M., Aebersold, R. and Ban, N. (2014) 'Architecture of the large subunit of the mammalian mitochondrial ribosome', *Nature*, 505(7484), pp. 515-9.

Guarente, L. (2011) 'Sirtuins, aging, and metabolism', *Cold Spring Harb Symp Quant Biol*, 76, pp. 81-90.

Guerrieri, F., Pellecchia, G., Lopriore, B., Papa, S., Esterina Liquori, G., Ferri, D., Moro, L., Marra, E. and Greco, M. (2002) 'Changes in ultrastructure and the occurrence of permeability transition in mitochondria during rat liver regeneration', *Eur J Biochem*, 269(13), pp. 3304-12.

Guo, Y., Ding, Q., Chen, L., Ji, C., Hao, H., Wang, J., Qi, W., Xie, X., Ma, J., Li, A., Jiang, X., Li, X. and Jiang, H. (2017) 'Overexpression of Heparin-Binding Epidermal Growth Factor-Like Growth Factor Mediates Liver Fibrosis in Transgenic Mice', *Am J Med Sci*, 354(2), pp. 199-210.

Gurung, P., Lukens, J.R. and Kanneganti, T.-D. (2015) 'Mitochondria: diversity in the regulation of the NLRP3 inflammasome', *Trends in Molecular Medicine*, 21(3), pp. 193-201.
Gustafsson, C.M., Falkenberg, M. and Larsson, N.G. (2016) 'Maintenance and Expression of Mammalian Mitochondrial DNA', *Annu Rev Biochem*, 85, pp. 133-60.
Gutierrez-Gonzalez, L., Deheragoda, M., Elia, G., Leedham, S.J., Shankar, A., Imber, C., Jankowski, J.A., Turnbull, D.M., Novelli, M., Wright, N.A. and McDonald, S.A. (2009) 'Analysis of the clonal architecture of the human small intestinal epithelium establishes a common stem cell for all lineages and reveals a mechanism for the fixation and spread of mutations', *J Pathol*, 217(4), pp. 489-96.
Haag, S., Sloan, K.E., Ranjan, N., Warda, A.S., Kretschmer, J., Blessing, C., Hubner, B., Seikowski, J., Dennerlein, S., Rehling, P., Rodnina, M.V. and Hobartner, C. (2016) 'NSUN3 and ABH1 modify the wobble position of mt-tRNAMet to expand codon recognition in mitochondrial translation', 35(19), pp. 2104-2119.
Hafner, A., Bulyk, M.L., Jambhekar, A. and Lahav, G. (2019) 'The multiple mechanisms that regulate p53 activity and cell fate', 20(4), pp. 199-210.
Haque, M.E. and Spremulli, L.L. (2008) 'Roles of the N- and C-terminal domains of mammalian mitochondrial initiation factor 3 in protein biosynthesis', *J Mol Biol*, 384(4), pp. 929-40.
Harman, D. (1956) 'Aging: a theory based on free radical and radiation chemistry', *J Gerontol*, 11(3), pp. 298-300.
Harman, D. (1972) 'The biologic clock: the mitochondria?', *J Am Geriatr Soc*, 20(4), pp. 145-7.
Hartley, D.P., Kolaja, K.L., Reichard, J. and Petersen, D.R. (1999) '4-Hydroxynonenal and Malondialdehyde Hepatic Protein Adducts in Rats Treated with Carbon Tetrachloride: Immunochemical Detection and Lobular Localization', *Toxicology and Applied Pharmacology*, 161(1), pp. 23-33.
Hartwell, L.H., Culotti, J. and Reid, B. (1970) 'Genetic control of the cell-division cycle in yeast. I. Detection of mutants', *Proc Natl Acad Sci U S A*, 66(2), pp. 352-9.
Hatta, S. (1985) 'Influence of plasma hormone levels on various stimulant-induced hepatic DNA synthesis in carbon tetrachloride-intoxicated rats', *Jpn J Pharmacol*, 37(1), pp. 77-84.
Hayashi, I. and Carr, B.I. (1985) 'DNA synthesis in rat hepatocytes: inhibition by a platelet factor and stimulation by an endogenous factor', *J Cell Physiol*, 125(1), pp. 82-90.
Hayden, M.S. and Ghosh, S. (2012) 'NF-kappaB, the first quarter-century: remarkable progress and outstanding questions', *Genes Dev*, 26(3), pp. 203-34.
Hayden, M.S. and Ghosh, S. (2014) 'Regulation of NF-κB by TNF family cytokines', *Semin Immunol*, 26(3), pp. 253-66.
Hayflick, L. and Moorhead, P.S. (1961) 'The serial cultivation of human diploid cell strains', *Experimental Cell Research*, 25(3), pp. 585-621.

He, X., Zhou, A., Lu, H., Chen, Y., Huang, G., Yue, X., Zhao, P. and Wu, Y. (2013) 'Suppression of Mitochondrial Complex I Influences Cell Metastatic Properties', *PLOS ONE*, 8(4), p. e61677.
Heinz, S., Freyberger, A., Lawrenz, B., Schladt, L., Schmuck, G. and Ellinger-Ziegelbauer, H. (2017) 'Mechanistic Investigations of the Mitochondrial Complex I Inhibitor Rotenone in the Context of Pharmacological and Safety Evaluation', *Sci Rep*, 7, p. 45465.
Hellerbrand, C., Stefanovic, B., Giordano, F., Burchardt, E.R. and Brenner, D.A. (1999) 'The role of TGFbeta1 in initiating hepatic stellate cell activation in vivo', *J Hepatol*, 30(1), pp. 77-87.
Herbener, G.H. (1976) 'A morphometric study of age-dependent changes in mitochondrial population of mouse liver and heart', *J Gerontol*, 31(1), pp. 8-12.
Herbst, A., Pak, J.W., McKenzie, D., Bua, E., Bassiouni, M. and Aiken, J.M. (2007) 'Accumulation of mitochondrial DNA deletion mutations in aged muscle fibers: evidence for a causal role in muscle fiber loss', *J Gerontol A Biol Sci Med Sci*, 62(3), pp. 235-45.
Herbst, A., Wanagat, J., Cheema, N., Widjaja, K., McKenzie, D. and Aiken, J.M. (2016) 'Latent mitochondrial DNA deletion mutations drive muscle fiber loss at old age', *Aging Cell*, 15(6), pp. 1132-1139.
Hernandez-Munoz, R., Sanchez-Sevilla, L., Martinez-Gomez, A. and Dent, M.A. (2003) 'Changes in mitochondrial adenine nucleotides and in permeability transition in two models of rat liver regeneration', *Hepatology*, 37(4), pp. 842-51.
Herrero, A. and Barja, G. (1997) 'Sites and mechanisms responsible for the low rate of free radical production of heart mitochondria in the long-lived pigeon', *Mech Ageing Dev*, 98(2), pp. 95-111.
Herscovitch, M., Comb, W., Ennis, T., Coleman, K., Yong, S., Armstead, B., Kalaitzidis, D., Chandani, S. and Gilmore, T.D. (2008) 'Intermolecular disulfide bond formation in the NEMO dimer requires Cys54 and Cys347', *Biochem Biophys Res Commun*, 367(1), pp. 103-8.
Hewitt, G., Jurk, D., Marques, F.D., Correia-Melo, C., Hardy, T., Gackowska, A., Anderson, R., Taschuk, M., Mann, J. and Passos, J.F. (2012) 'Telomeres are favoured targets of a persistent DNA damage response in ageing and stress-induced senescence', *Nat Commun*, 3, p. 708.
Higashi, T., Friedman, S.L. and Hoshida, Y. (2017) 'Hepatic stellate cells as key target in liver fibrosis', *Adv Drug Deliv Rev*, 121, pp. 27-42.
Higgins, G.M. (1931) 'Experimental pathology of the liver. Restoration of the liver of the white rat following partial surgical removal', *AMA Arch Pathol*, 12, pp. 186-202.
Hiona, A., Sanz, A., Kujoth, G.C., Pamplona, R., Seo, A.Y., Hofer, T., Someya, S., Miyakawa, T., Nakayama, C., Samhan-Arias, A.K., Servais, S., Barger, J.L., Portero-Otín, M., Tanokura, M., Prolla, T.A. and Leeuwenburgh, C. (2010) 'Mitochondrial DNA Mutations Induce Mitochondrial Dysfunction, Apoptosis and Sarcopenia in Skeletal Muscle of Mitochondrial DNA Mutator Mice', *PLOS ONE*, 5(7), p. e11468.

Hoenicke, L. and Zender, L. (2012) 'Immune surveillance of senescent cells--biological significance in cancer- and non-cancer pathologies', *Carcinogenesis*, 33(6), pp. 1123-6.
Holt, I.J., Lorimer, H.E. and Jacobs, H.T. (2000) 'Coupled leading- and lagging-strand synthesis of mammalian mitochondrial DNA', *Cell*, 100(5), pp. 515-24.
Hsu, H., Xiong, J. and Goeddel, D.V. (1995) 'The TNF receptor 1-associated protein TRADD signals cell death and NF-kappa B activation', *Cell*, 81(4), pp. 495-504.
Huang, T.T., Carlson, E.J., Kozy, H.M., Mantha, S., Goodman, S.I., Ursell, P.C. and Epstein, C.J. (2001) 'Genetic modification of prenatal lethality and dilated cardiomyopathy in Mn superoxide dismutase mutant mice', *Free Radic Biol Med*, 31(9), pp. 1101-10.
Huang, Z.Z., Li, H., Cai, J., Kuhlenkamp, J., Kaplowitz, N. and Lu, S.C. (1998) 'Changes in glutathione homeostasis during liver regeneration in the rat', *Hepatology*, 27(1), pp. 147-53.
Huh, C.G., Factor, V.M., Sanchez, A., Uchida, K., Conner, E.A. and Thorgeirsson, S.S. (2004) 'Hepatocyte growth factor/c-met signaling pathway is required for efficient liver regeneration and repair', *Proc Natl Acad Sci U S A*, 101(13), pp. 4477-82.
Huynen, M.A., Duarte, I., Chrzanowska-Lightowlers, Z.M. and Nabuurs, S.B. (2012) 'Structure based hypothesis of a mitochondrial ribosome rescue mechanism', *Biol Direct*, 7, p. 14.
Ichimura, H., Parthasarathi, K., Quadri, S., Issekutz, A.C. and Bhattacharya, J. (2003) 'Mechano-oxidative coupling by mitochondria induces proinflammatory responses in lung venular capillaries', *J Clin Invest*, 111(5), pp. 691-9.
Iimuro, Y. and Fujimoto, J. (2010) 'TLRs, NF-κB, JNK, and Liver Regeneration', *Gastroenterol Res Pract*, 2010.
Iimuro, Y., Nishiura, T., Hellerbrand, C., Behrns, K.E., Schoonhoven, R., Grisham, J.W. and Brenner, D.A. (1998) 'NFkappaB prevents apoptosis and liver dysfunction during liver regeneration', *J Clin Invest*, 101(4), pp. 802-11.
Inomoto, T., Tanaka, A., Mori, S., Jin, M.B., Sato, B., Yanabu, N., Tokuka, A., Kitai, T., Ozawa, K. and Yamaoka, Y. (1994) 'Changes in the distribution of the control of the mitochondrial oxidative phosphorylation in regenerating rabbit liver', *Biochim Biophys Acta*, 1188(3), pp. 311-7.
Iredale, J.P., Benyon, R.C., Pickering, J., McCullen, M., Northrop, M., Pawley, S., Hovell, C. and Arthur, M.J. (1998) 'Mechanisms of spontaneous resolution of rat liver fibrosis. Hepatic stellate cell apoptosis and reduced hepatic expression of metalloproteinase inhibitors', *J Clin Invest*, 102(3), pp. 538-49.
Ishihara, Y., Takemoto, T., Itoh, K., Ishida, A. and Yamazaki, T. (2015) 'Dual role of superoxide dismutase 2 induced in activated microglia: oxidative stress tolerance and convergence of inflammatory responses', *J Biol Chem*, 290(37), pp. 22805-17.
Ito, N., Kawata, S., Tamura, S., Kiso, S., Tsushima, H., Damm, D., Abraham, J.A., Higashiyama, S., Taniguchi, N. and Matsuzawa, Y. (1994) 'Heparin-binding EGF-like growth factor is a potent mitogen for rat hepatocytes', *Biochem Biophys Res Commun*, 198(1), pp. 25-31.

Iwai, M., Cui, T.X., Kitamura, H., Saito, M. and Shimazu, T. (2001) 'Increased secretion of tumour necrosis factor and interleukin 6 from isolated, perfused liver of rats after partial hepatectomy', *Cytokine*, 13(1), pp. 60-64.

Iyer, S.S., Pulskens, W.P., Sadler, J.J., Butter, L.M., Teske, G.J., Ulland, T.K., Eisenbarth, S.C., Florquin, S., Flavell, R.A., Leemans, J.C. and Sutterwala, F.S. (2009) 'Necrotic cells trigger a sterile inflammatory response through the Nlrp3 inflammasome', *Proc Natl Acad Sci U S A*, 106(48), pp. 20388-93.

Jeffrey, P.D., Tong, L. and Pavletich, N.P. (2000) 'Structural basis of inhibition of CDK-cyclin complexes by INK4 inhibitors', *Genes Dev*, 14(24), pp. 3115-25.

Jenner, P. (2003) 'Oxidative stress in Parkinson's disease', *Ann Neurol*, 53 Suppl 3, pp. S26-36; discussion S36-8.

Jho, E.H., Zhang, T., Domon, C., Joo, C.K., Freund, J.N. and Costantini, F. (2002) 'Wnt/beta-catenin/Tcf signaling induces the transcription of Axin2, a negative regulator of the signaling pathway', *Mol Cell Biol*, 22(4), pp. 1172-83.

Jiang, J.X. and Torok, N.J. (2013) 'Liver Injury and the Activation of the Hepatic Myofibroblasts', *Curr Pathobiol Rep*, 1(3), pp. 215-223.

Jiang, X., Chen, Y., Wei, H., Sun, R. and Tian, Z. (2013) 'Characterizing the lymphopoietic kinetics and features of hematopoietic progenitors contained in the adult murine liver in vivo', *PLoS One*, 8(10), p. e76762.

Jiang, Y., Liu, J., Waalkes, M. and Kang, Y.J. (2004) 'Changes in the gene expression associated with carbon tetrachloride-induced liver fibrosis persist after cessation of dosing in mice', *Toxicol Sci*, 79(2), pp. 404-10.

Jin, J., Iakova, P., Jiang, Y., Medrano, E.E. and Timchenko, N.A. (2011) 'The reduction of SIRT1 in livers of old mice leads to impaired body homeostasis and to inhibition of liver proliferation', *Hepatology*, 54(3), pp. 989-98.

Jin, J., Wang, G.L., Timchenko, L. and Timchenko, N.A. (2009) 'GSK3beta and aging liver', *Aging (Albany NY)*, 1(6), pp. 582-5.

Jirtle, R.L., Carr, B.I. and Scott, C.D. (1991) 'Modulation of insulin-like growth factor-II/mannose 6-phosphate receptors and transforming growth factor-beta 1 during liver regeneration', *J Biol Chem*, 266(33), pp. 22444-50.

Jones, P.L., Ping, D. and Boss, J.M. (1997) 'Tumor necrosis factor alpha and interleukin-1beta regulate the murine manganese superoxide dismutase gene through a complex intronic enhancer involving C/EBP-beta and NF-kappaB', *Mol Cell Biol*, 17(12), pp. 6970-81.

José Gómez-Lechón, M., Castelli, J., Guillén, I., o'Connor, E., Nakamura, T., Fabra, R. and Trullenque, R. (1995) 'Effects of hepatocyte growth factor on the growth and metabolism of human hepatocytes in primary culture', *Hepatology*, 21(5), pp. 1248-1254.

Jungermann, K. and Kietzmann, T. (2000) 'Oxygen: Modulator of metabolic zonation and disease of the liver', *Hepatology*, 31(2), pp. 255-260.

Jurk, D., Wilson, C., Passos, J.F., Oakley, F., Correia-Melo, C., Greaves, L., Saretzki, G., Fox, C., Lawless, C., Anderson, R., Hewitt, G., Pender, S.L., Fullard, N., Nelson, G., Mann, J., van de Sluis, B., Mann, D.A. and von Zglinicki, T. (2014) 'Chronic inflammation induces telomere dysfunction and accelerates ageing in mice', *Nat Commun*, 2, p. 4172.

Kaidi, A., Williams, A.C. and Paraskeva, C. (2007) 'Interaction between beta-catenin and HIF-1 promotes cellular adaptation to hypoxia', *Nat Cell Biol*, 9(2), pp. 210-7.

Kamata, H., Manabe, T., Oka, S., Kamata, K. and Hirata, H. (2002) 'Hydrogen peroxide activates IkappaB kinases through phosphorylation of serine residues in the activation loops', *FEBS Lett*, 519(1-3), pp. 231-7.

Kamenisch, Y., Fousteri, M., Knoch, J., von Thaler, A.-K., Fehrenbacher, B., Kato, H., Becker, T., Dollé, M.E.T., Kuiper, R., Majora, M., Schaller, M., van der Horst, G.T.J., van Steeg, H., Röcken, M., Rapaport, D., Krutmann, J., Mullenders, L.H. and Berneburg, M. (2010) 'Proteins of nucleotide and base excision repair pathways interact in mitochondria to protect from loss of subcutaneous fat, a hallmark of aging', *The Journal of Experimental Medicine*, 207(2), p. 379.

Kamiyama, Y., Ozawa, K. and Honjo, I. (1976) 'Changes in mitochondrial phosphorylative activity and adenylate energy charge of regenerating rabbit liver', *J Biochem*, 80(4), pp. 875-81.

Kan, N.G., Junghans, D. and Izpisua Belmonte, J.C. (2009) 'Compensatory growth mechanisms regulated by BMP and FGF signaling mediate liver regeneration in zebrafish after partial hepatectomy', *Faseb j*, 23(10), pp. 3516-25.

Kapoor, M. and Lozano, G. (1998) 'Functional activation of p53 via phosphorylation following DNA damage by UV but not gamma radiation', *Proc Natl Acad Sci U S A*, 95(6), pp. 2834-7.

Kaushal, P.S., Sharma, M.R., Booth, T.M., Haque, E.M., Tung, C.S., Sanbonmatsu, K.Y., Spremulli, L.L. and Agrawal, R.K. (2014) 'Cryo-EM structure of the small subunit of the mammalian mitochondrial ribosome', *Proc Natl Acad Sci U S A*, 111(20), pp. 7284-9.

Kazak, L., Reyes, A. and Holt, I.J. (2012) 'Minimizing the damage: repair pathways keep mitochondrial DNA intact', *Nature Reviews Molecular Cell Biology*, 13, p. 659.

Kerr, J.F., Wyllie, A.H. and Currie, A.R. (1972) 'Apoptosis: a basic biological phenomenon with wide-ranging implications in tissue kinetics', *Br J Cancer*, 26(4), pp. 239-57.

Khrapko, K., Kraytsberg, Y., De Grey, A.D.N.J., Vijg, J. and Schon, E.A. (2006) 'Does premature aging of the mtDNA mutator mouse prove that mtDNA mutations are involved in natural aging?', *Aging Cell*, 5(3), pp. 279-282.

Khrapko, K. and Vijg, J. (2007) 'Mitochondrial DNA mutations and aging: a case closed?', *Nat Genet*, 39(4), pp. 445-6.

Kietzmann, T. (2017) 'Metabolic zonation of the liver: The oxygen gradient revisited', *Redox Biol*, 11, pp. 622-630.
Kietzmann, T., Cornesse, Y., Brechtel, K., Modaressi, S. and Jungermann, K. (2001) 'Perivenous expression of the mRNA of the three hypoxia-inducible factor alpha-subunits, HIF1alpha, HIF2alpha and HIF3alpha, in rat liver', *Biochem J*, 354(Pt 3), pp. 531-7.
Kim, H.O., Kim, H.-S., Youn, J.-C., Shin, E.-C. and Park, S. (2011) 'Serum cytokine profiles in healthy young and elderly population assessed using multiplexed bead-based immunoassays', *Journal of Translational Medicine*, 9(1), p. 113.
Kim, I.H., Kisseleva, T. and Brenner, D.A. (2015) 'Aging and liver disease', *Curr Opin Gastroenterol*, 31(3), pp. 184-91.
Kim, K.H., Chen, C.C., Monzon, R.I. and Lau, L.F. (2013) 'Matricellular protein CCN1 promotes regression of liver fibrosis through induction of cellular senescence in hepatic myofibroblasts', *Mol Cell Biol*, 33(10), pp. 2078-90.
Kim, T.H., Mars, W.M., Stolz, D.B., Petersen, B.E. and Michalopoulos, G.K. (1997) 'Extracellular matrix remodeling at the early stages of liver regeneration in the rat', *Hepatology*, 26(4), pp. 896-904.
Kinoshita, T., Hirao, S., Matsumoto, K. and Nakamura, T. (1991) 'Possible endocrine control by hepatocyte growth factor of liver regeneration after partial hepatectomy', *Biochem Biophys Res Commun*, 177(1), pp. 330-5.
Kirkwood, T.B. (1997) 'The origins of human ageing', *Philos Trans R Soc Lond B Biol Sci*, 352(1363), pp. 1765-72.
Kirkwood, T.B.L. (1977) 'Evolution of ageing', *Nature*, 270(5635), pp. 301-304.
Kirkwood, T.B.L., Holliday, R., Maynard Smith, J. and Holliday, R. (1979) 'The evolution of ageing and longevity', *Proceedings of the Royal Society of London. Series B. Biological Sciences*, 205(1161), pp. 531-546.
Kischkel, F.C., Hellbardt, S., Behrmann, I., Germer, M., Pawlita, M., Krammer, P.H. and Peter, M.E. (1995) 'Cytotoxicity-dependent APO-1 (Fas/CD95)-associated proteins form a death-inducing signaling complex (DISC) with the receptor', *Embo j*, 14(22), pp. 5579-88.
Kiso, S., Kawata, S., Tamura, S., Inui, Y., Yoshida, Y., Sawai, Y., Umeki, S., Ito, N., Yamada, A., Miyagawa, J.I., Higashiyama, S., Iwawaki, T., Saito, M., Taniguchi, N., Matsuzawa, Y. and Kohno, K. (2003) 'Liver regeneration in heparin-binding EGF-like growth factor transgenic mice after partial hepatectomy', *Gastroenterology*, 124(3), pp. 701-707.
Klement, J.F., Rice, N.R., Car, B.D., Abbondanzo, S.J., Powers, G.D., Bhatt, P.H., Chen, C.H., Rosen, C.A. and Stewart, C.L. (1996) 'IkappaBalpha deficiency results in a sustained NF-kappaB response and severe widespread dermatitis in mice', *Mol Cell Biol*, 16(5), pp. 2341-9.

Knockaert, L., Berson, A., Ribault, C., Prost, P.-E., Fautrel, A., Pajaud, J., Lepage, S., Lucas-Clerc, C., Bégué, J.-M., Fromenty, B. and Robin, M.-A. (2011) 'Carbon tetrachloride-mediated lipid peroxidation induces early mitochondrial alterations in mouse liver', *Laboratory Investigation*, 92, p. 396.
Koch, A., Saran, S., Tran, D.D., Klebba-Farber, S., Thiesler, H., Sewald, K., Schindler, S., Braun, A., Klopfleisch, R. and Tamura, T. (2014) 'Murine precision-cut liver slices (PCLS): a new tool for studying tumor microenvironments and cell signaling ex vivo', *Cell Commun Signal*, 12, p. 73.
Kogure, K., Omata, W., Kanzaki, M., Zhang, Y.Q., Yasuda, H., Mine, T. and Kojima, I. (1995) 'A single intraportal administration of follistatin accelerates liver regeneration in partially hepatectomized rats', *Gastroenterology*, 108(4), pp. 1136-42.
Kokoszka, J.E., Coskun, P., Esposito, L.A. and Wallace, D.C. (2001) 'Increased mitochondrial oxidative stress in the Sod2 (+/−) mouse results in the age-related decline of mitochondrial function culminating in increased apoptosis', *Proceedings of the National Academy of Sciences*, 98(5), pp. 2278-2283.
Koliaki, C., Szendroedi, J., Kaul, K., Jelenik, T., Nowotny, P., Jankowiak, F., Herder, C., Carstensen, M., Krausch, M., Knoefel, Wolfram T., Schlensak, M. and Roden, M. (2015) 'Adaptation of Hepatic Mitochondrial Function in Humans with Non-Alcoholic Fatty Liver Is Lost in Steatohepatitis', *Cell Metabolism*, 21(5), pp. 739-746.
Kopsidas, G., Kovalenko, S.A., Kelso, J.M. and Linnane, A.W. (1998) 'An age-associated correlation between cellular bioenergy decline and mtDNA rearrangements in human skeletal muscle', *Mutat Res*, 421(1), pp. 27-36.
Koury, S.T., Bondurant, M.C., Koury, M.J. and Semenza, G.L. (1991) 'Localization of cells producing erythropoietin in murine liver by in situ hybridization', *Blood*, 77(11), pp. 2497-503.
Kovalovich, K., DeAngelis, R.A., Li, W., Furth, E.E., Ciliberto, G. and Taub, R. (2000) 'Increased toxin-induced liver injury and fibrosis in interleukin-6-deficient mice', *Hepatology*, 31(1), pp. 149-59.
Kraytsberg, Y., Simon, D.K., Turnbull, D.M. and Khrapko, K. (2009) 'Do mtDNA deletions drive premature aging in mtDNA mutator mice?', *Aging Cell*, 8(4), pp. 502-506.
Krishnan, K.J., Reeve, A.K., Samuels, D.C., Chinnery, P.F., Blackwood, J.K., Taylor, R.W., Wanrooij, S., Spelbrink, J.N., Lightowlers, R.N. and Turnbull, D.M. (2008) 'What causes mitochondrial DNA deletions in human cells?', *Nat Genet*, 40(3), pp. 275-9.
Krizhanovsky, V., Yon, M., Dickins, R.A., Hearn, S., Simon, J., Miething, C., Yee, H., Zender, L. and Lowe, S.W. (2008) 'Senescence of activated stellate cells limits liver fibrosis', *Cell*, 134(4), pp. 657-67.
Kroeger, K.M., Hashimoto, M., Kow, Y.W. and Greenberg, M.M. (2003) 'Cross-linking of 2-deoxyribonolactone and its beta-elimination product by base excision repair enzymes', *Biochemistry*, 42(8), pp. 2449-55.
Kroemer, G., Galluzzi, L. and Brenner, C. (2007) 'Mitochondrial membrane permeabilization in cell death', *Physiol Rev*, 87(1), pp. 99-163.

Ku, H.-H. and Sohal, R.S. (1993) 'Comparison of mitochondrial pro-oxidant generation and anti-oxidant defenses between rat and pigeon: possible basis of variation in longevity and metabolic potential', *Mechanisms of Ageing and Development*, 72(1), pp. 67-76.

Kubota, T., Miyagishima, M., Frye, C.S., Alber, S.M., Bounoutas, G.S., Kadokami, T., Watkins, S.C., McTiernan, C.F. and Feldman, A.M. (2001) 'Overexpression of tumor necrosis factor- alpha activates both anti- and pro-apoptotic pathways in the myocardium', *J Mol Cell Cardiol*, 33(7), pp. 1331-44.

Kudo, S., Mizuno, K., Hirai, Y. and Shimizu, T. (1990) 'Clearance and tissue distribution of recombinant human interleukin 1 beta in rats', *Cancer Res*, 50(18), pp. 5751-5.

Kujoth, G.C., Hiona, A., Pugh, T.D., Someya, S., Panzer, K., Wohlgemuth, S.E., Hofer, T., Seo, A.Y., Sullivan, R., Jobling, W.A., Morrow, J.D., Van Remmen, H., Sedivy, J.M., Yamasoba, T., Tanokura, M., Weindruch, R., Leeuwenburgh, C. and Prolla, T.A. (2005) 'Mitochondrial DNA mutations, oxidative stress, and apoptosis in mammalian aging', *Science*, 309(5733), pp. 481-4.

Kukat, C., Davies, K.M., Wurm, C.A., Spahr, H., Bonekamp, N.A., Kuhl, I., Joos, F., Polosa, P.L., Park, C.B., Posse, V., Falkenberg, M., Jakobs, S., Kuhlbrandt, W. and Larsson, N.G. (2015) 'Cross-strand binding of TFAM to a single mtDNA molecule forms the mitochondrial nucleoid', *Proc Natl Acad Sci U S A*, 112(36), pp. 11288-93.

Kukat, C. and Larsson, N.G. (2013) 'mtDNA makes a U-turn for the mitochondrial nucleoid', *Trends Cell Biol*, 23(9), pp. 457-63.

Kukat, C., Wurm, C.A., Spahr, H., Falkenberg, M., Larsson, N.G. and Jakobs, S. (2011) 'Super-resolution microscopy reveals that mammalian mitochondrial nucleoids have a uniform size and frequently contain a single copy of mtDNA', *Proc Natl Acad Sci U S A*, 108(33), pp. 13534-9.

Kuwahara, R., Kofman, A.V., Landis, C.S., Swenson, E.S., Barendswaard, E. and Theise, N.D. (2008) 'The hepatic stem cell niche: identification by label-retaining cell assay', *Hepatology*, 47(6), pp. 1994-2002.

Laoukili, J., Alvarez, M., Meijer, L.A., Stahl, M., Mohammed, S., Kleij, L., Heck, A.J. and Medema, R.H. (2008) 'Activation of FoxM1 during G2 requires cyclin A/Cdk-dependent relief of autorepression by the FoxM1 N-terminal domain', *Mol Cell Biol*, 28(9), pp. 3076-87.

Larsson, N.G. and Clayton, D.A. (1995) 'Molecular genetic aspects of human mitochondrial disorders', *Annu Rev Genet*, 29, pp. 151-78.

Larsson, N.G., Wang, J., Wilhelmsson, H., Oldfors, A., Rustin, P., Lewandoski, M., Barsh, G.S. and Clayton, D.A. (1998) 'Mitochondrial transcription factor A is necessary for mtDNA maintenance and embryogenesis in mice', *Nat Genet*, 18(3), pp. 231-6.

Lavin, M.F. and Gueven, N. (2006) 'The complexity of p53 stabilization and activation', *Cell Death Differ*, 13(6), pp. 941-50.

Lazarou, M., Thorburn, D.R., Ryan, M.T. and McKenzie, M. (2009) 'Assembly of mitochondrial complex I and defects in disease', *Biochim Biophys Acta*, 1793(1), pp. 78-88.

Le Couteur, D.G., Cogger, V.C., Markus, A.M., Harvey, P.J., Yin, Z.L., Ansselin, A.D. and McLean, A.J. (2001) 'Pseudocapillarization and associated energy limitation in the aged rat liver', *Hepatology*, 33(3), pp. 537-43.

Lebovitz, R.M., Zhang, H., Vogel, H., Cartwright, J., Jr., Dionne, L., Lu, N., Huang, S. and Matzuk, M.M. (1996) 'Neurodegeneration, myocardial injury, and perinatal death in mitochondrial superoxide dismutase-deficient mice', *Proc Natl Acad Sci U S A*, 93(18), pp. 9782-7.

Lehwald, N., Tao, G.Z., Jang, K.Y., Sorkin, M., Knoefel, W.T. and Sylvester, K.G. (2011) 'Wnt-beta-catenin signaling protects against hepatic ischemia and reperfusion injury in mice', *Gastroenterology*, 141(2), pp. 707-18, 718.e1-5.

Leithauser, F., Dhein, J., Mechtersheimer, G., Koretz, K., Bruderlein, S., Henne, C., Schmidt, A., Debatin, K.M., Krammer, P.H. and Moller, P. (1993) 'Constitutive and induced expression of APO-1, a new member of the nerve growth factor/tumor necrosis factor receptor superfamily, in normal and neoplastic cells', *Lab Invest*, 69(4), pp. 415-29.

Lenaz, G., Bovina, C., Castelluccio, C., Fato, R., Formiggini, G., Genova, M.L., Marchetti, M., Pich, M.M., Pallotti, F., Parenti Castelli, G. and Biagini, G. (1997) 'Mitochondrial complex I defects in aging', *Mol Cell Biochem*, 174(1-2), pp. 329-33.

Li, N., Ragheb, K., Lawler, G., Sturgis, J., Rajwa, B., Melendez, J.A. and Robinson, J.P. (2003) 'Mitochondrial complex I inhibitor rotenone induces apoptosis through enhancing mitochondrial reactive oxygen species production', *J Biol Chem*, 278(10), pp. 8516-25.

Li, Y., Huang, T.T., Carlson, E.J., Melov, S., Ursell, P.C., Olson, J.L., Noble, L.J., Yoshimura, M.P., Berger, C., Chan, P.H., Wallace, D.C. and Epstein, C.J. (1995) 'Dilated cardiomyopathy and neonatal lethality in mutant mice lacking manganese superoxide dismutase', *Nat Genet*, 11(4), pp. 376-81.

Libermann, T.A. and Baltimore, D. (1990) 'Activation of interleukin-6 gene expression through the NF-kappa B transcription factor', *Mol Cell Biol*, 10(5), pp. 2327-34.

Lightowlers, R.N., Chinnery, P.F., Turnbull, D.M. and Howell, N. (1997) 'Mammalian mitochondrial genetics: heredity, heteroplasmy and disease', *Trends Genet*, 13(11), pp. 450-5.

Lim, S. and Kaldis, P. (2013) 'Cdks, cyclins and CKIs: roles beyond cell cycle regulation', *Development*, 140(15), pp. 3079-93.

Lind, C., Sund, J. and Aqvist, J. (2013) 'Codon-reading specificities of mitochondrial release factors and translation termination at non-standard stop codons', *Nat Commun*, 4, p. 2940.

Lindroos, P.M., Zarnegar, R. and Michalopoulos, G.K. (1991) 'Hepatocyte growth factor (hepatopoietin A) rapidly increases in plasma before DNA synthesis and liver regeneration stimulated by partial hepatectomy and carbon tetrachloride administration', *Hepatology*, 13(4), pp. 743-50.

Lipski, R., Lippincott, D.J., Durden, B.C., Kaplan, A.R., Keiser, H.E., Park, J.H. and Levesque, A.A. (2012) 'p53 Dimers associate with a head-to-tail response element to repress cyclin B transcription', *PLoS One*, 7(8), p. e42615.

Liu, H., Sidiropoulos, P., Song, G., Pagliari, L.J., Birrer, M.J., Stein, B., Anrather, J. and Pope, R.M. (2000) 'TNF-alpha gene expression in macrophages: regulation by NF-kappa B is independent of c-Jun or C/EBP beta', *J Immunol*, 164(8), pp. 4277-85.

Liu, P. and Demple, B. (2010) 'DNA repair in mammalian mitochondria: Much more than we thought?', *Environ Mol Mutagen*, 51(5), pp. 417-26.

Liu, P., Qian, L., Sung, J.S., de Souza-Pinto, N.C., Zheng, L., Bogenhagen, D.F., Bohr, V.A., Wilson, D.M., 3rd, Shen, B. and Demple, B. (2008) 'Removal of oxidative DNA damage via FEN1-dependent long-patch base excision repair in human cell mitochondria', *Mol Cell Biol*, 28(16), pp. 4975-87.

Lodeiro, M.F., Uchida, A.U., Arnold, J.J., Reynolds, S.L., Moustafa, I.M. and Cameron, C.E. (2010) 'Identification of multiple rate-limiting steps during the human mitochondrial transcription cycle in vitro', *J Biol Chem*, 285(21), pp. 16387-402.

Logan, A., Shabalina, I.G., Prime, T.A., Rogatti, S., Kalinovich, A.V., Hartley, R.C., Budd, R.C., Cannon, B. and Murphy, M.P. (2014) 'In vivo levels of mitochondrial hydrogen peroxide increase with age in mtDNA mutator mice', *Aging Cell*, 13(4), pp. 765-8.

Lolli, G. and Johnson, L.N. (2005) 'CAK-Cyclin-dependent Activating Kinase: a key kinase in cell cycle control and a target for drugs?', *Cell Cycle*, 4(4), pp. 572-7.

Longley, M.J., Nguyen, D., Kunkel, T.A. and Copeland, W.C. (2001) 'The fidelity of human DNA polymerase gamma with and without exonucleolytic proofreading and the p55 accessory subunit', *J Biol Chem*, 276(42), pp. 38555-62.

Lopez-Armada, M.J., Carames, B., Martin, M.A., Cillero-Pastor, B., Lires-Dean, M., Fuentes-Boquete, I., Arenas, J. and Blanco, F.J. (2006) 'Mitochondrial activity is modulated by TNFalpha and IL-1beta in normal human chondrocyte cells', *Osteoarthritis Cartilage*, 14(10), pp. 1011-22.

Lopez-Armada, M.J., Riveiro-Naveira, R.R., Vaamonde-Garcia, C. and Valcarcel-Ares, M.N. (2013) 'Mitochondrial dysfunction and the inflammatory response', *Mitochondrion*, 13(2), pp. 106-18.

López-Fontal, R., Zeini, M., Través, P.G., Gómez-Ferrería, M., Aranda, A., Sáez, G.T., Cerdá, C., Martín-Sanz, P., Hortelano, S. and Boscá, L. (2010) 'Mice lacking thyroid hormone receptor Beta show enhanced apoptosis and delayed liver commitment for proliferation after partial hepatectomy', *PloS one*, 5(1), p. e8710 [Online]. Available at: http://europepmc.org/abstract/MED/20090848 http://europepmc.org/articles/PMC2806828?pdf=render http://europepmc.org/articles/PMC2806828 https://www.ncbi.nlm.nih.gov/pmc/articles/pmid/20090848/pdf/?tool=EBI https://www.ncbi.nlm.nih.gov/pmc/articles/pmid/20090848/?tool=EBI https://doi.org/10.1371/journal.pone.0008710 DOI: 10.1371/journal.pone.0008710 (Accessed: 2010).

Lopez-Otin, C., Blasco, M.A., Partridge, L., Serrano, M. and Kroemer, G. (2013) 'The hallmarks of aging', *Cell*, 153(6), pp. 1194-217.

Loud, A.V. (1968) 'A quantitative stereological description of the ultrastructure of normal rat liver parenchymal cells', *J Cell Biol*, 37(1), pp. 27-46.
Low, R.L. (2003) 'Mitochondrial Endonuclease G function in apoptosis and mtDNA metabolism: a historical perspective', *Mitochondrion*, 2(4), pp. 225-36.
Lu, S.C. (2009) 'Regulation of glutathione synthesis', *Mol Aspects Med*, 30(1-2), pp. 42-59.
Lucas, J.J., Hernandez, F., Gomez-Ramos, P., Moran, M.A., Hen, R. and Avila, J. (2001) 'Decreased nuclear beta-catenin, tau hyperphosphorylation and neurodegeneration in GSK-3beta conditional transgenic mice', *Embo j*, 20(1-2), pp. 27-39.
Lukas, J. and Bartek, J. (2004) 'Cell division: the heart of the cycle', *Nature*, 432(7017), pp. 564-7.
Lukas, J., Lukas, C. and Bartek, J. (2004) 'Mammalian cell cycle checkpoints: signalling pathways and their organization in space and time', *DNA Repair (Amst)*, 3(8-9), pp. 997-1007.
Lynch, A.M. and Lynch, M.A. (2002) 'The age-related increase in IL-1 type I receptor in rat hippocampus is coupled with an increase in caspase-3 activation', *Eur J Neurosci*, 15(11), pp. 1779-88.
Ma, H., Lee, Y., Hayama, T., Van Dyken, C., Marti-Gutierrez, N., Li, Y., Ahmed, R. and Koski, A. (2018) 'Germline and somatic mtDNA mutations in mouse aging', 13(7), p. e0201304.
Macip, S., Igarashi, M., Berggren, P., Yu, J., Lee, S.W. and Aaronson, S.A. (2003) 'Influence of induced reactive oxygen species in p53-mediated cell fate decisions', *Mol Cell Biol*, 23(23), pp. 8576-85.
Macip, S., Igarashi, M., Fang, L., Chen, A., Pan, Z.Q., Lee, S.W. and Aaronson, S.A. (2002) 'Inhibition of p21-mediated ROS accumulation can rescue p21-induced senescence', *Embo j*, 21(9), pp. 2180-8.
Maeda, S., Kamata, H., Luo, J.L., Leffert, H. and Karin, M. (2005) 'IKKbeta couples hepatocyte death to cytokine-driven compensatory proliferation that promotes chemical hepatocarcinogenesis', *Cell*, 121(7), pp. 977-90.
Maehara, K., Hasegawa, T. and Isobe, K.I. (2000) 'A NF-kappaB p65 subunit is indispensable for activating manganese superoxide: dismutase gene transcription mediated by tumor necrosis factor-alpha', *J Cell Biochem*, 77(3), pp. 474-86.
Malaquin, N., Tu, V. and Rodier, F. (2019) 'Assessing Functional Roles of the Senescence-Associated Secretory Phenotype (SASP)', *Methods Mol Biol*, 1896, pp. 45-55.
Malato, Y., Naqvi, S., Schurmann, N., Ng, R., Wang, B., Zape, J., Kay, M.A., Grimm, D. and Willenbring, H. (2011) 'Fate tracing of mature hepatocytes in mouse liver homeostasis and regeneration', *J Clin Invest*, 121(12), pp. 4850-60.
Manczak, M., Jung, Y., Park, B.S., Partovi, D. and Reddy, P.H. (2005) 'Time-course of mitochondrial gene expressions in mice brains: implications for mitochondrial dysfunction, oxidative damage, and cytochrome c in aging', *J Neurochem*, 92(3), pp. 494-504.
Maneiro, E., López-Armada, M.J., de Andres, M.C., Caramés, B., Martín, M.A., Bonilla, A., Del Hoyo, P., Galdo, F., Arenas, J. and Blanco, F.J. (2005) 'Effect of nitric oxide on mitochondrial respiratory activity of human articular chondrocytes', *Ann Rheum Dis*, 64(3), pp. 388-95.

Manibusan, M., Odin, M. and A Eastmond, D. (2007) 'Postulated Carbon Tetrachloride Mode of Action: A Review', *Journal of environmental science and health. Part C, Environmental carcinogenesis & ecotoxicology reviews*, 25, pp. 185-209.
Mansouri, A., Gattolliat, C.H. and Asselah, T. (2018) 'Mitochondrial Dysfunction and Signaling in Chronic Liver Diseases', *Gastroenterology*, 155(3), pp. 629-647.
Mao, S.A., Glorioso, J.M. and Nyberg, S.L. (2014) 'Liver regeneration', *Transl Res*, 163(4), pp. 352-62.
Marcelino, L.A. and Thilly, W.G. (1999) 'Mitochondrial mutagenesis in human cells and tissues', *Mutat Res*, 434(3), pp. 177-203.
Marchesini, G., Bua, V., Brunori, A., Bianchi, G., Pisi, P., Fabbri, A., Zoli, M. and Pisi, E. (1988) 'Galactose elimination capacity and liver volume in aging man', *Hepatology*, 8(5), pp. 1079-1083.
Margulis, L. (1971) 'The origin of plant and animal cells', *Am Sci*, 59(2), pp. 230-5.
Mariappan, N., Elks, C.M., Fink, B. and Francis, J. (2009) 'TNF-induced mitochondrial damage: a link between mitochondrial complex I activity and left ventricular dysfunction', *Free Radic Biol Med*, 46(4), pp. 462-70.
Marriott, H.M., Jackson, L.E., Wilkinson, T.S., Simpson, A.J., Mitchell, T.J., Buttle, D.J., Cross, S.S., Ince, P.G., Hellewell, P.G., Whyte, M.K. and Dockrell, D.H. (2008) 'Reactive oxygen species regulate neutrophil recruitment and survival in pneumococcal pneumonia', *Am J Respir Crit Care Med*, 177(8), pp. 887-95.
Mars, W.M., Zarnegar, R. and Michalopoulos, G.K. (1993) 'Activation of hepatocyte growth factor by the plasminogen activators uPA and tPA', *Am J Pathol*, 143(3), pp. 949-58.
Martin, W. and Muller, M. (1998) 'The hydrogen hypothesis for the first eukaryote', *Nature*, 392(6671), pp. 37-41.
Martin, W.F., Garg, S. and Zimorski, V. (2015) 'Endosymbiotic theories for eukaryote origin', *Philos Trans R Soc Lond B Biol Sci*, 370(1678), p. 20140330.
McConnell, B.B., Gregory, F.J., Stott, F.J., Hara, E. and Peters, G. (1999) 'Induced expression of p16(INK4a) inhibits both CDK4- and CDK2-associated kinase activity by reassortment of cyclin-CDK-inhibitor complexes', *Mol Cell Biol*, 19(3), pp. 1981-9.
McDonald, B., Pittman, K., Menezes, G.B., Hirota, S.A., Slaba, I., Waterhouse, C.C., Beck, P.L., Muruve, D.A. and Kubes, P. (2010) 'Intravascular danger signals guide neutrophils to sites of sterile inflammation', *Science*, 330(6002), pp. 362-6.
McDonald, P.P., Bald, A. and Cassatella, M.A. (1997) 'Activation of the NF-κB Pathway by Inflammatory Stimuli in Human Neutrophils', *Blood*, 89(9), pp. 3421-3433.
McDonald, S.A., Greaves, L.C., Gutierrez-Gonzalez, L., Rodriguez-Justo, M., Deheragoda, M., Leedham, S.J., Taylor, R.W., Lee, C.Y., Preston, S.L., Lovell, M., Hunt, T., Elia, G., Oukrif, D., Harrison, R., Novelli, M.R., Mitchell, I., Stoker, D.L., Turnbull, D.M., Jankowski, J.A. and Wright, N.A. (2008)

'Mechanisms of field cancerization in the human stomach: the expansion and spread of mutated gastric stem cells', *Gastroenterology*, 134(2), pp. 500-10.
McGowan, J.A., Strain, A.J. and Bucher, N.L. (1981) 'DNA synthesis in primary cultures of adult rat hepatocytes in a defined medium: effects of epidermal growth factor, insulin, glucagon, and cyclic-AMP', *J Cell Physiol*, 108(3), pp. 353-63.
Mederacke, I., Hsu, C.C., Troeger, J.S., Huebener, P., Mu, X., Dapito, D.H., Pradere, J.P. and Schwabe, R.F. (2013) 'Fate tracing reveals hepatic stellate cells as dominant contributors to liver fibrosis independent of its aetiology', *Nat Commun*, 4, p. 2823.
Mehlhorn, R.J. (1991) 'Ascorbate- and dehydroascorbic acid-mediated reduction of free radicals in the human erythrocyte', *Journal of Biological Chemistry*, 266(5), pp. 2724-2731.
Melov, S., Doctrow, S.R., Schneider, J.A., Haberson, J., Patel, M., Coskun, P.E., Huffman, K., Wallace, D.C. and Malfroy, B. (2001) 'Lifespan extension and rescue of spongiform encephalopathy in superoxide dismutase 2 nullizygous mice treated with superoxide dismutase-catalase mimetics', *J Neurosci*, 21(21), pp. 8348-53.
Meyer, K.C., Rosenthal, N.S., Soergel, P. and Peterson, K. (1998) 'Neutrophils and low-grade inflammation in the seemingly normal aging human lung', *Mech Ageing Dev*, 104(2), pp. 169-81.
Miao, L. and St Clair, D.K. (2009) 'Regulation of superoxide dismutase genes: implications in disease', *Free Radic Biol Med*, 47(4), pp. 344-56.
Michalopoulos, G.K. (2007) 'Liver regeneration', *J Cell Physiol*, 213(2), pp. 286-300.
Michalopoulos, G.K. and DeFrances, M.C. (1997) 'Liver regeneration', *Science*, 276(5309), pp. 60-6.
Michikawa, Y., Mazzucchelli, F., Bresolin, N., Scarlato, G. and Attardi, G. (1999) 'Aging-dependent large accumulation of point mutations in the human mtDNA control region for replication', *Science*, 286(5440), pp. 774-9.
Minczuk, M., He, J., Duch, A.M., Ettema, T.J., Chlebowski, A., Dzionek, K., Nijtmans, L.G., Huynen, M.A. and Holt, I.J. (2011) 'TEFM (c17orf42) is necessary for transcription of human mtDNA', *Nucleic Acids Res*, 39(10), pp. 4284-99.
Miralles Fusté, J., Shi, Y., Wanrooij, S., Zhu, X., Jemt, E., Persson, Ö., Sabouri, N., Gustafsson, C.M. and Falkenberg, M. (2014) 'In vivo occupancy of mitochondrial single-stranded DNA binding protein supports the strand displacement mode of DNA replication', *PLoS Genet*, 10(12), p. e1004832.
Mitra, J., Dai, C.Y., Somasundaram, K., El-Deiry, W.S., Satyamoorthy, K., Herlyn, M. and Enders, G.H. (1999) 'Induction of p21(WAF1/CIP1) and inhibition of Cdk2 mediated by the tumor suppressor p16(INK4a)', *Mol Cell Biol*, 19(5), pp. 3916-28.
Mitra, K., Wunder, C., Roysam, B., Lin, G. and Lippincott-Schwartz, J. (2009) 'A hyperfused mitochondrial state achieved at G1-S regulates cyclin E buildup and entry into S phase', *Proc Natl Acad Sci U S A*, 106(29), pp. 11960-5.

Mittal, M., Siddiqui, M.R., Tran, K., Reddy, S.P. and Malik, A.B. (2014) 'Reactive oxygen species in inflammation and tissue injury', *Antioxid Redox Signal*, 20(7), pp. 1126-67.

Miyaoka, Y., Ebato, K., Kato, H., Arakawa, S., Shimizu, S. and Miyajima, A. (2012) 'Hypertrophy and unconventional cell division of hepatocytes underlie liver regeneration', *Curr Biol*, 22(13), pp. 1166-75.

Miyaoka, Y. and Miyajima, A. (2013) 'To divide or not to divide: revisiting liver regeneration', *Cell Div*, 8(1), p. 8.

Moiseeva, O., Bourdeau, V., Roux, A., Deschenes-Simard, X. and Ferbeyre, G. (2009) 'Mitochondrial dysfunction contributes to oncogene-induced senescence', *Mol Cell Biol*, 29(16), pp. 4495-507.

Montella, L., Masci, A.M., Merkabaoui, G., Perna, F., Vitiello, L., Racioppi, L. and Palmieri, G. (2003) 'B-cell lymphopenia and hypogammaglobulinemia in thymoma patients', *Ann Hematol*, 82(6), pp. 343-7.

Moolten, F.L. and Bucher, N.L. (1967) 'Regeneration of rat liver: transfer of humoral agent by cross circulation', *Science*, 158(3798), pp. 272-4.

Morgan, M.J. and Liu, Z.G. (2011) 'Crosstalk of reactive oxygen species and NF-kappaB signaling', *Cell Res*, 21(1), pp. 103-15.

Moustakas, A. and Kardassis, D. (1998) 'Regulation of the human p21/WAF1/Cip1 promoter in hepatic cells by functional interactions between Sp1 and Smad family members', *Proc Natl Acad Sci U S A*, 95(12), pp. 6733-8.

Muller-Hocker, J., Aust, D., Rohrbach, H., Napiwotzky, J., Reith, A., Link, T.A., Seibel, P., Holzel, D. and Kadenbach, B. (1997) 'Defects of the respiratory chain in the normal human liver and in cirrhosis during aging', *Hepatology*, 26(3), pp. 709-19.

Munscher, C., Muller-Hocker, J. and Kadenbach, B. (1993) 'Human aging is associated with various point mutations in tRNA genes of mitochondrial DNA', *Biol Chem Hoppe Seyler*, 374(12), pp. 1099-104.

Murphy, M.P. (2009) 'How mitochondria produce reactive oxygen species', *Biochem J*, 417(1), pp. 1-13.

Nagino, M., Tanaka, M., Nishikimi, M., Nimura, Y., Kubota, H., Kanai, M., Kato, T. and Ozawa, T. (1989) 'Stimulated rat liver mitochondrial biogenesis after partial hepatectomy', *Cancer Res*, 49(17), pp. 4913-8.

Nakamura, T., Tomita, Y., Hirai, R., Yamaoka, K., Kaji, K. and Ichihara, A. (1985) 'Inhibitory effect of transforming growth factor-beta on DNA synthesis of adult rat hepatocytes in primary culture', *Biochem Biophys Res Commun*, 133(3), pp. 1042-50.

Nakano, S., Suzuki, T., Kawarada, L., Iwata, H., Asano, K. and Suzuki, T. (2016) 'NSUN3 methylase initiates 5-formylcytidine biogenesis in human mitochondrial tRNA(Met)', *Nat Chem Biol*, 12(7), pp. 546-51.

Navarro, A. and Boveris, A. (2007) 'The mitochondrial energy transduction system and the aging process', *Am J Physiol Cell Physiol*, 292(2), pp. C670-86.
Neckelmann, N., Li, K., Wade, R.P., Shuster, R. and Wallace, D.C. (1987) 'cDNA sequence of a human skeletal muscle ADP/ATP translocator: lack of a leader peptide, divergence from a fibroblast translocator cDNA, and coevolution with mitochondrial DNA genes', *Proc Natl Acad Sci U S A*, 84(21), pp. 7580-4.
Nejak-Bowen, K., Orr, A., Bowen, W.C., Jr. and Michalopoulos, G.K. (2013) 'Conditional genetic elimination of hepatocyte growth factor in mice compromises liver regeneration after partial hepatectomy', *PLoS One*, 8(3), p. e59836.
Nekhaeva, E., Bodyak, N.D., Kraytsberg, Y., McGrath, S.B., Van Orsouw, N.J., Pluzhnikov, A., Wei, J.Y., Vijg, J. and Khrapko, K. (2002) 'Clonally expanded mtDNA point mutations are abundant in individual cells of human tissues', *Proceedings of the National Academy of Sciences*, 99(8), pp. 5521-5526.
Nelson, G., Kucheryavenko, O., Wordsworth, J. and von Zglinicki, T. (2018) 'The senescent bystander effect is caused by ROS-activated NF-kappaB signalling', *Mech Ageing Dev*, 170, pp. 30-36.
Nelson, G., Wordsworth, J., Wang, C., Jurk, D., Lawless, C., Martin-Ruiz, C. and von Zglinicki, T. (2012) 'A senescent cell bystander effect: senescence-induced senescence', *Aging Cell*, 11(2), pp. 345-9.
Neupert, W. and Herrmann, J.M. (2007) 'Translocation of proteins into mitochondria', *Annu Rev Biochem*, 76, pp. 723-49.
Nevzorova, Y.A., Tolba, R., Trautwein, C. and Liedtke, C. (2015) 'Partial hepatectomy in mice', *Lab Anim*, 49(1 Suppl), pp. 81-8.
Nikolich-Žugich, J. (2014) 'Aging of the T Cell Compartment in Mice and Humans: From No Naive Expectations to Foggy Memories', *The Journal of Immunology*, 193(6), pp. 2622-2629.
Nishida, K., Ohta, Y., Kongo, M. and Ishiguro, I. (1996) 'Response of endogenous reduced glutathione through hepatic glutathione redox cycle to enhancement of hepatic lipid peroxidation with the development of acute liver injury in mice intoxicated with carbon tetrachloride', *Res Commun Mol Pathol Pharmacol*, 93(2), pp. 198-218.
Nishikawa, Y., Wang, M. and Carr, B.I. (1998) 'Changes in TGF-beta receptors of rat hepatocytes during primary culture and liver regeneration: increased expression of TGF-beta receptors associated with increased sensitivity to TGF-beta-mediated growth inhibition', *J Cell Physiol*, 176(3), pp. 612-23.
Noguchi, S., Ohba, Y. and Oka, T. (1991) 'Effect of salivary epidermal growth factor on wound healing of tongue in mice', *Am J Physiol*, 260(4 Pt 1), pp. E620-5.
Nooteboom, M., Johnson, R., Taylor, R.W., Wright, N.A., Lightowlers, R.N., Kirkwood, T.B., Mathers, J.C., Turnbull, D.M. and Greaves, L.C. (2010) 'Age-associated mitochondrial DNA mutations lead to small but significant changes in cell proliferation and apoptosis in human colonic crypts', *Aging Cell*, 9(1), pp. 96-9.

Norddahl, G.L., Pronk, C.J., Wahlestedt, M., Sten, G., Nygren, J.M., Ugale, A., Sigvardsson, M. and Bryder, D. (2011) 'Accumulating mitochondrial DNA mutations drive premature hematopoietic aging phenotypes distinct from physiological stem cell aging', *Cell Stem Cell*, 8(5), pp. 499-510.
Noureddin, M., Yates, K.P., Vaughn, I.A., Neuschwander-Tetri, B.A., Sanyal, A.J., McCullough, A., Merriman, R., Hameed, B., Doo, E., Kleiner, D.E., Behling, C. and Loomba, R. (2013) 'Clinical and histological determinants of nonalcoholic steatohepatitis and advanced fibrosis in elderly patients', *Hepatology*, 58(5), pp. 1644-54.
Nunnari, J. and Suomalainen, A. (2012) 'Mitochondria: In Sickness and in Health', *Cell*, 148(6), pp. 1145-1159.
Nurse, P. and Thuriaux, P. (1980) 'Regulatory genes controlling mitosis in the fission yeast Schizosaccharomyces pombe', *Genetics*, 96(3), pp. 627-37.
Nurse, P., Thuriaux, P. and Nasmyth, K. (1976) 'Genetic control of the cell division cycle in the fission yeast Schizosaccharomyces pombe', *Mol Gen Genet*, 146(2), pp. 167-78.
O'Mahony, M.S. and Schmucker, D.L. (1994) 'Liver disease in the elderly', *Semin Gastrointest Dis*, 5(4), pp. 197-206.
Oakley, F. and Mann, D.A. (2015) 'Chapter 15 - Stellate Cell Depletion Models', in Gandhi, C.R. and Pinzani, M. (eds.) *Stellate Cells in Health and Disease*. Boston: Academic Press, pp. 251-270.
Oberhammer, F.A., Pavelka, M., Sharma, S., Tiefenbacher, R., Purchio, A.F., Bursch, W. and Schulte-Hermann, R. (1992) 'Induction of apoptosis in cultured hepatocytes and in regressing liver by transforming growth factor beta 1', *Proc Natl Acad Sci U S A*, 89(12), pp. 5408-12.
Oe, S., Lemmer, E.R., Conner, E.A., Factor, V.M., Leveen, P., Larsson, J., Karlsson, S. and Thorgeirsson, S.S. (2004) 'Intact signaling by transforming growth factor beta is not required for termination of liver regeneration in mice', *Hepatology*, 40(5), pp. 1098-105.
Ogawa, K., Suzuki, K., Okutsu, M., Yamazaki, K. and Shinkai, S. (2008) 'The association of elevated reactive oxygen species levels from neutrophils with low-grade inflammation in the elderly', *Immun Ageing*, 5, p. 13.
Ogrodnik, M., Miwa, S., Tchkonia, T., Tiniakos, D., Wilson, C.L., Lahat, A., Day, C.P., Burt, A., Palmer, A., Anstee, Q.M., Grellscheid, S.N., Hoeijmakers, J.H.J., Barnhoorn, S., Mann, D.A., Bird, T.G., Vermeij, W.P., Kirkland, J.L., Passos, J.F., von Zglinicki, T. and Jurk, D. (2017) 'Cellular senescence drives age-dependent hepatic steatosis', *Nature Communications*, 8, p. 15691.
Ohtani, N., Zebedee, Z., Huot, T.J., Stinson, J.A., Sugimoto, M., Ohashi, Y., Sharrocks, A.D., Peters, G. and Hara, E. (2001) 'Opposing effects of Ets and Id proteins on p16INK4a expression during cellular senescence', *Nature*, 409(6823), pp. 1067-70.
Ojala, D., Montoya, J. and Attardi, G. (1981) 'tRNA punctuation model of RNA processing in human mitochondria', *Nature*, 290(5806), pp. 470-474.

Olinga, P. and Schuppan, D. (2013) 'Precision-cut liver slices: a tool to model the liver ex vivo', *J Hepatol*, 58(6), pp. 1252-3.

Otera, H. and Mihara, K. (2012) 'Mitochondrial Dynamics: Functional Link with Apoptosis', *International Journal of Cell Biology*, 2012, p. 10.

Owusu-Ansah, E., Yavari, A., Mandal, S. and Banerjee, U. (2008) 'Distinct mitochondrial retrograde signals control the G1-S cell cycle checkpoint', *Nature Genetics*, 40, p. 356.

Packer, L. and Fuehr, K. (1977) 'Low oxygen concentration extends the lifespan of cultured human diploid cells', *Nature*, 267(5610), pp. 423-5.

Paish, H.L., Reed, L.H., Brown, H., Bryan, M.C., Govaere, O., Leslie, J., Barksby, B.S., Garcia Macia, M., Watson, A., Xu, X., Zaki, M.Y.W., Greaves, L., Whitehall, J., French, J., White, S.A., Manas, D.M., Robinson, S.M., Spoletini, G., Griffiths, C., Mann, D.A., Borthwick, L.A., Drinnan, M.J., Mann, J. and Oakley, F. (2019) 'A Bioreactor Technology for Modeling Fibrosis in Human and Rodent Precision-Cut Liver Slices', *Hepatology*.

Palade, G.E. (1953) 'An electron microscope study of the mitochondrial structure', *J Histochem Cytochem*, 1(4), pp. 188-211.

Paranjpe, S., Bowen, W.C., Bell, A.W., Nejak-Bowen, K., Luo, J.H. and Michalopoulos, G.K. (2007) 'Cell cycle effects resulting from inhibition of hepatocyte growth factor and its receptor c-Met in regenerating rat livers by RNA interference', *Hepatology*, 45(6), pp. 1471-7.

Park, B.K. (1982) 'Assessment of the drug metabolism capacity of the liver', *Br J Clin Pharmacol*, 14(5), pp. 631-51.

Park, S.Y., Gifford, J.R., Andtbacka, R.H., Trinity, J.D., Hyngstrom, J.R., Garten, R.S., Diakos, N.A., Ives, S.J., Dela, F., Larsen, S., Drakos, S. and Richardson, R.S. (2014) 'Cardiac, skeletal, and smooth muscle mitochondrial respiration: are all mitochondria created equal?', *Am J Physiol Heart Circ Physiol*, 307(3), pp. H346-52.

Pascucci, B., Lemma, T., Iorio, E., Giovannini, S., Vaz, B., Iavarone, I., Calcagnile, A., Narciso, L., Degan, P., Podo, F., Roginskya, V., Janjic, B.M., Van Houten, B., Stefanini, M., Dogliotti, E. and D'Errico, M. (2012) 'An altered redox balance mediates the hypersensitivity of Cockayne syndrome primary fibroblasts to oxidative stress', *Aging Cell*, 11(3), pp. 520-9.

Passos, J.F., Nelson, G., Wang, C., Richter, T., Simillion, C., Proctor, C.J., Miwa, S., Olijslagers, S., Hallinan, J., Wipat, A., Saretzki, G., Rudolph, K.L., Kirkwood, T.B. and von Zglinicki, T. (2010) 'Feedback between p21 and reactive oxygen production is necessary for cell senescence', *Mol Syst Biol*, 6, p. 347.

Passos, J.F., Saretzki, G., Ahmed, S., Nelson, G., Richter, T., Peters, H., Wappler, I., Birket, M.J., Harold, G., Schaeuble, K., Birch-Machin, M.A., Kirkwood, T.B. and von Zglinicki, T. (2007) 'Mitochondrial dysfunction accounts for the stochastic heterogeneity in telomere-dependent senescence', *PLoS Biol*, 5(5), p. e110.

Pavletich, N.P. (1999) 'Mechanisms of cyclin-dependent kinase regulation: structures of Cdks, their cyclin activators, and Cip and INK4 inhibitors', *J Mol Biol*, 287(5), pp. 821-8.
Payne, B.A. and Chinnery, P.F. (2015) 'Mitochondrial dysfunction in aging: Much progress but many unresolved questions', *Biochim Biophys Acta*, 1847(11), pp. 1347-53.
Payne, B.A., Wilson, I.J., Yu-Wai-Man, P., Coxhead, J., Deehan, D., Horvath, R., Taylor, R.W., Samuels, D.C., Santibanez-Koref, M. and Chinnery, P.F. (2013) 'Universal heteroplasmy of human mitochondrial DNA', *Hum Mol Genet*, 22(2), pp. 384-90.
Pellicoro, A., Ramachandran, P., Iredale, J.P. and Fallowfield, J.A. (2014) 'Liver fibrosis and repair: immune regulation of wound healing in a solid organ', *Nat Rev Immunol*, 14(3), pp. 181-94.
Perugorria, M.J., Latasa, M.U., Nicou, A., Cartagena-Lirola, H., Castillo, J., Goni, S., Vespasiani-Gentilucci, U., Zagami, M.G., Lotersztajn, S., Prieto, J., Berasain, C. and Avila, M.A. (2008) 'The epidermal growth factor receptor ligand amphiregulin participates in the development of mouse liver fibrosis', *Hepatology*, 48(4), pp. 1251-61.
Petersen, S., Saretzki, G. and von Zglinicki, T. (1998) 'Preferential accumulation of single-stranded regions in telomeres of human fibroblasts', *Exp Cell Res*, 239(1), pp. 152-60.
Pinti, M., Cevenini, E., Nasi, M., De Biasi, S., Salvioli, S., Monti, D., Benatti, S., Gibellini, L., Cotichini, R., Stazi, M.A., Trenti, T., Franceschi, C. and Cossarizza, A. (2014) 'Circulating mitochondrial DNA increases with age and is a familiar trait: Implications for "inflamm-aging"', *Eur J Immunol*, 44(5), pp. 1552-62.
Pinzani, M. and Rombouts, K. (2004) 'Liver fibrosis: from the bench to clinical targets', *Dig Liver Dis*, 36(4), pp. 231-42.
Planas-Paz, L., Orsini, V. and Boulter, L. (2016) 'The RSPO-LGR4/5-ZNRF3/RNF43 module controls liver zonation and size', 18(5), pp. 467-79.
Poole, A.M. and Gribaldo, S. (2014) 'Eukaryotic origins: How and when was the mitochondrion acquired?', *Cold Spring Harb Perspect Biol*, 6(12), p. a015990.
Popow, J., Alleaume, A.M., Curk, T., Schwarzl, T., Sauer, S. and Hentze, M.W. (2015) 'FASTKD2 is an RNA-binding protein required for mitochondrial RNA processing and translation', *Rna*, 21(11), pp. 1873-84.
Posse, V., Shahzad, S., Falkenberg, M., Hallberg, B.M. and Gustafsson, C.M. (2015) 'TEFM is a potent stimulator of mitochondrial transcription elongation in vitro', *Nucleic Acids Res*, 43(5), pp. 2615-24.
Pradere, J.P., Kluwe, J., De Minicis, S., Jiao, J.J., Gwak, G.Y., Dapito, D.H., Jang, M.K., Guenther, N.D., Mederacke, I., Friedman, R., Dragomir, A.C., Aloman, C. and Schwabe, R.F. (2013) 'Hepatic macrophages but not dendritic cells contribute to liver fibrosis by promoting the survival of activated hepatic stellate cells in mice', *Hepatology*, 58(4), pp. 1461-73.
Prattichizzo, F., De Nigris, V., La Sala, L., Procopio, A.D., Olivieri, F. and Ceriello, A. (2016) '“Inflammaging” as a Druggable Target: A Senescence-Associated Secretory

Phenotype—Centered View of Type 2 Diabetes', *Oxidative Medicine and Cellular Longevity*, 2016, p. 10.

Premoli, A., Paschetta, E., Hvalryg, M., Spandre, M., Bo, S. and Durazzo, M. (2009) 'Characteristics of liver diseases in the elderly: a review', *Minerva Gastroenterol Dietol*, 55(1), pp. 71-8.

Prieto-Martin, A., Montoya, J. and Martinez-Azorin, F. (2004) 'Phosphorylation of rat mitochondrial transcription termination factor (mTERF) is required for transcription termination but not for binding to DNA', *Nucleic Acids Res*, 32(7), pp. 2059-68.

Pyo, C.W., Choi, J.H., Oh, S.M. and Choi, S.Y. (2013) 'Oxidative stress-induced cyclin D1 depletion and its role in cell cycle processing', *Biochim Biophys Acta*, 1830(11), pp. 5316-25.

Ramesh, S., Qi, X.J., Wildey, G.M., Robinson, J., Molkentin, J., Letterio, J. and Howe, P.H. (2008) 'TGF beta-mediated BIM expression and apoptosis are regulated through SMAD3-dependent expression of the MAPK phosphatase MKP2', *EMBO Rep*, 9(10), pp. 990-7.

Rampersad, S.N. (2012) 'Multiple applications of Alamar Blue as an indicator of metabolic function and cellular health in cell viability bioassays', *Sensors (Basel)*, 12(9), pp. 12347-60.

Rayess, H., Wang, M.B. and Srivatsan, E.S. (2012) 'Cellular senescence and tumor suppressor gene p16', *Int J Cancer*, 130(8), pp. 1715-25.

Rebelo, A.P., Dillon, L.M. and Moraes, C.T. (2011) 'Mitochondrial DNA transcription regulation and nucleoid organization', *J Inherit Metab Dis*, 34(4), pp. 941-51.

Reed, S.I., Ferguson, J. and Groppe, J.C. (1982) 'Preliminary characterization of the transcriptional and translational products of the Saccharomyces cerevisiae cell division cycle gene CDC28', *Mol Cell Biol*, 2(4), pp. 412-25.

Rehman, H., Liu, Q., Krishnasamy, Y., Shi, Z., Ramshesh, V.K., Haque, K., Schnellmann, R.G., Murphy, M.P., Lemasters, J.J., Rockey, D.C. and Zhong, Z. (2016) 'The mitochondria-targeted antioxidant MitoQ attenuates liver fibrosis in mice', *Int J Physiol Pathophysiol Pharmacol*, 8(1), pp. 14-27.

Reyes, A., Kazak, L., Wood, S.R., Yasukawa, T., Jacobs, H.T. and Holt, I.J. (2013) 'Mitochondrial DNA replication proceeds via a 'bootlace' mechanism involving the incorporation of processed transcripts', *Nucleic Acids Res*, 41(11), pp. 5837-50.

Ricci, J.E., Munoz-Pinedo, C., Fitzgerald, P., Bailly-Maitre, B., Perkins, G.A., Yadava, N., Scheffler, I.E., Ellisman, M.H. and Green, D.R. (2004) 'Disruption of mitochondrial function during apoptosis is mediated by caspase cleavage of the p75 subunit of complex I of the electron transport chain', *Cell*, 117(6), pp. 773-86.

Richter, C., Park, J.W. and Ames, B.N. (1988) 'Normal oxidative damage to mitochondrial and nuclear DNA is extensive', *Proc Natl Acad Sci U S A*, 85(17), pp. 6465-7.

Rocha, M.C., Grady, J.P., Grunewald, A., Vincent, A., Dobson, P.F., Taylor, R.W., Turnbull, D.M. and Rygiel, K.A. (2015) 'A novel immunofluorescent assay to investigate oxidative phosphorylation

deficiency in mitochondrial myopathy: understanding mechanisms and improving diagnosis', *Sci Rep*, 5, p. 15037.
Rosales, C., Lowell, C.A., Schnoor, M. and Uribe-Querol, E. (2017) 'Neutrophils: Their Role in Innate and Adaptive Immunity 2017', 2017, p. 9748345.
Ross, J.M. (2011) 'Visualization of mitochondrial respiratory function using cytochrome c oxidase/succinate dehydrogenase (COX/SDH) double-labeling histochemistry', *J Vis Exp*, (57), p. e3266.
Ross, J.M., Stewart, J.B., Hagstrom, E., Brene, S., Mourier, A., Coppotelli, G., Freyer, C., Lagouge, M., Hoffer, B.J., Olson, L. and Larsson, N.G. (2013) 'Germline mitochondrial DNA mutations aggravate ageing and can impair brain development', *Nature*, 501(7467), pp. 412-5.
Rossmanith, W. (2011) 'Localization of human RNase Z isoforms: dual nuclear/mitochondrial targeting of the ELAC2 gene product by alternative translation initiation', *PLoS One*, 6(4), p. e19152.
Russo, A.A., Jeffrey, P.D. and Pavletich, N.P. (1996) 'Structural basis of cyclin-dependent kinase activation by phosphorylation', *Nat Struct Biol*, 3(8), pp. 696-700.
Saelens, X., Festjens, N., Vande Walle, L., van Gurp, M., van Loo, G. and Vandenabeele, P. (2004) 'Toxic proteins released from mitochondria in cell death', *Oncogene*, 23(16), pp. 2861-74.
Saito, H. and Papaconstantinou, J. (2001) 'Age-associated Differences in Cardiovascular Inflammatory Gene Induction during Endotoxic Stress', *Journal of Biological Chemistry*, 276(31), pp. 29307-29312.
Sakamaki, T., Casimiro, M.C., Ju, X., Quong, A.A., Katiyar, S., Liu, M., Jiao, X., Li, A., Zhang, X., Lu, Y., Wang, C., Byers, S., Nicholson, R., Link, T., Shemluck, M., Yang, J., Fricke, S.T., Novikoff, P.M., Papanikolaou, A., Arnold, A., Albanese, C. and Pestell, R. (2006) 'Cyclin D1 determines mitochondrial function in vivo', *Mol Cell Biol*, 26(14), pp. 5449-69.
Sakamoto, T., Liu, Z., Murase, N., Ezure, T., Yokomuro, S., Poli, V. and Demetris, A.J. (1999) 'Mitosis and apoptosis in the liver of interleukin-6-deficient mice after partial hepatectomy', *Hepatology*, 29(2), pp. 403-11.
Salazar-Roa, M. and Malumbres, M. (2017) 'Fueling the Cell Division Cycle', *Trends Cell Biol*, 27(1), pp. 69-81.
Salminen, A., Kauppinen, A. and Kaarniranta, K. (2012) 'Emerging role of NF-kappaB signaling in the induction of senescence-associated secretory phenotype (SASP)', *Cell Signal*, 24(4), pp. 835-45.
Sanyal, A.J., Campbell-Sargent, C., Mirshahi, F., Rizzo, W.B., Contos, M.J., Sterling, R.K., Luketic, V.A., Shiffman, M.L. and Clore, J.N. (2001) 'Nonalcoholic steatohepatitis: association of insulin resistance and mitochondrial abnormalities', *Gastroenterology*, 120(5), pp. 1183-92.
Sanz, A. (2016) 'Mitochondrial reactive oxygen species: Do they extend or shorten animal lifespan?', *Biochim Biophys Acta*, 1857(8), pp. 1116-1126.

Sanz, A., Fernandez-Ayala, D.J., Stefanatos, R.K. and Jacobs, H.T. (2010) 'Mitochondrial ROS production correlates with, but does not directly regulate lifespan in Drosophila', *Aging (Albany NY)*, 2(4), pp. 200-23.

Saretzki, G., Murphy, M.P. and von Zglinicki, T. (2003) 'MitoQ counteracts telomere shortening and elongates lifespan of fibroblasts under mild oxidative stress', *Aging Cell*, 2(2), pp. 141-3.

Sasarman, F., Antonicka, H., Horvath, R. and Shoubridge, E.A. (2011) 'The 2-thiouridylase function of the human MTU1 (TRMU) enzyme is dispensable for mitochondrial translation', *Hum Mol Genet*, 20(23), pp. 4634-43.

Sastre, J., Pallardo, F.V., Pla, R., Pellin, A., Juan, G., O'Connor, J.E., Estrela, J.M., Miquel, J. and Vina, J. (1996) 'Aging of the liver: age-associated mitochondrial damage in intact hepatocytes', *Hepatology*, 24(5), pp. 1199-205.

Satoh, M., Adachi, K., Suda, T., Yamazaki, M. and Mizuno, D. (1991) 'TNF-driven inflammation during mouse liver regeneration after partial hepatectomy and its role in growth regulation of liver', *Mol Biother*, 3(3), pp. 136-47.

Sayre, L.M., Smith, M.A. and Perry, G. (2001) 'Chemistry and biochemistry of oxidative stress in neurodegenerative disease', *Curr Med Chem*, 8(7), pp. 721-38.

Scaffidi, C., Schmitz, I., Krammer, P.H. and Peter, M.E. (1999) 'The role of c-FLIP in modulation of CD95-induced apoptosis', *J Biol Chem*, 274(3), pp. 1541-8.

Schaper, F., Siewert, E., Gomez-Lechon, M.J., Gatsios, P., Sachs, M., Birchmeier, W., Heinrich, P.C. and Castell, J. (1997) 'Hepatocyte growth factor/scatter factor (HGF/SF) signals via the STAT3/APRF transcription factor in human hepatoma cells and hepatocytes', *FEBS Lett*, 405(1), pp. 99-103.

Schmidt-Arras, D. and Rose-John, S. (2016) 'IL-6 pathway in the liver: From physiopathology to therapy', *J Hepatol*, 64(6), pp. 1403-15.

Schmidt, O., Pfanner, N. and Meisinger, C. (2010) 'Mitochondrial protein import: from proteomics to functional mechanisms', *Nat Rev Mol Cell Biol*, 11(9), pp. 655-67.

Schmucker, D.L. (2005) 'Age-related changes in liver structure and function: Implications for disease ?', *Exp Gerontol*, 40(8-9), pp. 650-9.

Schmucker, D.L., Mooney, J.S. and Jones, A.L. (1978) 'Stereological analysis of hepatic fine structure in the Fischer 344 rat. Influence of sublobular location and animal age', *J Cell Biol*, 78(2), pp. 319-37.

Schmucker, D.L. and Sanchez, H. (2011) 'Liver regeneration and aging: a current perspective', *Curr Gerontol Geriatr Res*, 2011, p. 526379.

Schnabl, B., Purbeck, C.A., Choi, Y.H., Hagedorn, C.H. and Brenner, D. (2003) 'Replicative senescence of activated human hepatic stellate cells is accompanied by a pronounced inflammatory but less fibrogenic phenotype', *Hepatology*, 37(3), pp. 653-64.

Scholten, D., Trebicka, J., Liedtke, C. and Weiskirchen, R. (2015) 'The carbon tetrachloride model in mice', *Lab Anim*, 49(1 Suppl), pp. 4-11.

Schoonbroodt, S. and Piette, J. (2000) 'Oxidative stress interference with the nuclear factor-kappa B activation pathways', *Biochem Pharmacol*, 60(8), pp. 1075-83.
Schulze-Osthoff, K., Beyaert, R., Vandevoorde, V., Haegeman, G. and Fiers, W. (1993) 'Depletion of the mitochondrial electron transport abrogates the cytotoxic and gene-inductive effects of TNF', *Embo j*, 12(8), pp. 3095-104.
Schwabe, R.F., Seki, E. and Brenner, D.A. (2006) 'Toll-Like Receptor Signaling in the Liver', *Gastroenterology*, 130(6), pp. 1886-1900.
Schwall, R.H., Robbins, K., Jardieu, P., Chang, L., Lai, C. and Terrell, T.G. (1993) 'Activin induces cell death in hepatocytes in vivo and in vitro', *Hepatology*, 18(2), pp. 347-56.
Sciacco, M., Bonilla, E., Schon, E.A., DiMauro, S. and Moraes, C.T. (1994) 'Distribution of wild-type and common deletion forms of mtDNA in normal and respiration-deficient muscle fibers from patients with mitochondrial myopathy', *Hum Mol Genet*, 3(1), pp. 13-9.
Seki, S., Habu, Y., Kawamura, T., Takeda, K., Dobashi, H., Ohkawa, T. and Hiraide, H. (2000) 'The liver as a crucial organ in the first line of host defense: the roles of Kupffer cells, natural killer (NK) cells and NK1.1 Ag+ T cells in T helper 1 immune responses', *Immunol Rev*, 174, pp. 35-46.
Sekine, S., Lan, B.Y., Bedolli, M., Feng, S. and Hebrok, M. (2006) 'Liver-specific loss of beta-catenin blocks glutamine synthesis pathway activity and cytochrome p450 expression in mice', *Hepatology*, 43(4), pp. 817-25.
Selzner, N., Selzner, M., Odermatt, B., Tian, Y., Van Rooijen, N. and Clavien, P.A. (2003) 'ICAM-1 triggers liver regeneration through leukocyte recruitment and Kupffer cell-dependent release of TNF-alpha/IL-6 in mice', *Gastroenterology*, 124(3), pp. 692-700.
Serizawa, H. (1998) 'Cyclin-dependent kinase inhibitor p16INK4A inhibits phosphorylation of RNA polymerase II by general transcription factor TFIIH', *J Biol Chem*, 273(10), pp. 5427-30.
Shackelford, R.E., Kaufmann, W.K. and Paules, R.S. (2000) 'Oxidative stress and cell cycle checkpoint function', *Free Radic Biol Med*, 28(9), pp. 1387-404.
Sharma, M.R., Koc, E.C., Datta, P.P., Booth, T.M., Spremulli, L.L. and Agrawal, R.K. (2003) 'Structure of the mammalian mitochondrial ribosome reveals an expanded functional role for its component proteins', *Cell*, 115(1), pp. 97-108.
Shenkar, R., Navidi, W., Tavare, S., Dang, M.H., Chomyn, A., Attardi, G., Cortopassi, G. and Arnheim, N. (1996) 'The mutation rate of the human mtDNA deletion mtDNA4977', *Am J Hum Genet*, 59(4), pp. 772-80.
Shimada, K., Crother, T.R., Karlin, J., Dagvadorj, J., Chiba, N., Chen, S., Ramanujan, V.K., Wolf, A.J., Vergnes, L., Ojcius, D.M., Rentsendorj, A., Vargas, M., Guerrero, C., Wang, Y., Fitzgerald, K.A., Underhill, D.M., Town, T. and Arditi, M. (2012) 'Oxidized mitochondrial DNA activates the NLRP3 inflammasome during apoptosis', *Immunity*, 36(3), pp. 401-14.

Shimizu, S., Narita, M. and Tsujimoto, Y. (1999) 'Bcl-2 family proteins regulate the release of apoptogenic cytochrome c by the mitochondrial channel VDAC', *Nature*, 399(6735), pp. 483-7.

Shoffner, J.M., Lott, M.T., Voljavec, A.S., Soueidan, S.A., Costigan, D.A. and Wallace, D.C. (1989) 'Spontaneous Kearns-Sayre/chronic external ophthalmoplegia plus syndrome associated with a mitochondrial DNA deletion: a slip-replication model and metabolic therapy', *Proc Natl Acad Sci U S A*, 86(20), pp. 7952-6.

Sipes, I.G., el Sisi, A.E., Sim, W.W., Mobley, S.A. and Earnest, D.L. (1991) 'Reactive oxygen species in the progression of CCl4-induced liver injury', *Adv Exp Med Biol*, 283, pp. 489-97.

Skrtic, S., Wallenius, V., Ekberg, S., Brenzel, A., Gressner, A.M. and Jansson, J.O. (1999) 'Hepatocyte-stimulated expression of hepatocyte growth factor (HGF) in cultured rat hepatic stellate cells', *J Hepatol*, 30(1), pp. 115-24.

Slaba, I., Wang, J., Kolaczkowska, E., McDonald, B., Lee, W.Y. and Kubes, P. (2015) 'Imaging the dynamic platelet-neutrophil response in sterile liver injury and repair in mice', *Hepatology*, 62(5), pp. 1593-605.

Sohal, R.S., Svensson, I., Sohal, B.H. and Brunk, U.T. (1989) 'Superoxide anion radical production in different animal species', *Mech Ageing Dev*, 49(2), pp. 129-35.

Soleimanpour-Lichaei, H.R., Kuhl, I., Gaisne, M., Passos, J.F., Wydro, M., Rorbach, J., Temperley, R., Bonnefoy, N., Tate, W., Lightowlers, R. and Chrzanowska-Lightowlers, Z. (2007) 'mtRF1a is a human mitochondrial translation release factor decoding the major termination codons UAA and UAG', *Mol Cell*, 27(5), pp. 745-57.

Sologub, M., Litonin, D., Anikin, M., Mustaev, A. and Temiakov, D. (2009) 'TFB2 is a transient component of the catalytic site of the human mitochondrial RNA polymerase', *Cell*, 139(5), pp. 934-44.

Spelbrink, J.N., Li, F.Y., Tiranti, V., Nikali, K., Yuan, Q.P., Tariq, M., Wanrooij, S., Garrido, N., Comi, G., Morandi, L., Santoro, L., Toscano, A., Fabrizi, G.M., Somer, H., Croxen, R., Beeson, D., Poulton, J., Suomalainen, A., Jacobs, H.T., Zeviani, M. and Larsson, C. (2001) 'Human mitochondrial DNA deletions associated with mutations in the gene encoding Twinkle, a phage T7 gene 4-like protein localized in mitochondria', *Nat Genet*, 28(3), pp. 223-31.

Srivastava, P. and Panda, D. (2007) 'Rotenone inhibits mammalian cell proliferation by inhibiting microtubule assembly through tubulin binding', *Febs j*, 274(18), pp. 4788-801.

St-Pierre, J., Buckingham, J.A., Roebuck, S.J. and Brand, M.D. (2002) 'Topology of Superoxide Production from Different Sites in the Mitochondrial Electron Transport Chain', *Journal of Biological Chemistry*, 277(47), pp. 44784-44790.

St-Pierre, J., Drori, S., Uldry, M., Silvaggi, J.M., Rhee, J., Jager, S., Handschin, C., Zheng, K., Lin, J., Yang, W., Simon, D.K., Bachoo, R. and Spiegelman, B.M. (2006) 'Suppression of reactive oxygen species and neurodegeneration by the PGC-1 transcriptional coactivators', *Cell*, 127(2), pp. 397-408.

St-Pierre, J., Lin, J., Krauss, S., Tarr, P.T., Yang, R., Newgard, C.B. and Spiegelman, B.M. (2003) 'Bioenergetic analysis of peroxisome proliferator-activated receptor gamma coactivators 1alpha and 1beta (PGC-1alpha and PGC-1beta) in muscle cells', *J Biol Chem*, 278(29), pp. 26597-603.

Stadler, J., Bentz, B.G., Harbrecht, B.G., Di Silvio, M., Curran, R.D., Billiar, T.R., Hoffman, R.A. and Simmons, R.L. (1992) 'Tumor necrosis factor alpha inhibits hepatocyte mitochondrial respiration', *Ann Surg*, 216(5), pp. 539-46.

Stamp, C., Zupanic, A., Sachdeva, A., Stoll, E.A., Shanley, D.P., Mathers, J.C., Kirkwood, T.B.L., Heer, R., Simons, B.D., Turnbull, D.M. and Greaves, L.C. (2018) 'Predominant Asymmetrical Stem Cell Fate Outcome Limits the Rate of Niche Succession in Human Colonic Crypts', *EBioMedicine*, 31, pp. 166-173.

Stanger, B.Z. (2015) 'Cellular homeostasis and repair in the mammalian liver', *Annu Rev Physiol*, 77, pp. 179-200.

Stein, G.H., Drullinger, L.F., Soulard, A. and Dulic, V. (1999) 'Differential roles for cyclin-dependent kinase inhibitors p21 and p16 in the mechanisms of senescence and differentiation in human fibroblasts', *Mol Cell Biol*, 19(3), pp. 2109-17.

Stocco, D.M., Cascarano, J. and Wilson, M.A. (1977) 'Quantitation of mitochondrial DNA, RNA, and protein in starved and starved-refed rat liver', *J Cell Physiol*, 90(2), pp. 295-306.

Stocco, D.M. and Hutson, J.C. (1978) 'Quantitation of mitochondrial DNA and protein in the liver of Fischer 344 rats during aging', *J Gerontol*, 33(6), pp. 802-9.

Stocker, E. and Heine, W.D. (1971) 'Regeneration of liver parenchyma under normal and pathological conditions', *Beitr Pathol*, 144(4), pp. 400-8.

Strasberg, S.M. (2005) 'Nomenclature of hepatic anatomy and resections: a review of the Brisbane 2000 system', *J Hepatobiliary Pancreat Surg*, 12(5), pp. 351-5.

Su, A.I., Guidotti, L.G., Pezacki, J.P., Chisari, F.V. and Schultz, P.G. (2002) 'Gene expression during the priming phase of liver regeneration after partial hepatectomy in mice', *Proc Natl Acad Sci U S A*, 99(17), pp. 11181-6.

Sun, S.C., Ganchi, P.A., Ballard, D.W. and Greene, W.C. (1993) 'NF-kappa B controls expression of inhibitor I kappa B alpha: evidence for an inducible autoregulatory pathway', *Science*, 259(5103), pp. 1912-5.

Suryadinata, R., Sadowski, M. and Sarcevic, B. (2010) 'Control of cell cycle progression by phosphorylation of cyclin-dependent kinase (CDK) substrates', *Biosci Rep*, 30(4), pp. 243-55.

Suzuki, H., Toyoda, M., Horiguchi, N., Kakizaki, S., Ohyama, T., Takizawa, D., Ichikawa, T., Sato, K., Takagi, H. and Mori, M. (2009) 'Hepatocyte growth factor protects against Fas-mediated liver apoptosis in transgenic mice', *Liver Int*, 29(10), pp. 1562-8.

Szymonik-Lesiuk, S., Czechowska, G., Stryjecka-Zimmer, M., Slomka, M., Madro, A., Celinski, K. and Wielosz, M. (2003) 'Catalase, superoxide dismutase, and glutathione peroxidase activities in various rat tissues after carbon tetrachloride intoxication', *J Hepatobiliary Pancreat Surg*, 10(4), pp. 309-15.

Taguchi, N., Ishihara, N., Jofuku, A., Oka, T. and Mihara, K. (2007) 'Mitotic phosphorylation of dynamin-related GTPase Drp1 participates in mitochondrial fission', *J Biol Chem*, 282(15), pp. 11521-9.

Takada, Y., Mukhopadhyay, A., Kundu, G.C., Mahabeleshwar, G.H., Singh, S. and Aggarwal, B.B. (2003) 'Hydrogen peroxide activates NF-kappa B through tyrosine phosphorylation of I kappa B alpha and serine phosphorylation of p65: evidence for the involvement of I kappa B alpha kinase and Syk protein-tyrosine kinase', *J Biol Chem*, 278(26), pp. 24233-41.

Takahashi, A., Ohtani, N., Yamakoshi, K., Iida, S., Tahara, H., Nakayama, K., Nakayama, K.I., Ide, T., Saya, H. and Hara, E. (2006) 'Mitogenic signalling and the p16INK4a-Rb pathway cooperate to enforce irreversible cellular senescence', *Nat Cell Biol*, 8(11), pp. 1291-7.

Takamura, K., Tsuchida, K., Miyake, H., Tashiro, S. and Sugino, H. (2005) 'Activin and activin receptor expression changes in liver regeneration in rat', *J Surg Res*, 126(1), pp. 3-11.

Takehara, T., Hayashi, N., Mita, E., Kanto, T., Tatsumi, T., Sasaki, Y., Kasahara, A. and Hori, M. (1998) 'Delayed Fas-mediated hepatocyte apoptosis during liver regeneration in mice: hepatoprotective role of TNF alpha', *Hepatology*, 27(6), pp. 1643-51.

Tanimizu, N., Nakamura, Y., Ichinohe, N., Mizuguchi, T., Hirata, K. and Mitaka, T. (2013) 'Hepatic biliary epithelial cells acquire epithelial integrity but lose plasticity to differentiate into hepatocytes in vitro during development', *J Cell Sci*, 126(Pt 22), pp. 5239-46.

Tao, Y., Wang, M. and Chen, E. (2017) 'Liver Regeneration: Analysis of the Main Relevant Signaling Molecules', 2017, p. 4256352.

Tarlow, B.D., Finegold, M.J. and Grompe, M. (2014) 'Clonal tracing of Sox9+ liver progenitors in mouse oval cell injury', *Hepatology*, 60(1), pp. 278-89.

Tauchi, H. and Sato, T. (1968) 'Age Changes in Size and Number of Mitochondria of Human Hepatic Cells', *Journal of Gerontology*, 23(4), pp. 454-461.

Taylor, R.W., Barron, M.J., Borthwick, G.M., Gospel, A., Chinnery, P.F., Samuels, D.C., Taylor, G.A., Plusa, S.M., Needham, S.J., Greaves, L.C., Kirkwood, T.B. and Turnbull, D.M. (2003) 'Mitochondrial DNA mutations in human colonic crypt stem cells', *J Clin Invest*, 112(9), pp. 1351-60.

Taylor, R.W. and Turnbull, D.M. (2005) 'Mitochondrial DNA mutations in human disease', *Nature Reviews Genetics*, 6(5), pp. 389-402.

Temperley, R., Richter, R., Dennerlein, S., Lightowlers, R.N. and Chrzanowska-Lightowlers, Z.M. (2010a) 'Hungry codons promote frameshifting in human mitochondrial ribosomes', *Science*, 327(5963), p. 301.

Temperley, R.J., Wydro, M., Lightowlers, R.N. and Chrzanowska-Lightowlers, Z.M. (2010b) 'Human mitochondrial mRNAs--like members of all families, similar but different', *Biochim Biophys Acta*, 1797(6-7), pp. 1081-5.

Tewari, M., Dobrzanski, P., Mohn, K.L., Cressman, D.E., Hsu, J.C., Bravo, R. and Taub, R. (1992) 'Rapid induction in regenerating liver of RL/IF-1 (an I kappa B that inhibits NF-kappa B, RelB-p50, and c-Rel-p50) and PHF, a novel kappa B site-binding complex', *Mol Cell Biol*, 12(6), pp. 2898-908.

Theilgaard-Monch, K., Knudsen, S., Follin, P. and Borregaard, N. (2004) 'The transcriptional activation program of human neutrophils in skin lesions supports their important role in wound healing', *J Immunol*, 172(12), pp. 7684-93.

Thornborrow, E.C. and Manfredi, J.J. (1999) 'One mechanism for cell type-specific regulation of the bax promoter by the tumor suppressor p53 is dictated by the p53 response element', *J Biol Chem*, 274(47), pp. 33747-56.

Tierney, D.J., Haas, A.L. and Koop, D.R. (1992) 'Degradation of cytochrome P450 2E1: selective loss after labilization of the enzyme', *Arch Biochem Biophys*, 293(1), pp. 9-16.

Tomiya, T., Ogata, I. and Fujiwara, K. (1998) 'Transforming growth factor alpha levels in liver and blood correlate better than hepatocyte growth factor with hepatocyte proliferation during liver regeneration', *Am J Pathol*, 153(3), pp. 955-61.

Traverso, J.J., Manoranjan, V.S., Bishop, A.R., Rasmussen, K.O. and Voulgarakis, N.K. (2015) 'Allostery through protein-induced DNA bubbles', *Sci Rep*, 5, p. 9037.

Treuting, P.M., Dintzis, S.M. and Montine, K.S. (2018) *Comparative anatomy and histology : a mouse, rat, and human atlas*.

Trifunovic, A. and Larsson, N.G. (2008) 'Mitochondrial dysfunction as a cause of ageing', *J Intern Med*, 263(2), pp. 167-78.

Trifunovic, A., Wredenberg, A., Falkenberg, M., Spelbrink, J.N., Rovio, A.T., Bruder, C.E., Bohlooly, Y.M., Gidlof, S., Oldfors, A., Wibom, R., Tornell, J., Jacobs, H.T. and Larsson, N.G. (2004) 'Premature ageing in mice expressing defective mitochondrial DNA polymerase', *Nature*, 429(6990), pp. 417-23.

Tsuchida, T. and Friedman, S.L. (2017) 'Mechanisms of hepatic stellate cell activation', *Nature Reviews Gastroenterology &Amp; Hepatology*, 14, p. 397.

Turrens, J.F. and Boveris, A. (1980) 'Generation of superoxide anion by the NADH dehydrogenase of bovine heart mitochondria', *Biochem J*, 191(2), pp. 421-7.

Uchiyama, S., Shimizu, T. and Shirasawa, T. (2006) 'CuZn-SOD deficiency causes ApoB degradation and induces hepatic lipid accumulation by impaired lipoprotein secretion in mice', *J Biol Chem*, 281(42), pp. 31713-9.

Ungvari, Z., Orosz, Z., Rivera, A., Labinskyy, N., Xiangmin, Z., Olson, S., Podlutsky, A. and Csiszar, A. (2007) 'Resveratrol increases vascular oxidative stress resistance', *Am J Physiol Heart Circ Physiol*, 292(5), pp. H2417-24.

United Nations (2017) *World Population Ageing*. New York: Nations, U. [Online]. Available at: https://www.un.org/en/development/desa/population/theme/ageing/WPA2017.asp.

Vaamonde-Garcia, C., Courties, A., Pigenet, A., Laiguillon, M.C., Sautet, A., Houard, X., Kerdine-Romer, S., Meijide, R., Berenbaum, F. and Sellam, J. (2017) 'The nuclear factor-erythroid 2-related factor/heme oxygenase-1 axis is critical for the inflammatory features of type 2 diabetes-associated osteoarthritis', *J Biol Chem*, 292(35), pp. 14505-14515.

Vaamonde-Garcia, C., Riveiro-Naveira, R.R., Valcarcel-Ares, M.N., Hermida-Carballo, L., Blanco, F.J. and Lopez-Armada, M.J. (2012) 'Mitochondrial dysfunction increases inflammatory responsiveness to cytokines in normal human chondrocytes', *Arthritis Rheum*, 64(9), pp. 2927-36.

Valle, I., Alvarez-Barrientos, A., Arza, E., Lamas, S. and Monsalve, M. (2005) 'PGC-1alpha regulates the mitochondrial antioxidant defense system in vascular endothelial cells', *Cardiovasc Res*, 66(3), pp. 562-73.

van der Giezen, M. (2011) 'Mitochondria and the Rise of Eukaryotes', *BioScience*, 61, pp. 594-601.

Van Haute, L., Powell, C.A. and Minczuk, M. (2017) 'Dealing with an Unconventional Genetic Code in Mitochondria: The Biogenesis and Pathogenic Defects of the 5-Formylcytosine Modification in Mitochondrial tRNA(Met)', *Biomolecules*, 7(1).

Van Raamsdonk, J.M. and Hekimi, S. (2012) 'Superoxide dismutase is dispensable for normal animal lifespan', *Proc Natl Acad Sci U S A*, 109(15), pp. 5785-90.

Vega-Avila, E. and Pugsley, M.K. (2011) 'An overview of colorimetric assay methods used to assess survival or proliferation of mammalian cells', *Proc West Pharmacol Soc*, 54, pp. 10-4.

Venugopal, S.K., Wu, J., Catana, A.M., Eisenbud, L., He, S.Q., Duan, Y.Y., Follenzi, A. and Zern, M.A. (2007) 'Lentivirus-mediated superoxide dismutase1 gene delivery protects against oxidative stress-induced liver injury in mice', *Liver Int*, 27(10), pp. 1311-22.

Vermeulen, K., Van Bockstaele, D.R. and Berneman, Z.N. (2003) 'The cell cycle: a review of regulation, deregulation and therapeutic targets in cancer', *Cell Proliferation*, 36(3), pp. 131-149.

Vermulst, M., Bielas, J.H., Kujoth, G.C., Ladiges, W.C., Rabinovitch, P.S., Prolla, T.A. and Loeb, L.A. (2007) 'Mitochondrial point mutations do not limit the natural lifespan of mice', *Nature Genetics*, 39, p. 540.

Vermulst, M., Wanagat, J., Kujoth, G.C., Bielas, J.H., Rabinovitch, P.S., Prolla, T.A. and Loeb, L.A. (2008) 'DNA deletions and clonal mutations drive premature aging in mitochondrial mutator mice', *Nat Genet*, 40(4), pp. 392-4.

Villarroya, M., Prado, S., Esteve, J.M., Soriano, M.A., Aguado, C., Perez-Martinez, D., Martinez-Ferrandis, J.I., Yim, L., Victor, V.M., Cebolla, E., Montaner, A., Knecht, E. and Armengod, M.E. (2008) 'Characterization of human GTPBP3, a GTP-binding protein involved in mitochondrial tRNA modification', *Mol Cell Biol*, 28(24), pp. 7514-31.

Vivo, M., Matarese, M., Sepe, M., Di Martino, R., Festa, L., Calabrò, V., La Mantia, G. and Pollice, A. (2015) 'MDM2-mediated degradation of p14ARF: a novel mechanism to control ARF levels in cancer cells', *PLoS One*, 10(2), p. e0117252.

Vogel, F., Bornhovd, C., Neupert, W. and Reichert, A.S. (2006) 'Dynamic subcompartmentalization of the mitochondrial inner membrane', *J Cell Biol*, 175(2), pp. 237-47.

W. S. Liu, V., Zhang, C., W. Linnane, A. and Nagley, P. (1997) 'Quantitative allele-specific PCR: Demonstration of age-associated accumulation in human tissues of the A→G mutation at nucleotide 3243 in mitochondrial DNA', *Human Mutation*, 9, pp. 265-271.

Wallace, D.C., Ye, J.H., Neckelmann, S.N., Singh, G., Webster, K.A. and Greenberg, B.D. (1987) 'Sequence analysis of cDNAs for the human and bovine ATP synthase beta subunit: mitochondrial DNA genes sustain seventeen times more mutations', *Curr Genet*, 12(2), pp. 81-90.

Wallin, I.E. (1926) 'BACTERIA AND THE ORIGIN OF SPECIES', *Science*, 64(1651), pp. 173-5.

Wang, B., Gao, C. and Ponder, K.P. (2005) 'C/EBPbeta contributes to hepatocyte growth factor-induced replication of rodent hepatocytes', *J Hepatol*, 43(2), pp. 294-302.

Wang, B., Zhao, L., Fish, M., Logan, C.Y. and Nusse, R. (2015) 'Self-renewing diploid Axin2(+) cells fuel homeostatic renewal of the liver', *Nature*, 524(7564), pp. 180-5.

Wang, C., Li, Z., Lu, Y., Du, R., Katiyar, S., Yang, J., Fu, M., Leader, J.E., Quong, A., Novikoff, P.M. and Pestell, R.G. (2006) 'Cyclin D1 repression of nuclear respiratory factor 1 integrates nuclear DNA synthesis and mitochondrial function', *Proc Natl Acad Sci U S A*, 103(31), pp. 11567-72.

Wang, C. and Youle, R.J. (2009) 'The role of mitochondria in apoptosis*', *Annu Rev Genet*, 43, pp. 95-118.

Wang, G.J., Nutter, L.M. and Thayer, S.A. (1997) 'Insensitivity of cultured rat cortical neurons to mitochondrial DNA synthesis inhibitors: evidence for a slow turnover of mitochondrial DNA', *Biochem Pharmacol*, 54(1), pp. 181-7.

Wang, J. (2018) 'Neutrophils in tissue injury and repair', *Cell Tissue Res*, 371(3), pp. 531-539.

Wang, S. and El-Deiry, W.S. (2003) 'TRAIL and apoptosis induction by TNF-family death receptors', *Oncogene*, 22(53), pp. 8628-33.

Wang, X., Quail, E., Hung, N.J., Tan, Y., Ye, H. and Costa, R.H. (2001) 'Increased levels of forkhead box M1B transcription factor in transgenic mouse hepatocytes prevent age-related proliferation defects in regenerating liver', *Proc Natl Acad Sci U S A*, 98(20), pp. 11468-73.

Wang, Z., Fan, M., Candas, D., Zhang, T.Q., Qin, L., Eldridge, A., Wachsmann-Hogiu, S., Ahmed, K.M., Chromy, B.A., Nantajit, D., Duru, N., He, F., Chen, M., Finkel, T., Weinstein, L.S. and Li, J.J. (2014) 'Cyclin B1/Cdk1 coordinates mitochondrial respiration for cell-cycle G2/M progression', *Dev Cell*, 29(2), pp. 217-32.

Watanabe, K., Shibuya, S., Koyama, H., Ozawa, Y., Toda, T., Yokote, K. and Shimizu, T. (2013) 'Sod1 loss induces intrinsic superoxide accumulation leading to p53-mediated growth arrest and apoptosis', *Int J Mol Sci*, 14(6), pp. 10998-1010.

Weber, L.W., Boll, M. and Stampfl, A. (2003) 'Hepatotoxicity and mechanism of action of haloalkanes: carbon tetrachloride as a toxicological model', *Crit Rev Toxicol*, 33(2), pp. 105-36.

Wera, O., Lancellotti, P. and Oury, C. (2016) 'The Dual Role of Neutrophils in Inflammatory Bowel Diseases', *J Clin Med*, 5(12).

White, M.J., DiCaprio, M.J. and Greenberg, D.A. (1996) 'Assessment of neuronal viability with Alamar blue in cortical and granule cell cultures', *J Neurosci Methods*, 70(2), pp. 195-200.

Williams, M.D., Van Remmen, H., Conrad, C.C., Huang, T.T., Epstein, C.J. and Richardson, A. (1998) 'Increased oxidative damage is correlated to altered mitochondrial function in heterozygous manganese superoxide dismutase knockout mice', *J Biol Chem*, 273(43), pp. 28510-5.

Williams, S.L., Huang, J., Edwards, Y.J., Ulloa, R.H., Dillon, L.M., Prolla, T.A., Vance, J.M., Moraes, C.T. and Zuchner, S. (2010) 'The mtDNA mutation spectrum of the progeroid Polg mutator mouse includes abundant control region multimers', *Cell Metab*, 12(6), pp. 675-82.

Wilson, L., Yang, Q., Szustakowski, J.D., Gullicksen, P.S. and Halse, R. (2007) 'Pyruvate induces mitochondrial biogenesis by a PGC-1 alpha-independent mechanism', *Am J Physiol Cell Physiol*, 292(5), pp. C1599-605.

Winterbourn, C.C., Kettle, A.J. and Hampton, M.B. (2016) 'Reactive Oxygen Species and Neutrophil Function', *Annual Review of Biochemistry*, 85(1), pp. 765-792.

Witzany, G. (2006) 'Serial Endosymbiotic Theory (set): the biosemiotic update', *Acta Biotheor*, 54(2), pp. 103-17.

Wolpe, S.D., Sherry, B., Juers, D., Davatelis, G., Yurt, R.W. and Cerami, A. (1989) 'Identification and characterization of macrophage inflammatory protein 2', *Proc Natl Acad Sci U S A*, 86(2), pp. 612-6.

Wong, H. and Riabowol, K. (1996) 'Differential CDK-inhibitor gene expression in aging human diploid fibroblasts', *Experimental Gerontology*, 31(1), pp. 311-325.

Wright, M.C., Issa, R., Smart, D.E., Trim, N., Murray, G.I., Primrose, J.N., Arthur, M.J., Iredale, J.P. and Mann, D.A. (2001) 'Gliotoxin stimulates the apoptosis of human and rat hepatic stellate cells and enhances the resolution of liver fibrosis in rats', *Gastroenterology*, 121(3), pp. 685-98.

Wu, X., Li, L. and Jiang, H. (2016) 'Doa1 targets ubiquitinated substrates for mitochondria-associated degradation', *J Cell Biol*, 213(1), pp. 49-63.

Wynne, H.A., Cope, L.H., Mutch, E., Rawlins, M.D., Woodhouse, K.W. and James, O.F. (1989) 'The effect of age upon liver volume and apparent liver blood flow in healthy man', *Hepatology*, 9(2), pp. 297-301.

Xiao, G.H., Jeffers, M., Bellacosa, A., Mitsuuchi, Y., Vande Woude, G.F. and Testa, J.R. (2001) 'Anti-apoptotic signaling by hepatocyte growth factor/Met via the phosphatidylinositol 3-kinase/Akt and mitogen-activated protein kinase pathways', *Proc Natl Acad Sci U S A*, 98(1), pp. 247-52.

Yakes, F.M. and Van Houten, B. (1997) 'Mitochondrial DNA damage is more extensive and persists longer than nuclear DNA damage in human cells following oxidative stress', *Proc Natl Acad Sci U S A*, 94(2), pp. 514-9.

Yakubovskaya, E., Guja, K.E., Eng, E.T., Choi, W.S., Mejia, E., Beglov, D., Lukin, M., Kozakov, D. and Garcia-Diaz, M. (2014) 'Organization of the human mitochondrial transcription initiation complex', *Nucleic Acids Res*, 42(6), pp. 4100-12.

Yakubovskaya, E., Mejia, E., Byrnes, J., Hambardjieva, E. and Garcia-Diaz, M. (2010) 'Helix unwinding and base flipping enable human MTERF1 to terminate mitochondrial transcription', *Cell*, 141(6), pp. 982-93.

Yamada, Y., Kirillova, I., Peschon, J.J. and Fausto, N. (1997) 'Initiation of liver growth by tumor necrosis factor: deficient liver regeneration in mice lacking type I tumor necrosis factor receptor', *Proc Natl Acad Sci U S A*, 94(4), pp. 1441-6.

Yamada, Y., Webber, E.M., Kirillova, I., Peschon, J.J. and Fausto, N. (1998) 'Analysis of liver regeneration in mice lacking type 1 or type 2 tumor necrosis factor receptor: requirement for type 1 but not type 2 receptor', *Hepatology*, 28(4), pp. 959-70.

Yang, D., Oyaizu, Y., Oyaizu, H., Olsen, G.J. and Woese, C.R. (1985) 'Mitochondrial origins', *Proc Natl Acad Sci U S A*, 82(13), pp. 4443-7.

Yang, L., Magness, S.T., Bataller, R., Rippe, R.A. and Brenner, D.A. (2005) 'NF-kappaB activation in Kupffer cells after partial hepatectomy', *Am J Physiol Gastrointest Liver Physiol*, 289(3), pp. G530-8.

Yang, S., Tan, T.M., Wee, A. and Leow, C.K. (2004) 'Mitochondrial respiratory function and antioxidant capacity in normal and cirrhotic livers following partial hepatectomy', *Cell Mol Life Sci*, 61(2), pp. 220-9.

Yang, W. and Hekimi, S. (2010) 'A mitochondrial superoxide signal triggers increased longevity in Caenorhabditis elegans', *PLoS Biol*, 8(12), p. e1000556.

Yasuda, H., Mine, T., Shibata, H., Eto, Y., Hasegawa, Y., Takeuchi, T., Asano, S. and Kojima, I. (1993) 'Activin A: an autocrine inhibitor of initiation of DNA synthesis in rat hepatocytes', *J Clin Invest*, 92(3), pp. 1491-6.

Yasukawa, T., Reyes, A., Cluett, T.J., Yang, M.Y., Bowmaker, M., Jacobs, H.T. and Holt, I.J. (2006) 'Replication of vertebrate mitochondrial DNA entails transient ribonucleotide incorporation throughout the lagging strand', *Embo j*, 25(22), pp. 5358-71.

Yasukawa, T., Yang, M.Y., Jacobs, H.T. and Holt, I.J. (2005) 'A bidirectional origin of replication maps to the major noncoding region of human mitochondrial DNA', *Mol Cell*, 18(6), pp. 651-62.

Yen, T.C., Chen, Y.S., King, K.L., Yeh, S.H. and Wei, Y.H. (1989) 'Liver mitochondrial respiratory functions decline with age', *Biochem Biophys Res Commun*, 165(3), pp. 944-1003.
Yoshioka, Y., Kitao, T., Kishino, T., Yamamuro, A. and Maeda, S. (2006) 'Nitric Oxide Protects Macrophages from Hydrogen Peroxide-Induced Apoptosis by Inducing the Formation of Catalase', *The Journal of Immunology*, 176(8), p. 4675.
Zajicek, G., Oren, R. and Weinreb, M., Jr. (1985) 'The streaming liver', *Liver*, 5(6), pp. 293-300.
Zhang, C., Bills, M., Quigley, A., Maxwell, R.J., Linnane, A.W. and Nagley, P. (1997) 'Varied prevalence of age-associated mitochondrial DNA deletions in different species and tissues: a comparison between human and rat', *Biochem Biophys Res Commun*, 230(3), pp. 630-5.
Zhang, C., Linnane, A.W. and Nagley, P. (1993) 'Occurrence of a particular base substitution (3243 A to G) in mitochondrial DNA of tissues of ageing humans', *Biochem Biophys Res Commun*, 195(2), pp. 1104-10.
Zhang, D., Chen, G., Manwani, D., Mortha, A., Xu, C., Faith, J.J., Burk, R.D., Kunisaki, Y., Jang, J.E., Scheiermann, C., Merad, M. and Frenette, P.S. (2015) 'Neutrophil ageing is regulated by the microbiome', *Nature*, 525(7570), pp. 528-32.
Zhang, D., Mott, J.L., Chang, S.W., Denniger, G., Feng, Z. and Zassenhaus, H.P. (2000) 'Construction of transgenic mice with tissue-specific acceleration of mitochondrial DNA mutagenesis', *Genomics*, 69(2), pp. 151-61.
Zhang, Q., Raoof, M., Chen, Y., Sumi, Y., Sursal, T., Junger, W., Brohi, K., Itagaki, K. and Hauser, C.J. (2010) 'Circulating mitochondrial DAMPs cause inflammatory responses to injury', *Nature*, 464(7285), pp. 104-7.
Zhang, Y., Chong, E. and Herman, B. (2002) 'Age-associated increases in the activity of multiple caspases in Fisher 344 rat organs', *Exp Gerontol*, 37(6), pp. 777-89.
Zhang, Y., Xiong, Y. and Yarbrough, W.G. (1998) 'ARF promotes MDM2 degradation and stabilizes p53: ARF-INK4a locus deletion impairs both the Rb and p53 tumor suppression pathways', *Cell*, 92(6), pp. 725-34.
Zheng, L., Zhou, M., Guo, Z., Lu, H., Qian, L., Dai, H., Qiu, J., Yakubovskaya, E., Bogenhagen, D.F., Demple, B. and Shen, B. (2008) 'Human DNA2 is a mitochondrial nuclease/helicase for efficient processing of DNA replication and repair intermediates', *Mol Cell*, 32(3), pp. 325-36.
Zheng, W., Khrapko, K., Coller, H.A., Thilly, W.G. and Copeland, W.C. (2006) 'Origins of human mitochondrial point mutations as DNA polymerase gamma-mediated errors', *Mutat Res*, 599(1-2), pp. 11-20.
Zhong, Z., Umemura, A., Sanchez-Lopez, E., Liang, S., Shalapour, S., Wong, J., He, F., Boassa, D., Perkins, G., Ali, S.R., McGeough, M.D., Ellisman, M.H., Seki, E., Gustafsson, A.B., Hoffman, H.M., Diaz-Meco, M.T., Moscat, J. and Karin, M. (2016) 'NF-kappaB Restricts Inflammasome Activation via Elimination of Damaged Mitochondria', *Cell*, 164(5), pp. 896-910.

Zhou, D., Chrest, F.J., Adler, W., Munster, A. and Winchurch, R.A. (1993) 'Increased production of TGF-beta and Il-6 by aged spleen cells', *Immunol Lett*, 36(1), pp. 7-11.
Zhou, R., Yazdi, A.S., Menu, P. and Tschopp, J. (2011) 'A role for mitochondria in NLRP3 inflammasome activation', *Nature*, 469(7329), pp. 221-5.
Zhou, W., Cao, L., Jeffries, J., Zhu, X., Staiger, C.J. and Deng, Q. (2018) 'Neutrophil-specific knockout demonstrates a role for mitochondria in regulating neutrophil motility in zebrafish', 11(3).
Zindy, F., Quelle, D.E., Roussel, M.F. and Sherr, C.J. (1997) 'Expression of the p16INK4a tumor suppressor versus other INK4 family members during mouse development and aging', *Oncogene*, 15(2), pp. 203-11.
Zinovkina, L.A. (2018) 'Mechanisms of Mitochondrial DNA Repair in Mammals', *Biochemistry (Moscow)*, 83(3), pp. 233-249.
Zmijewski, J.W., Lorne, E., Zhao, X., Tsuruta, Y., Sha, Y., Liu, G., Siegal, G.P. and Abraham, E. (2008) 'Mitochondrial respiratory complex I regulates neutrophil activation and severity of lung injury', *Am J Respir Crit Care Med*, 178(2), pp. 168-79.